REPORT DOCUMENTATION PAGE		READ INSTRUCTIONS BEFORE COMPLETING FORM
1. REPORT NUMBER AR 5	2. GOVT ACCESSION NO. AD-A119688	3. RECIPIENT'S CATALOG NUMBER
4. TITLE (and Subtitle) Theoretical Studies Relating to the Interaction of Radiation with Matter: Atomic Collision Processes Occurring in the Presence of Radiation Fields		5. TYPE OF REPORT & PERIOD COVERED Interim 8/1/81 - 7/31/82
		6. PERFORMING ORG. REPORT NUMBER
7. AUTHOR(s) P.R. Berman		8. CONTRACT OR GRANT NUMBER(s) N00014-77-C-0553
9. PERFORMING ORGANIZATION NAME AND ADDRESS Prof. P.R. Berman Physics Dept. - New York University 4 Washington Place, New York, N.Y. 10003		10. PROGRAM ELEMENT, PROJECT, TASK AREA & WORK UNIT NUMBERS
11. CONTROLLING OFFICE NAME AND ADDRESS Office of Naval Research Resident Representative New York 715 Broadway - New York, N.Y. 10003		12. REPORT DATE Sept. 15, 1982
		13. NUMBER OF PAGES 140
14. MONITORING AGENCY NAME & ADDRESS(if different from Controlling Office)		15. SECURITY CLASS. (of this report) Unclassified
		15a. DECLASSIFICATION/DOWNGRADING SCHEDULE

16. DISTRIBUTION STATEMENT (of this Report)

Approved for public release; distribution unlimited

17. DISTRIBUTION STATEMENT (of the abstract entered in Block 20, if different from Report)

DTIC
SELECTED
SEP 28 1982
H

18. SUPPLEMENTARY NOTES

19. KEY WORDS (Continue on reverse side if necessary and identify by block number)

Laser Spectroscopy, Optical Collisions, Radiative Collisions, Velocity-Changing Collisions, Two-Level System, Atomic Coherence, Zeeman Coherence, Dressed-Atom Picture, Degenerate Four-Wave Mixing, Collision Kernel, Photon Echo

20. ABSTRACT (Continue on reverse side if necessary and identify by block number)

Work is reported in the areas of:-
(1) Two-Level Atom & Radiation Pulse
(2) Effects of Collisions on Atomic Coherences
(3) Collision Effects in Degenerate-Four-Wave-Mixing
(4) Laser-Assisted Collisions
(5) Laser Spectroscopy of Na
(6) Heating of a Vapor via Laser Assisted Collisions

DD FORM 1473 EDITION OF 1 NOV 55 IS OBSOLETE
1 JAN 73
S/N 0102-LF-014-6601

AD A119688

DTIC FILE COPY

·Annual Report (AR5)

Title: "Theoretical Studies Relating to the Interaction of Radiation
with Matter: Atomic Collision Processes Occurring in the Presence
of Radiation Fields"

Supported by the U.S. Office of Naval Research

Contract No.: N00014-77-C-0553

Report of Period: August 1, 1981 - July 31, 1982

Date of Report: September 15, 1982

Accession For

NTIS GRA&I	
DTIC TAB	☐
Unannounced	☐
Justification	

By

Distribution/

Availability Codes

| Dist | Avail and/or Special |

A

DTIC COPY INSPECTED 2

Research has been carried out in the areas of (1) Collision kernels and laser spectroscopy, (2) Laser-assisted collisions, (3) Heating and cooling via collisionally-aided radiative excitation (4) Collisional processes in 4-wave mixing experiments (5) Laser Spectroscopy of Na (6) Radiative collisions involving surfaces and (7) Two-level problem plus radiation pulse.

1. Collision Kernels and Laser Spectroscopy (P. Berman, R. Shakeshaft)

In an atomic vapor, a quantity of physical interest is the collision kernel $W_{ii}(\vec{v}' \to \vec{v})$ giving the probability density per unit time that an atom in state i undergoes a change of velocity from $\vec{v}'$ to $\vec{v}$, owing to collisions with perturber atoms. For atoms in a superposition of states i and j there is an alalogous "kernel" $W_{ij}(\vec{v}' \to \vec{v})$ (it need not be definite) which describes the effects of collisions on atomic state coherences. The coherence kernel is important in problems relating to atomic spectroscopy where an external radiation field creates a linear superposition of atomic states. The coherence kernel specifies the manner in which collisions modify superposition states; in turn the collision-induced modification alters the absorptive and dispersive properties of the vapor. A complete analysis of the line shapes associated with laser spectroscopy can be achieved only with an understanding of the collision kernels. Conversely, the line shapes can be used to provide information on collisional processes occurring within the vapor.

Formal expressions for the collision kernels exist[1], but limited progress had been achieved in gaining physical insight into those ex- pressions for the case when the collisional interactions for states i and

- 1 -

j differ appreciably (as they will for most electronic transition).
Classically, the i and j state populations would follow different
trajectories during a collision, and it is not obvious that a collision
trajectory can be assigned to the atomic coherence (superposition state).

Using arguments based on the uncertainty principle, we have
shown[2*,3*,4*,5*,6*] that collisions can be divide$^?$ roughly into two
regions. Let b_o be some characteristic impact parameter in the scattering
process. For collisions having impact parameters $b < b_o$, collisions may
be treated classically leading to classical population kernels and
vanishing coherence kernels. The coherence kernel vanishes owing to a
spatial separation of the state i and j collision trajectories. On the
other hand, collisions having $b > b_o$ must be treated quantum-mechanically.
These collisions give rise to diffractive scattering contributions to
both the population and coherence kernels.

The interpretation based on the Uncertainty Principle represents
the first, simple unifying explanation of the manner in which collisions
affect the physical observables associated with an atomic system. We
have shown[4] that the diffractive velocity changes should depend only
on the active atom mass and not the perturber to active atom mass ratio.
Dramatic experimental evidence for these conclusions has been provided
by a series of experiments carried out by Hartmann's group at Columbia
using Li, Na and Tℓ as the active atoms in photon echo experiments.
This work is serving to stimulate experimental efforts by other groups.

*Asterisks on references indicate that the reference is appended to
this report.

- 2 -

A comprehensive summary[7] of the physical processes underlying collisions in atomic vapors and the corresponding implications for spectroscopy has been prepared in conjunction with lectures given at the 1982 Les Houches Summer School in "New Trends in Atomic Physics."

2. Laser-Assisted Collisions (P. Berman, E.J. Robinson)

A review article on Collisionally-Aided Radiative Excitation (CARE) and Radiatively Assisted Inelastic Collisions (RAIC) was written[8*] In this article, simple physical arguments were given to explain the detuning and field strength dependence of cross sections for laser assisted collisions.

Recently, we predicted that final state coherences could be created by RAIC.[9] Motivated by the theory, A. Deaurre performed an experiment to test its predictions. Her results[10] provided the first experimental evidence for coherences created by RAIC and were in excellent agreement with theory.

3. Cooling or Heating via CARE (P. Berman)

Several years ago,[11] we predicted that cooling or heating of an atomic vapor could be achieved using Collisionally-Aided Radiative Excitation (CARE). In Prof. Stroke's laboratory, we are now trying to carry out an experiment of this type. The reaction under investigation is

$$Na\ (3S_{1/2}) + X + \hbar\Omega \rightarrow Na\ (3P_{1/2}) + X$$
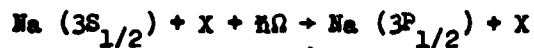
where X is a rare gas atom.

The energy defect between the photon energy $\hbar\Omega$ and the $3P_{1/2}-3S_{1/2}$ transition frequency is provided by a corresponding change in the translational energy of the Na - rare gas system. To probe this energy change, the velocity distribution of the excited state Na atoms is monitored using the transition to the 4D state. Calculations were made which indicated that heating of the Na should be detectable by this scheme using a positive energy defect and heavy rare gas perturbers. Preliminary results[12*] confirm this heating effect. Work on this experiment will continue into next year.

4.   Collisional Processes in 4-Wave Mixing (P. Berman)

In the past several years, there has been considerable interest in 4-wave mixing and in phase conjugate optics.[13] Recently, several attempts to include collisional effects into the theory of such processes have appeared. "New", "collision induced" resonances have been predicted and observed.[14] Although there have been some attempts at physical explanations of these resonances, there appears to be room for a more fundamental understanding of their origin. Moreover, 4-wave mixing experiments offer a convenient vehicle for studying the effects of velocity-changing collisions on Zeeman coherences, a problem that continues to elude a simple physical interpretation.

In collaboration with Dr. J. Lam, we have begun a systematic study of collision effects in 4-wave mixing experiments. It is our hope to

provide a coherent picture of the collision-induced resonances and to incorporate the effects of velocity changing collisions into the line shape formulas. Calculations have begun and we have already concluded that the standard interpretations of some of the resonances appearing in 4-wave mixing are in error.

5. Laser Spectroscopy of Na (C. Feuillade)

Owing to a favorable resonance transition frequency, Na has been the favorite choice of experimentalists in laser spectroscopic studies. The fine and hyperfine structure of Na leads to a multitude of levels, even in the Na ground state. There have been no rigorous calculations that properly incorporate the effects of fine and hyperfine structure, collisional effects and optical pumping effects with Na as the active atom in a laser spectroscopy experiment. However, it is clear that optical pumping of the ground state, in particular, can severely modify the laser spectroscopic line shapes.

Due to the fundamental importance of the Na system in laser spectroscopy, we have begun a project to include all fine and hyperfine structure of the 3S, 3P and 4D levels of Na, interacting with two laser fields. Both steady state and transient solutions will be sought, to clearly isolate the effects of optical pumping. Eventually, collisional effects will be included. Progress to date includes the development of a large computer code to include all the relevant levels and allow for arbitrary polarization of the laser fields.

6. Radiative Collisions Involving Surfaces   (P. Berman, E. Robinson)

In collaboration with Prof. Rajan (NYU), we have started some preliminary studies of atom-surface interactions in the presence of laser fields. While some problems have been identified, little progress has been made in developing the theory. Still, in the long term, this appears to be a fruitful area for investigation.

7. Two-level Atom plus Radiation Pulse   (E. Robinson, A. Bambini, P. Berman)

Research continues in the fundamentally important problem of a two-level system coupled by a radiation pulse. In the large detuning limit, we were able to show that certain classes of coupling pulses having the same asymptotic Fourier transforms will yield transition probabilities that are related to each other by a simple scaling transformation.[15*] Methods for evaluating the transition probabilities in the large-detuning limit have also been developed.

8. Miscellaneous

Previous work has been published relating to the effects of collisions on Zeeman coherences[16*], the dressed atom picture as applied to laser spectroscopy[17*], and the eigenvalue problem for the two-level atom plus radiation pulse problem.[18*] In addition, a Comment[19*], was published correcting and clarifying some recent work[20] yielding sub-natural line width resolution.

- 6 -

References

1. See, for example, P.R. Berman, Phys. Reps. $\underline{43}$, 101 (1978); Adv. At. Mol. Phys. $\underline{13}$, 57 (1977).

2. R. Kachru, T.J. Chen, T.W. Mossberg, S.R. Hartmann and P.R. Berman, Phys. Rev. Letters $\underline{47}$, 902 (1981).

3. T.W. Mossberg, R. Kachru, T.J. Chen, S.R. Hartmann and P.R. Berman, in Laser Spectroscopy V, edited by A.R.W. McKellar, T. Oka and B. Stoicheff (Springer-Verlag, Berlin, 1981) p. 208.

4. P.R. Berman, T.W. Mossberg and S.R. Hartmann, Phys. Rev. A$\underline{25}$, 2550 (1982).

5. P.R. Berman, App. Physics $\underline{28B}$, 190 (1982).

6. L. Spruch and R. Shakeshaft, to appear in proceedings of VII International Atomics Physics Conference.

7. P.R. Berman, to appear.

8. P.R. Berman and E.J. Robinson, to appear in Photon-Assisted Collisions, published by Gordon and Breach.

9. P.R. Berman, Phys. Rev. A$\underline{22}$, 1838, 1848 (1980).

10. A. Debarre, J. Phys. B$\underline{15}$, 1693 (1982).

11. P.R. Berman and S. Stenholm, Opt. Commun. $\underline{24}$, 155 (1978).

12. M. Tawil, P.R. Berman, E. Giacobino, O. Redi, H.H. Stroke, and R. Vetter, Bull. Am. Phys. Soc. $\underline{27}$, 473 (1982).

13. For a review, see, R.L. Abrams, J.F. Lam, R.C. Lind, D.G. Steel and P.F. Liao, to appear in Optical Phase Conjugation, edited by R.A. Fisher (Academic Press, New York, 1982).

References - Con't.

14. See, for example, M. Dagenais, Phys. Rev. A26, 869 (1982); N. Bloembergen, M.C. Downer and L.J. Roghberg, to appear in Proceedings of VII International Atomic Physics Conference and references therein.

15. E.J. Robinson and P.R. Berman, submitted to Phys. Rev. A.

16. J.L. LeGouët and P.R. Berman, Phys. Rev. A24, 1831 (1981); A25, E.3429 (1982).

17. P.R. Berman and R. Salomaa, Phys. Rev. A25, 2667 (1982).

18. E.J. Robinson, Phys. Rev. A24, 2239 (1981).

19. P.R. Berman, Phys. Rev. Lett. 48, 366 (1982).

20. F. Shimizu, K. Umezu and H. Takuma, Phys. Rev. Lett. 47, 825 (1981).

Measurement of a Total Atomic-Radiator-Perturber Scattering Cross Secti

R. Kachru,[a] T. J. Chen, and S. R. Hartmann

Columbia Radiation Laboratory, Department of Physics, Columbia University, New York, New York 10027

and

T. W. Mossberg

Department of Physics, Harvard University, Cambridge, Massachusetts 02138

and

P. R. Berman

Department of Physics, New York University, New York, New York 10003
(Received 9 June 1981)

From work on the $2S$-$2P_{1/2}$ transition of atomic ^{7}Li, perturbed by noble gases, and use of the photon-echo technique, the first measurement of a "total" atomic-radiator-perturber scattering cross section is reported. The phase-changing, inelastic, *and veloc-ity-changing* aspects of collisions contribute to this cross section, which is significantly larger than the corresponding pressure-broadening cross section. Typical velocity changes are found to be roughly one percent of the mean thermal speed.

PACS numbers: 32.70.Jz, 34.40.+n, 34.90.+q, 42.65.Gv

In most spectroscopy experiments, one monitors the dipole moment of the system under investigation. The collisional perturbation of optical dipoles or "optical radiators" represents an interesting problem, since it requires one to understand the way in which collisions affect a superposition state. At first glance, it might seem than any collision destroys the superposition state since the states a and b involved in the optical transition generally follow different collision trajectories.[1,2] The notion of distinct trajectories, however, is a classical one which is known to fail for large-impact-parameter collisions. Thus the dipole moment or optical coherence is not necessarily destroyed in such large impact-parameter collisions.[3] Despite the fact that state-dependent trajectory effects seem to play a crucial role in determining the fate of the optical dipoles, for reasons to be discussed below, steady-state spectroscopy experiments are not overly sensitive[4] to such effects. As a result traditional theories of pressure broadening,[5] in which collisions are assumed to affect only the phases of the optical dipoles, have been successful in explaining these experiments. Only recently has the effect of velocity-changing collisions been put in better perspective.[6] To identify clearly the effects of velocity-changing collisions on optical dipoles experimentally, coherent transient techniques offer unique possibilities.[7]

We present here results of a photon-echo study of $2S$-$2P_{1/2}$ Li radiators perturbed by noble-gas atoms which provide *the first comprehensive picture of the quantum-mechanical velocity-changing aspect of collisions*.[3,7] We measure a total radiator-perturber scattering cross section σ_t (representing the combined effect of the inelastic, phase-changing, and velocity-changing aspects of collisions), and find that it is significantly larger than the broadening cross sections deduced from

spectral line measurements. Fitting our data by a phenomenological collision kernel allows us to estimate the average velocity change experienced by a radiator in those collisions which produce identifiable velocity changes.

Assume that the two photon-echo-excitation pulses propagate along $\hat{z}$ and occur at the times $t = 0$ and $t = \tau$. The phase of a radiator residing at a particular location $\vec{r}$ in the sample is given[8] (for $t > \tau$) by $\exp[-i(\varphi - \vec{k} \cdot \vec{r})]$, where

$$\varphi(t) \equiv - \int_0^\tau [\omega(t') + \vec{k} \cdot \vec{v}(t')]dt' + \int_\tau^t [\omega(t') + \vec{k} \cdot \vec{v}(t')]dt', \tag{1}$$

$\omega(t')$ $[\vec{v}(t')]$ is the instantaneous oscillation frequency [velocity] of the radiator, and $\vec{k}$ is the common wave vector of the excitation pulses. In the absence of collisions, $\omega(t')$ and $\vec{v}(t')$ are time independent so that $\varphi(t_e = 2\tau) = 0$ (i.e., Doppler dephasing is eliminated) and an echo is emitted along $\hat{z}$.

In the presence of collisions, the echo intensity I_e is degraded by the factor $\langle \exp[-i\varphi(2\tau)] \rangle^2$, where the angle brackets indicate an ensemble average. While a more detailed calculation of the collisionally induced modification of the echo amplitude will be given elsewhere, we can, roughly speaking, evaluate this factor by considering collisions to be divided into two groups, i.e., those having impact parameters, b, less than or greater than the Weisskopf radius b_W.[5] For $b < b_W$, classical trajectory notions are valid and because of the separation-of-trajectories argument, one is led to the conclusion that the dipole moment is destroyed in a collision. In traditional pressure-broadening theories, phase changes in this region are large enough to destroy the optical coherence. A broadening cross section σ_B can be calculated using either theoretical picture (loss of dipoles because of phase changes or distinct trajectories) and, interestingly, both approaches lead to the same value. For collisions with $b > b_W$, the distinct-trajectory argument fails and one must perform a quantum mechanical calculation. Collisions for which $b > b_W$ give rise to all veloc-

ity-changing effects in which the dipole moment may be preserved and the small phase changes which occur in these collisions (which for simplicity we neglect) contribute to the pressure-induced shifts in spectral profiles. We can understand the success of traditional theories of pressure broadening despite their neglect of velocity-changing effects by noting that collisions with $b > b_W$ generally give rise only to small-angle ($\theta \lesssim \lambda_B/b_W \ll 1$, where λ_B is the deBroglie wavelength of Li) diffractive scattering. The small velocity changes associated with diffractive scattering do not significantly modify the output of most steady-state spectroscopic experiments. For large τ, however, photon-echo experiments can be sensitive to the velocity changes resulting from even diffractive scattering.

Thus collisions with $b < b_W$ can be viewed as "inelasticlike" and accordingly lead to a decrease in echo intensity by the factor

$$\exp(-4nv_r\sigma_B\tau), \tag{2}$$

where n is the perturber number density, $v_r = (8k_B T/\pi\mu)^{1/2}$ is the mean perturber-radiator relative speed, k_B is Boltzman's constant, T is the absolute temperature, μ is the radiator-perturber reduced mass, and σ_B is the τ-independent broadening cross section. Velocity-changing collisions decrease the echo intensity by the factor[9]

$$\exp[-4nv_r\tau\sigma_v(\tau)], \tag{3a}$$

where

$$\sigma_v(\tau) = \sigma_v^0 \left\{ 1 - \tau^{-1} \int_0^\tau d\tau' \int_{-\infty}^{\infty} \exp[ik\tau'(\Delta v_z)]g(\Delta v_z)d(\Delta v_z) \right\}, \tag{3b}$$

σ_v^0 is the total cross section for velocity changing collisions, $k = |\vec{k}|$, and the collision kernel $g(\Delta v_z)$ gives the probability of a particular change in the z component of velocity Δv_z. Over all, the echo intensity varies as

$$I_e(n, \tau) = I_e^0 \exp[-4nv_r\tau\sigma_{eff}(\tau)], \tag{4a}$$

where

$$\sigma_{eff}(\tau) = \sigma_B + \sigma_v(\tau), \tag{4b}$$

and I_e^0 is the $n = 0$ echo intensity. Since the root mean square change in Δv_z is finite for any realistic $g(\Delta v_z)$, $\sigma_v(\tau) = \alpha\tau^2$ for sufficiently small τ
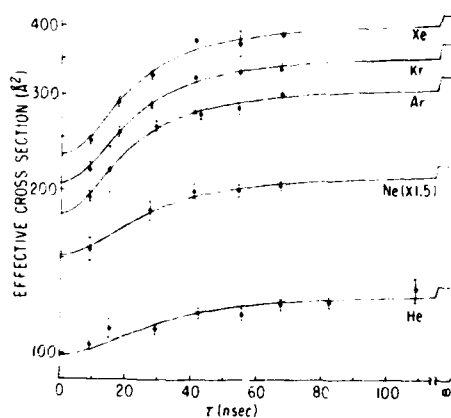
903

FIG. 1. Plot of $\sigma_{eff}(\tau)$ vs τ. Error bars represent statistical uncertainty. At right we show σ_t.

and

$$\sigma_{eff}(\tau) = \sigma_B + \alpha\tau^2 \quad \text{(short } \tau\text{).} \tag{5}$$

Here α depends on the details of $g(\Delta v_z)$. Therefore, $\sigma_{eff}(\tau = 0) \equiv \sigma_B$. On the other hand, $\sigma_v(\tau \to \infty) = \sigma_v^0$, which implies that $\sigma_{eff}(\tau \to \infty) = \sigma_t \equiv \sigma_B + \sigma_v^0$.

The excitation pulses used in our experiment on the 6708-Å $2S$-$2P_{1/2}$ transition of ^{7}Li have a 6-GHz spectral width, a 4.5-nsec temporal width, and a peak power of a few watts. The two pulses, optically split from the single output pulse of an N_2-laser–pumped dye laser, were collimated to a 4-mm diameter, and directed through a stainless-steel heat-pipe–type cell containing Li of natural isotopic concentrations. The cell, maintained at 525 ± 15 K (implying a Li pressure of $\approx 10^{-6}$ Torr), had a vapor region approximately 10 cm in length. For reasons described elsewhere,[3] we used excitation pulses of orthogonal linear polarization in short-τ measurements.

Excitation pulses of parallel polarization, which, depending on τ, produce echo signals 10 to 100 times larger than pulses of orthogonal polarization, were used for long-τ measurements, where radiative decay of the $2P_{1/2}$ state weakened the echo signal (by ≈ 1600 times for $\tau \approx 100$ nsec). Measurements in the intermediate-τ regime revealed no polarization dependence of observed cross sections.

We have measured I_e vs n (maximum $n \approx 10^{16}$ cm^{-3}) for various fixed τ, and used Eq. (4a) to calculate $\sigma_{eff}(\tau)$. In Fig. 1, we plot $\sigma_{eff}(\tau)$ vs τ for each noble-gas perturber. We obtained values of σ_B by using our two shortest-τ measurements of $\sigma_{eff}(\tau)$ for each perturber and extrapolating, according to Eq. (5), back to $\sigma_{eff}(\tau = 0) = \sigma_B$. These values of σ_B are presented in Table I along with the values of σ_B obtained in traditional line-broadening experiments.[10] Except in the case of He, we find that the measurements are in good agreement.

We attempt to reproduce $\sigma_v(\tau)$ [computed using our value of σ_B and Eq. (4b)] and hence $\sigma_{eff}(\tau)$ by inserting various $g(\Delta v_z)$ in Eq. (3b). For $g(\Delta v_z) = (\pi u_0)^{-1/2} \exp(-\Delta v_z^2/u_0^2)$, we obtain the solid lines shown in Fig. 1. The least-squares-fit values of the free parameters σ_v^0 and u_0 are shown in Table I. The quality of the fits is quite good. A Lorentzian kernel of the form $g(\Delta v_z) = (u_0/\pi)/(u_0^2 + \Delta v_z^2)$ [but with $g(\Delta v_z) = 0$ for $\Delta v_z \gg u_0$] produces a better fit to $\sigma_v(\tau)$ for Li-He collisions, but a poorer fit for the other perturbers. These results, as well as the ratio $\sigma_B/\sigma_v^0 \approx 1.0$ observed in our experiment, are in qualitative agreement with a theory based on a quantum mechanical hard-sphere model of collisions.

The derived values of u_0 and σ_v^0 depend somewhat on our choice for $g(\Delta v_z)$. We note, however, that our measurements are sensitive to all velocity changes $\Delta v_z > \Delta v_z^{min} \equiv 1/k\tau_{max}$ (τ_{max} is our

TABLE I. Various cross sections involved in this work (see text). The G and L in parentheses indicate results obtained with a Gaussian and a Lorentzian collision kernel, respectively.

Perturber	σ_B [a] (Å^2)	σ_B [b,c] (Å^2)	σ_v^0 (G) (Å^2)	σ_v^0 (L) (Å^2)	u_0 (G) (cm/sec)	u_0 (L) (cm/sec)	σ_a [d] (Å^2)	σ_t (G) (Å^2)	σ_t (L) (Å^2)
He	99	86(3)	34	49	1060	247	130	133	148
Ne	101	104(4)	47	90	1140	187	150	149	191
Ar	181	164(8)	145	207	1400	340	400	326	388
Kr	206	211(9)	170	236	1320	335	440	376	442
Xe	233	265(10)	200	289	1320	315	510	433	522

[a] This work.
[b] Scaled from 628 to 525 K according to $(1/T)^{1/5}$.
[c] Ref. 10.
[d] Ref. 11.

904

maximum pulse separation). Our value for Δv_z^{min} is less than the characteristic diffractive velocity change $v_D \equiv v_r \lambda_B / \sqrt{\sigma_t}$. The fact that the scattering is diffractive in nature restricts our choice of $g(\Delta v_z)$ to functions which are relatively flat in the region $\Delta v_z \lesssim v_D$. With this restriction, we do not expect our derived value of σ_v^0 to differ greatly from those shown in Table I. If a heavier radiator is used, the corresponding values of $u_0 \approx v_D$ could be smaller and the region in which velocity changes are seen (i.e., $ku_0 \tau \gtrsim 1$) might no longer be accessible. It is perhaps for this reason that velocity-changing effects were not seen in a coherent-transient experiment with I_2 as the radiator.[12]

Recent treatments of radiator-perturber scattering have shown that the net polarization in a medium obeys a quantum mechanical transport equation.[13,14] This equation contains a loss term whose real part, which corresponds to the time rate of change of the polarization's magnitude, is given by $m v_r (\sigma_a + \sigma_b)/2$, where σ_a (σ_b) corresponds to the cross section for ground-state (excited-state) radiator-perturber scattering. Since this is the only term important to the long-time behavior of the photon echo, we equate our σ_t with $(\sigma_a + \sigma_b)/2$.

The cross section σ_a has been measured by atomic-beam techniques.[11] In Table I, we list, for each perturber, the velocity-selected value of σ_a obtained at the velocity v_r. Our values of $\sigma_t = \sigma_B + \sigma_v^0$, based on both Lorentzian and Gaussian kernels, are also presented. Since the long-range part of the potential should, to a reasonable approximation, determine the magnitude of the scattering cross section, we expect (at least for Ar, Kr, and Xe) that $\sigma_b / \sigma_a \approx (C_6^b / C_6^a)^{2/5}$, where C_6^b (C_6^a) is the coefficient of the Van der Waals portion of the potential. Assuming that $C_6 = 2\epsilon r_m^6$, where ϵ is the potential well depth and r_m is the internuclear separation at which the potential is minimum [as is true of a Lennard-Jones (6, 12) potential], we can use the potential calculation of Baylis[15] to find that $(C_6^b / C_6^a)^{2/5}$ falls between 1 and 1.6, depending on the perturber and which of the possible excited-state potentials is considered. This implies that σ_t should be between 1 and 1.3 times σ_a. Our data are reasonably consistent with this result.

Our results clearly demonstrate the role played by velocity-changing collisions. Their contribution to the echo signal underlines the importance of quantum mechanical scattering effects in collisions undergone by an optical dipole.

[(a)]Present address: Molecular Physics Laboratory, SRI International, Menlo Park, Cal. 94025.

[1]In the case of transitions between similar levels (e.g., the vibrational-rotational levels of a single molecular electronic state) collisional phase changes do not occur, and collisional velocity changes produce marked effects. See R. H. Dicke, Phys. Rev. 89, 472 (1953); C. J. Borde, in Laser Spectroscopy III, edited by J. L. Hall and J. L. Carssten (Springer-Verlag, Berlin, 1977), p. 121.

[2]P. R. Berman, Phys. Rep. 43, 101 (1978), and Adv. At. Mol. Phys. 13, 57 (1977), and references therein.

[3]The first evidence of collisional velocity changes affecting an optical radiator involving dissimilar states was reported by T. W. Mossberg, R. Kachru, and S. R. Hartmann, Phys. Rev. Lett. 44, 73 (1980).

[4]A method of observing the effect of velocity-changing collisions on the line shape of optical transitions involving three coupled energy levels has recently been proposed [J. L. LeGouët and P. R. Berman, Phys. Rev. A 17, 52 (1978)]; however, experiments have thus far failed to detect the effect [P. Cahuzac, J. L. LeGouët, P. E. Toschek, and R. Vetter, Appl. Phys. 20, 83 (1979)].

[5]Two recent reviews with additional references are W. R. Hindmarsh and J. M. Farr, Prog. Quantum Electron. 2, 139 (1972); E. L. Lewis, Phys. Rep. 58, 1 (1980).

[6]S. Avrillier, C. J. Borde, J. Picant, and N. Tran Minh, in Spectral Line Shapes, edited by B. Wende (Walter de Gruyter, Berlin, 1981).

[7]The power of the photon-echo technique in the study of collisional velocity changes (in the absence of phase-changing effects) was demonstrated by P. R. Berman, J. M. Levy, and R. G. Brewer, Phys. Rev. A 11, 1668 (1975). See also B. Comaskey, R. E. Scotti, and R. L. Shoemaker, Opt. Lett. 6, 45 (1981).

[8]R. Kachru, T. W. Mossberg, and S. R. Hartmann, J. Phys. B 13, L363 (1980).

[9]A. Flusberg, Opt. Commun. 29, 123 (1979).

[10]N. Lwin, thesis, University of Newcastle upon Tyne, 1976 (unpublished), as reported by Lewis, Ref. 5.

[11]P. Dehmer and L. Wharton, J. Chem. Phys. 57, 4821 (1972).

[12]R. G. Brewer and A. Z. Genack, Phys. Rev. Lett. 36, 959 (1976); R. G. Brewer and S. S. Kano, in Nonlinear Behavior of Molecules, Atoms and Ions in Electric, Magnetic or Electromagnetic Fields, edited by L. Neal (Elsevier, Amsterdam, 1979), p. 45.

[13]P. R. Berman, Phys. Rev. A 5, 927 (1972).

[14]G. Nienhuis, J. Quant. Spectrosc. Radiat. Transfer 20, 275 (1978).

[15]W. E. Baylis, J. Chem. Phys. 51, 2665 (1969).

Noble Gas Induced Relaxation of the Li 3S-3P Transition Spanning the Short Term Impact Regime to the Long Term Asymptotic Regime

T.W. Mossberg*, R. Kachru+, T.J. Chen, S.R. Hartmann

Columbia Radiation Laboratory, Department of Physics, Columbia University
538 W. 120th. St., New York, NY 10027, USA, and

P.R. Berman

Department of Physics, New York University, 4 Washington Place
New York, NY 10003, USA

Photon echoes have a Doppler free character which allows one to study relaxation processes which would otherwise be hidden in the inhomogeniously broadened spectral profile. It has recently been shown, for example, that contrary to expection, a radiating atom in a linear superposition of dissimilar electronic states can undergo identifiable velocity changing collisions [1]. Studies of this nature require an examination of the sub-Doppler region of the spectral line shape. The effect manifests itself, in the case of photon echoes, in a dependence of the effective relaxation cross section σ_{eff} on the excitation pulse separation τ. In this paper we report measurements in Li vapor where τ can be increased into the regime where σ_{eff} once again becomes independent of τ. In the limit $\tau = 0$ we measure σ_0 which is the phase changing cross section as calculated by Baranger [2] while in the large τ limit we measure σ_∞ the average total scattering cross section of the ground and the excited states. Our data at intermediate values of τ is used to determine the form of the scattering kernel and the average velocity change per collision. These measurements are for the 2S-2P superposition states in atomic Li perturbed by each of the noble gases. For He perturbers the scattering kernel is found to be Lorentzian, for the other perturbers it is Gaussian.

We use a N_2 laser pumped dye laser to generate a 4.5 nsec light pulse at the 6708 Å 2S-2P$_{1/2}$ transition of ^{7}Li. The pulse which has a 6 GHz spectral width is attenuated, split, delayed an amount τ, recombined, and directed into a cell, whose effective length is 10 cm, at 525 $\pm$ 15°K containing the Li vapor (at ~10^{-6} torr). For short values of τ the polarizations of the photon echo excitation pulses were orthogonal in order to reduce the effects of detector saturation which arose because of the non instantaneous response the Pockels cell shutters used for their protection.

For a superposition state relaxing at an effective rate $\Gamma_{eff} = nv\,\sigma_{eff}$ where n is the perturber density, v is the average relative velocity of the collision partners and σ_{eff} is an effective cross section, the corresponding echo intensity will decay according to

$$I = I_0 \exp(-4\Gamma_{eff}\tau) \tag{1}$$

and since Γ_{eff} varies linearly with perturber pressure P

$$I(P) = I(0)\exp(-\beta P) \tag{2}$$

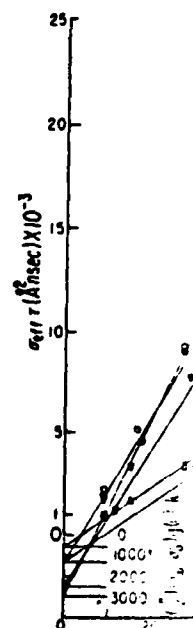* Present Address: Dept. of Physics, Harvard University, Cambridge, MA 02138, USA
+ Present Address: Molecular Physics Lab., SRI International, Menlo Park

where the const.
perturber and t-
values of τ by ~
gas pressure. T

$$\sigma_{eff} = \Gamma_{eff}/nv$$

In fig. (1) w
σ_{eff} as a functi
of the Li atom w.
to a phase change
collisions occur
lisions have a d
σ_{eff} on τ. Our
creases at a lar;
levels off consi.

Echoes in the
volume large cor
any atom experie-
preciable fracti
have taken in th
reinforce the e:
increases and th
proceeds up to a

where the constant β, which we measure directly, is characteristic of the perturber and the collision process. We determine β at several discrete values of τ by measuring the echo intensity as a function of the perturber gas pressure. The value of σ_{eff} is obtained from

$$\sigma_{eff} = \Gamma_{eff}/nv = \beta P/4nv\tau. \qquad (3)$$

In fig. (1) we summarize our work by plotting all measured values of σ_{eff} as a function of τ. A dependence on τ arises because each collision of the Li atom with a perturber gives rise to a velocity change in addition to a phase change of the Li superposition state. If only phase changing collisions occured σ_{eff} would be independent of τ. Velocity changing collisions have a delayed effect which manifests itself in a dependence of σ_{eff} on τ. Our data indicates that at the shortest values of τ σ_{eff} increases at a large and relatively constant rate while at higher τ it levels off considerably.

Echoes in the optical regime (photon echoes) are generally formed in a volume large compared to the wavelength of the optical transition. Thus any atom experiencing a velocity change sufficient to displace it an appreciable fraction of a wavelength from the position it would otherwise have taken in the phased array which radiates the echo will not necessarily reinforce the echo signal. As τ is increased the resulting displacement increases and the effect of a particular velocity change is enhanced. This proceeds up to a point that being when τ is so large that all atoms experi-
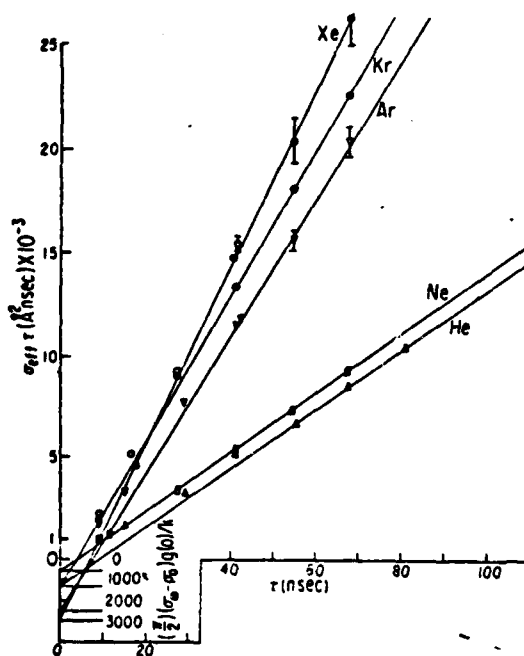

Fig. 1 Plot of $\sigma_{eff}(\tau)$ versus τ. Error bars represent statistical uncertainty.

encing a velocity change are effectively eliminated from the echo formation processes. The data of fig. (1) at large τ shows this effect clearly in the weakening dependence of σ_{eff} on τ.

In what may be called the collision kernel approximation Flusberg [3] has shown that σ_{eff} may be expressed as

$$\sigma_{eff} = \sigma_0 + \sigma_v \left[1-(1/\tau) \int_0^\tau dt \; \tilde{g}(kt)\right] \qquad (4)$$

where $\sigma_0(\sigma_v)$ is the phase changing (velocity changing) cross section and

$$g(kt) = \int_{-\infty}^{\infty} \exp(ikt\Delta v) \; g(\Delta v) \; d(\Delta v). \qquad (5)$$

The collision kernel $g(\Delta v)$ gives the probability of a particular change Δv in the component of the velocity along the laser pulse direction. For $k\tau \ll 1$

$$\sigma_{eff} = \sigma_0 + \sigma_v \frac{1}{6} k^2\tau^2 \langle\Delta v^2\rangle \qquad (6)$$

where $\langle\Delta v^2\rangle$ is the second moment of the collision kernel. For $k\tau \gg 1$

$$\sigma_{eff} = \sigma_0 + \sigma_v \left[1 - \pi g(0)/2k\tau\right] \qquad (7)$$

where $g(0)$ is the amplitude of the collision kernel at $\Delta v = 0$.

Our data at short τ does not fit (6) well, shorter excitation pulses would have been required to enter the regime where this approximation is valid. Our data does suffice however to use (6) to estimate σ_0 and we find that except for He we agree to within a few percent with measurements of σ_0 made from line broadening experiments [4]. Our estimate of σ_0 for He runs ~10% high.

The solid line curves of fig. (1) were obtained using an explicit form of the collision kernel. For all perturbers except He we have used a Gaussian kernel

$$g(\Delta v) = (1/\sqrt{\pi} \; u_0)\exp(-\Delta v^2/u_0^2) \qquad (8)$$

while for He we have used the Lorentzian kernel

$$g(\Delta v) = (u_0/\pi)/(u_0^2 + \Delta v^2). \qquad (9)$$

We vary u_0 and σ_v to obtain the best fit. All relevant parameters are tabulated in table I.
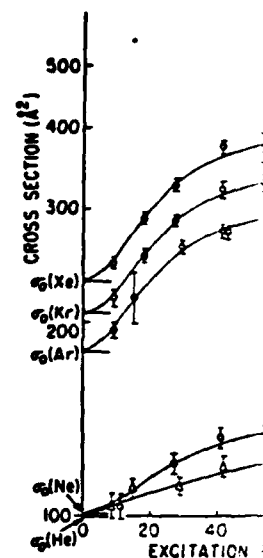
Table 1

Perturber	σ_0	σ_v	$\sigma_\infty = \sigma_0+\sigma_v$	u_0	$\sigma_\infty \; \sigma_0+\sigma_v$ (from fig.2)
He	99 Å^2	49 Å^2	148 Å^2	247 cm/sec	146
Ne	101	47	148	1140	146
Ar	181	145	326	1400	338
Kr	206	170	376	1320	356
Xe	233	200	434	1320	434

An alternative r-- a function of τ, see

$$\sigma_{eff} = (\sigma_0 + \sigma_v)\tau -$$

and we should obtain yields $\sigma_0 + \sigma_v = \sigma_\infty$ with $g(0)$. The valu calculated from the

REFERENCE

1. T.W. Mossberg, R.
2. Michel Baranger,
3. A. Flusberg, Opt.
4. N. Lwin, Thesis
   by E. L. Lewis,

ormation
ly in

g [3].

(4)

n and

(5)

ange Δv
For

(6)

> 1

(7)

lses
on is
ve
rements
) for

t form
a

(8)

(9)

:s are

fig.2)

An alternative proceedure for presenting our data is to plot $\sigma_{eff}\tau$ as a function of τ, see fig. (2), in which case we expect that from (7)

$$\sigma_{eff} = (\sigma_0 + \sigma_v)\tau - \sigma_v \, \pi g(0)/2k \qquad (10)$$

and we should obtain an assumptotic fit to a straight line whose slope yields $\sigma_0 + \sigma_v = \sigma_\infty$ and whose negative intercept yields the product of σ_v with $g(0)$. The values of $\sigma_0 + \sigma_v = \sigma_\infty$ so obtained are compared with that calculated from the data of table I.
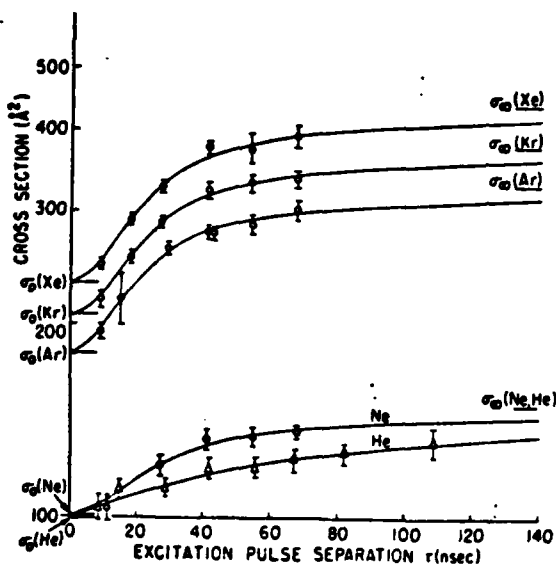
Fig. 2 $\sigma_{eff}\tau$ plotted versus τ.

REFERENCE

1. T.W. Mossberg, R. Kachru, and S.R. Hartmann, Phys. Rev. Lett. 44, 73 (1980).
2. Michel Baranger, Physics Rev. 111, 481 (1958).
3. A. Flusberg, Opt. Commun. 29, 123 (1979).
4. N. Lwin, Thesis (University of Newcastle upon Tyne) 1976, as reported by E. L. Lewis, Phys. Rep. 59, 1 (1980).

Collision kernels and laser spectroscopy

P. R. Berman

Physics Department, New York University, 4 Washington Place, New York, New York 10003

T. W. Mossberg

Department of Physics, Harvard University, Cambridge, Massachusetts 02138

S. R. Hartmann

Columbia Radiation Laboratory, Department of Physics, Columbia University, New York, New York 10027

(Received 24 August 1981)

Collisional processes occurring within an atomic vapor can be conveniently described in terms of collision kernels. The population kernel $W_{ii}(\vec{v}' \rightarrow \vec{v})$ gives the probability density per unit time that an "active" atom in state i undergoes a collision with a perturber that changes the active atom's velocity from $\vec{v}'$ to $\vec{v}$. For active atoms in a linear superposition of states i and j, there is an analogous *coherence kernel* $W_{ij}(\vec{v}' \rightarrow \vec{v})$ $(i \neq j)$ reflecting the effects of collisions on the off-diagonal density-matrix element ρ_{ij}. In this work, we discuss the general properties of the collision kernels which characterize a two-level active atom which, owing to the action of a radiation field, is in a linear superposition of its two levels. Using arguments based on the uncertainty principle, we show that collisions can be divided roughly into the following two categories: (1) collisions having impact parameters less than some characteristic radius which may be described classically and (2) collisions having impact parameters larger than this characteristic radius which give rise to diffractive scattering and must be treated using a quantum-mechanical theory. For the population kernels, collisions of type (1) can lead to a large-angle scattering component, while those of type (2) lead to a small-angle (diffractive) scattering component. For the coherence kernel, however, assuming that the collisional interaction for states i and j differ appreciably, only collisions of type (2) contribute, and the coherence kernel contains a small-angle scattering component only. The absence of a large-angle scattering component in the coherence kernel is linked to a collision-induced spatial separation of the trajectories associated with states i and j. Interestingly enough, the width of the diffractive kernel, as measured in the laboratory frame, is found to be insensitive to the perturber to active-atom mass ratio. To illustrate these features, a specific calculation of the kernels is carried out using a hard-sphere model for the scattering. The relationship of the present description of collisions to that of traditional pressure-broadening theory in which trajectory separation effects are ignored is discussed. It is explained why traditional pressure-broadening theory correctly describes collision effects in linear spectroscopy, but fails to provide an adequate description of some saturation spectroscopy and photon-echo experiments in which velocity-changing collisions associated with the coherence kernel play a significant role. An expression for the collisionally modified photon-echo amplitude is derived which clearly displays the role played by velocity-changing collisions associated with the coherence kernel.

I. INTRODUCTION

Emission and absorption spectra have traditionally provided the blueprints from which most of our data concerning the energy-level structure of atoms and molecules could be derived. The precision of this data is limited by one's inability to resolve structure that lies within the widths of the various spectral lines. In low-density atomic vapors, the linewidth is determined mainly by the Doppler effect (i.e., atoms moving at different velocities absorb or emit Doppler-shifted frequencies), although both the natural widths of the levels and collisions within the vapor contribute somewhat. One of the most exciting achievements in spectroscopy over the last decade has been the

development of methods wherein the Doppler width is partially or totally suppressed. The development of these "Doppler-free" methods in both time (e.g., photon-echo) and frequency (e.g., saturation spectroscopy) domain experiments has been made possible in large part by the advances in laser technology. With the removal of the Doppler broadening, the line shapes increasingly reflect the effects of collisional processes occurring in the vapor. It is not surprising, therefore, that the progress in laser spectroscopy has been accompanied by a renewed interest in understanding (1) the manner in which collisions modify the line shapes and (2) the extent to which laser spectroscopy can be used as a probe of collisional processes in vapors.

In order to illustrate the role played by collisions in atomic spectroscopy, we consider an ensemble of two-level "active" atoms immersed in a low-density vapor of "perturber" atoms. The levels of each active atom (labeled 1 and 2) are coupled by a radiation field. The active atoms undergo binary collisions with the perturbers (active-atom—active-atom collisions are neglected). The collisions are assumed to be adiabatic in the sense that they possess insufficient energy to induce transitions between the active-atom's levels. Under these conditions, one may seek to determine the manner in which these elastic collisions affect the physical observables associated with the active atoms.

The problem can be approached by investigating in detail a collision between an active atom and a perturber (Fig. 1). The active atom, which is prepared in a linear superposition of its two levels by a radiation field, generally experiences a collisional interaction which is different for states 1 and 2. From a classical viewpoint, the collisional interaction (acting analogously to a Stern-Gerlach magnet) separates the populations (conveniently represented by density matrix elements ρ_{11} and ρ_{22}) along the distinct trajectories shown in Fig. 1. Since the populations scatter independently, the

FIG. 1. Picture of a collision between an active atom A and stationary perturber P. There is no obvious classical trajectory to associate with the atomic "coherence" ρ_{12}.

possibility of distinct post-collision trajectories poses no conceptual difficulties. The scattering for each state i ($i = 1,2$) is determined by the differential cross section $\sigma_i(\theta) = |f_i(\theta)|^2$ for the elastic scattering of an active atom in state i by a perturber atom.[1]

The populations ρ_{ii}, however, are not the only relevant quantities in considering the interaction of radiation with matter. The polarization of the vapor directly influences its absorptive and dispersive properties. If the dipole moment operator of our two-level atom is $\hat{\mu}$ and if states 1 and 2 have opposite parity, then the polarization of the system is proportional to $\langle \hat{\mu} \rangle = \vec{\mu}_{12}\rho_{21} + \vec{\mu}_{21}\rho_{12}$, where $\vec{\mu}_{ij}$ is the ij matrix element of $\hat{\mu}$ and ρ_{ij} is the ij density-matrix element (i.e., $\rho_{ij} = a_i a_j^*$, where a_i is the state i probability amplitude). Consequently, the absorptive and dispersive properties of the medium are influenced by collisional perturbations of the "atomic coherence" ρ_{12} (or ρ_{21}).

Collisions appear to affect ρ_{12} in a particularly simple way. Since the collision shown in Fig. 1 leads to a spatial separation of states 1 and 2, ρ_{12} vanishes following the collision. Thus, using a classical picture of a collision, one is led to distinct trajectories for the populations ρ_{11} and ρ_{22} and to a vanishing of the coherence ρ_{12}.

While the classical picture of a collision given in Fig. 1 is useful in providing some insight into the effects of collisions on the various density-matrix elements, it is not sufficient to obtain a total picture of the scattering. Using arguments based on the uncertainty principle, we will show that, within certain limits, the classical picture is valid for small-impact parameter collisions. However, for large-impact parameter collisions, the quantum theory must be used. Quantum-mechanical effects give rise to diffractive scattering contributions for the populations and to nonvanishing values of ρ_{12} following a collision.

The discussion of a single collision given above would be appropriate to a crossed atomic-beam experiment in which the center-of-mass energy is constant for all collisions. In an atomic vapor, however, the perturbers have some velocity distribution which must be averaged over. For the vapor, the quantity of interest is the collision kernel $W_{ii}(\vec{v}' \rightarrow \vec{v})$ giving the probability density per unit time that an active atom in state i changes its velocity from $\vec{v}'$ to $\vec{v}$ in undergoing a collision with a perturber. The corresponding rate for such collisions is denoted by $\Gamma_i(\vec{v}')$. The kernel is proportional to the differential scattering cross section
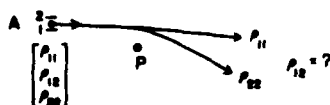
averaged over the perturber velocity distribution consistent with conservation of momentum and energy. For off-diagonal density-matrix elements, one can also define a "kernel" $W_{12}(\vec{v}' \to \vec{v})$ and "rate" $\Gamma_{12}^{vc}(\vec{v}')$, although these quantities, now dependent on $f_1 f_2^*$, need no longer be positive definite. Formal expressions for $W_{12}(\vec{v}' \to \vec{v})$ and $\Gamma_{12}^{vc}(\vec{v}')$ have been given,[2,3] but there has been, with two recent exceptions,[4,5] little progress in obtaining a satisfactory physical interpretation or actual evaluation of the "coherence kernel" $W_{12}(\vec{v}' \to \vec{v})$.[6] It is the purpose of this paper to provide a simple physical picture of the scattering process that leads to an intuitive understanding of the nature of $W_{12}(\vec{v}' \to \vec{v})$.

It has already been noted that collisional perturbations of ρ_{12} affect the absorptive properties of a medium. Thus, one might imagine that collision induced modifications of absorption or emission line shapes are intimately connected with the coherence kernel $W_{12}(\vec{v}' \to \vec{v})$. Since $W_{12}(\vec{v}' \to \vec{v})$ is strongly influenced by the trajectory effects shown in Fig. 1, it appears that such trajectory effects are critical in calculating the effects of collisions on spectral line shapes. However, it is well known that traditional theories of pressure broadening,[7] which totally ignore trajectory effects of the type shown in Fig. 1 and consider collisions to produce only phase changes in ρ_{12}, have been very successful in explaining most spectral profiles. How, one may ask, can a theory that ignores trajectory separation effects still produce correct results? It is a second purpose of this paper to provide an answer to this question.

[There *is* a range of experimental situations where trajectory effects are known to be important.[8] In such experiments, however, the states involved in the transition (usually vibrational, rotational, or rf transitions) experience nearly identical collisional interactions and, consequently, follow the *same* collisional trajectory. Trajectory effects lead to a *narrowing* of spectral lines in linear spectroscopy and to a signal with a unique signature in photon-echo experiments.[9] In this paper, however, we shall be concerned only with situations where the collisional interaction for states 1 and 2 differs somewhat (the precise conditions are given below) as is generally the case for electronic transitions. Only recently has an experiment been performed that clearly indicates the importance of trajectory effects for an electronic transition.[10,11]]

In Sec. II, the uncertainty principle is used to obtain a simple physical picture of the scattering.

It is shown that collisions can be divided roughly into two regions. For small-impact parameter collisions, the scattering can be given a classical interpretation; the distinct trajectories for states 1 and 2 shown in Fig. 1 then lead to a vanishing of ρ_{12} following the collision. On the other hand, for large-impact parameter collisions (leading to diffractive scattering), the classical picture fails and a quantum-mechanical calculation of ρ_{12} is needed. A specific evaluation of the coherence kernel and rates is made in Sec. III using a model potential based on hard-sphere scattering. The various features discussed in Sec. II are illustrated by this example. In Sec. IV, the role that the coherence kernel plays in affecting various spectroscopic line shapes is discussed. The reason for the success of traditional pressure-broadening theories is explained in this section. Finally, a calculation of a collisionally modified photon-echo signal is given in Sec. V. The role played by trajectory effects is clearly reflected in the expression for the echo amplitude.

For simplicity, the calculations carried out in Secs. II – V are made assuming a high ratio of perturber to active atom mass. In Appendix A, the calculations are extended to allow for an arbitrary mass ratio. It is shown that *the width of the coherence kernel is effectively independent of the ratio of perturber to active-atom mass* and depends only on the active-atom mass and collision cross section.

It is implicitly assumed throughout this work that an *impact approximation* is valid. All relevant frequencies (e.g., collision rates, atom-field detunings, Rabi frequencies) are assumed to be small in comparison with the inverse duration time of a collision. The validity of the impact approximation implies that only binary collisions need be considered and that these collisions produce a time rate of change for ρ_{ij} which is independent of other contributions to $\partial \rho_{ij}/\partial t$.

II. QUALITATIVE PICTURE OF SCATTERING

Before discussing the effects of collisions on ρ_{12} and the corresponding coherence kernel $W_{12}(\vec{v}' \to \vec{v})$, it is instructive to review some aspects of elastic scattering theory. Thus, we shall first consider the elastic scattering of an active atom in state *l*. To simplify the discussion we take the perturber as stationary (ratio of perturber to active-atom mass much greater than unity), but the results of this section are perfectly general if all vari-

ables are taken as those in the center-of-mass system. Moreover, we neglect such effects as orbiting, rainbow, and glory scattering which, although important in certain cases,[12] are not particularly relevent to the subject matter at hand.

A. Population kernel

The regions of validity of a classical picture of scattering can be established by using the uncertainty principle. Consider a collision characterized by an impact parameter b leading to scattering at an angle θ. For a classical picture to be valid, one must have

$$\Delta b < b, \quad \Delta\theta < \theta , \qquad (1)$$

where Δb and $\Delta\theta$ are the uncertainties in b and θ, respectively. On the other hand, it follows from the uncertainty principle that $\Delta p_t \Delta b \geq \hbar$, where Δp_t is the uncertainty in the transverse component of the active atom's momentum. Since $\Delta p_t \equiv m \Delta v_t \approx m v \Delta\theta = \hbar k \Delta\theta$ [m is the active-atom mass, $k \equiv m v / \hbar$, and v is the active-atom speed], the uncertainty principle requires that

$$k \Delta b \Delta\theta \gtrsim 1 . \qquad (2)$$

Setting $\Delta b = b$ and $\Delta\theta = \theta$, one sees that conditions (1) and (2) can both be satisfied provided

$$\theta \gg 1/(kb) . \qquad (3)$$

Let b_i represent some characteristic range for scattering by the perturber of active atoms in the state i. For typical interaction potentials, it follows that a classical description of the scattering is valid if

$$\theta \gg \theta_i^d \equiv 1/(kb_i) . \qquad (4)$$

In fact, it is well known[12] that the quantum-mechanical expression for the differential scattering cross section reduces to the corresponding classical one if condition (4) is satisfied (neglecting any effects of rainbow scattering). Clearly, Eq. (4) is meaningful only if $kb_i > 1$.

On th ϵ other hand, for $\theta < \theta_i^d$ one can no longer expect the classical picture of scattering to remain appropriate. In an atomic vapor, k is typically of order 10^9 cm^{-1} and b_i is of order 10 Å so that $\theta_i^d \approx 0.01 \ll 1$. In effect, the angle θ_i^d separates the scattering into two distinct regions. For $\theta \gg \theta_i^d$ (corresponding to collisions having $b < b_i$), the scattering may be described classically. For $\theta \ll \theta_i^d$ (corresponding to collisions having $b > b_i$)

the scattering may be considered diffractive in nature and must be described quantum mechanically. [For other than purely repulsive potentials, the $\theta < \theta_i^d$ region also has (relatively weak) contributions from some collisions having $b < b_i$ ("glory scattering").[12] As noted earlier, effects such as orbiting or rainbow and glory scattering are neglected in this work.]

The above results imply that the collision kernel for elastic scattering in state i can be written as the sum of two terms corresponding to classical large-angle scattering and quantum-mechanical diffractive scattering, respectively.[13] There is recent experimental evidence that supports this conclusion.[14]

B. Coherence kernel

We are now in a position to discuss the effects of a collision on ρ_{12}. The interaction potential is assumed to be state dependent and it is further assumed that there are two characteristic lengths b_1 and b_2 associated with the scattering for states 1 and 2, respectively. For the sake of definiteness, we take $b_2 > b_1$. The question to be answered is the following: For what scattering angles, if any, may a classical picture be used to describe the effects of the scattering on ρ_{12}?

The question must first be clarified since the criterion we shall use to judge the validity of a classical picture is different than that used in the case of single-state elastic scattering. Scattering for ρ_{12} will be classified as "classical" if the trajectories associated with the elastic scattering from states 1 and 2 are distinct and nonoverlapping (see Fig. 1). A consequence of this classification is that ρ_{12} is zero following any classically described collision, since the spatial overlap of states 1 and 2 vanishes as a result of the collision.

An uncertainty principle argument can once again be used to obtain the classical region. Let θ_1 and θ_2 be the scattering angles associated with states 1 and 2 for a collision having impact parameter b. The criterion for a classical collision is then

$$\Delta b < b; \quad \Delta\theta < |\theta_2 - \theta_1| , \qquad (5)$$

where $\Delta\theta$ is the uncertainty in θ for a collision with impact parameter b. The restriction imposed by the uncertainty principle is still given by Eq. (2), which may be combined with Eq. (5) to give

$$|\theta_2 - \theta_1| > 1/(kb) \qquad (6)$$

as the distinct trajectory condition.

Equation (6) can be given a very interesting interpretation in terms of a parameter appearing in conventional theories of pressure broadening. An active atom in state i sees a potential $V(r)$ produced by a perturber, where r is the active-atom—perturber separation. The scattering angle θ_i, calculated assuming small-angle scattering, is

$$\theta_i = v_t/v \simeq -\frac{1}{\hbar k} \int \frac{\partial V_i(r)}{\partial b} dt , \qquad (7)$$

where the integral is along the time parameterized collision trajectory $r(b,v,t)$. Setting $\partial V_i/\partial b = -\kappa b^{-1} V_i$ (κ is the constant of order unity) and substituting Eq. (7) into (6), one obtains the distinct trajectory condition[15]

$$\frac{1}{\hbar} \left| \int [V_2(b,t) - V_1(b,t)] dt \right| > \kappa^{-1} \simeq 1 . \qquad (8)$$

The value of b, denoted by b_W, for which the left-hand side of Eq. (8) equals unity is the Weisskopf radius of pressure-broadening theory.[7] Equation (8) implies that the maximum impact parameter for which the distinct trajectory condition holds is $b \simeq b_W$; consequently, Eq. (6) is valid only for

$$b < b_W \qquad (9)$$

(distinct trajectory condition). The consistency of the entire approach requires that

$$kb_W \gg 1 . \qquad (10)$$

One is led to the following result. For scattering angles corresponding to collisions having an impact parameter $b < b_W$, a classical picture is possible provided that Eq. (10) is valid. These classical collisions result in a complete destruction of ρ_{12} owing to the separation of trajectories for states 1 and 2. For diffractive scattering, corresponding to collisions having impact parameters $b > b_W$, a quantum-mechanical calculation is needed. In this case, ρ_{12} does not vanish following the collision (see Fig. 2). [Notice that the impact parameter separating the classical and quantum scattering domains differs somewhat for the populations and the coherences. The b_i associated with the populations may be calculated using Eqs. (3), (4), and (7).]

If $kb_W < 1$, a quantum-mechanical approach is needed for all scattering angles. In this limit the scattering is almost identical for states 1 and 2 ($b_W = 0$ for state-independent scattering) and there is non-negligible spatial overlap of the state 1 and 2 trajectories. In this work, we assume that the interaction potentials for the two levels differ sufficiently to insure that Eq. (10) holds for most atoms
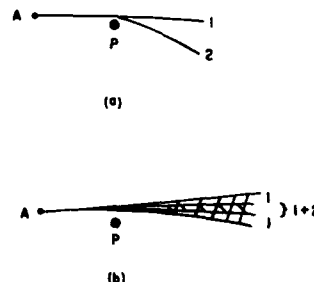

(a)

(b)

FIG. 2. Effects of collisions on ρ_{12} can be *roughly* visualized as shown in this figure when $kb_W = b_W/\lambdabar \gg 1$. For collisions having impact parameter $b < b_W$ (a), the trajectories for states 1 and 2 are distinct and nonoverlapping following the collision, leading to a destruction of ρ_{12}. For collisions with $b > b_W$ (b), scattering is diffractive in nature. The overlap of the diffractive scattering cones for states 1 and 2 leads to nondestructive velocity-changing collisions associated with ρ_{12}.

in the vapor. Typically $b_W \approx 5-10$ Å for electronic transitions so that $kb_W \approx 100 \gg 1$.

The qualitative structure of the coherence kernel $W_{12}(\vec{v}' \rightarrow \vec{v})$ is now evident. In contrast to the population kernels, the coherence kernel *vanishes* in the large-angle scattering region owing to the separation of trajectory effects. For diffractive scattering, a quantum-mechanical calculation of $W_{12}(\vec{v}' \rightarrow \vec{v})$ is needed. Thus, the coherence kernel is effectively nonzero for diffractive scattering only. The consequences of this conclusion are discussed in Sec. IV.

In this section, a qualitative picture of the scattering process was given. In Sec. III, a coherence kernel is explicitly calculated assuming a simple form for the interaction potential. The calculation serves to illustrate the various features discussed in this section. The reader not interested in the details of the model-potential calculation can proceed to Sec. IV without loss of continuity.

III. MODEL-POTENTIAL CALCULATION

The qualitative properties of the collision kernels discussed in Sec. II are relatively insensitive to the form of the interaction potential. Therefore, for the sake of simplicity, we assume that the state i scattering potential can be represented as an impenetrable sphere of radius b_i (with $b_2 > b_1$). It should be noted, however, that the calculations presented below may easily be generalized to spherically symmetric potentials of an arbitrary nature.

To further simplify the calculations, we assume that the perturber is stationary, although a generalization of the results of this section to allow for an arbitrary active-atom-to-perturber-mass ratio is given in Appendix A. This section is organized as follows: A. The scattering amplitude for hard-sphere scattering is given and an exponential approximation to it, valid for diffractive scattering, is obtained. B. The collision kernel $W_{ll}(\vec{v}' \rightarrow \vec{v})$ and the rate $\Gamma_l(\vec{v})$ for this scattering of populations are calculated. C. The coherence kernel $W_{12}(\vec{v}' \rightarrow \vec{v})$ and the rate $\Gamma_{12}^{vc}(\vec{v})$ are evaluated. D. The coherence kernel and the rate are averaged over a transverse velocity distribution to obtain a one-dimensional kernel $W_{12}(\vec{v}'_z \rightarrow \vec{v}_z)$ and rate $\Gamma_{12}^{vc}(v_z)$ that appear in theories of laser spectroscopy.

A. Scattering amplitude

The scattering amplitude for elastic scattering of an active atom in state j by the perturber is

$$f_j(\theta) = \frac{1}{ik} \sum_{l=0}^{\infty} (l + \tfrac{1}{2})(e^{2i\eta_l^j} - 1) P_l(\cos\theta) , \quad (11)$$

where the η_l^j are the elastic scattering phase shifts. For hard-sphere scattering, the η_l^j are equal to

$$\tan^{-1}[j_l(kb_j)/n_l(kb_j)] ,$$

where j_l and n_l are spherical Bessel and Neumann functions, respectively.

If $\theta \gg (1/kb_j)^{1/3}$ (classical region), a standard calculation using the method of stationary phase gives[12,16]

$$f_j(\theta) = -(b_j/2)e^{i\phi_j(\theta)}, \quad \theta \gg (kb_j)^{-1/3}$$

where
                                                              (12a)

$$\phi_j(\theta) = -2kb_j \sin\frac{\theta}{2} . \quad (12b)$$

The differential cross section $|f_j(\theta)|^2 = b_j^2/4$ is just the classical result for hard-sphere scattering. Thus, for $\theta \gg (kb_j)^{-1/3}$, one regains the classical result, in agreement with the qualitative discussion of Sec. II.

For small-angle scattering $\theta \ll 1$, one can replace $P_l(\cos\theta)$ by the zero-order Bessel function $J_0((l + \tfrac{1}{2})\theta)$.[17] With this substitution, Eq. (11) becomes

$$f_j(\theta) = \frac{1}{ik} \sum_{l=0}^{\infty} (l + \tfrac{1}{2})(e^{2i\eta_l^j} - 1) J_0((l + \tfrac{1}{2})\theta) . \quad (13)$$

Using some simple properties of the spherical Bessel functions, one can show that η_l^j is large and varies linearly with l for $l < L_j \equiv kb_j$ and that $\eta_l^j \rightarrow 0$ very rapidly for $l > L_j$. Thus, for $l < L_j$ the term containing $e^{2i\eta_l^j}$ varies rapidly and averages to zero (there is no point of stationary phase[18]) while, for $l > L_j$, $(e^{2i\eta_l^j} - 1) \approx 0$. Equation (13) may then be approximated by[19]

$$f_j(\theta) \approx (i/k) \sum_{l=0}^{L_j} (l + \tfrac{1}{2}) J_0((l + \tfrac{1}{2})\theta) . \quad (14)$$

By transforming the sum (14) into an integral, one finally obtains[18]

$$f_j(\theta) \approx ib_j J_1(kb_j\theta)/\theta, \quad \theta \ll (kb_j)^{-1/3} . \quad (15)$$

The differential cross section

$$|f_j(\theta)|^2 = b_j^2 [J_1(kb_j\theta)]^2/\theta^2$$

contains a central peak and smaller side lobes typical of the diffraction pattern produced by an opaque object. Most of the scattering is contained in a cone of half angle $\theta \approx 4/kb_j$.

Equation (15) is valid not only in the diffractive cone $\theta < (kb_j)^{-1}$, but also in a range $(kb_j)^{-1} < \theta < (kb_j)^{-1/3}$. Inside the diffractive cone, Eq. (15) can be approximated by

$$f_j(\theta) \approx \tfrac{1}{2} ikb_j \exp(-\tfrac{1}{8} k^2 b_j^2 \theta^2) \quad kb_j\theta \lesssim 1 . \quad (16)$$

Although Eq. (16) is valid for diffractive scattering, if Eq. (16) rather than Eq. (15) is used in calculating collision rates and one-dimensional collision kernels, the results may differ by as much as 20% from the true hard-spheres values. [The results differ because the calculations require integrations in a range where Eq. (16) is not strictly valid.] Despite this discrepancy, we shall use Eq. (16) in subsequent calculations, owing to its simple analytical form. Given the spirit of this illustrative example, the slight errors which are introduced are not overly significant. For completeness, however, results using the correct amplitude (15) are given in Appendix B.

B. Population kernels

The population density in velocity space $\rho_{ll}(\vec{v}, t)$ satisfies a transport-type equation in which the collision terms are of the form[3]

$$\frac{\partial \rho_{ll}(\vec{v},t)}{\partial t}\bigg|_{\text{coll}} = -\Gamma_i(v)\rho_{ll}(\vec{v},t)$$

$$+ \int W_{ll}(\vec{v}\,'\rightarrow\vec{v})\rho_{ll}(\vec{v}\,',t)d\vec{v}\,' \ . \tag{17}$$

The first term on the right-hand side is the loss at rate $\Gamma_i(v)$ of population density $\rho_{ll}(\vec{v},t)$, while the second term gives the increase of $\rho_{ll}(\vec{v},t)$ resulting from collisions which change the velocity from $\vec{v}\,'$ to $\vec{v}$. The collision kernel $W_{ll}(\vec{v}\,'\rightarrow\vec{v})$ gives the probability density per unit time that a collision changes the active-atom velocity from $\vec{v}\,'$ to $\vec{v}$ and is related to the differential scattering cross section by[3]

$$W_{ll}(\vec{v}\,'\rightarrow\vec{v}) = Nv\,|f_i(v,\theta)|^2 v^{-2}\delta(v-v') \ , \tag{18}$$

where N is the perturber density and θ is the angle between $\vec{v}$ and $\vec{v}\,'$. The delta function ensures conservation of energy. The collision rate $\Gamma_i(v)$ is defined as

$$\Gamma_i(v) = \int W_{ll}(\vec{v}\rightarrow\vec{v}\,')d\vec{v}\,' \ , \tag{19}$$

which, together with Eq. (18) yields

$$\Gamma_i(v) = Nv\sigma_i(v) \ , \tag{20a}$$

where

$$\sigma_i(v) = \int |f_i(v,\theta)|^2 d\Omega_v \tag{20b}$$

is the total elastic state i scattering cross section. Equation (20) is in the standard form for a collision rate.

For hard-sphere scattering, the collision kernel, obtained from Eqs. (12), (16), and (18) is

$$W_{ll}(\vec{v}\,'\rightarrow\vec{v}) = Nv^{-1}\delta(v-v')$$
$$\times \begin{cases} b_i^2/4, & \theta >> (kb_i)^{-1/3} \\ (k^2b_i^4/4)\exp(-\tfrac{1}{4}k^2b_i^2\theta^2), & \theta \lesssim (kb_i)^{-1} \ . \end{cases} \tag{21}$$

It contains a part corresponding to classical scattering for $\theta >> (kb_i)^{-1/3}$ and the quantum-mechanical contribution of diffractive scattering for $\theta < (kb_i)^{-1}$. The collision cross section, obtained from Eqs. (19)–(21) is

$$\sigma_i = 2\pi b_i^2 \ , \tag{22}$$

a well-known result for hard-sphere scattering in the high-energy limit. The classical and diffractive scattering each contribute πb_i^2 to the total cross section.[20]

It is instructive to use the optical theorem and Eq. (18) to rewrite Eq. (17) in the form

$$\frac{\partial \rho_{ll}(\vec{v},t)}{\partial t}\bigg|_{\text{coll}} = -\tfrac{1}{2}[\Gamma_i(v)+\Gamma_i^*(v)]\rho_{ll}(\vec{v},t) + Nv^{-1}\int f_i(v,\theta)f_i^*(v,\theta)\delta(v-v')\rho_{ll}(\vec{v}\,',t)d\vec{v}\,' \ , \tag{23a}$$

where

$$\Gamma_j(v) = Nv(4\pi/ik)f_j(v,0) \tag{23b}$$

and $f(v,0)$ is a forward-scattering amplitude. In general $\Gamma_i(v)$ is complex, but, for hard-sphere scattering

$$\Gamma_i(v) = Nv(2\pi b_i^2) \tag{24}$$

is real.

C. Coherence kernel

The collisional time rate of change of the coherence density is given by[2,3]

$$\frac{\partial \rho_{12}(\vec{v},t)}{\partial t}\bigg|_{\text{coll}} = -\tfrac{1}{2}[\Gamma_1(v)+\Gamma_2^*(v)]\rho_{12}(\vec{v},t)$$

$$+ \int W_{12}(\vec{v}\,'\rightarrow\vec{v})\rho_{12}(\vec{v}\,',t)d\vec{v}\,' \ , \tag{25}$$

where

$$W_{12}(\vec{v}\,'\rightarrow\vec{v}) = Nvf_1(v,\theta)f_2^*(v,\theta)v^{-2}\delta(v-v') \ . \tag{26}$$

It may be noticed that Eq. (25) may be obtained from Eq. (23) by the substitution $f_1^*(v,\theta) \rightarrow f_2^*(v,\theta)$. The "rate" $\Gamma_{12}^{rc}(v)$ associated with the

coherence kernel is defined by

$$\Gamma_{12}^{vc}(v) = \int W_{12}(\vec{v} \rightarrow \vec{v}')d\vec{v}' \tag{27a}$$

$$= Nv\sigma_{12}^{vc}(v) , \tag{27b}$$

where

$$\sigma_{12}^{vc}(v) = \int f_1(v,\theta)f_2^*(v,\theta)d\Omega_v . \tag{28}$$

For hard-sphere scattering in the classical region $\theta >> (kb_j)^{-1/3}$, the collision kernel obtained from Eqs. (26) and (12), is

$$W_{12}(\vec{v}' \rightarrow \vec{v}) = Nv^{-1}(b_1 b_2/4)\delta(v - v')e^{i\phi(\theta)} , \tag{29a}$$

where

$$\phi(\theta) = 2k(b_2 - b_1)\sin(\theta/2) . \tag{29b}$$

If $k(b_2 - b_1) >> 1$, as assumed,[21] $W_{12}(\vec{v}' \rightarrow \vec{v})$ varies very rapidly with $\vec{v}'$ and the integral term in Eq. (25) averages to zero. Thus, *effectively*, $W_{12}(\vec{v}' \rightarrow \vec{v})$ is zero in the classical scattering region, a conclusion reached in Sec. II using the distinct trajectory argument. On the other hand, for diffractive scattering $\theta < (kb_j)^{-1}$, the collision kernel obtained using Eqs. (26) and (16), is

$$W_{12}(\vec{v}' \rightarrow \vec{v}) = \tfrac{1}{4}Nv^{-1}\delta(v - v')k^2 b_1^2 b_2^2$$

$$\times \exp[-\tfrac{1}{8}k^2(b_1^2 + b_2^2)\theta^2] . \tag{30}$$

As predicted in Sec. II, the coherence kernel is nonvanishing only in the diffractive scattering domain.

Using Eqs. (27) and (30), one can derive a velocity-changing coherence cross section and rate

$$\sigma_{12}^{vc} = 2\pi b_1^2 b_2^2/(b_1^2 + b_2^2) , \tag{31a}$$

$$\Gamma_{12}^{vc}(v) = Nv\sigma_{12}^{vc} . \tag{31b}$$

For future reference, we also define a "total" cross section σ_{12}^t and rate $\Gamma_{12}^t(v)$ by

$$\sigma_{12}^t = \tfrac{1}{2}(\sigma_1 + \sigma_2) = \pi(b_1^2 + b_2^2) , \tag{32a}$$

$$\Gamma_{12}^t(v) = Nv\sigma_{12}^t , \tag{32b}$$

and a phase-interrupting cross section σ_{12}^{ph} and rate $\Gamma_{12}^{ph}(v)$ by

$$\sigma_{12}^{ph} = \sigma_{12}^t - \sigma_{12}^{vc} = \pi(b_1^4 + b_2^4)/(b_1^2 + b_2^2) , \tag{33a}$$

$$\Gamma_{12}^{ph}(v) = Nv\sigma_{12}^{ph} . \tag{33b}$$

[The corresponding values of $W_{12}(\vec{v}' \rightarrow \vec{v})$, σ_{12}^{vc}, σ_{12}^t, and σ_{12}^{ph} obtained using the scattering amplitude (15) instead of (16) are given in Appendix B. They differ at most by $\approx 20\%$ from these values.]

D. One-dimensional coherence kernel

A situation of practical importance in laser spectroscopy involves the interaction of atoms with one or more single-mode laser fields. Assuming the fields to propagate in the $\pm z$ direction, one is led to the conclusion that, in the absence of collisions, the density-matrix element $\rho_{12}(\vec{v},t)$ may be factored as

$$\rho_{12}(\vec{v},t) = \rho_{12}(\vec{v}_t)\rho_{12}(v_z,t) , \tag{34}$$

where $\vec{v}_t$ is a velocity transverse to the z axis. The transverse component of the density-matrix element may be taken as constant in time since it is unaffected by the atom-field interaction. While this is no longer rigorously true when collisions occur,[22] one might still assume Eq. (34) to hold to a first approximation. In that case one can insert Eq. (34) into Eq. (25), and integrate over $\vec{v}_t$ to obtain

$$\frac{\partial \rho_{12}(v_z,t)}{\partial t}\bigg|_{coll} = -\Gamma_{12}^t(v_z)\rho_{12}(v_z,t) + \int_{-\infty}^{\infty} W_{12}(v_z' \rightarrow v_z)\rho_{12}(v_z',t)dv_z' , \tag{35}$$

where the one-dimensional kernel $W_{12}(v_z' \rightarrow v_z)$ is defined as

$$W_{12}(v_z' \rightarrow v_z) = \int W_{12}(\vec{v}' \rightarrow \vec{v})\rho_{12}(\vec{v}_t')d\vec{v}_t'd\vec{v}_t , \tag{36}$$

and the one-dimensional total collision rate is $\Gamma_{12}^t(v)_z = \tfrac{1}{2}[\Gamma_1(v_z) + \Gamma_2(v_z)]$, where

$$\Gamma_j(v_z) = \int \Gamma_j(v)\rho_{12}(\vec{v}_t)d\vec{v}_t . \tag{37}$$

In addition, a one-dimensional velocity-changing coherence rate $\Gamma_{12}^{vc}(v_z)$ can be defined by

$$\Gamma_{12}^{vc}(v_z) = \int \Gamma_{12}^{vc}(v)\rho_{12}(\vec{v}_t)d\vec{v}_t = \int W_{12}(v_z \rightarrow v_z')d_z' . \tag{38}$$

In order to carry out the calculations implicit in Eqs. (30)–(38), we assume $\rho_{12}(\vec{v}_t)$ is described by a thermal distribution

$$\rho_{12}(\vec{v}_t) = (\pi u^2)^{-1} \exp(-v_t^2/u^2) ,$$
(39)

where u is the most probable active-atom speed. Substituting Eqs. (30) and (39) into Eq. (36) and recalling that $k = mv/\hbar$, one may obtain the coherence kernel

$$W_{12}(v_z' \rightarrow v_z) = \tfrac{1}{4} N (\pi u^4)^{-1} (b_1^2 b_2^2/\hbar^2) \int v \delta(v-v') \exp(-v^2\theta^2/u^2\theta_0^2) \exp(-v_t'^2/u^2) d\vec{v}_t' d\vec{v}_t ,$$
(40)

where

$$\lambdabar = \hbar/u ,$$
(41)

$$\theta_0^2 = 8\lambdabar^2/(b_1^2+b_2^2) << 1 ,$$
(42)

$$v^2 = v_t^2 + v_z^2; \quad v'^2 = v_t'^2 + v_z'^2 ,$$
(43)

and

$$\cos\theta = \vec{v}\cdot\vec{v}'/v^2 .$$
(44)

The integrals in Eq. (40) are not overly difficult to evaluate. Writing $d\vec{v}_t = v_t dv_t d\phi_t$ and $d\vec{v}_t' = v_t' dv_t' d\phi_t'$, one can integrate Eq. (40) over v_t' to arrive at

$$W_{12}(v_z' \rightarrow v_z) = \tfrac{1}{4} N (\pi u^4)^{-1} (b_1^2 b_2^2/\hbar^2) \int_0^{2\pi} d\varphi_t \int_0^{2\pi} d\varphi_t' \int_0^{\infty} v_t dv_t v^2 \exp(-v^2\bar{\theta}^2/u^2\theta_0^2) \exp(-v_t^2/u^2) ,$$
(45)

where $\bar{\theta}$ is θ evaluated at $v_t'^2 = v_t^2 + v_z^2 - v_z'^2$ and terms of order $(v_z^2 - v_z'^2)/u^2$ are neglected owing to the diffractive nature of the scattering ($\bar{\theta} \le \theta_0 << 1$). For $\bar{\theta} << 1$, one can use Eq. (44) to obtain

$$\bar{\theta}^2 = \frac{(v_z - v_z')^2}{v_t^2} + \frac{v_t^2}{v^2}(\varphi_t - \varphi_t')^2 .$$
(46)

After Eq. (46) is substituted into Eq. (45), the remaining integrals can easily be evaluated to yield the coherence kernel

$$W_{12}(v_z' \rightarrow v_z) = N\sigma_{12}^{vc}\theta_0^{-1} \exp[-(v_z-v_z')^2/\theta_0^2 u^2] \exp\left[\frac{-2|(v_z-v_z')v_z'|}{\theta_0 u^2}\right] \left[\frac{1}{2} + \frac{v_z'^2}{u^2} + \frac{|v_z'(v_z-v_z')|}{\theta_0 u^2}\right] ,$$
(47)

where σ_{12}^{vc} is given by Eq. (31). In terms of dimensionless variables

$$x = (v_z - v_z')/\theta_0 u ,$$
(48a)

$$y = v_z'/u \approx v_z/u ,$$
(48b)

Eq. (47) may be written

$$W_{12}(x,y) = N\sigma_{12}^{vc}\theta_0^{-1} e^{-x^2} e^{-2|xy|}(\tfrac{1}{2} + y^2 + |xy|) .$$
(49)

The coherence kernel (47) [or (49)], is centered at $x = (v_z - v_z')/\theta_0 u = 0$ and has a width $|v_z - v_z'| \approx u\theta_0 << u$ if $|y| < 1$. (If $|y| >> 1$, the width is of order $u\theta_0/|y|$.) For $|y| = |v_z'|/u >> 1$, the kernel becomes exponential. The one-dimensional coherence kernel is displayed in Fig. 3 for several values of y. It is this type of kernel that one expects to encounter in laser spectroscopy experi-

ments.

[It is interesting to note that the kernel width remains of order $\theta_0 u$ independent of the active-atom-to-perturber mass ratio (see discussion in Appendix A). As the perturber to active-atom mass ratio decreases, there is a decrease in the scattering angle as measured in the laboratory frame relative to that measured in the center-of-mass frame; however, this effect is exactly compensated by an increase in the diffractive scattering cone in the center-of-mass system [the scattering angle varies as (reduced mass)$^{-1/2}$]. Thus, the kernel width is always of order $\theta_0 u \propto [m(\sigma_{12}^i)^{1/2}]^{-1}$. A low-mass active atom must be used to maximize the coherence kernel width. The fact that the kernel width increases with decreasing σ_{12}^i is reasonable; smaller obstacles produce larger diffraction cones.]

The various one-dimensional rates can also be calculated. From Eqs. (38), (49), and (31) one finds
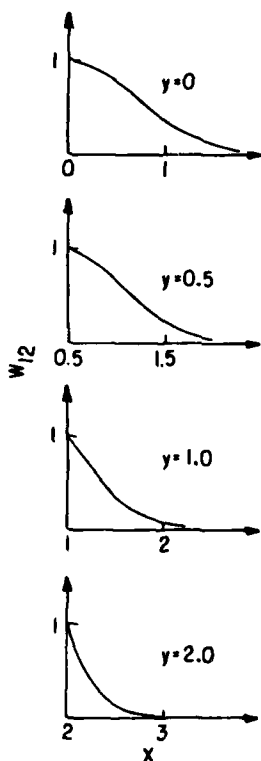
$$\Gamma_{12}^{ph}(y) = \Gamma_{12}^{t}(y) - \Gamma_{12}^{vc}(y) = Nu_z(y)\sigma_{12}^{ph}$$

$$= Nu_z(y) \left[\frac{\pi(b_1^4 + b_2^4)}{b_1^2 + b_2^2} \right] . \tag{54}$$

IV. COLLISION KERNELS IN LASER SPECTROSCOPY

It remains to determine the manner in which the collision kernels and rates modify the observables which are measured in various experiments. The reason for the success of traditional pressure-broadening theories in explaining many types of spectral line shapes will emerge naturally from this discussion.

In order to observe the effects of population kernels, the first step is to selectively excite (or deplete) a velocity subset of active atoms in state i. This selectivity can generally be achieved by using a narrow-band laser of frequency Ω to excite a transition having frequency ω. Only those atoms with velocity $v_z = (\Omega - \omega)/K$, where $\vec{K} = K\hat{z}$ is the laser propagation vector, will see a Doppler-shifted frequency that is resonant with the transition frequency. In this manner, one can excite a longitudinal velocity subset of atoms with velocities v_z centered at $(\Omega - \omega)/K$ having a width in velocity space of order $u_0 = \gamma/K$, where γ is some effective width (natural plus collision) associated with the transition.

Collisions will now modify the population density only if the collision-induced velocity changes produced within the velocity-selected state's lifetime is greater than or of the order of u_0. That is, for collisions to produce noticeable effects, they must significantly alter the velocity distribution created in the excitation process. Typically, $u_0/u \simeq 0.01$, so that both large-angle and diffractive scattering can modify the population density. The population density of the velocity-selected state may be monitored by measuring the absorption of a second laser on the same or another transition containing the level in question.[2,3] Such effects have been observed using both steady-state[23] and coherent transient[14,24] techniques. It might be noted that collision-induced changes in population densities can also be measured using a standing-wave photon-echo technique.[25]

FIG. 3. One-dimensional coherence collision kernel $W_{12}(\vec{v}_z' \rightarrow \vec{v}_z)$ as a function of $x = (v_z - v_z')/\theta_0 u$ for several values of $y = v_z'/u$. The kernel is in units of $N\sigma_{12}^{vc}\theta_0^{-1}(\frac{1}{2} + y^2)$ so that $W_{12} = 1$ at $x = 0$. Only positive x and y are shown since $W_{12}(x,y) = W_{12}(-x,y) = W_{12}(x,-y)$.

$$\Gamma_{12}^{vc}(y) = Nu_z(y)\sigma_{12}^{vc} = Nu_z(y) \left[\frac{2\pi b_1^2 b_2^2}{b_1^2 + b_2^2} \right] , \tag{50}$$

where $u_z(y)$ is the value of v averaged over the transverse velocity distribution, i.e.,

$$u_z(y) = (\pi u^2)^{-1} \int d\vec{v}_t (v_t^2 + y^2 u^2)^{1/2} e^{-v_t^2/u^2}$$

$$= |y| + (\pi^{1/2}/2)e^{y^2}[1 - \Phi(|y|)] , \tag{51}$$

where Φ is the error function. From Eqs. (37), (39), (24), (51), (32), and (33), one obtains

$$\Gamma_i(y) = Nu_z(y)\sigma_i = Nu_z(y)(2\pi b_i^2) , \tag{52}$$

$$\Gamma_{12}^{t}(y) = \frac{1}{2}[\Gamma_1(y) + \Gamma_2(y)] = Nu_z(y)\sigma_{12}^{t}$$

$$= Nu_z(y)[\pi(b_1^2 + b_2^2)] , \tag{53}$$

and

Coherence kernel

It is much more difficult to detect the velocity changes associated with the coherence kernel

$W_{12}(\vec{v}' \to \vec{v})$ than with the population kernel $W_{ii}(\vec{v}' \to \vec{v})$ owing to two factors. First, *the coherence kernel is limited to diffractive scattering*, whereas the population kernel contains a large-angle scattering component that is more easily detectable. Second, the effective lifetime for coherences is generally significantly smaller than that for populations (see discussion below); consequently, there may occur too few collisions within the coherence lifetime to produce a measurable effect. Therefore, it requires some analysis to determine the feasibility of measuring velocity changes associated with the coherence kernel.

In the rest frame of the active atom, the effect of a laser field $\vec{E} = \hat{i} E_0 \cos \Omega' t$ is to produce a "coherence" $\rho_{12}(\vec{v}, t)$ which essentially follows the field dependence, i.e., $\rho_{12}(\vec{v}, t) = \tilde{\rho}_{12}(\vec{v}, t) e^{+i\Omega' t}$.[26] The frequency Ω' seen in the atomic rest frame is equal to $\Omega - K v_z$ for a laser field of frequency Ω and propagation vector $K = K\hat{z}$. Thus, $\rho_{12}(\vec{v}, t)$ varies as

$$\rho_{12}(\vec{v}, t) = \tilde{\rho}_{12}(\vec{v}, t) e^{i\Omega t} e^{-iK v_z t}, \qquad (55)$$

where $\tilde{\rho}_{12}(\vec{v}, t)$ is generally a slowly varying function of $\vec{v}$ and t. Assuming that $\tilde{\rho}_{12}(\vec{v}, t)$ can be factored as in Eq. (34), one can substitute Eq. (55) into Eq. (25) and average over $\vec{v}_t$ to obtain

$$\frac{\partial \tilde{\rho}_{12}(v_z, t)}{\partial t}\bigg|_{coll} = -\Gamma_{12}^t(v_z)\tilde{\rho}_{12}(v_z, t) + \int W_{12}(v_z' \to v_z) e^{-iK(v_z - v_z')t} \tilde{\rho}_{12}(v_z', t) dv_z', \qquad (56)$$

which is the analog of Eq. (35).

We wish to examine Eq. (56) as it applies to linear spectroscopy, saturation spectroscopy, and photon-echo experiments. To do so, it is useful to draw some general conclusions concerning Eq. (56). First, there is always some effective coherence lifetime τ associated with $\tilde{\rho}_{12}$ which is determined by the natural and collisional widths of the levels, as well as the width of the velocity distribution represented by $\tilde{\rho}_{12}(v_z, t)$ (τ^{-1} is approximately equal to the linewidth observed in linear spectroscopy). Second, the coherence kernel limits $|v_z - v_z'|$ to values [see Eq. (47)]

$$|v_z - v_z'| \lesssim u\theta_0 \equiv \delta u \ll u, \qquad (57a)$$

$$\delta u = \frac{(8\pi)^{1/2}\hbar}{m(\sigma_{12}^t)^{1/2}}. \qquad (57b)$$

Consequently, if $K\delta u\tau \ll 1$ and if $\tilde{\rho}_{12}(v_z', t)$ is slowly varying compared with $W_{12}(v_z' \to v_z)$, the integral term in Eq. (56) may be approximated by $\Gamma_{12}^{vc}(v_z)\rho_{12}(v_z, t)$ if use is made of Eq. (38).[27] Thus, using Eq. (54), one finds

$$\frac{\partial \tilde{\rho}_{12}(v_z, t)}{\partial t}\bigg|_{coll} = -\Gamma_{12}^{ph}(v_z)\tilde{\rho}_{12}(v_z, t), \qquad (58a)$$

provided

$$K\delta u\tau \ll 1;$$

$$\left| \frac{1}{\tilde{\rho}_{12}} \frac{d\tilde{\rho}_{12}}{dv_z'} \right| \ll \left| \frac{1}{W_{12}(v_z' \to v_z)} \frac{dW_{12}(v_z' \to v_z)}{dv_z'} \right|. \qquad (58b)$$

Equation (58a) is precisely the equation used in traditional pressure-broadening theories![7,2,3]

We are let to conclude that traditional pressure-broadening theories give accurate results *provided* that Eq. (58b) is satisfied. Although the theory presented in this work and traditional pressure-broadening theories lead to the same formal result when Eq. (58b) is satisfied, the interpretation of the result is very different in the two theories. In our case, it is the separation of trajectories that leads to a destruction rate $\Gamma_{12}^{ph}(v) \approx Nv b_W$ is (recall b_W the Weisskopf radius), while, in traditional theories, it is large phase shifts for collisions having $b < b_W$ which destroy ρ_{12}. Thus, despite the fact that the neglect of trajectory effects cannot be justified, one is still at liberty to use the results of conventional pressure-broadening theories,[7] provided that Eq. (58b) is valid.[28] We now analyze some typical experimental situations to determine whether or not Eq. (58) can be used and to determine under what conditions the velocity changes associated with the coherence kernel may be detected.

Linear spectroscopy. In linear spectroscopy, there is no velocity selectivity and $\tilde{\rho}_{12}(v_z, t)$ is a thermal distribution having width u. The effective coherence time owing to this distribution is $\tau = (Ku)^{-1}$ at low pressure (leading to a width $\simeq \tau^{-1} \simeq Ku \simeq$ Doppler width) and decreases with increasing pressure. Under these conditions, Eq. (58b) is always satisfied, implying that linear spectroscopy may be described using conventional pressure-broadening theories. The net effect of collisions is a broadening of the spectral profiles.[29]

Saturation spectroscopy. In saturation spectroscopy, one selectively excites a velocity distribution of width $u_0 \approx (\gamma_{12} + \Gamma_{12}^{ph})/K$, where γ_{12} is the natural width associated with the $1-2$ transition. The effective coherence time, determined by the natural and collisional decay of ρ_{12}, is of order $\tau = (\gamma_{12} + \Gamma_{12}^{ph})^{-1}$. Thus, the width of $\rho_{12}(v_z,t)$ compared with that of $W_{12}(v_z' \to v_z)$ is roughly equal to $(\gamma_{12} + \Gamma_{12}^{ph})/K\delta u$, which may be of order unity at low pressures ($\Gamma_{12}^{ph} < \gamma_{12}$) but grows with increasing pressure. The quantity $K\delta u \tau$ is roughly equal to $K\delta u /(\gamma_{12} + \Gamma_{12}^{ph})$, which decreases with increasing pressure. Consequently, Eq. (58b) may be marginally violated at low pressures but should be valid at pressures where $\Gamma_{12}^{ph} >> \gamma_{12}$. At low pressures, the velocity-changing effects could introduce distortions into the saturation spectroscopy line shapes.[30] In order to observe deviations from Eq. (58a), systems having large K,[31] small γ_{12}, and an active atom with low mass should be sought. An attempt to observe velocity-changing effects on optical coherences was recently carried out with Xe as the active atom.[32] Although the method used produces line shapes that are sensitive to velocity changes associated with optical coherences, the value of K (infrared transitions) and the large mass of the Xe active atoms were not ideal for observing the effect. No direct evidence of the effects of velocity-changing collisions associated with the coherence kernel was found.[32]

Photon echoes. The photon-echo experiment is described in more detail in Sec. V. It turns out that the second inequality in Eq. (58b) is always satisfied. However, as described below, it is possible to arrange the experimental conditions such that $K\delta u \tau > 1$. In this limit, Eq. (58a) is no longer valid and the photon-echo signal reflects the effects of velocity changes associated with the coherence kernel $W_{12}(v_z' \to v_z)$. Recently, the first experimental evidence of this effect on an electronic transition was reported.[10,11]

V. PHOTON ECHO

A. General features

A photon-echo experiment offers an excellent method for monitoring the coherence ρ_{12}. In the absence of collisions and spontaneous decay, the photon echo signal is formed as follows[2,9,33]:

(1) At $t = 0$, a short pulse of radiation (propagation vector $\vec{K} = K\hat{z}$) creates a coherence

$$\rho_{12}(z,v_z,0) = CW(v_z)e^{-iKz},$$

where C is a constant.

(2) Between $t = 0$ and $t = T$, the coherence evolves freely as

$$\rho_{12}(z,v_z,t) = CW(v_z)e^{-iKz}e^{i(\omega + Kv_z)t},$$

where ω is the transition frequency. As seen in the laboratory frame, this frequency is Doppler shifted by Kv_z. The Doppler shifts cause the dipoles to dephase relative to each other.

(3) A second short pulse at $t = T$, also having $\vec{K} = K\hat{z}$, is chosen to produce a net effect[34] of changing the sign of the $(\omega + Kv_z)$ phase factor.[2,9,33] Thus, at time $t = T$, following the second pulse,

$$\rho_{12}(z,v_z,T) = C'W(v_z)e^{-iKz}e^{-i(\omega + Kv_z)T},$$

where C' is a constant. For $t > T$, the coherence once again evolves freely as

$$\rho_{12}(z,v_z,t) = C'W(v_z)e^{-iKz}e^{-i(\omega + Kv_z)T}e^{i(\omega + Kv_z)(t-T)}$$

$$= C'W(v_z)e^{-iKz}e^{i(\omega + Kv_z)(t - 2T)}. \qquad (59)$$

The dipoles, which dephased in the period $0 < t < T$, begin to rephase for $t > T$. At $t = 2T$, they are all in phase an an "echo" signal is emitted. Any interference of this dephasing-rephasing process or loss of ρ_{12} owing to spontaneous decay results in a decrease in echo amplitude. Thus the photon echo serves as a sensitive probe of the coherence ρ_{12}.

Spontaneous decay results in a decrease of ρ_{12} by a factor $\exp(-\gamma_{12}t)$ and a corresponding decrease in the echo amplitude (γ_{12} is the natural width associated with the transition). The collisional time rate of change of ρ_{12} given in Eq. (35) also modifies the echo amplitude. When the effects of both spontaneous decay and collisions are incorporated into the calculation, the resulting expression for the echo amplitude produced at $t = 2T$ is[9,35]

$$A(T) = \int_{-\infty}^{\infty} W(v_z)A(v_z,T)dv_z, \qquad (60a)$$

where

$$A(v_z,T) = A_0 \exp\left[-2\gamma_{12}T - 2\Gamma_{12}^t(v_z)T + 2\int_0^T dt \int_{-\infty}^{\infty} dv_z'\, W_{12}(v_z' \to v_z)\cos[K(v_z - v_z')t]\right] \qquad (60b)$$

is the contribution to the echo amplitude from atoms having velocity v_z.

Before specifically evaluating Eq. (60b) using the kernel (47), we can note several general features of the result (60b). The width of the coherence kernel $W_{12}(v_z' \rightarrow v_z)$ is roughly $\delta u = u\theta_0 << u$. If $K\delta uT << 1$, the velocity changes associated with the diffractive scattering region produce effects too small to be detected. In this limit, Eq. (60b) reduces to

$$A(v_z,T) \simeq A_0 \exp\{-2[\gamma_{12}+\Gamma_{12}^{ph}(v_z)]T\} ,$$

$$K\delta uT << 1 \quad (61)$$

where Eqs. (38) and (54) have been used. For times T such that diffractive scattering effects are negligible, the loss of echo amplitude arises from spontaneous decay (γ_{12} term) and the destruction of ρ_{12} produced by the separation of trajectory effect [$\Gamma_{12}^{ph}(v_z)$ term].

On the other hand, if $k\delta uT > 1$, the velocity changes associated with the diffractive scattering region lead to phase changes in ρ_{12} that are large enough to *further reduce the echo amplitude* from the value (61) produced by spontaneous decay and *separation of trajectory effects. In the limit that $K\delta uT >> 1$*, the integral term in Eq. (60b) averages to zero[36] and the echo amplitude becomes

$$A(v_z,T) = A_0 \exp\{-2[\gamma_{12}+\Gamma_{12}'(v_z)]T\} ,$$

$$K\delta uT >> 1 . \quad (62)$$

The reduction of echo amplitude is now caused by spontaneous decay, separation of trajectory effects, *and* diffractive coherent scattering. The rate of echo decay, $\Gamma_{12}'(v_z)$, in the long-time domain is larger than the rate $\Gamma_{12}^{ph}(v_z)$ in the short-time domain.

As the pulse separation T is increased, the effects of diffractive coherence scattering on the echo amplitude become more pronounced. For $K\delta uT >> 1$, every scattering event, on average, contributes to the collisional exponential loss term appearing in Eq. (62).

One may ask why the photon-echo method is distinctly superior to saturation spectroscopy in revealing these effects since the effective coherence lifetime $\tau \simeq [\gamma_{12}+\Gamma_{12}^{ph}(v_z)]^{-1}$ is the *same* in both cases. The answer to this question lies in the way in which the diffractive scattering affects the respective line shapes. In saturation spectroscopy, diffractive scattering produces corrections to *linewidths* of order $K\delta u\tau$; since $K\delta u\tau$ is generally less than unity the distortion of the line shape is usually difficult to observe. In photon-echo experiments, however, diffractive scattering produces corrections of order $k\delta uT$ which may be arbitrarily large. Of course, the effective coherence lifetime is playing a role by reducing the signal strength by a factor $\exp(-2T/\tau)$, which is much less than unity when $K\delta uT >> 1$. However, since echo signals are intrinsically large, measurements in the region where $T/\tau \lesssim 5$ are readily performed; such measurements[10,11] have led to a clear demonstration of the effects of diffractive scattering on coherences. The spectral resolution of echo signals obtained with pulse separations $T > 1/\gamma_{12}$ is less than the natural width associated with the $1-2$ transition.

B. Specific evaluation of echo amplitude

The integral appearing in Eq. (60b) is

$$I = \int_{-\infty}^{\infty} dv_z' \, W_{12}(v_z' \rightarrow v_z)\frac{\sin[K(v_z-v_z')T]}{K(v_z-v_z')} . \quad (63)$$

If the dimensionless variables $x = (v_z-v_z')/\delta u$ and $y = v_z/u \simeq v_z'/u$ given in Eq. (48) are reintroduced and the coherence kernel (49) substituted into Eq. (63), one obtains

$$I(y,\Theta) = 2N\sigma_{12}^{vc}uT\Theta^{-1}\int_0^{\infty} dx \, e^{-x^2-2x|y|}(\tfrac{1}{2}+y^2+x|y|)\sin(\Theta x)/x , \quad (64)$$

where

$$\Theta = K\delta uT = \theta_0(KuT) , \quad (65)$$

and θ_0 is defined by Eq. (42). The integrals are tabulated[17] and one may write Eq. (64) as

$$I(y,\Theta) = Nu\sigma_{12}^{vc}TY(y,\Theta) , \quad (66)$$

where

$$Y(y,\Theta) = 2 \sum_{n=0}^{\infty} \left[-\frac{\Theta^2}{2} \right]^n \frac{e^{y^2/2}}{2n+1} [2^{-1/2} D_{-(2n+1)}(\sqrt{2}|y|) + |y| D_{-2n}(\sqrt{2}|y|)] \;, \tag{67}$$

and D_n is a parabolic cylinder function.[17] Combining Eqs. (60b) and (63)—(67), we obtain

$$A(yu,T) = A_0 \exp\{-2[\gamma_{12} + \Gamma_{12}'(yu)]T + 2Nu\sigma_{12}^{vc} TY(y,\Theta)\} \;. \tag{68}$$

Equation (68) must now be averaged over a Maxwellian distribution in yu to arrive at the echo amplitude (60a). The integration must be done numerically. For illustrative purposes, we present two approximate methods for performing this average.

Method 1. If only a narrow range of velocities is excited by the laser pulse[37] such that $|y| \ll 1$, one can set $y = 0$ in Eq. (68) and use Eqs. (68), (60a), (51), and (53) to obtain the echo amplitude

$$A(T) = A_0 \exp\{-2[\gamma_{12} + Nu_x(0)[\sigma_{12}' - \sigma_{12}^{vc}\Theta^{-1}\sqrt{\pi}\Phi(\Theta/2)]]T\} \;, \tag{69}$$

where Φ is the error function and $u_x(0) = u\sqrt{\pi}/2$ is the average value of v for $v_z = 0$.[38] We note that

$$\ln[A(T)/A_0] \sim \begin{cases} -2[\gamma_{12} + Nu_x(0)(\sigma_{12}^{ph} + \sigma_{12}^{vc}\Theta^2/12)]T, & \Theta \ll 1 \\ -2[\gamma_{12} + Nu_x(0)(\sigma_{12}' - \sigma_{12}^{vc}\sqrt{\pi}/\Theta)]T, & \Theta \gg 1 \end{cases} \tag{70}$$

and recall that $\Theta = K\delta uT$.

Method 2. If $W(v_z)$ is a Maxwellian distribution having width u, the assumption $|y| \ll 1$ no longer holds. As a rough approximation, however, we can average the *exponent* in Eq. (68) over y rather than the exponential. In this manner, one finds[39]

$$A(T) = A_0 \exp\left\{-2\left\{\gamma_{12} + N\bar{v}\left[\sigma_{12}' - \sigma_{12}^{vc} \sum_{n=0}^{\infty}\left[-\frac{\Theta^2}{2}\right]^n \frac{1}{(2n+1)(2n+1)!!}\right]\right\}T\right\} \;, \tag{71}$$

where $\bar{v} = 2u/\sqrt{\pi}$ is the average speed and the sum is a representation of the generalized hypergeometric function $_2F_2(\frac{1}{2},1;\frac{3}{2},\frac{3}{2};-\Theta^2/4)$. For small and large Θ, Eq. (71) may be written

$$\ln[A(T)/A_0] \sim \begin{cases} -2[\gamma_{12} + N\bar{v}(\sigma_{12}^{ph} + \sigma_{12}^{vc}\Theta^2/18)]T, & \Theta \ll 1 \\ -2[\gamma_{12} + N\bar{v}(\sigma_{12}' - \sigma_{12}^{vc}\pi^{3/2}/2\Theta)]T, & \Theta \gg 1 \;. \end{cases} \tag{72}$$

The results expressed by Eqs. (70) and (72) are of a quite general nature.[8] For $\Theta \ll 1$

$$\ln[A(T)/A_0] \sim -2\gamma_{12}T - 2N\tilde{u}\sigma_{12}^{ph}T - 2cN\tilde{u}\sigma_{12}^{vc}K^2(\delta u)^2 T^3, \quad K\delta uT \ll 1 \tag{73}$$

where c is a constant and $\tilde{u}$ some effective average speed. The T^3 dependence is a signature of velocity-changing effects. For $\Theta \gg 1$,

$$\ln[A(T)/A_0] \sim -2\gamma_{12}T - 2N\tilde{u}\sigma_{12}'T - 2c'N\tilde{u}\sigma_{12}^{vc}/K\delta u, \quad K\delta uT \gg 1 \;, \tag{74}$$

where c' is a constant.

To isolate the effects of collisions, we define a quantity

$$B(\Theta) = -\{\ln[A(T)/A_0] + 2\gamma_{12}T\}/(2N\tilde{u}\sigma_{12}^{ph}T) \;, \tag{75}$$

which will have asymptotic limits

$$B(\Theta) \sim \begin{cases} 1 + c(\sigma_{12}^{vc}/\sigma_{12}^{ph})\Theta^2, & \Theta \ll 1 \\ \sigma_{12}'/\sigma_{12}^{ph}, & \Theta \gg 1 \;. \end{cases} \tag{76}$$

The ratio of $B(\Theta)$ in the high- and low-Θ limits is

$$\mathscr{R} = \frac{B(\Theta)(\Theta \gg 1)}{B(\Theta)(\Theta \ll 1)} = \frac{\sigma_{12}'}{\sigma_{12}^{ph}} = \frac{(b_1^2 + b_2^2)^2}{b_1^4 + b_2^4} \;, \tag{77}$$

where Eqs. (53) and (54) have been used.

As a specific example, we calculate $B(\Theta)$ using the approximation (71) (for which $u = \bar{v}$) and find

$$B(\Theta) = 1 + \frac{2b_1^2 b_2^2}{b_1^4 + b_2^4} \left[1 - \sum_{n=0}^{\infty} \left(-\frac{\Theta^2}{2} \right)^n \frac{1}{(2n+1)(2n+1)!!} \right]. \tag{78}$$

In Fig. 4, $B(\Theta)$ is graphed for several values of (b_1/b_2). For $\Theta \gg 1$, $B(\Theta)$ asymptotically approaches the ratio $\mathcal{R}$ given by Eq. (77). The ratio $\mathcal{R} = \sigma'_{12}/\sigma_{12}^{ph}$ varies from 1 to 2 as (b_1/b_2) varies from 0 to 1. It should be noted that the general conclusions reached in this section are model independent. In particular, the echo amplitude varies as $\exp(-2\Gamma_{12}^{ph}T)$ for short times ($K\delta uT \ll 1$) and as $\exp(-2\Gamma'_{12}T)$ for long times ($K\delta uT \gg 1$).

The curves shown in Fig. 4 are in qualitative agreement with recent experimental results on photon echoes in Li perturbed by rare gases.[11] Velocity-changing effects were also observed with Na as the active atom; the Na mass is small enough to give rise to a δu large enough [Eq. (57b)] to produce $K\delta uT > 1$ for the pulse separations in that experiment.[10] In a coherent transient experiment on an electronic transition of I_2,[40] only the exponential decay of the echo amplitude typical of the short-time domain was observed. The large iodine mass leads to a small δu [Eq. (57b)]; consequently; $K\delta uT$ may remain small for the time scales used in that experiment.

VI. SUMMARY

When atoms that have been created in a superposition state by a radiation field undergo elastic collisions in an atomic vapor, two distinct types of effects occur. There is a modification of both the
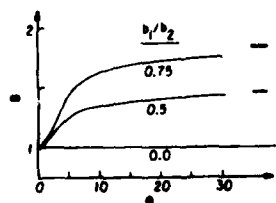

FIG. 4. Graph of $B(\Theta)$ which characterizes the photon-echo signal [Eq. (78)] as a function of $\Theta = K\delta uT$ for $b_1/b_2 = 0, 0.5, 0.75$. The small horizontal lines on the right side of the graph indicate the asymptotic value of $B(\Theta)$ as $\Theta \to \infty$.

population-velocity distributions $\rho_{ii}(\bar{v},t)$ and the coherence density $\rho_{ij}(\bar{v},t)$ ($i \neq j$) produced by the scattering events. The processes can be characterized by collision kernels $W_{ii}(\bar{v}' \to \bar{v})$ and $W_{ij}(\bar{v}' \to \bar{v})$, respectively. In this work, we have discussed the population kernels $W_{ii}(\bar{v}' \to \bar{v})$, but have concentrated our efforts in obtaining a physical picture of the coherence kernel $W_{ij}(\bar{v}' \to \bar{v})$. To do so, we have considered a system of two-level active atoms interacting with a radiation field and undergoing collisions with perturber atoms. The collision interaction experienced by the atom in each state was assumed to differ appreciably, as is usually the case for electronic transitions.

Using arguments based on the uncertainty principle, we showed that collisions can be roughly divided into two regions. Collisions having an impact parameter less than some characteristic radius may be described classically, while large-impact parameter collisions, giving rise to diffractive scattering, must be treated using a quantum-mechanical approach. As a consequence of this result, the population kernel may be written as the sum of a large-scale (classical) scattering term plus a term containing the effects of diffractive scattering.

The collision-induced modifications of the atomic coherences produced by these two types of collisions are somewhat more interesting. For small-impact parameter collisions, there are distinct nonoverlapping trajectories associated with the scattering for each atomic state. Since there is no spatial overlap of states 1 and 2 following such collisions, these collisions destroy ρ_{12} and lead simply to a decay rate for ρ_{12}. Quantum mechanically, the classical separation of trajectories is represented by a rapid variation with angle of the phase of the product of the amplitudes $f_1 f_2^*$. Large-impact parameter collisions, on the other hand, lead to overlapping diffractive scattering for the two states. Consequently, the coherence kernel $W_{12}(\bar{v}' \to \bar{v})$ possesses a diffractive component only arising from these large-impact parameter collisions. The width of the coherence kernel is effectively independent of the perturber to active-atom mass ratio.

Trajectory effects are seen to play an important role in determining the collision-induced changes

in the coherence ρ_{12}. The coherence ρ_{12} is related to the atomic polarization, which, in turn, is directly linked to the spectral properties of the medium. It seems somewhat paradoxical, therefore, that traditional pressure-broadening theories, in which separation of trajectory effects are neglected and in which collisions are assumed to affect only the phases of the optical dipoles, are so successful in describing spectroscopic line shapes. This apparent paradox was resolved in Sec. IV, where it was shown that traditional pressure-broadening may be used provided the velocity-changes associated with the coherence kernel are too small to be detectable in a given experiment. Thus, although the interpretations are different in the two approaches, the results can be identical. In linear spectroscopy, traditional pressure-broadening theory is always valid, if, as assumed, the collisional interaction differs appreciably for the two states between which the optical transition occurs. Traditional pressure-broadening theory is no longer applicable if the velocity changes associated with the diffractive coherence kernel $W_{12}(\vec{v}' \rightarrow \vec{v})$ can be experimentally measured. Such effects should be marginally observable in saturation spectroscopy and have been observed for the first time in photon-echo experiments.[10,11]

To illustrate various features of the problem, we adopted a simple model of hard-sphere scattering to describe the collisions. The results, however, are quite general and can be easily extended to arbitrary potentials. The hard-sphere model enabled us to obtain closed-form expressions for the various collision kernels and rates. In addition, we used the model to calculate an expression for the photon-echo amplitude, which clearly indicates the

importance of velocity-changing collisions associated with $W_{12}(\vec{v}' \rightarrow \vec{v})$. If one uses a more realistic interaction potential, the resulting expressions must be evaluated numerically.

It should be noted that the semiclassical approach used in this work is valid only if the de Broglie wavelength of the atoms (in the center-of-mass reference frame) is much smaller that the characteristic Weisskopf collision radius b_W. Moreover, any effects of orbiting or of rainbow or glory scattering have been neglected. A rigorous discussion of the validity of the semiclassical approach has been given by Avrillier, Borde, Picart, and Tran Minh.[4] A calculation is in progress which is designed to determine the conditions under which our general approach to calculating the coherence kernel retains its validity.

ACKNOWLEDGMENTS

APPENDIX A

In Appendix A, the results of Sec. III are generalized to allow for an arbitrary perturber to active-atom mass ratio. The collision kernel is given by[2,3]

$$W_{ij}(\vec{v}' \rightarrow \vec{v}) = N \left[\frac{m}{\mu} \right]^3 \int d\vec{v}'_r \int d\vec{v}_r W_p(\vec{v}' - \vec{v}'_r) \delta \left[\vec{v}_r - \vec{v}'_r - \frac{m}{\mu}(\vec{v} - \vec{v}') \right] v_r^{-1} \delta(v_r - v'_r) F_{ij}(v'_r, |\vec{v}_r - \vec{v}'_r|) .$$

(A1)

The quantities appearing in Eq. (A1) are the product of scattering amplitudes in the center-of-mass system

$$F_{ij}(v'_r, |\vec{v}_r - \vec{v}'_r|) = f_i(v'_r, |\vec{v}_r - \vec{v}'_r|) f_j^*(v'_r, |\vec{v}_r - \vec{v}'_r|) ,$$

(A2)

the perturber velocity distribution

$$W_p(\vec{v}_p) = (\pi u_p^2)^{-3/2} \exp(-v_p^2/u_p^2) ,$$

(A3)

where u_p is the most probable perturber speed, and the reduced mass μ. Equation (A1) represents the collision kernel in the center-of-mass frame averaged over the perturber velocity distribution consistent with conservation of momentum and energy.

Integrating Eq. (A1) over $\vec{v}_r'$ and setting

$$\vec{\eta} = (m/\mu)(\vec{v} - \vec{v}') , \qquad (A4)$$

one finds

$$W_{ij}(\vec{v}' \to \vec{v}) = N(m/\mu)^3 \int d\vec{v}_r W_p(\vec{v}' - \vec{v}_r + \vec{\eta}) \delta(v_r - |\vec{v}_r - \vec{\eta}|) v_r^{-1} F_{ij}(v_r, \eta) . \qquad (A5)$$

The angular integrals can be carried without too much difficulty[5,13,41] and one may obtain

$$W_{ij}(\vec{v}' \to \vec{v}) = N(m/\mu)^3 (2\pi)\eta^{-1} W_p(\tfrac{1}{2}\vec{\eta} + \vec{v}') \int_0^\infty q\, dq \, \exp(-q^2/u_p^2) I_0(2qv_s/u_p^2) F_{ij}((q^2 + \tfrac{1}{4}\eta^2)^{1/2}, \eta)) , \qquad (A6)$$

where

$$v_s = (vv'/|\vec{v} - \vec{v}'|)\sin\theta , \qquad (A7)$$

θ is the angle between $\vec{v}'$ and $\vec{v}$, and I_0 is a modified Bessel function.

When the exponential approximation to the scattering amplitude (16) is used, one has

$$F_{ij}(v_r, \eta) = \tfrac{1}{4} k_r^2 b_i^2 b_j^2 \exp[-\tfrac{1}{8} k_r^2 (b_i^2 + b_j^2)\theta_r^2] , \qquad (A8)$$

where

$$\vec{k}_r = \mu \vec{v}_r / \hbar \qquad (A9)$$

and

$$\theta_r = 2\sin^{-1}(\eta/2v_r) \qquad (A10)$$

are the k vector and scattering angle, respectively, in the center-of-mass frame. Substituting Eqs. (A8)–(A10) into (A6) and assuming $\theta_r \ll 1$ (diffractive scattering region), we find

$$W_{ij}(\vec{v}' \to \vec{v}) \simeq \frac{N}{\sqrt{\pi}} \left[\frac{m}{\mu} \right]^3 \frac{b_i^2 b_j^2 \exp[-\eta^2/(\theta_0' u_r)^2]}{4\lambda_r^2 u_p \eta} \exp\left[-\left[\frac{\eta}{2} + \frac{\vec{v}' \cdot \vec{\eta}}{\eta} \right]^2 \frac{1}{u_p^2} \right] u_r^{-2}[v'^2 + \tfrac{1}{4}\eta^2 + u_p^2 - (\vec{v}' \cdot \vec{\eta}/\eta)^2] , \qquad (A11)$$

where

$$\vec{\eta} = (m/\mu)(\vec{v} - \vec{v}') ,$$

$$\lambda_r = \hbar/\mu u_r , \qquad (A12)$$

$$u_r^2 = u^2 + u_p^2 , \qquad (A13)$$

and

$$(\theta_0')^2 = 8\lambda_r^2/(b_i^2 + b_j^2) \ll 1 . \qquad (A14)$$

The various collision rates defined by Eqs. (19), (27), (32), and (33) are easily calculated starting from Eq. (A1). One finds

$$\Gamma_i(v) = N u_r(v)(2\pi b_i^2) , \qquad (A15a)$$

$$\Gamma_{12}'(v) = N u_r(v)[\pi(b_1^2 + b_2^2)] , \qquad (A15b)$$

$$\Gamma_{12}^{v_2}(v) = N u_r(v) \left[\frac{2\pi b_1^2 b_2^2}{b_1^2 + b_2^2} \right] , \qquad (A15c)$$

$$\Gamma_{12}^{\text{ph}}(v) \approx N u_r(v) \left[\frac{\pi(b_1^4 + b_2^4)}{b_1^2 + b_2^2} \right] , \tag{A15d}$$

where $u_r(v)$ is the active-atom perturber relative speed averaged over the perturber velocity distribution, i.e.,

$$u_r(u_p z) = \int W_p(\vec{v}_p) |\vec{v} - \vec{v}_p| d\vec{v}_p$$

$$= \pi^{-1/2} u_p e^{-z^2} [1 + 2\pi^{1/2} z^{-1}(1 + 2z^2) e^{z^2} \Phi(z)] , \tag{A16a}$$

with

$$z = v/u_p . \tag{A16b}$$

[Note that as $u_p \rightarrow 0$ and $\mu \rightarrow m$, one regains the results of Sec. III. If $u \rightarrow 0$, and $\mu \rightarrow m_p$ (perturber mass), $W_{12}(\vec{v}' \rightarrow \vec{v}) \sim \Gamma_{12}^{\text{vc}}(v) \delta(\vec{v} - \vec{v}')$, and $u_r(u_p z) \sim u_r(0) = 2\pi^{-1/2} u_p$.]

To obtain the one-dimensional kernel, one multiplies Eq. (A1) by $W(\vec{v}_t')$ and integrates over $\vec{v}_t$ and $\vec{v}_t'$. The resulting integrals can be reduced to a triple integral[5,13,41] of the form

$$W_{ij}(v_z' \rightarrow v_z) = 4\pi^{-1/2} \beta \kappa \int_0^\infty ds_t \int_0^\infty dq \int_{-\infty}^\infty dp \, e^{-\beta^2(p-y)^2} \exp[-\kappa^{-1}(q^2 + q_0^2)] F_{12}((q_0^2 + p^2 + q^2)^{1/2}, \eta) , \tag{A17}$$

where

$$\beta = u/u_p = (m_p/m)^{1/2} , \tag{A18}$$

$$\kappa = (1 + \beta^2)/\beta^2 , \tag{A19}$$

$$\vec{s} = (\vec{v} - \vec{v}')/u = \vec{s}_t + s_z \hat{z} , \tag{A20}$$

$$q_0^2 = s_t^{-2} (\tfrac{1}{2} \kappa s^2 + p s_z)^2 , \tag{A21}$$

and

$$y = v_z'/u . \tag{A22}$$

With the kernel given by the exponential approximation (A8), Eq. (A17) may be integrated to give

$$W_{12}(v_z' \rightarrow v_z) = \tfrac{1}{2} N \sigma_{12}^{\text{vc}}(\theta_0')^{-1} e^{-\beta^2 x^2}$$

$$\times \{ [\tfrac{1}{2} + \beta^{-2} + y^2 + x\bar{y}(1 - \beta^{-2}) - x^2] e^{-2x\bar{y}}[1 + \Phi(\bar{y} - x)]$$

$$+ [\tfrac{1}{2} + \beta^{-2} + y^2 - x\bar{y}(1 - \beta^{-2}) - x^2] e^{2x\bar{y}}[1 - \Phi(\bar{y} + x)] + 2\pi^{-1/2} x e^{-\bar{y}^2} e^{-x^2} \} , \tag{A23}$$

where

$$x = |v_z - v_z'| / (\beta u \theta_0') , \tag{A24}$$

$$y = v_z'/u ,$$

$$\bar{y} = \beta y = v_z'/u_p , \tag{A25}$$

$$\theta_0' = \kappa \theta_0 . \tag{A26}$$

The kernel (A23) reduces to Eq. (49) in the limit $\beta \rightarrow \infty$ and has a width of order $\theta_0 u$ for $|y| \lesssim 1$. For $\beta << 1$ and $|y| \lesssim 1$, the effective width of the kernel is of order $\beta \theta_0' u = \kappa \beta \theta_0 u = (1 + \beta^2)^{1/2} \theta_0 u \approx \theta_0 u$. Thus, *regardless of the ratio of perturber to active-atom mass ratio*, the kernel width (for $|y| \lesssim 1$) is of order

$$u \theta_0 = 2\sqrt{2} \lambda u / (b_1^2 + b_2^2)^{1/2}$$

$$= 2(2\pi)^{1/2} \hbar/m (\sigma_{12}')^{1/2} . \tag{A27}$$

This somewhat surprising result arises from the cancellation of two effects. As m_p/m (or β) decreases, there is an *increase* in the size of the diffraction cone in the center-of-mass system [recall that $\theta_r \propto (\mu u_r)^{-1}$

$=(1+\beta^{-2})^{1/2}\theta_0]$. This effect is compensated by a *decrease* in the scattering angle as measured in the laboratory frame. Thus, the collision width depends primarily on the active-atom mass and total collision cross section.

In Fig. 5, the kernel

$$W_{12}(0 \rightarrow \beta u\theta_0', x) = N\sigma_{12}^{vc}(\theta_0')^{-1}e^{-\beta^2 x^2}\{(\tfrac{1}{2}+\beta^{-2}-x^2)[1-\Phi(x)]+\pi^{-1/2}xe^{-x^2}\} \tag{A28}$$

is plotted as a function of

$$(1+\beta^2)^{1/2}x = v_z/u\theta_0 = v_z/\delta u \tag{A29}$$

for several values of β. The $\beta=0.1$ and $\beta=10$ curves correspond to asymptotic limits of the kernel for the cases $\beta \ll 1$ and $\beta \gg 1$ respectively; thus the kernel width is seen to vary only slightly with β. In practice, σ' normally increases with increasing β, implying a corresponding decrease in the kernel width. Smaller collision cross sections produce a larger diffractive-scattering cone.

The various one-dimensional rates are still given by Eqs. (A15) if one replaces v by v_z and $u_r(v)$ by $u_z(v_z)$, where $u_z(v_z)$ is the relative speed averaged over the perturber and transverse active-atom velocity distributions, i.e.,

$$u_z(v_z) = \int W(\vec{v}_t)W_p(\vec{v}_p)|\vec{v}-\vec{v}_p|d\vec{v}_p d\vec{v}_t , \tag{A30}$$

where

$$\vec{v} = \vec{v}_t + v_z\hat{z} .$$

Explicitly,[41] one finds

$$u_z(uy) = u_p\left[\beta y\Phi(\beta y)+\pi^{-1/2}e^{-\beta^2 y^2}\left[1+\pi^{1/2}\int_0^\infty dx\, e^{-x^2/\kappa^2\beta^2}\cosh(2yx/\sqrt{\kappa})[1-\Phi(x/\kappa\beta^2)]\right]\right] . \tag{A31}$$

APPENDIX B

In Appendix B, we derive expressions for the various collision kernels and rates using the amplitude (15) for hard-sphere scattering instead of its exponential approximation (16). Moreover, the cross sections are also calculated directly using Eq. (11) to illustrate the origin of the distinct trajectory approximation $k(b_2-b_1) \gg 1$.

Using Eqs. (A2) and (15), we find

$$F_{ij}(v_r,\eta) = b_i b_j \theta_r^{-2} J_1(k_r b_i \theta_r) J_1(k_r b_j \theta_r) , \tag{B1}$$

where θ_r is given by Eq. (A10). If Eq. (B1) is substituted into Eq. (A6) and the assumption $\theta_r \ll 1$ is used, one may obtain [cf. Eqs. (A11)–(A14)]

$$W_{ij}(\vec{v}' \rightarrow \vec{v}) = \frac{N}{\sqrt{\pi}}\left[\frac{m}{\mu}\right]^3\frac{b_i b_j u_r^2}{u_p\eta^3}J_1\left[\frac{b_i\eta}{u_r\lambda_r}\right]J_1\left[\frac{b_j\eta}{u_r\lambda_r}\right]$$

$$\times \{\exp[-(\tfrac{1}{2}\eta+\vec{v}'\cdot\vec{\eta}/\eta)^2/u_p^2]\}u_r^{-2}[v'^2+\tfrac{1}{4}\eta^2+u_p^2-(\vec{v}'\cdot\vec{\eta}/\eta)^2] , \tag{B2}$$

where $\vec{\eta} = (m/\mu)(\vec{v}-\vec{v})$. Equation (B2) reduces to Eq. (A11) if $b\eta/u_r\lambda_r \ll 1$.

The rate obtained from Eqs. (27), (A1), and (B1) is

$$\Gamma_{ij}^{vc}(v) = Nu_r(v)\int d\Omega_r b_i b_j \theta_r^{-2}J_1(k_r b_i \theta_r)$$

$$\times J_1(k_r b_j \theta_r) , \tag{B3}$$

where $u_r(v)$ is given by Eq. (A16). If $k_r(b_2-b_1) \gg 1$, the θ_r integral can be replaced by an integral from 0 to ∞. In that case, for $b_2 > b_1$, one finds[17]

$$\Gamma_{ij}^{vc}(v) = Nu_r(v)(\pi b_i^2) \quad b_i \leq b_j . \tag{B4}$$

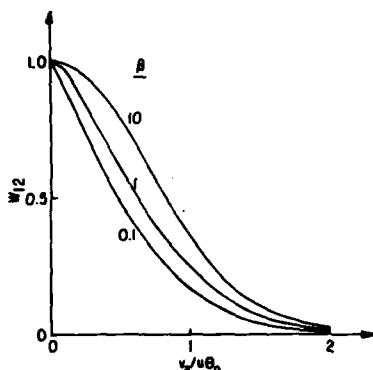Thus, the various cross sections and rates defined in Eqs. (19) and (31)–(33) are given by ($b_2 > b_1$)

FIG. 5. Graphs of the one-dimensional kernel $W_{12}(0 \to v_z)$ as a function of $(1+\beta^2)^{1/2}x = v_z/u\theta_0$ for several values of $\beta = u/u_p = (m_p/m)^{1/2}$. Notice that the width of the kernel is essentially independent of β, although its shape changes somewhat. The kernel is in units of $N\sigma_{12}^{vc}(\theta_0^r)^{-1}$ and is normalized such that $W_{12}(0 \to 0) = 1$.

$$\sigma_i = 2\pi b_i^2 , \tag{B5a}$$

$$\sigma_{12}^{vc} = \pi b_1^2 , \tag{B5b}$$

$$\sigma_{12}^t = \pi(b_1^2 + b_2^2) , \tag{B5c}$$

$$\sigma_{12}^{ph} = \pi b_2^2 , \tag{B5d}$$

and $\Gamma(v) = Nu_r(v)\sigma$. The cross section σ_{12}^{vc} can differ by as much as 17% from that calculated using the exponential approximation to the scattering amplitude [see Eq. (31)].

Integral expressions for the one-dimensional kernels and rates can be easily obtained using Eqs. (36), (39), (A1), (B1), and (27). Without explicitly writing expressions for these quantities, we note that for large enough $|\vec{v} - \vec{v}'|$ or $|\vec{v}_z - \vec{v}_z'|$, it is possible for the population kernel to have side lobes and for the coherence kernel to go negative (the exponential approximation always gives a positive kernel). This feature is already seen in Eq. (B2). Near the "center" of the kernel, $|v_z - v_z'| < u\theta_0$, the exponential approximation (16) produces a collision kernel that has the same form as the one calculated using the correct amplitude (15).

To finish this appendix (and article), we calculate σ_{12}^{vc} directly from Eq. (11) without using the assumption that $k(b_2 - b_1) \gg 1$. Using the definition

$$\sigma_{ij}^{vc} = \text{Re} \int f_i(\theta) f_j^*(\theta) d\Omega \tag{B6}$$

along with Eq. (11) for $f_i(\theta)$, one easily derives

$$\sigma_{ij}^{vc} = 4\pi k^{-2} \sum_{l=0}^{\infty} (l + \tfrac{1}{2}) [2\sin^2\eta_l^{(1)} \sin^2\eta_l^{(2)} + \tfrac{1}{2}\sin(2\eta_l^{(1)})\sin(2\eta_l^{(2)})] , \tag{B7}$$

where

$$\eta_l^{(i)} = \tan^{-1}[j_l(kb_i)/n_l(kb_i)] \tag{B8}$$

is the state-i hard-sphere scattering phase shift. Using the properties of the spherical Bessel functions,[17] one can show that $\eta_l^{(i)} \sim 0$ exponentially for $l < L_i$ so that the $\cos(2\eta_l^i)$ terms average to zero. One is left with

$$L_i = kb_i \tag{B9}$$

(assuming $b_i < b_j$). Equation (B7) may be rewritten as

$$\sigma_{ij}^{vc} = 2\pi k^{-2} \sum_{l=0}^{L_i} l[1 - \cos(2\eta_l^{(j)}) - \cos(2\eta_l^{(j)}) + \cos(\eta_l^{(j)} - \eta_l^{(i)})] . \tag{B10}$$

Again, using the properties of the Bessel functions,[17] one can show that the η_l^i are large for $l < L_i$ so that the $\cos(2\eta_l^i)$ terms average to zero. One is left with

$$\sigma_{ij}^{vc} = 4\pi k^{-2} \sum_{l=0}^{L_i} l \sin^2[(\eta_l^{(j)} - \eta_l^{(i)})/2] . \tag{B11}$$

For $i = j$, Eqs. (B9) and (B11) yield $\sigma_i = 2\pi b_i^2$, the quantum-mechanical result for high-energy hard-sphere scattering. For $i \neq j$, one can approximate[17]

$$\eta_l^{(2)} - \eta_l^{(1)} = l(\psi_2 - \psi_1) - l(\tan\psi_2 - \tan\psi_1) , \tag{B12}$$

where

$$\psi_l = \cos^{-1}(l/L_i) .$$

Since $l/L_i \ll 1$ for most l in the sum,

$$\psi_l - \tan\psi_l \simeq \frac{\pi}{2} - \frac{l}{2L_i} - \frac{L_i}{l} ,$$

such that

$$\eta_l^{(2)} - \eta_l^{(1)} \approx -k(b_2 - b_1) + \frac{l^2}{2}\frac{(b_2 - b_1)}{kb_1 b_2} . \tag{B13}$$

Combining Eqs. (B13) and (B11) and changing the

sum to an integral, one finally obtains

$$\sigma_{12}^{vc} = \pi b_1^2 + \frac{4\pi b_1 b_2}{k(b_2-b_1)} \sin\left[\frac{kb_1(b_2-b_1)}{4b_2}\right]$$

$$\times \cos\left[\frac{k(b_2-b_1)(4b_2-b_1)}{4b_2}\right] . \qquad (B14)$$

If $b_2 = b_1$, $\sigma_{12}^{vc} = 2\pi b_1^2$, but for $k(b_2-b_1) \gg 1$, $\sigma_{12}^{vc} \simeq \pi b_1^2$, in agreement with the result (B5b) derived *from diffractive scattering only*. Thus, if $k(b_2-b_1) \gg 1$, diffractive scattering only contributes to the coherence kernel.

---

[1]The perturber atoms are assumed to be nonreactive and simply provide an effective scattering potential which is different for states 1 and 2 of the active atom.

[2]P. R. Berman, Adv. At. Mol. Phys. 13, 57 (1977), and references therein.

[3]P. R. Berman, Phys. Rep. 43, 101 (1978).

[4]S. Avrillier, C. J. Borde, J. Picart, and N. Tran Minh, in *Proceedings of the 5th International Conference on Spectral Line Shapes,* edited by B. Wende (de Gruyter, Berlin, 1981), and (unpublished).

[5]S. Avrillier, Doctorat D'Etat thesis, University of Paris, North, 1978 (unpublished).

[6]An attempt to explain the coherence kernel for the magnetic substates of a given level has been given recently. See, J. L. LeGouët and P. R. Berman, Phys. Rev. A 24, 1831 (1981).

[7]See, for example, R. G. Breene, Jr., *The Shift and Shape of Spectral Lines* (Pergamon, New York, 1961); M. Baranger, in *Atomic and Molecular Processes,* edited by D. R. Bates (Academic, New York, 1962), Chap. 13; H. R. Griem, in *Plasma Spectroscopy* (McGraw-Hill, New York, 1964), Chap. 4; J. T. Jeffries, *Spectral Line Formation* (Blaisdell, Waltham, Massachusetts, 1968); I. I. Sobelman, *Introduction to the Theory of Atomic Spectra* (Pergamon, New York, 1972); S. Y. Chen and M. Takeo, Rev. Mod. Phys. 29, 20 (1957); J. Cooper, *ibid.* 39, 167 (1967).

[8]For a discussion of this effect (often referred to as "Dicke narrowing" [R. H. Dicke, Phys. Rev. 89, 872 (1953)], see P. R. Berman, Appl. Phys. (Germany) 6, 283 (1975), Sec. 5 and references therein.

[9]P. R. Berman, J. M. Levy, and R. G. Brewer, Phys. Rev. A 11, 1668 (1975); B. Comasky, R. E. Scotti, and R. L. Shoemaker, Opt. Lett. 6, 45 (1981).

[10]T. W. Mossberg, R. Kachru, and S. R. Hartmann, Phys. Rev. Lett. 44, 73 (1980).

[11]R. Kachru, T. J. Chen, T. W. Mossberg, S. R. Hartmann, and P. R. Berman, Phys. Rev. Lett. 47, 902 (1981).

[12]See, e.g., M. S. Child, *Molecular Collision Theory* (Academic, London, 1974), Chaps. 1–5.

[13]Population kernels of this type are discussed in A. P. Kolchenko, S. G. Rautian, and A. M. Shalagin, Nucl. Phys. Inst. Semiconductor Phys. Internal Report (unpublished).

[14]M. Gorlicki, A. Peuriot, and M. Dumont, J. Phys.
Lett. (Paris) 41, L275 (1980).

[15]Equation (8) is strictly true only for smoothly varying potentials for which the impulse approximation may be used. For hard-sphere scattering, condition (8) is replaced by $k(b_2-b_1) \gg 1$.

[16]The stationary phase method is valid only if $kb_j\theta^3 \gg 1$. This result may be obtained by using the asymptotic expansion

$$P_l(\cos\theta) \sim \cos[(l+\tfrac{1}{2})\theta - \pi/4]$$

and an approximation form for the phase shifts

$$\eta_l = (l+\tfrac{1}{2})(\beta - \tan\beta) - \pi/4 ,$$

valid for $kb_j \gg 1$ [the angle β is defined by $\cos\beta \approx (l+\tfrac{1}{2})/kb_j$]. The net phase appearing in Eq. (11) becomes

$$\phi = -(l+\tfrac{1}{2})(\theta - 2\beta + 2\tan\beta) + \pi/4 .$$

The point of stationary phase is given by $(l+\tfrac{1}{2}) = kb_j\cos(\theta/2)$ (classical result). If $kb_j\theta^3 < 1 \ll kb_j\theta$, then the phase ϕ is a linear function of l and there is no point of stationary phase (equivalently, the third derivative term neglected in the stationary phase method is not negligible). Consequently, Eq. (12) is valid in the range $\theta \gg (kb_j)^{-1/3}$, which is more limited than $\theta \gg (kb_j)^{-1}$.

[17]I. S. Gradshteyn and I. M. Ryzhik, *Tables of Integrals, Series, and Products* (Academic, New York, 1965).

[18]There is no point of stationary phase provided $kb_j\theta^3 \ll 1$, (see Ref. 16). This condition limits the range of validity of Eq. (15).

[19]If, for $\theta \ll 1$, one expands $P_l(\cos\theta)$ as

$$\{J_0(x) + (\theta^2/4)[(2x)^{-1}J_1(x) - J_2(x) + \tfrac{1}{6}xJ_3(x)]\}$$

(see Ref. 17), the leading correction to Eq. (14) can be shown to be of order

$$k^2b_j^2\theta^4 \ll (kb_j)^{-2/3} \ll 1 ,$$

where the first inequality follows from the condition stated in Ref. 18.

[20]In integrating the classical contribution over solid angle, one must exclude a region $\theta < (kb_j)^{-1/3}$. This exclusion leads to corrections of order $(kb_j)^{-2/3} \ll 1$.

[21]For a smoothly varying potential, the condition

$k(b_2-b_1)>>1$ would be replaced by Eq. (8).

[22]For example, if atoms having a large v_z are selected, collisions can transfer some of this "heat" to the transverse velocities.

[23]C. Bréchignac, R. Vetter, and P. R. Berman, J. Phys. Lett. (Paris) **39**, L231 (1978); Phys. Rev. A **17**, 1609 (1978); P. F. Liao, J. E. Bjorkholm, and P. R. Berman, *ibid.* **21**, 1927 (1980).

[24]T. W. Hänsch, I. S. Shahin, and A. L. Schawlow, Phys. Rev. Lett. **27**, 707 (1971); J. Brochard and P. Cahuzac, J. Phys. B **9**, 2027 (1976); P. Cahuzac and X. Drago, Opt. Commun. **24**, 63 (1978); T. W. Mossberg, A. Flusberg, R. Kachru, and S. R. Hartmann, Phys. Rev. Lett. **42**, 1665 (1979).

[25]R. Kachru, T. W. Mossberg, E. Whittaker, and S. R. Hartmann, Opt. Commun. **31**, 223 (1979); T. W. Mossberg, R. Kachru, E. Whittaker, and S. R. Hartmann, Phys. Rev. Lett. **43**, 851 (1979); see also J. L. LeGouët and P. R. Berman, Phys. Rev. A **20**, 1105 (1979), and references therein.

[26]We assume that $|\Omega'-\omega|/(\Omega'+\omega)<<1$, where ω is the transition frequency ("rotating-wave" or resonance approximation).

[27]Owing to the narrow width of the coherence kernel, one can interchange v_z and v_z' at will.

[28]If the condition $k_r b_W>>1$ is violated [see Eq. (A9) for the definition of k_r] owing to a very small perturber to active-atom mass ratio (e.g., electron perturbers), then the neglect of trajectory effects can be justified. However, if $k_r b_W>>1$ as is assumed in this work, a unified picture of the collisions mechanism is achieved only when trajectory effects are incorporated into the theory.

[29]For scattering potentials other than hard sphere, collisions usually produce a shift as well as a broadening of the profiles.

[30]J. L. LeGouët and P. R. Berman, Phys. Rev. A **17**, 52 (1978). In this paper, an approximation for the coherence kernel, similar in spirit to the one derived in this work, was used.

[31]Actually, it is combinations of the K's for the various transitions which enter (see Refs. 2 and 3).

[32]P. Cahuzac, J. L. LeGouët, P. E. Toschek, and R. Vetter, Appl. Phys. (Germany) **20**, 83 (1979).

[33]See, for example, I. D. Abella, N. A. Kurnit, and S. R. Hartmann, Phys. Rev. **141**, 391 (1966); M. Scully, M. J. Stephen, and D. C. Burnham, *ibid.* **171**, 213 (1968); S. R. Hartmann, Sci. Am. **218**, 32 (1968); C. H. Wang, C. K. N. Patel, R. E. Slusher, and W. J. Tomlinson, Phys. Rev. **179**, 294 (1969); R. L. Shoemaker, in *Laser and Coherence Spectroscopy*, edited by J. T. Steinfeld (Plenum, New York, 1978), p. 197; T. W. Mossberg, R. Kachru, S. R. Hartmann, and A. M. Flusberg, Phys. Rev. A **20**, 1976 (1979).

[34]For simplicity, we take the pulse to be resonant with the atomic transition, i.e., $K=\omega/c$.

[35]A. Flusberg, Opt. Commun. **29**, 123 (1979).

[36]A somewhat more careful evaluation of Eq. (60b) in the limit $K\delta uT>>1$ gives

$$A(v_z,T)=\exp\{-2[\gamma_{12}+\Gamma'_{12}(v_z)]T$$
$$+2\pi K^{-1}W_{12}(v_z\to v_z)\}.$$

The last term follows from Eq. (60b) if

$$\int_0^T \cos[K(v_z-v_z')t]dt$$

is replaced by $\pi K^{-1}\delta(v_z-v_z')$.

[37]A smooth Fourier-transform-limited pulse of duration $\Delta\tau$ excites a velocity bandwith $\Delta v_z\approx(K\Delta\tau)^{-1}$. If $\Delta\tau$ is chosen such that $Ku<\Delta\tau<<T$, only a fraction of the Maxwellian distribution is excited.

[38]Taking $y=0$ in Eq. (49) implies a Gaussian kernel. Equation (69) agrees with a related calculation (Ref. 9) in which a Gaussian kernel was used.

[39]Rather than directly averaging the exponent in Eq. (68), it is easier to perform the averaging in the exponent of Eq. (60b).

[40]R. G. Brewer and A. Z. Genack, Phys. Rev. Lett. **36**, 959 (1976).

[41]P. F. Liao, J. E. Bjorkholm, and P. R. Berman, Phys. Rev. A **21**, 1927 (1980), Appendix. Note that a factor of 2 is missing in the second term in the exponent in Eq. (A4) of this reference and that, in Eq. (A8), one should replace $\sqrt{2}$ by $\sqrt{\pi}$.

Laser Spectroscopy

Collision Kernels and Laser Spectroscopy

P. R. Berman

Physics Department, New York University, New York, NY 10003, USA

PACS: 07.65

Collisional processes occurring within an atomic vapor can be conveniently described in terms of collision kernels. One can speak about both the population kernels $W_{ii}(v' \to v)$ and coherence kernels $W_{ij}(v' \to v)$ $[i \neq j]$ associated with the vapor. The population kernel represents the probability density per unit time that an atom in state i undergoes a collision taking it from velocity v' to v; in essence, it determines the manner in which collisions affect the population density $\rho_{ii}(v, t)$. Analogously, the coherence kernel can be used to describe the effects of collisions on off-diagonal density matrix elements $\rho_{ij}(v, t)$; however, since $W_{ij}(v' \to v)$ is associated with atomic state coherences, it is not positive definite and has no simple classical analogue. The collision kernels are directly related to scattering amplitudes and, as such, can provide important information on collisional processes occurring within an atomic vapor. Moreover, new methods involving laser spectroscopy enable one to experimentally measure these kernels.

A theoretical analysis of the general properties of the collision kernels has been carried out. In addition, the manner in which these kernels are reflected in line shapes associated with linear and nonlinear spectroscopy has been examined. It is shown that collisions can be roughly divided into two categories. Collisions having impact parameters less than some characteristics radius h_0 can be described classically, while those collisions having impact parameter greater than h_0 must be treated quantum-mechanically. The large impact parameter collisions are associated with diffractive scattering. As a result of this division, the population kernel contains components representing both large-angle and diffractive scattering. However, assuming that the collisional interaction for states i and j differ appreciably, the coherence kernel $W_{ij}(v' \to v)$ is found to have a diffractive scattering component only. The absence of a large-angle scattering component in the coherence kernel can be linked to a collisionally-induced spatial separation of the i and j state collision trajectories.

Laser spectroscopy provides an effective means for measuring the kernels. It is shown that steady-state nonlinear laser spectroscopy provides a convenient method for determining the large-angle scattering component of the population kernel, while coherent transient techniques (e.g. delayed saturated absorption, photon echoes, stimulated echoes) can be used to monitor both the coherence kernel and the diffractive scattering component of the population kernel. A discussion of the type of information one can hope to obtain from these studies will be given. Moreover, the connection with traditional pressure broadening theories will be noted.

Collision Studies of Highly Excited Atomic States Using a New cw Four-Wave Mixing Spectroscopy Technique

J. F. Lam, D. G. Steel, and R. A. McFarlane

Hughes Research Laboratories, Malibu, CA 90265, USA

PACS: 07.65

This paper describes measurements of buffer gas collision rates with high lying atomic states on sodium using a new Doppler free spectroscopy technique. The approach uses two narrow band stabilized tunable dye lasers at frequencies Ω_1 and Ω_2 in a two photon four-wave mixing experiment. With two separate wavelengths we are able to eliminate the usually large intermediate state detuning that results when two photon resonant degenerate four-wave mixing is used to study a three level system. By appropriate geometry, the signal in our approach is generated by a pure two-quantum excitation with no stepwise contribution. We are thus able to examine collision physics affecting the final state without being obscured by intermediate state effects. We anticipate that this technique will be extremely powerful in investigating collisional effects on the Rydberg series. The ability for this technique to produce large signals even for collision studies of highly excited states overcomes sensitivity problems due to large intermediate state detuning using degenerate two-photon absorption [1]. It also provides an important laser spectroscopy measurement of collisional effects giving rise to broadening and level shifts in the frequency domain in contrast to earlier measure-
ments of broadening in the time domain using pulsed lasers [2, 3].

The analysis begins by assuming a cascade up three level system. The geometry involves a backward pump, E_b, at frequency Ω_1 (resonant with the first transition at frequency ω_{21}) and a forward pump, E_f, and probe, E_p, at frequency Ω_2 (resonant with the second transition out of level 2 at frequency ω_{32}). We assume that the forward and backward pumps are arranged to be counterpropagating and the probe beam is nearly collinear with the forward pump. We further assume that the level energies in the cascade-up three-level system are given by $E_3 > E_2 > E_1$. In this geometry the physical origin of the signal (which is nearly counterpropagating to the probe wave) arises from a four-wave mixing interaction generated by a two-photon coherence between levels 1 and 3 induced by the simultaneous interaction of E_f and E_b. In collinear geometry the resonance condition that must be satisfied in order for all four waves to interact with the same velocity group is given by $\Omega_2 - \omega_{32} = -(k_2/k_1)(\Omega_1 - \omega_{21})$. Using the density matrix approach and calculating the polarization using perturbation theory to third order in the fields [4] we find in the Doppler limit the frequency response is a Lorentzian whose linewidth is given by the two-photon linewidth γ_{13} plus a normally small correction factor, $(k_2/k_1 - 1)\gamma_{12}$, which under certain conditions gives rise to subnatural linewidths [5].

Effects of dephasing collisions are included phenomenologically to the density matrix by adding a pressure dependent complex parameter γ_{ij}^{ph} to $\gamma_{ij}(i \neq j)$. Hence the presence of buffer gas (in the form of ground state noble gas perturbers) will broaden and shift

HEAVY PARTICLE COLLISIONS

Larry Spruch[*] and Robin Shakeshaft[†]

[*]Physics Department, New York University
New York, NY 10003 U.S.A.

[†]Physics Department, University of Southern California
Los Angeles, CA 90007 U.S.A.

I. INTRODUCTION

The speaker (LS) is on record as believing that occasionally, for all its obvious disadvantages, talks should be given by those who had not been deeply involved, if at all, in the subject to be covered. Possible advantages include great freedom in the choice of topics, the lack of a compulsion to cover every detail of the topics chosen, and an objectivity (if some ignorance) in accreditation. Neither of us had been knowledgeable in two of the three topics we have chosen. To avoid pitfalls in our treatment of the third, asymmetric charge transfer, we have given a completely qualitative discussion of developments in that area.

We have obviously chosen areas we believe to be of particular significance, but having picked three areas, we cannot begin to give the details necessary for a thorough understanding. Our primary purpose is to interest those who have not read the original papers in doing so.

II. NUCLEAR RESONANCES AND THE PROBABILITY OF K-SHELL IONIZATION

If atomic physics has been enjoying a renaissance because of

new developments within the field, it is also true that there are areas of atomic physics which are so well understood that agreement between theory and experiment exceeds that in any other field of physics. It is for the latter reason that an area of interplay between atomic physics and another branch of physics can be extremely useful in studying that other branch. Thus, for example, relatively long nuclear half-lives, longer than perhaps picoseconds, can be measured directly, while relatively short nuclear half-lives, shorter than perhaps 10^{-21} seconds, can be determined by measuring the associated half-width, but intermediate half-lives can be difficult to measure by either approach. Now the orbital period of a K-shell electron in a nucleus of atomic number Z is of order $(2\pi a_0/Z)/(Ze^2/\hbar)$ or roughly $10^{-16}/Z^2$ seconds. One can then hope to determine intermediate nuclear half-lives if one can find a measurable effect of the nuclear half-life on a K-shell electron. Consider, for example, the scattering through an angle θ in the center of mass frame of a nuclear projectile P and a target nucleus T, with atomic numbers Z_P and Z_T, respectively. The incident relative kinetic energy $E_i = \frac{1}{2}Mv_i^2$, with M the reduced nuclear mass, is assumed to be in the neighborhood of a resonance with a half-life Δt. (We will talk of ionization, but the argument would be the same for excitation.) We let $P(\text{ion}) = P_{fi}(E_i,\theta)$ be the ratio of the probability of the ionization of the K-shell electron in the course of the nuclear scattering process to the probability that there is no ionization during the nuclear scattering. Ionization is from the initial (1s) state i, with normalized wave function $\phi_i(\vec{r})$, to the final continuum state with normalized wave function $\phi_f(\vec{r})$. We will find that $P(\text{ion})$ will depend upon Δt. We expect a significant effect if the nuclear width $\Gamma = \hbar/\Delta t$ is at most of the order of the binding energy U_K of the K-shell electron, or, equivalently, if the half-life or time-delay is at least of the order of the orbital period of the K-shell electron.

In section II we use capital letters for nuclear energies, momenta, coordinates (but not velocities), wave functions, and scattering amplitudes, and small letters for the corresponding electronic properties. We have $\vec{K}_i\hbar = M\vec{v}_i$ and $\vec{K}_f\hbar$ for the incident and emergent relative momenta of the nuclei, E_i and E_f for the associated energies, R for the P-T separation and V for the P-T interaction, ϵ_i for the initial K-shell energy of the electron (e⁻) and ϵ_f for the e⁻ energy in its final ionized state, and r for the T-e⁻ separation. We introduce ω via $E_i - E_f = \hbar\omega = \epsilon_f - \epsilon_i$. We will study the problem both in the semi-classical approximation (SCA) and, in the context of quantum theory, in the distorted wave Born approximation (DWBA). We now list a number of approximations which we will make in both the SCA and the DWBA. We will later list additional approximations to be made separately in the SCA and DWBA approximations. The approximations which are made more for convenience of discussion than out of dire necessity are indicated by a star. With the approximations we will make, the mathematics is trivial; in the discussion below the most difficult step is the integration of an exponential. The hard

part is of course the justification of the approximations.

i) *The recoil of T can be neglected.

ii) The P-e⁻ interaction can be treated as a perturbation; a necessary condition for the validity of (ii) is that $Z_p \ll Z_T$.

' iii) The e⁻-e⁻ interactions in the neutral target atom can be neglected.

We note that the ejected K-shell electrons have a continuous energy spectrum and therefore provide a poor signature for ionization; a good signature is provided by the X-ray radiation or by one of the Auger electron lines which follow the ionization. (Since the X-ray is emitted by an electron whose initial state is any of a number of p-states --- primarily the 2p state --- with equally populated projections of the angular momentum, and whose final state is an s-state, the X-ray radiation will be spherically symmetric.)

A. The Semi-Classical Approximation

iv') The electron will be treated quantum mechanically, but we assume that the motions of both P and T can be described classically. Indeed, in the lab frame, it follows from assumption (i) that T is always at rest.

v') We assume further that P has an impact parameter of zero with respect to T and moves with constant momentum $K_i\hbar$ from time $t = -\infty$ to $t = -\tfrac{1}{2}\Delta t$, with $R(t) = \vec{K}_i v_i(t + \tfrac{1}{2}\Delta t)$ in this interval, that P then collides with T, the two forming a composite system (with $\vec{R}(t) = 0$) for a time interval Δt, that is, until $t = +\tfrac{1}{2}\Delta t$, and that P then departs with constant momentum $K_f\hbar$, with $\vec{R}(t) = \vec{K}_f v_i(t-\tfrac{1}{2}\Delta t)$. (For inelastic nuclear scattering, one would simply replace v_i by v_f, the outgoing relative velocity, in this last expression.) The angle θ between $\vec{K}_f$ and $\vec{K}_i$ is fixed by the location of the detector.

The electron is subject to a perturbation H' which for the moment we write simply as $H'(\vec{r},\vec{R}(t))$. The amplitude a_{fi} that the electron will be in a final state f at $t = +\infty$ if it was in an initial state i at $t = -\infty$ is then given, in first order time-dependent perturbation theory, by

$$i\hbar a_{fi} = \int_{-\infty}^{\infty} e^{i\omega t} H'_{fi}[\vec{R}(t)]dt . \quad (2.1)$$

where

$$H'_{fi}[\vec{R}(t)] = \int d^3r \, \phi_f^*(\vec{r}) H'[\vec{r},\vec{R}(t)]\phi_i(\vec{r}) . \quad (2.2)$$

The dependence of a_{fi} on θ and E_i (through the presence of $\vec{R}(t)$) is often suppressed. With the changes of variables $t \to t \pm \tfrac{1}{2}\Delta t$, we can rewrite Eq. (2.1) as

$$i\hbar a_{fi} = \exp(-\tfrac{1}{2}i\omega\Delta t)[i\omega^{-1}H'_{fi}(0) + I(-\infty,0;\vec{K}_i)]$$

$$+ \exp(\tfrac{1}{2}i\omega\Delta t)[-i\omega^{-1}H'_{fi}(0) + I(0,\infty;\vec{K}_f)] . \quad (2.3)$$

where

$$I(a,b;\vec{K}) \equiv \int_a^b \exp(i\omega t)H'_{fi}(\vec{K}v_i t)dt . \quad (2.4)$$

We then have

$$P(ion) \equiv P_{fi}(E_i,\theta) = |a_{fi}(E_i,\theta)|^2 . \quad (2.5)$$

To proceed further, we would use

$$H'[\vec{r},\vec{R}(t)] = -Z_p e^2/|\vec{r}-\vec{R}(t)| . \quad (2.6)$$

Since P(ion) depends upon a_{fi} which in turn depends upon Δt (through the interference of the two terms in Eq. (2.3) for a_{fi}), a comparison of a theoretical estimate and experimental determination of P(ion) gives an estimate of Δt.

B. A Quantum Approach, in the DWBA

In addition to assuming the validity of the DWBA, we make the following assumptions.

iv") *The nuclear scattering process is an elastic one.

v") *The question of the P-T interaction V did not explicitly arise in the SCA. In the DWBA we need not specify V but we will assume that it is spin-independent and spherically symmetric, that is, that $V = V(R)$. The effects of V(R) are contained in the exact elastic nuclear scattering amplitudes which will appear; these will be denoted in general by $F(\vec{K} \to \vec{K}')$, with $\vec{K}$ denoting an arbitrary

emergent direction, and by $F(\hat{k}_f \leftarrow \hat{k}_i) \equiv F_{el}(E,\theta)$ for the scattering process of interest.

vi") θ, the angle of scattering of P, is not small.

vii") The dimension over which the effects of V are significant is very small compared to the dimension a_o/Z_T of the K-shell. This is eminently reasonable with regard to the nuclear component of V, and it is not unreasonable even with regard to the Coulomb component of V, since large-angle nuclear scattering is determined largely by V(R) at small R.

viii") We often neglect the difference between K_i and K_f (but never when either appears in an exponent).

Note that, as opposed to the SCA, the DWBA preserves conservation of linear and angular momentum and of energy.

We now invoke the DWBA, as discussed in Taylor (1972), for example, to write for the ionization amplitude $f(ion) \equiv f_{fi}(E_i,\theta)$

$$f(ion) = -(M/2\pi\hbar^2)\langle \psi^{(-)}_{\vec{K}_f}(\vec{R})|H'_{fi}(\vec{R})|\psi^{(+)}_{\vec{K}_i}(\vec{R})\rangle \quad . \quad (2.7)$$

where, in our present time-independent formalism, $H'_{fi}(\vec{R})$ differs from the $H'_{fi}[\vec{R}(t)]$ of Eq. (2.2) only in the replacement of $H'[\vec{r},\vec{R}(t)]$ by the time-independent form $H'(\vec{r},\vec{R})$. As $R \sim \infty$, the exact nuclear scattering wave function $\psi^{(+)}_{\vec{K}_i}$ behaves as

$$\psi^{(+)}_{\vec{K}_i}(\vec{R}) \sim e^{i\vec{K}_i\cdot\vec{R}} + F(\hat{R} \leftarrow \vec{K}_i)(e^{iK_iR}/R) \quad . \quad (2.8)$$

Similarly, since $\psi^{(-)*}_{\vec{K}} = \psi^{(+)}_{-\vec{K}}$, we have

$$\psi^{(-)*}_{\vec{K}_f}(\vec{R}) \sim e^{-i\vec{K}_f\cdot\vec{R}} + F(\hat{R} \leftarrow -\vec{K}_f)(e^{iK_fR}/R) \quad . \quad (2.9)$$

In line with approximation vii"), only the asymptotic forms of the nuclear wave functions are relevant. (Note that these forms contain the exact elastic scattering amplitudes.) The insertion of (2.8) and (2.9) into Eq. (2.7) gives four terms. We now make a peaking approximation:

ix") We drop all contributions involving exponentials which contain $\vec{k}_i$ or K_i and $\vec{k}_f$ or K_f unless the exponent can almost vanish, and we approximate any factor $g(\hat{k}_i,\hat{k}_f)$ of such an exponential by its

value for the direction(s) $\hat{k}_i$ and/or $\hat{k}_f$ at which the exponent almost vanishes. We therefore drop the term proportional to $\exp i(\vec{K}_i-\vec{K}_f)\cdot\vec{R}$ since the exponent is negligible only for θ very small, a region we have excluded, and we drop the term proportional to $R^{-2}\exp i(K_i+K_f)R$. In the coefficients of the terms with $\exp i(\vec{K}_i\cdot\vec{R} + K_fR)$ and $\exp i(-\vec{K}_f\cdot\vec{R} + K_iR)$, we approximate $\hat{R}$ by $-\hat{k}_i$ and by $\hat{k}_f$, respectively. Further, we use

$$K_i-K_f = (K_i^2-K_f^2)/(K_i + K_f) \approx (2M/\hbar^2)\hbar\omega/(2K_i) = \omega/v_i \quad .$$

Finally, since the angle of scattering is the same, we use rotational invariance to give $F(-\hat{k}_i \leftarrow -\hat{k}_f) = F(\hat{k}_i \leftarrow \hat{k}_f) = F_{el}(E_f,\theta)$, the last step following by definition. we drop terms in $\exp(\pm\tfrac{1}{2})(K_i + K_f)R$ after having performed the angular integration over $d\hat{R}$, and we approximate $1/K_f$ by $1/K_i$ to arrive at

$$\tilde{f}(ion) = F_{el}(E_i,\theta)\int_0^\infty H'_{fi}(\hat{k}_f R)e^{i\omega R/v_i}\,dR/v_i$$

$$+ F_{el}(E_f,\theta)\int_0^\infty H'_{fi}(-\hat{k}_i R)e^{-i\omega R/v_i}\,dR/v_i \quad .$$

Setting $t = -R/v_i$ in the second integral and $t = R/v_i$ in the first, and introducing

$$Q \equiv F_{el}(E_f,\theta)/F_{el}(E_i,\theta) \quad . \quad (2.10)$$

we have

$$P(ion) \sim |f(ion)/F_{el}(E_i,\theta)|^2 =$$

$$|I(0,\infty;\hat{k}_f) + QI(-\infty,0;\hat{k}_i)|^2 /\hbar^2 \quad (2.11)$$

where the I's, defined by Eq. (2.4), are precisely those which appeared in the SCA.

We will be concerned with the case $\hbar\omega \ll E_i$, for the probability of the electron picking up an energy comparable to E_i is negligible. If we are off resonance, it follows that we can approximate K_f by K_i and therefore Q by 1, so that P(ion) is independent of $F_{el}(E_i,\theta)$, as is to be expected; with H' treated in first order perturbation theory, for a non-resonant nuclear reaction, the back reaction of the electron on P can be neglected, f(ion) is proportional

to F_{el}, and P(ion) is independent of F_{el}. For a resonant nuclear reaction, on the other hand, the slight change from E_i to E_f can be very important. In other words, in the time independent DWBA, with the further approximation of using the asymptotic forms of the nuclear scattering wave functions, the dependence of P(ion) on the half-life of the compound nucleus originates in the strong E dependence of $F(E,\theta)$ near a resonance. More precisely, on physical grounds we might expect the energy $\hbar\omega$ given up to the K electron to be of order U_K. (Formally, this follows from the quantum matrix element $H_{fi}[\vec{R}]$ for the electron defined by Eq. (2.2) with $H'[\vec{r},R(t)]$ replaced by $H'[\vec{r},\vec{R}]$. Thus, with a factor $\exp(-Z_T r/a_o)$ from ϕ_{i1} and in the approximation in which ϕ_f is proportional to $\exp(i\vec{k}_f \cdot \vec{r})$, we expect $H_{fi}[\vec{R}]$ to fall off rapidly for k_f larger than Z_T/a_o.) If $F(E,\theta)$ is to vary significantly as E varies by an amount U_K, one must have $\Gamma \lesssim U_K$.

C. Comparison of the SCA and the DWBA

Even though energy, momentum and angular momentum are conserved in the DWBA but not in the SCA, there is a close relation between the two approaches, and indeed we have already seen that they involve the identical I integrals. The analogy can be pursued further if $\omega\Delta t \ll 1$, and if we can approximate $F(E_f,\theta) = F(E_i - \hbar\omega, \theta)$ by $F(E,\theta) - \hbar\omega\partial F(E,\theta)/\partial E$, evaluated at $E = E_i$, so that, using the quantum mechanical time delay τ defined by

$$\tau = \tau(E,\theta) = -i\hbar\partial\ell nF(E,\theta)/\partial E \quad,$$

we can write $Q = 1 - i\omega\tau$. In the SCA, we then have from Eqs. (2.5) and (2.3), writing the latter with an over-all factor $\exp(\frac{1}{2}i\omega\Delta t)$ and then using $\exp(-i\omega\Delta t) \simeq 1 - i\omega\Delta t$,

$$\hbar^2 P(ion) = \left|(1-i\omega\Delta t)I(-\infty,0;\vec{k}_i) + I(0,\infty;\vec{k}_f) + \Delta t H'_{fi}(0)\right|^2 . \quad (2.12)$$

To obtain P(ion) in the DWBA from Eq. (2.12) for P(ion) in the SCA, we must drop the last term and replace Δt by τ in the first term. The SCA and DWBA estimates of P(ion) may not be quite as close as they seem to be. Firstly, Δt is real while $\Delta\tau$ can be complex. Secondly, the DWBA P(ion) has no $H'_{fi}(0)$ term. Indeed, in the SCA, the $H'_{fi}(0)$ term originates in the $P-e^-$ interaction during the time P is at $R = 0$, while in the DWBA we used the asymptotic forms of $\Psi_i^{(+)}$ and $\Psi_f^{(-)}$, which are surely incorrect for small R and in particular at $R = 0$. To obtain the DWBA analog of the $H'_{fi}(0)$ term, one must expand the nuclear wave functions (not their asymptotic forms) in partial waves, and study the monopole component of H', originating in the region $R < r$. The point is that the possibility of P penetrating the classically forbidden region is rather larger for the

resonant than for the non-resonant case. Nevertheless, when all is said and done, the contribution from the region $R < r$ will normally be quite small; the monopole contribution can be significant, but its inclusion does not change the form of Eq. (2.12), though a slight redefinition is necessary.

We close this section with a few comments on the literature.

Similar processes had been considered earlier, but the present process was first considered, in the SCA, by Ciocchetti and Molinari (1965). Blair et al. (1978) recorded, without proof, the DWBA theoretical result. The analysis presented above follows very closely that of Feagin and Kocbach (1981). A proof of the DWBA result, somewhat of a tour de force, has been given by Blair and Anholt (1982). (The Appendix of this paper contains a study of various SCA analyses.) See also McVoy and Weidenmuller (1982). The first experiment showing the effect of the nuclear half-life on the ionization probability was described in the paper by Blair et al., referred to just above. In that experiment on ^{58}Ni and in a second on ^{88}Sr by Chemin et al. (1981), protons were elastically scattered across a resonance for which Γ was comparable in magnitude to U_K, and the effect was both expected and seen. In an experiment by Duinker et al. (1980) on the scattering of protons by ^{12}C across a resonance, the effect was seen even though it is not expected, since here Γ is much larger than U_K; this problem has not yet been resolved. A short but very nice review of a number of experiments which deeply involve the interplay of atomic and nuclear physics, not just the effect of a nuclear resonance on K-shell ionization considered here, has been given by Merzbacher (1982). See also "Two Notes on Sec. II" just before the list of references.

III. EFFECT OF COLLISIONS ON THE EMISSION OF RADIATION

A. Introduction

Consider a medium containing N two-level one-electron atoms. The n-th atom has the normalized wave function

$$\Psi^n(\vec{r}_n,\vec{R}_n,t) = A_1^n(\vec{R}_n,t)\psi_1(\vec{r}_n) + A_2^n(\vec{R}_n,t)\psi_2(\vec{r}_n) \quad, \quad (3.1)$$

where $\vec{R}_n$ locates the center of mass of the atom and where $\vec{r}_n$ is the electron coordinate relative to the atom's center of mass. The polarization (dipole moment density) of the medium at position $\vec{X}$ and time t is

$$\vec{P}(\vec{X},t) = N\vec{er}_{12}\rho_{12}(\vec{X},t) + c.c. \quad, \quad (3.2)$$

where

$$\vec{r}_{12} = \int d\vec{r} \psi_1(\vec{r}) \vec{r} \psi_2(\vec{r})^* \ , \tag{3.3}$$

and where, assuming no correlations between atoms, ρ_{12} is an off-diagonal element of the ensemble average density matrix:

$$\rho_{ij}(\vec{X},t) = \frac{1}{N} \sum_{n=1}^{N} A_i^n(\vec{X},t) A_j^n(\vec{X},t)^* \ . \tag{3.4}$$

The *polarization of the medium* or, equivalently, the "coherence" $\rho_{12}(\vec{X},t)$, governs the response of the medium to both an applied field and (as in spontaneous emission) to the vacuum field.

The population densities of states 1 and 2 in a macroscopically small region centered at X are $\rho_{11}(X,t)$ and $\rho_{22}(X,t)$, respectively. The total fractions of atoms in states 1 and 2 are $\int \rho_{11}(X,t)dX$ and $\int \rho_{22}(X,t)dX$. The populations change due to pumping and spontaneous emission (natural decay). Changes in populations due to collision induced transitions are neglected here. Changes in the coherence ρ_{12} occur because of pumping, natural decay, dipole dephasing between atoms of different velocities (Doppler broadening), and collisional decay (pressure broadening). We consider two-level atoms which do not interact with one another, and which can emit and absorb radiation and scatter from stationary (infinitely massive structureless) perturbers. Recently, new insight has been gained into the understanding of collisional effects on the coherence. We describe here the modern view of collisional effects on ρ_{12}, following closely the work of Berman (1975) and Berman et al. (1982).

B. Qualitative Discussion

Traditionally, the destruction of ρ_{12} by collisions is attributed to a loss of coherence of the phases for different values of n (phase interruption) of the products $A_1^n(\vec{R}_n,t)A_2^n(\vec{R}_n,t)^*$. (The traditional theory is described by, among others, Sobel'man (1972).) However, an alternative explanation, applicable in the classical regime, is that collisions destroy ρ_{12} by reducing the overlap of $A_1^n(\vec{R}_n,t)$ and $A_2^n(\vec{R}_n,t)^*$. To see this, we assume for simplicity that the collision is impulsive and that the scattering angle is small compared to unity. The effective potential between an active atom in state i and a perturber is, to a <u>first approximation</u>,

$$V_i(\vec{R}) = \int \phi_i(\vec{r})^* V(\vec{r},\vec{R}) \phi_i(\vec{r}) d\vec{r} \ , \tag{3.5}$$

where $\vec{R}$ is the atom-perturber separation and $V(\vec{r},\vec{R})$ is their interaction. An atom entering a collision with momentum $\hbar k$ in state i will scatter through an angle θ_i given approximately by

$$\theta_i = -\frac{1}{\hbar k} \int_{-\infty}^{\infty} \frac{\partial V_i(\vec{R})}{\partial b} dt \ , \tag{3.6}$$

where in the integrand we may write $\vec{R} = \vec{b} + \vec{v}t$, with $\vec{b}$ and $\vec{v}$ the impact parameter and velocity of the incident atom. Assuming the diffraction angle $1/(kb)$ to be small, the scattering is classical if

$$\theta_i \gg 1/(kb) \ . \tag{3.7}$$

If this condition is satisfied, the population $\rho_{ii}(\vec{R},t)$ follows a classical trajectory. The trajectories for the two populations are classically distinguishable if

$$|\theta_2 - \theta_1| \gg 1/(kb) \ , \tag{3.8}$$

in which case the overlap of $A_1^n(\vec{R}_n,t)$ and $A_2^n(\vec{R}_n,t)$ is effectively zero after the collision. Therefore, assuming that the above inequalities hold, if an atom enters a collision in a superposition state, so that initially $\rho_{12} \neq 0$, the separation of population trajectories results in ρ_{12} vanishing after the collision. While this view differs from the traditional (phase interruption) view, the difference is not so great when one considers the manner in which the overlap $A_1^n(\vec{R}_n,t)A_2^n(\vec{R}_n,t)^*$ vanishes in the classical limit; the quantum-mechanical overlap acquires a large phase which varies rapidly with $\vec{R}_n$ and the overlap vanishes when averaged over slight variations of $\vec{R}_n$. It is interesting to combine Eqs. (3.6) and (3.8); approximating $\partial V_i/\partial b$ by V_i/b, Eq. (3.8) becomes

$$\hbar^{-1}|\int[V_2(R) - V_1(R)]dt| \gg 1 \ . \tag{3.9}$$

The value of b for which the left-hand-side equals unity is denoted as b_w, the "Weisskopf radius". For $b < b_w$ collisions are classical and destroy ρ_{12} through trajectory separation (or phase interruption in the traditional view). For $b > b_w$ the scattering is nonclassical and does not destroy ρ_{12}. Thus ρ_{12} survives collisions only in the *diffractive zone*, that is, for $b > b_w$ and therefore in a narrow forward scattering cone.

C. Quantitative Discussion: Transport Equations

A more quantitative discussion requires the use of transport equations for the density matrix. To begin, we consider a beam of one-level atoms, each of mass m and incident velocity $\vec{v}$, scattering from a collection of perturbers with volume density N. The transport equation, in the form of Eq. (3.14b) below, could be written down without derivation simply on the basis of physical principles. However, we sketch a derivation here since it facilitates the derivation of the somewhat more complicated transport equations for two-level atoms. The atoms in the incident beam are assumed to have wavepackets of similar form but random impact parameters. Thus the normalized incoming wavepacket of a typical atom is

$$\phi_{in}(\vec{k}) = \exp(-i\vec{b}\cdot\vec{k})\phi_o(\vec{k})$$

where $\phi_o(\vec{k})$ is independent of the impact parameter $\vec{b}$ and is sharply peaked when $\vec{k}$ equals $m\vec{v}/\hbar$. After a collision, an atom is represented by the outgoing wavepacket $\phi_{out}(\vec{k})$, where (Taylor, 1972)

$$\phi_{out}(\vec{k}) = \phi_{in}(\vec{k}) + (1/\pi)\int d\vec{k}'\delta(k^2-k'^2)f(\vec{k}'\rightarrow\vec{k})\phi_{in}(\vec{k}'); \quad (3.10)$$

$f(\vec{k}'\rightarrow\vec{k})$ is the scattering amplitude. The ensemble average probability densities before and after the collision are $\rho_{in}(\vec{k})$ and $\rho_{out}(\vec{k})$, respectively, where the domain of integration is the cross section, area A of the incident beam,

$$\rho_a(\vec{k}) = (1/A)\int d^2b|\phi_a(\vec{k})|^2 \quad , \quad [\pm \rho_{in}(\vec{k}) = |\phi_o(\vec{k})|^2] \quad , \quad (3.11)$$

with a in or out. Now on average the beam encounters one perturber in the time interval $\tau = 1/(NvA)$. The collision rate of change of the probability density $\rho_{11}(\vec{k},t) \equiv \rho(\vec{k},t)$ is therefore

$$\frac{\partial\rho(\vec{k},t)}{\partial t}\bigg|_{coll} = \frac{\rho_{out}(\vec{k})-\rho_{in}(\vec{k})}{\tau}$$

$$= Nv\int d^2b \, [|\phi_{out}(\vec{k})|^2 - |\phi_{in}(\vec{k})|^2] \quad . \quad (3.12)$$

If Eq. (3.10) is used to substitute for $\phi_{out}(\vec{k})$ in Eq. (3.12), the integration over b may be done by assuming A to be sufficiently large that we can use, for $\vec{k}\neq\vec{k}'$

$$\int d^2b \, \phi_{in}^*(\vec{k}')\phi_{in}(\vec{k}) = (2\pi)^2\delta^2(\vec{k}_\perp' - \vec{k}_\perp)\phi_o^*(\vec{k}')\phi_o(\vec{k}) \quad , \quad (3.13)$$

where $\vec{k}_\perp$ denotes the component of $\vec{k}$ perpendicular to $\vec{v}$. An integration over the variable k' may then be done using the fact that $\phi_o(\vec{k}')$ is highly localized — see the analogous discussion of Taylor (1972), pages 49-51. Setting $\rho_{in}(\vec{k}) = \rho(\vec{k},t)$, the following transport equation is obtained:

$$\frac{\partial\rho(\vec{k},t)}{\partial t}\bigg|_{coll} = -\Gamma(\vec{k})\rho(\vec{k},t) + \int d\vec{k}'W(\vec{k}'\rightarrow\vec{k})\rho(\vec{k}',t) \quad , \quad (3.14a)$$

where, with $\sigma(\vec{k})$ denoting the total cross section,

$$W(\vec{k}'\rightarrow\vec{k}) = Nv|f(\vec{k}'\rightarrow\vec{k})|^2 \, k^{-2}\delta(k-k') \quad , \quad (3.15)$$

$$\Gamma(\vec{k}) = 4\pi(N\hbar/m)Imf(\vec{k}\rightarrow\vec{k}) = Nv\sigma(\vec{k}) = \int d\vec{k}'W(\vec{k}\rightarrow\vec{k}') \quad . \quad (3.16)$$

Note that k = k' in Eq. (3.14a) since the perturbers do not recoil. Further, k = mv/ℏ since $\phi_o(\vec{k})$ is highly localized. However, since Eq. (3.14a) is linear, it applies when $\rho_{in}(\vec{k})$ is a superposition of densities localized in different regions of k-space; hence $\rho(\vec{k},t)$ may represent a broad distribution in $\vec{k}$-space. From Eqs. (3.15) and (3.16), Eq. (3.14a) can be written in the more transparent form

$$\frac{\partial\rho(\vec{k},t)}{\partial t}\bigg|_{coll} = -Nv\sigma(\vec{k})\rho(\vec{k},t)+Nv\int d\vec{k}'|f(\vec{k}'\rightarrow\vec{k})|^2\rho(\vec{k}',t). \quad (3.14b)$$

The transport equations for the density matrix $\rho_{ij}(\vec{k},t)$, with $\rho_{ij}(\vec{k},t)$ the momentum space analog of $\rho_{ij}(\vec{R},t)$ of Eq. (3.4), of two-level atoms can be derived similarly if collision induced transitions between the two levels are neglected. We have (Berman, 1975)

$$\frac{\partial\rho_{11}(\vec{k},t)}{\partial t}\bigg|_{coll} = -\Gamma_{11}^{vc}(\vec{k})\rho_{11}(\vec{k},t) + \int d\vec{k}'W_{11}(\vec{k}'\rightarrow\vec{k})\rho_{11}(\vec{k}',t), \quad (3.17a)$$

$$\frac{\partial\rho_{12}(\vec{k},t)}{\partial t}\bigg|_{coll} = -(\Gamma_{12}^{ph}(\vec{k}) + \Gamma_{12}^{vc}(\vec{k}))\rho_{12}(\vec{k},t)$$

$$+ \int d\vec{k}'W_{12}(\vec{k}'\rightarrow\vec{k})\rho_{12}(\vec{k}',t) \quad , \quad (3.17b)$$

where, if $f_i(\vec{k}\rightarrow\vec{k}')$ is the scattering amplitude for an atom in state i,

$$W_{ij}(\vec{k}'\rightarrow\vec{k}) = Nvf_i(\vec{k}'\rightarrow\vec{k})f_j^*(\vec{k}'\rightarrow\vec{k})k^{-2}\delta(k-k') \quad , \quad (3.18)$$

$$\Gamma^{vc}_{ij}(\vec{k}) = \int d\vec{k}' W_{ij}(\vec{k} \rightarrow \vec{k}') \quad . \tag{3.19}$$

$$\Gamma^{ph}_{12}(\vec{k}) = -2\pi i N(\hbar/m)[f_1(\vec{k} \rightarrow \vec{k}) - f_2^*(\vec{k} \rightarrow \vec{k})] - \Gamma^{vc}_{12}(\vec{k}) \quad . \tag{3.20}$$

The superscript vc denotes velocity changing. If velocity changing collisions are neglected, that is, if $W_{ij}(\vec{k} \rightarrow \vec{k}') = \tilde{W}_{ij}(\vec{k}) \delta^3(\vec{k}' - \vec{k})$ so that $\Gamma^{vc}_{ij}(\vec{k}) = \tilde{W}_{ij}(\vec{k})$, the integral term and the term in Γ^{vc}_{ij} cancel in Eqs. (3.17), and these equations reduce to the much simpler equations of the traditional pressure broadening theory:

$$\frac{\partial \rho_{ii}(\vec{k},t)}{\partial t}\bigg|_{coll} = 0 \quad . \tag{3.21a}$$

$$\frac{\partial \rho_{12}(\vec{k},t)}{\partial t}\bigg|_{coll} = -\Gamma^{ph}_{12}(\vec{k}) \rho_{12}(\vec{k},t) \quad . \tag{3.21b}$$

With velocity changing collisions neglected, Γ^{ph}_{12} is, in the traditional view, the collision decay rate due to phase interruption of the atomic dipole. If velocity changing collisions are allowed but if the scattering amplitudes f_1 and f_2 are equal, it follows from Eqs. (3.18)-(3.20) and the optical theorem that $\Gamma^{ph}_{12}(\vec{k}) = 0$; thus there is no phase interruption of the atomic dipole during the collision if the atom scatters as a structureless entity.

The qualitative analysis of the previous subsection indicates that, in general, $W_{12}(\vec{k} \rightarrow \vec{k}')$ vanishes in the classical scattering regime due to trajectory separation. (More accurately, W_{12} oscillates rapidly and the integral over the classical region vanishes.) W_{12} gives a nonvanishing contribution only in the diffractive scattering region. Thus any departure from a transport equation for ρ_{12} of the form of Eq. (3.21b) arises from diffractive scattering. Such a departure may be observed by creating a photon echo, as we now briefly discuss.

D. Laser Spectroscopy

Suppose that a single-mode laser of frequency Ω interacts with the atoms. Assume the laser field $\vec{E}$ propagates in the z direction, i.e., $\vec{E} = \vec{E}_0 \cos(Kz - \Omega t)$. In the absence of collisions and under appropriate initial conditions $\rho_{12}(\vec{k},t)$ factors into

$$\rho_{12}(\vec{k},t) = \rho_{12}(\vec{k}_T) \rho_{12}(k_z,t) \tag{3.22}$$

where, following convention, we use $\rho_{12}(x)$ to denote different

functions for different arguments x, and where $\vec{k}_T$ is the component of $\vec{k}$ perpendicular to the z-axis. This factorization is assumed to hold, to a first approximation, in the presence of collisions. Substituting into Eq. (3.17b), integrating over k_T, and defining the normalization of $\rho_{12}(\vec{k}_T)$ --- it is not defined by Eq. (3.22) --- to be $\int \rho_{12}(\vec{k}_T) d^2 k_T = 1$, we find

$$\frac{\partial \rho_{12}(k_z,t)}{\partial t}\bigg|_{coll} = -[\Gamma^{vc}_{12}(k_z) + \Gamma^{ph}_{12}(k_z)] \rho_{12}(k_z,t)$$

$$+ \int dk'_z W_{12}(k'_z \rightarrow k_z) \rho_{12}(k'_z,t) \quad . \tag{3.23}$$

$$W_{12}(k'_z \rightarrow k_z) = \int d^2 k_T \int d^2 k'_T W_{12}(\vec{k}' \rightarrow \vec{k}) \rho_{12}(\vec{k}'_T) \quad . \tag{3.24}$$

$$\Gamma^\beta_{12}(k_z) = \int d^2 k_T \Gamma^\beta_{12}(\vec{k}) \rho_{12}(\vec{k}_T) \quad , \tag{3.25}$$

where β is vc or ph.

The field frequency seen in the rest frame of an atom is $\tilde{\Omega} = \Omega - Kv_z$ (Doppler shift) where $K = \Omega/c$ and $v_z = \hbar k_z/m$. If $|\tilde{\Omega} - \omega| \ll |\tilde{\Omega} + \omega|$, where ω is the transition frequency for the two atomic levels, $\rho_{12}(k_z,t)$ will oscillate in time with the field as $\rho_{12}(k_z,t) = \tilde{\rho}_{12}(k_z,t) \exp(i\Omega t)$ where $\tilde{\rho}_{12}(k_z,t)$ varies slowly with time (rotating wave approximation). From Eq. (3.23), we then have (Berman et al., 1982)

$$\frac{\partial \tilde{\rho}_{12}(k_z,t)}{\partial t}\bigg|_{coll} = -[\Gamma^{vc}_{12}(k_z) + \Gamma^{ph}_{12}(k_z)] \tilde{\rho}_{12}(k_z,t)$$

$$+ \int dk'_z W_{12}(k'_z \rightarrow k_z) \exp[iK(v_z - v'_z)t] \tilde{\rho}_{12}(k'_z,t) \quad . \tag{3.26}$$

(Note that since we are concerned here with collisional effects, we have not included a term originating in $(\partial/\partial t)\exp(i\tilde{\Omega}t)$.) This equation governs the collision rate of change of ρ_{12} in the presence of a single-mode laser. To obtain the full rate of change of ρ_{12} with time, the impact approximation is assumed. In this approximation a collision is regarded as instantaneous compared to all other relevant time scales. Then $\partial\rho_{12}/\partial t|_{coll}$ can be simply added to the time derivative $\partial\rho_{12}/\partial t|_{rad}$ due to coupling with the radiation field to give the full time derivative.

Only the diffractive scattering contributes to the integral of

Eq. (3.26). Now diffractive scattering occurs in a very narrow forward cone (assuming the atoms are not moving too slowly) and so the accompanying velocity changes are small. Let δv be the characteristic value of the velocity change $v'_z - v_z$ in the diffractive region. A coherence $\tilde{\rho}_{12}(k_z,0)$ which is prepared at time $t = 0$ will subsequently decay: let τ_c be the coherence lifetime. If $K\delta v \tau_c \ll 1$ the exponential in the integrand of Eq. (3.26) may be set equal to unity. Further, $\tilde{\rho}_{12}(k_z,t)$ is expected to vary slowly over the diffractive region so that it may be taken out of the integral of Eq. (3.26) at the value $\tilde{\rho}_{12}(k_z,t)$. In this case, the term in Γ_{12}^{vc} cancels the integral term and Eq. (3.26) reduces to the traditional equation

$$\left.\frac{\partial \tilde{\rho}_{12}(k_z,t)}{\partial t}\right|_{coll} = -\Gamma_{12}^{ph}(k_z)\tilde{\rho}_{12}(k_z,t) \ , \qquad (3.27)$$

leading to the prediction that $\tilde{\rho}_{12}$ has the decay rate $\mathrm{Re}\Gamma_{12}^{ph}(k_z)+\gamma_{12}$, where γ_{12} is the natural decay rate. (If the experimental situation involves a distribution of k_z, we must average over k_z and include the free induction decay rate due to a relative dephasing of atomic dipoles with different velocities.) However, suppose instead that $K\delta v \tau_c \gg 1$. For $t > 1/(K\delta v)$ the exponential oscillates rapidly over the diffractive region and the integral in Eq. (3.26) vanishes so we obtain (Berman et al., 1982)

$$\left.\frac{\partial \tilde{\rho}_{12}(k_z,t)}{\partial t}\right|_{coll} = -[\Gamma_{12}^{vc}(k_z) + \Gamma_{12}^{ph}(k_z)]\tilde{\rho}_{12}(k_z,t) \ , \qquad (3.28)$$

leading to the prediction of the larger decay rate $\mathrm{Re}[\Gamma_{12}^{vc}(k_z) + \Gamma_{12}^{ph}(k_z)] + \gamma_{12}$. Now τ_c, the effective coherence lifetime of ρ_{12}, depends on the experimental situation. Without going into the details of a photon echo --- a lucid discussion is given in Sargent et al., 1974 --- suffice it to say that in a photon echo experiment τ_c can be made large; the condition $K\delta v \tau_c \gg 1$ can therefore be attained and the larger decay rate confirmed. This was done recently (Mossberg et al., 1980), establishing for the first time the influence of diffractive scattering on the emission of radiation.

IV. ASYMMETRIC CHARGE TRANSFER

A measure of the great practical importance of the charge transfer process is the very considerable experimental and theoretical effort devoted to that process. The areas in which significant progress has very recently been recorded include atom capture as well as electron capture, the eikonal approximation, and versions of the Glauber approximation. Unfortunately, space permits only one topic, an important step in our understanding of asymmetric charge transfer.

To appreciate this step, it will be useful to consider earlier developments in asymmetric and symmetric charge transfer. There have been a number of relatively recent reviews in these areas (Basu et al., 1978; Belkić et al., 1979; Shakeshaft and Spruch, 1979; Shakeshaft, 1982), and we limit ourselves to some brief comments.

We wish to consider electron capture by a projectile P (a bare nucleus of charge $Z_p e$) incident with a high velocity $\vec{v}$ on a neutral atom. The target nucleus T has a charge $Z_T e$, and the process is

$$P^{(Z_p)} + Atom \longrightarrow P^{(Z_p-1)} + Ion^{(+1)} \ .$$
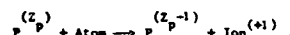
One must and can do better (Briggs and Taulbjerg, 1979) but we assume that all electron-electron interactions are negligible. In a Born expansion in a non-relativistic context, the n-th term represents the contribution associated with n scatterings. We make one remark on potential scattering (scattering by a target with no internal degrees of freedom) before considering charge transfer. The Born expansion, for sufficiently large incident energy E and f... many potentials, is a convergent expansion in powers of V/E, where V is a characteristic value of V. The first Born term therefore dominates for sufficiently large E for potential scattering.

We begin our consideration of charge transfer by studying the symmetric case, for which $Z_p = Z_T \equiv Z$. In the first Born term, the main contribution originates in components of the target and final bound state wave functions for which the velocity of the electron is comparable with $\vec{v}$, and those amplitudes are very small for v large --- more precisely, for $v \gg e^2/\hbar$, a characteristic electron velocity in the initial and final state --- even if, as we do for simplicity, we consider capture from and to ground states. The second Born term can be described roughly as follows. The electron can initially have a small speed, for it is given a speed close to v in a close collision with P. The electron then moves, in this intermediate state, almost as a free particle. (The uncertainty in its energy is $\Delta E \approx p \Delta p/m \approx \hbar v/a$, with a an atomic dimension, so that $\Delta E/E$ falls off as $1/v$, but the off-the-energy shell component gives a significant contribution). The electron is then scattered elastically by T, emerging with velocity close to $\vec{v}$, and is captured. The second Born term dominates over the first even though it involves an additional collision (and therefore an additional factor, proportional to e^2, which often suggests that the term involved is of higher order) because the second Born term does not require high speed components in the initial and final bound states. It is widely believed, though it has not been proved, that higher order Born terms are dominated by the second, for they suffer from having still further factors of e^2, and they have no compensating advantages since the second Born term already allows low velocities in

the initial and final states.

For many applications of great current interest, one has Z_p small, say unity, but $Z_T \gtrsim 5$, and incident energies E such that v is rather large compared to $Z_p e^2/\hbar$ but not compared to $Z_T e^2/\hbar$. It is then inappropriate to ignore multiple e^--T collisions; rather, all e^--T collisions must be included. However, we can continue to ignore multiple e^--P collisions. In the present asymmetric analog of the second Born term in the symmetric case, the electron in the intermediate state is described by a Coulomb wave rather than by a plane wave. A natural starting point is to assume that the Coulomb wave is on the energy shell. This amounts to the impulse approximation, developed largely in this context by Briggs (1977) and also by Kocbach (1980) and Amundsen and Jakubassa (1980). While this approach gives good results at larger incident energies, theory and experiment begin to disagree at energies rather above the value at which the disagreement had been expected. The point is that the off-the-energy-shell component of the intermediate state wave function --- now a Coulomb wave --- must be retained. The analysis is tricky, and requires further approximations. It is a major achievement that the final result is obtained in tractable form: the predicted asymmetric charge transfer cross section differs from the impulse approximation prediction by a rather simple factor, one which gives considerably better agreement with the data at lower energies. We note incidentally that this work not only provides a theoretical foundation for asymmetric charge transfer but also provides much deeper insight into a number of earlier approaches, placing them in a hierarchy of successive approximations. See Macek and Taulbjerg (1981), Briggs, Macek and Taulbjerg, to be published, and Macek and Alston, to be published.

Two Notes on Sec. II:

1) Many intermediate nuclear half-lives can be determined by means independent of the measurement of P(ion) --- most generally by matching scattering data to the Breit-Wigner formula, but also by using special techniques, such as channeling. One time interval which might be determined most easily by a measurement of P(ion) is the time interval during which two heavy ions remain in one another's neighborhood in the course of a scattering process.

2) The argument of the first paragraph of Sec. II can be reversed; one can use a detailed knowledge of the properties of a nuclear resonance to determine an atomic property. Thus, let us rewrite the equation above Eq. (2.10) as

$$f(ion) = F_{e\ell}(E_i,\theta)A + F_{e\ell}(E_f,\theta)B$$

where A and B depend only upon atomic properties. This form remains valid even if one includes contributions from small values of R. Now assume, for example, that the nuclear resonant state is an $s_{\frac{1}{2}}$ state, and choose θ to be $90°$ so that the only relevant interference term arises from the monopole term, with both P and e^- emerging in spherically symmetric distributions. One can then show that $B = A^*$. If one were not at a resonance, one would have $F_{e\ell}(E_i,\theta) \approx F_{e\ell}(E_f,\theta)$, and therefore $f(ion) \approx 2 F_{e\ell}(E_i,\theta)ReA$. At resonance, however, one can also, at least in principle, determine the imaginary component of A. It is not clear however if theory and experiment are now good enough to determine ImA. (See Blair et al., 1978, and references therein.)

References

Amundsen, P.A. and D. Jakubassa, 1980, Charge transfer in asymmetric heavy-ion collisions, J. Phys. B, 13:L467.

Basu, D., S.C. Mukherjee and D.P. Sural, 1978, Electron capture processes in ion-atom collisions, Physics Reports, 42:145.

Belkic, Dz., R. Gayet and A. Salin, 1979, Electron capture in high-energy ion-atom collisions, Physics Reports, 56:279.

Berman, P.R., T.W. Mossberg and S.R. Hartman, 1982, Collision kernels and laser spectroscopy, Phys. Rev. A, 25:2550.

Blair, J.S., P. Dyer, K.A. Snover, and T.A. Trainor, 1978, Nuclear "time-delay" and X-ray-proton coincidences near a nuclear scattering resonance, Phys. Rev. Lett., 41:1712.

Blair, J. and R. Anholt, 1982, Theory of K-shell ionization during nuclear resonance scattering, Phys. Rev. A, 25:907.

Briggs, J.S., 1977, Impact-parameter formulation of the impulse approximation for charge exchange, J. Phys. B, 10:3075.

Briggs, J.S. and K. Taulbjerg, 1979, Charge transfer by a double-scattering mechanism involving target electrons, J. Phys. B, 12:2565.

Briggs, J., J. Macek, and K. Taulbjerg, Theory of asymmetric charge transfer, Comment. At. Mol. Phys., in press.

Chemin, J.F., R. Anholt, Ch. Stoller, W.E. Meyerhoff, and P.A. Amundsen, 1981, Measurement of ^{85}Sr K-shell ionization probability across the nuclear elastic-scattering resonance at 5060 keV, Phys. Rev. A, 24:1218.

Ciochetti, G. and A. Molinari, 1965, K electron shell ionization and nuclear reactions, Nuovo Cimento, 40B:69.

Duinker, W., J. van Eck, and A. Niehaus, 1980, Experimental evidence for the influence of inner-shell ionization on resonant nuclear scattering, Phys. Rev. Lett., 45:2102.

Feagin, J.M. and L. Kocbach, 1981, Inner-shell excitation in central collisions of light ions with atoms: an interplay between atomic and nuclear processes, J. Phys. B: At. Mol. Phys., 14:4349.

Kocbach, L., 1980, Impulse approximation calculations for capture

of K-shell electrons by fast light nuclei, J. Phys. B, 13:L665.

Macek, J. and K. Taulbjerg, 1981, Correction to Z_p/Z_T expansions for electron capture, Phys. Rev. Lett., 46:170.

Macek, J. and S. Alston, Theory of electron capture from a hydrogen-like ion by a bare ion, Phys. Rev. A, in press.

McVoy, K.W. and H.A. Weidenmüller, 1982, Analysis of K-shell ionization accompanying nuclear scattering, Phys. Rev. A, 25:1462.

Merzbacher, E., 1982, The interplay between nuclear and atomic phenomena in ion-atom collisions, in Proceedings of the Divisional Conference of the European Physical Society on "Nuclear and Atomic Physics with Heavy Ions", Bucharest, Romania, June 1981, to be published.

Mossberg, T.W., R. Kachru and S.R. Hartmann, 1980, Observation of collisional velocity changes associated with atoms in a superposition of dissimilar electronic states, Phys. Rev. Lett., 44:73.

Sargent, M., M.O. Scully and W.E. Lamb, 1974, Chap. 13, in "Laser Physics", Addison-Wesley, Reading.

Shakeshaft, R., 1982, Atomic rearrangement collisions at asymptotically high impact velocities, in "Invited Papers of the XII International Conference on the Physics of Electronic and Atomic Collisions", Gatlinberg, Tennessee, July 1981, S. Datz (editor), North Holland, Amsterdam.

Shakeshaft, R. and L. Spruch, 1979, Mechanism for charge transfer (or for the capture of any light particle) at asymptotically high impact velocities, Rev. Mod. Phys., 51:369.

Sobel'man, I.I., 1972, Chap. 10, in "Introduction to the Theory of Atomic Spectra", Pergamon, New York.

Taylor, J.R., 1972, in "Scattering Theory", Wiley, New York.

COMBINED RADIATION FIELD - COLLISIONAL EXCITATION OF ATOMS

PAUL R. BERMAN and EDWARD J. ROBINSON
Physics Department, New York University, 4 Washington
Place, New York, New York 10003 U.S.A.

__Abstract__ The physical principles underlying the com-
bined radiation field - collisional excitation of atoms
are reviewed. A discussion of both collisionally-
aided radiative excitation ("optical collisions") and
radiatively-aided inelastic collisions ("radiative
collisions") is presented.

INTRODUCTION

The purpose of this paper is to present a simple discussion
of atomic transitions induced by the simultaneous action of
a laser field and a collision.

Consider a reaction of the general form

$$A_i + B_i + \hbar\Omega \rightarrow A_f + B_f, \tag{1}$$

where $A_{i,f}$ and $B_{i,f}$ are internal states of two atoms A and
B undergoing a collision and Ω is the frequency of an
applied radiation field. If, in the absence of the colli-
sion, one finds

$$A_i + \hbar\Omega \rightarrow A_i$$

$$B_i + \hbar\Omega \rightarrow B_i$$

while, in the absence of the external field, one has

$$A_i + B_i \rightarrow A_i + B_i.$$

1

the reaction (1) is of a type that requires the simultaneous presence of both a collisional interaction and external radiation field if either or both final atomic states are to differ from the initial ones. One may then speak of "laser-assisted collisions" or "collisionally-assisted light absorption". These are processes which have been the focus of a large number of experimental[1-16] and theoretical[17-46] investigations in the last decade. In this work, we discuss the physical principles underlying such reactions; more detailed theoretical treatments may be found in the literature.

Reactions of the form (1) may be further classified into two categories. The first of these we refer to as Collisionally-Aided Radiative Excitation[37] (CARE) and has been designated by others as "optical collisions".[19] The CARE reaction is easy to visualize (see Fig. 1). An atom A
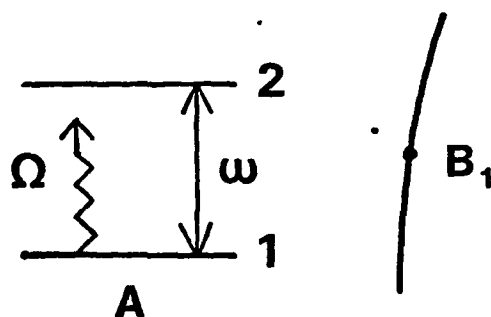

Figure 1. A schematic representation of the CARE reaction $A_1 + B_1 + \hbar\Omega \rightarrow A_2 + B_1$. A laser field of frequency Ω is incident on atom A and can drive the 1-2 transition when atom A undergoes a collision with a ground state perturber B.

is irradiated by a laser field whose frequency Ω is close

COMBINED RADIATION FIELD - COLLISIONAL EXCITATION

enough to that of an atomic transition for a two-level
approximation to be valid. The field's frequency is de-
tuned from exact resonance by an amount Δ which is large
compared to the natural and Doppler widths of the transi-
tion, but small compared to the thermal energy divided by $\hbar$.
With such a large detuning, the probability for the field
to excite atom A is negligibly small. However, if A under-
goes a collision with atom B while interacting with the
field, the probability for excitation can be greatly en-
hanced. The energy mismatch $\hbar\Delta$ between the photon and
atomic transition energies is compensated for by a corres-
ponding change in the translational energy of the colliding
atoms.

The second class of reactions of the type (1) we refer
to as Radiatively-Aided Inelastic Collisions[37] (RAIC) and
has been designated by others as "radiative collisions"[17]
or "LICET - Laser Induced Collisional Excitation Trans-
fer".[3] Atoms A and B are prepared in initial states A_i and
B_i and, as a consequency of the combined atom-atom and atom-
field interactions, they emerge in some new final states
A_f and B_f. The process is depicted schematically in Fig. 2.

The transition between initial and final states is
assumed to be highly improbable or energetically forbidden
in the absence of the applied field. Thus, one can view
the photon as providing the energy to assist the inelastic
transition $A_i + B_i \rightarrow A_f + B_f$. In general the RAIC cross-
section will be largest if the photon frequency is chosen
to be resonant with the energy difference between initial
and final composite atomic states. However, as in CARE,
significant excitation can occur under off-resonance condi-
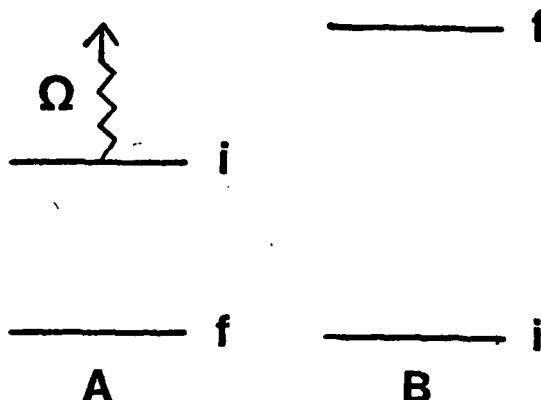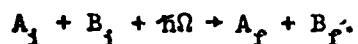tions, with the energy mismatch again compensated by a

3

Figure 2.   Atoms A and B undergo a collision in the pre-
sence of radiation. The field frequency Ω is approxi-
mately equal to a transition frequency in the composite
AB system. The RAIC reaction is of the form
$A_i + B_i + \hbar\Omega \rightarrow A_f + B_f$.

change in translational energy.

Before examining CARE and RAIC in greater detail, it is
useful to review the problem of the interaction of a radia-
tion pulse with a two-level atomic system.

ATOM + PULSE

In this section, we examine the interaction of a two-level
atom with a radiation pulse whose electric field of polari-
zation $\hat{\epsilon}$ may be represented by

$$\underline{E}(t) = \hat{\epsilon}E_o(t)\cos(\Omega t),$$

The smooth pulse envelope function $E_o(t)$ is assumed to

COMBINED RADIATION FIELD – COLLISIONAL EXCITATION

vanish as $t \to \pm\infty$ and to vary slowly in comparison with $\cos(\Omega t)$. The difference $|\Omega - \omega|$, where ω is the atomic transition frequency, is taken to be much less than $(\omega + \Omega)$, allowing one to neglect the "anti-rotating" components of the field. For an atom which is in its lower state 1 at $t = -\infty$, we seek the probability that it is excited to state 2 following its interaction with the pulse. Taking the atom-field interaction to be

$$V(t) = -\underline{\mu}\cdot\underline{E}(t),$$

where $\underline{\mu}$ is the atomic dipole moment operator, one may use Schrödinger's equation to obtain the time evolution equations for the state amplitudes. In the interaction representation and with the neglect of the anti-rotating components of the field, one finds

$$\dot{a}_1 = -i\chi(t)\, e^{i\Delta t}\, a_2\, . \qquad\qquad \text{(2a)}$$

$$\dot{a}_2 = -i\chi(t)\, e^{-i\Delta t}\, a_1, \qquad\qquad \text{(2b)}$$

where $\Delta = \Omega - \omega$ is the detuning, $\chi(t) = \mu E_o(t)/2\hbar$ is the coupling parameter, and $\mu = \langle 1|\underline{\mu}\cdot\hat{\varepsilon}|2\rangle = \mu^*$. The frequency $\chi(t)$ is sometimes referred to as the Rabi frequency.

The problem is conveniently described in terms of the following parameters: (1) the pulse duration T, (2) the frequency $f = \dot{\chi}(t)/\chi(t)$ which determines the frequency components characterizing the pulse, (3) the natural lifetimes of states 1 and 2 which are taken to be much longer than T, justifying the omission of decay terms in Eqs. (2), (4) the detuning Δ, and (5) the Rabi frequency $\chi(t)$. As a simplification, we set $f \approx T^{-1}$, which is a good approximation for smooth pulses.

5

P. R. BERMAN AND E. J. ROBINSON

If the detuning and envelope function are such that $|\Delta|T \gg 1$, the pulse contains negligibly small Fourier components at the frequency needed to compensate for the detuning. In this limit, the pulse is said to be adiabatic. That is, the excitation probability following the passage of the pulse is vanishingly small, i.e., proportional to $\exp(-2|\Delta|T)$ for typical envelope functions. It is interesting to note that the excitation probability remains exponentially small regardless of field strength $\chi(t)$, reflecting the fact that the Fourier components needed to effect the excitation are essentially absent. As the field strength $\chi(t)$ increases, the excitation probability, which is proportional to $A^2 = |\int_{-\infty}^{\infty}\chi(t)dt|^2$ for $A^2 \ll 1$, exhibits some type of saturation behavior for $A^2 > 1$. Thus, without some additional interaction, an adiabatic pulse cannot appreciably excite the atom. The "additional interaction" can be provided by a collision.

CARE

Assume that the atom undergoes a collision with a perturber during its interaction with the adiabatic radiation pulse. This collision occurs on a time scale τ_c (typically 10^{-12} sec for the thermal atoms under consideration here) which is short compared to T (typically 10^{-9} sec). The perturber can be considered as providing an effective time-dependent potential which modifies the energy separation of states 1 and 2 in a transient manner. If $\hbar V_i(t)$ is the collision-induced modification of level i's energy, then the instantaneous transition frequency is

$$\omega(t) = \omega + V_{LS}(t),$$

6

COMBINED RADIATION FIELD - COLLISIONAL EXCITATION

where

$$V_{LS}(t) = V_2(t) - V_1(t).$$

It is implicitly assumed that $V_1(t) \neq V_2(t)$, as is generally the case if levels 1 and 2 belong to different electronic configurations.[47] The collision does not have sufficient energy to couple levels 1 and 2 in the absence of the field (see Fig. 1).

The effect of the collision-induced transient variation of the transition frequency is to introduce appreciable Fourier components into the excitation mechanism at frequencies up to $\omega_c = \tau_c^{-1} \gg T^{-1}$. These added Fourier components lead to a new contribution to the excitation probability which is much larger than the $\exp(-2|\Delta|T)$ term associated with the atom-adiabatic pulse interaction. This "collisionally-assisted" contribution leads to a CARE reaction of the form

$$A_1 + B_1 + \hbar\Omega \rightarrow A_2 + B_2.$$

The state amplitudes now evolve according to

$$\dot{a}_1 = -i\chi(t)\exp[i\Delta t - i\int_0^t V_{LS}(t')dt']a_2 \tag{3a}$$

$$\dot{a}_2 = -i\chi(t)\exp[-i\Delta t + i\int_0^t V_{LS}(t')dt']a_1, \tag{3b}$$

subject to the initial conditions

$$a_1(-\infty) = 1, \quad a_2(-\infty) = 0. \tag{3c}$$

In order to discuss CARE, it is useful to again refer to the various time scales in the problem. The collision duration, $\tau_c(b,v_r) \approx b/v_r$, where b is the impact parameter and v_r the interatomic speed associated with a collision, is an important time parameter. Although $\tau_c(b,v_r)$ varies

7

from collision to collision, we can define a representative time $\tau_c \equiv \tau_c(b_o, \bar{v}_r)$ in which $\bar{v}_r$ is the average interatomic relative speed and b_o is an impact parameter chosen to guarantee that τ_c is "representative". Generally speaking, b_0 will be that impact parameter for which the phase $\int_{-\infty}^{\infty} V_{LS}(b, \bar{v}_r, t)dt$ takes on a value of order unity; a typical value for b_o is 10^{-7}cm. The dimensionless parameters which enter our considerations are $|\Delta|T$ which turns out to be unimportant, $|\Delta|\tau_c$ which critically categorizes the detuning, $\chi(t)T$ which represents the strength of the atom-field interaction before and after the collision, and χT which represents the strength of the atom-field interaction during the collision. The field strength $\chi(t)$ is approximately constant during a collision and χ represents some characteristic value of $|\chi(t)|$ for the pulse. As noted above, $\tau_c/T \ll 1$.

Weak Fields: $\chi T \ll 1$

For weak fields, the excitation probability can be calculated from Eqs. (3) using first-order perturbation theory. The results depend critically on the value of $|\Delta|\tau_c$.

If $|\Delta|\tau_c \ll 1$, the only change in state amplitude a_2 during the collision arises from the level-shifting term. The collision acts to provide a sudden change in the phase ϕ of a_2, given by $\phi(b, v_r) = \int_{-\infty}^{\infty} V_{LS}(b, v_r, t)dt$. This impulse destroys the adiabatic response of the two-level system, and gives a final state amplitude

$$a_2 = -i[\int_{-\infty}^{t_c} \chi(t') e^{-i\Delta t'}dt' + e^{i\phi}\int_{t_c}^{\infty}\chi(t')e^{-i\Delta t'}dt']$$

$$= -2i[\chi(t_c)/\Delta]e^{-i\Delta t_c}e^{i\phi/2}\sin(\phi/2),$$

where t_c is the time at which the collision occurs. Setting $|\chi(t_c)| \equiv \chi$, one obtains the excitation probability

8

COMBINED RADIATION FIELD – COLLISIONAL EXCITATION

$$|a_2(b,v_r,\infty)|^2 = 4(\chi/\Delta)^2 \sin^2[\phi(b,v_r)/2] \qquad (4)$$

and the corresponding CARE cross section

$$\sigma_c(v_r) = 2\pi \int_0^\infty |a_2(b,v_r,\infty)|^2 b\,db \qquad (5a)$$

$$\approx 2(\chi/\Delta)^2 (\pi b_0^2). \qquad (5b)$$

The result (4-5) is known as the "impact limit" since τ_c is smaller than any other time scale in the problem. The impact cross-section is independent of the sign of Δ since the Fourier transform of the collision interaction is flat over the range of Δ represented by $|\Delta|\tau_c \ll 1$.

The impact result can be viewed in an alternative manner. If we were to suddenly interrupt the atom-radiation pulse interaction at any time t_c, we would, on average, find a population $[\chi(t_c)/\Delta]^2$ in the upper state. The CARE cross-section is equal to the product of this excitation probability and the collision cross section $(\approx \pi b_0^2)$.

If $|\Delta|\tau_c > 1$, the phase induced in a_2 during the collision by the detuning is not negligible, and the impact result is not valid. As we have seen, one consequence of the collision is to shorten the relevant time from T to τ_c, so that appreciable Fourier components up to τ_c^{-1} are introduced. If this were all that occurred, one would expect a CARE transition probability that varied as $\exp[-2|\Delta| \tau_c(b,v_r)]$. However, there is an additional effect, whose origin may be seen in Fig. 3, which modifies this result. In drawing the energy levels in Fig. 3, we have chosen $V_{LS}(t) < 0$; the case for arbitrary $V_{LS}(t)$ may be treated by an obvious generalization of the method given below.
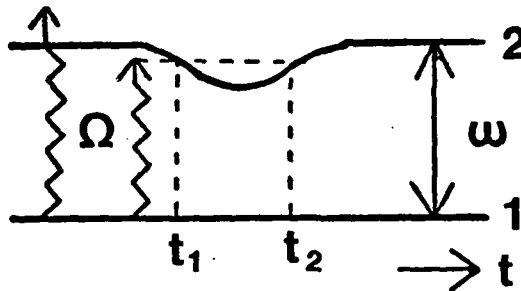
9

Figure 3. Energy levels of atom A during a collision. "Instantaneous resonances" $[\Omega \approx \omega(t)]$ can occur for detunings $\Delta < 0$ only; for $\Delta > 0$, the collision detunes the atomic transition further from resonance.

The CARE cross section is a strongly asymmetric function of Δ when $|\Delta|\tau_c > 1$. For a given $\Delta < 0$, collisions can always produce $\omega(t) \approx \Omega$ for short times during the collision;[48] i.e., the systems become instantaneously resonant with the field. Such times are labeled t_1 and t_2 in Fig. 3. The phase of a_2 varies rapidly owing to the factor $\exp(-i\Delta t)$, except at t_1 and t_2, where the oscillation is suppressed by the factor $\exp[i \int_{\bullet}^{t} V_{LS}(t')dt']$. The major contributions to the excitation amplitude are provided by these times of stationary phase. The corresponding CARE cross-section varies as an inverse power law in $|\Delta|$, instead of the exponential that characterizes other regimes. The fact that the points of stationary phase provide the major contributions to $a_2(\infty)$ is linked to the condition $|\Delta|\tau_c > 1$. That is, the (pulse + collision) does not contain the Fourier components at Δ to appreciably excite the atom; in this case the instantaneous resonances become a critical feature. In the

10

COMBINED RADIATION FIELD - COLLISIONAL EXCITATION

impact limit, the system of (pulse + collision) does
have appreciable Fourier coefficients at Δ so that the
presence or absence of instantaneous resonances does not
affect the excitation amplitude.

In contrast to the $\Delta < 0$ case, for $\Delta > 0$ the colli-
sion pushes the levels further away from resonance (see
Fig. 3). The net result of this level displacement is
that the nonresonant side of the CARE cross section falls
off exponentially as a fractional power of $|\Delta|\tau_c$, even
after one averages over impact parameter.[19,46,49,50]
Thus, the CARE cross-section exhibits a marked asymmetry,
with an inverse power law dependence on $|\Delta|$ on one side,
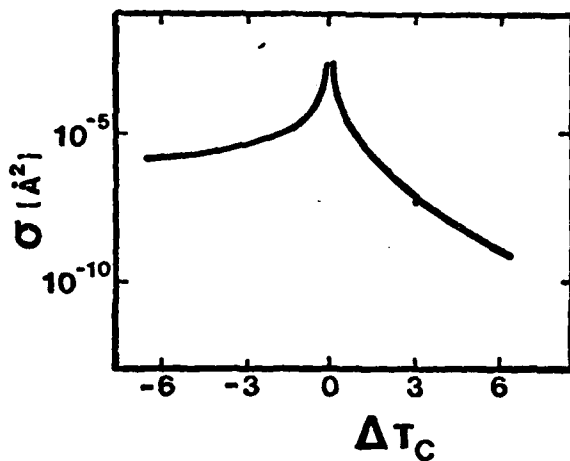and an exponential decay on the other. A typical pro-
file is shown in Fig. 4.

Figure 4. CARE cross section as a function of $|\Delta|\tau_c$
in the weak field limit, $\chi\tau_c \simeq 1.0\times10^{-4}$. This cross
section is drawn for a level-shifting term which varies
as R^{-6} (R is the interatomic separation) and a value
$b_o \simeq 1.1\times10^{-7}$ cm (see Ref. 37).

11

It should be noted that CARE cross-section in the weak-field regime can also be obtained using traditional pressure broadening theories of linear absorption or emission.[49-52]

Strong Fields: $\chi T > 1$

As long as $\chi < |\Delta|$, the previous perturbative treatment is valid and the CARE cross-section is proportional to χ^2. If both $\chi T > 1$ and $\chi > |\Delta|$, the perturbation theory fails, and a strong field theory is required. Space limitations preclude a detailed description of such a theory, which is conveniently developed using a quantized-field – dressed-atom approach, but we cite some of the results.

For $\chi > |\Delta|$ and $\chi\tau_c < 1$ (which implies $|\Delta|\tau_c \ll 1$), one is still in the impact domain since the collision time τ_c is the shortest time scale in the problem. If the atom – radiation pulse interaction is interrupted at some arbitrary time, one would find an upper state population approximately equal to 1/2 since the field is sufficiently strong ($\chi T > 1$) to lead to equal populations, on average, in levels 1 and 2. (This factor of 1/2 should be compared with the average population $(\chi/\Delta)^2$ found in the weak field case). Thus, in this limit, the CARE cross-section is approximately equal to $\pi b_o^2/2$, independent of both Δ and χ.

For $\chi > |\Delta|$ and $\chi\tau_c > 1$, an impact theory can no longer be used. During the collision, the field is strong enough to lead to rapid oscillations (so-called Rabi oscillations) in the state amplitudes. Since $\chi > |\Delta|$, these Rabi oscillations provide the dominant phase variation for the state amplitudes; the effective detuning in the problem becomes χ instead of $|\Delta|$. There is no possi-
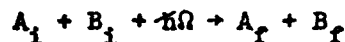
12

bility of "instantaneous resonances" here; consequently, the excitation probability varies as $\exp[-2\chi\tau_c(b,v_r)]$. Just as in the weak-field result for the $\Delta > 0$ case, the CARE cross-section obtained after averaging over impact parameter falls off exponentially as a fractional power of $\chi\tau_c$.[19]

RAIC

A typical RAIC reaction of the form

$$A_i + B_i + \hbar\Omega \rightarrow A_f + B_f$$

is illustrated in Fig. 2. In going from the initial to final state in the composite AB system, a number of intermediate states may play a role. However, by summing over these states and neglecting the effect of small variations in nonresonant energy denominators, one may reduce the problem to that for a two-level system coupled by an effective operator $U(t)$ which is proportional to the product of the radiation field amplitude and the collisional interaction. Explicitly we write

$$U(t) = \hbar(\chi/\bar{\omega})\, V_c(t),$$

where $\bar{\omega}$ is some representative frequency denominator ($\bar{\omega} \gg \chi$) and $V_c(t)$ is the collisional interaction. Since $U(t) = 0$ in the absence of a collision, the RAIC interaction occurs during the collision only. Thus the pulse time T plays no role at all in RAIC - the relevant time scale in the problem is the collision duration τ_c.

The initial and final state amplitudes for the combined AB system (see Fig. 2) obey the equations

13

P. R. BERMAN AND E. J. ROBINSON

$$\dot{a}_i = -i(\chi/\bar{\omega})V_c(t)\exp[i\Delta t - i\int_0^t V_{LS}(t')dt']\,a_f \qquad (6a)$$

$$\dot{a}_f = -i(\chi/\bar{\omega})V_c(t)\exp[-i\Delta t + i\int_0^t V_{LS}(t')dt']\,a_i, \qquad (6b)$$

where

$$\Delta = \hbar\Omega - (E_f - E_i)$$

and $V_{LS}(t)$ is the same collisional energy level shift en-
countered in CARE. An additional contribution to level
shifts resulting from the AC Stark effect will not be dis-
cussed here, but can be included by redefining the energy
levels at their Stark-shifted values.

Weak Fields

A perturbative treatment is valid provided $|a_f(t)| \ll 1$,
in which case

$$|a_f(\infty)| \simeq |(\chi/\bar{\omega})\int_{-\infty}^{\infty} V_c(t)\exp[-i\Delta t + i\int_0^t V_{LS}(t')dt']dt|.$$

If $|\Delta|\tau_c \ll 1$, the amplitude for excitation is independent
of Δ. For $|\Delta|\tau_c > 1$, one again finds an asymmetric line ow-
ing to the effects of instantaneous resonances which occur
for one sign of Δ but not the other.[53]

The functional forms of $V_c(t)$ and $V_{LS}(t)$ determine
where the maximum RAIC cross section occurs as a function
of Δ. In a typical situation, the time-dependence of
$V_c(t)$ and $V_{LS}(t)$ is roughly similar and the maximum RAIC
cross section occurs for $\Delta \simeq 0$. However, the RAIC maximum
may occur for $\Delta \neq 0$ if the duration associated with $V_c(t)$
is much smaller than that associated with $V_{LS}(t)$, as
might be the case in RAIC charge transfer[33], where, for
an interatomic separation $R(t)$, $V_c(t) \propto \exp[-CR(t)]$,
while $V_{LS}(t) \propto [R(t)]^{-n}$. Under these conditions, the

14

COMBINED RADIATION FIELD – COLLISIONAL EXCITATION

collisional coupling is significant only when $V_{LS}(t)$ is producing a relatively large variation in the atoms' energy levels. Since the effective level separation of the composite AB system is no longer $E_f - E_i$ during the time that the collisional coupling occurs, it is not surprising that the maximum RAIC cross section can be displaced from $\Delta = 0$.

Strong Fields

To get some idea of strong field effects, consider Eqs. (6) in the limit that $\Delta = 0$ and with the level-shifting term set equal to zero. In that case, the upper state probability varies as

$$|a_2(b,v_r,\infty)|^2 = \sin^2[\phi_R(b,v_r)],$$

where

$$\phi_R(b,v_r) = (\chi/\bar\omega)\int_{-\infty}^{\infty} V_c(b,v_r,t)dt.$$

The RAIC cross-section is equal to πb_R^2 where b_R is an impact parameter for which ϕ_R is of order unity. For a power law potential $V_c(t) \propto [R(t)]^{-n}$, $n \geq 3, \phi_R \propto \chi/b^{n-1}v_r$ and b_R^2 varies as $(\chi/v_r)^{2\alpha}$ with $\alpha = (n-1)^{-1}$. The RAIC cross-section, which is proportional to χ^2 for weak fields, varies as $\chi^{2/(n-1)}$ (i.e. as the square root of the intensity for n=3) in the strong field limit. For strong fields, owing to the fact that $b_R \propto \chi^\alpha$, large impact parameter collisions only are important and V_{LS} plays a minor role for such collisions. The line width is determined by the inverse collision time $\tau_c^{-1} = v_r/b_R \propto v_r^{\alpha+1}\chi^{-\alpha}$; the RAIC profile narrows with increasing field strength.

The ratio b_R/b_o can be used as a measure of the field strength. If $b_R > b_o$, one is in the strong field region since the upper state amplitude saturates at radii where the level-shifting effect is unimportant. On the other hand, for $b_R \ll b_o$, the collisional coupling can not overcome the effects of level-shifting and a perturbative treatment is valid. Typically[4], the transition from weak to strong field occurs for field strengths of order $10^8 W/cm^2$. The strong field effects in RAIC and CARE are fundamentally different. In RAIC, the upper state probability is truly saturated by the field-collisional interaction. In CARE, on the other hand, the upper state probability amplitude is always small if $\chi\tau_c \gg 1$. It is the rapid Rabi oscillations that lead to a decreasing CARE cross section with increasing χ when $\chi\tau_c \gg 1$ and $\chi/|\Delta| > 1$.

CONCLUSION

We have presented explanations of the physical processes underlying combined radiation field-collisional excitation of atomic systems. Alternative approaches could involve a "dressed-atom" description or a molecular-state basis calculation. For a meaningful theoretical description of CARE and RAIC, one must use accurate interatomic potentials and average all results over the spatial and temporal extent of the laser pulse. It may be noted, however, that experimental investigations of CARE and RAIC have revealed many of the qualitative features discussed above.

COMBINED RADIATION FIELD – COLLISIONAL EXCITATION

a lecture given by PRB at the College de France in January, 1980.

REFERENCES

1. S. E. Harris, R. W. Falcone, W. R. Green, D. B. Lidow, J. C. White, and J. F. Young, in _Tunable Lasers and Applications_, edited by A. Moorandian, T. Jaeger, and P. Stokseth (Springer-Verlag, New York, 1976) p. 193, and references therein.
2. R.W. Falcone, W. R. Green, J. C. White, and S. E. Harris, Phys. Rev. A. 15, 1533 (1977).
3. Ph. Cahuzac and P. E. Toschek, Phys. Rev. Lett. 36, 462 (1978).
4. S.E. Harris, J. F. Young, W. R. Green, R. W. Falcone, J. Lukasik, J. C. White, J. R. Willison, M. D. Wright, and G. A. Zdasiuk, in _Laser Spectroscopy IV_, edited by H. Walther and K. W. Rothe (Springer-Verlag, Berlin, 1979) pp. 349-359, and references therein.
5. S. E. Harris, J. F. Young, R. W. Falcone, W. R. Green, D. B. Lidow, J. Lukasik, J. C. White, M. D. Wright, and G. A. Zdasiuk, _Proceedings of the Seventh International Conference on Atomic Physics_, edited by D. Kleppner and F.M. Pipkin (Plenum, New York, 1981) pp. 407-428, and references therein.
6. C. Brechignac, Ph. Cahuzac, and P. E. Toschek, Phys. Rev. A 21, 1969 (1980).
7. J. C. White, R. R. Freeman and P. F. Liao, Opt. Lett. 5, 120 (1980).
8. D. L. Rousseau, G. D. Patterson, and P. F. Williams, Phys. Rev. Lett. 34, 1306 (1975).
9. J. L. Carlsten and A. Szöke, Phys. Rev. Lett. 36, 667 (1976); J. Phys. B 9, L231 (1976).
10. A. M. Bonch-Bruevich, S. G. Przhibel'skii, A. A. Fedorov, and V. V. Khromov, Sov. Phys.-JETP 44, 909 (1976).
11. R. D. Driver and J. L. Snider, J. Phys. B 10, 595 (1977).
12. J. L. Carlsten, A. Szöke, and M. G. Raymer, Phys. Rev. A 15, 1029 (1977).
13. M. G. Raymer, J. L. Carlsten, and G. Pichler, J. Phys. B 12, L119 (1979).
14. P. F. Liao, J. E. Bjorkholm, and P. R. Berman, Phys. Rev. A 20, 1489 (1979).

P. R. BERMAN AND E. J. ROBINSON

15. A. M. Bonch-Bruevich, T. A. Vartanyan, and V. V. Khromov, Sov. Phys.-JETP 51, 271 (1980).
16. A. Corney and J. V. M. McGinley, J. Phys. B. 14, 3047 (1981).
17. L. I. Gudzenko and S. I. Yakovlenko, Sov. Phys.-JETP 35, 877 (1972).
18. S. I. Yakovlenko, Sov. Phys.-JETP 64, 2020 (1973).
19. V. S. Lisitsa and S. I. Yakovlenko, Sov. Phys.-JETP 39, 759 (1974).
20. S. E. Harris and D. B. Lidow, Phys. Rev. Lett. 33, 674 (1974); 34, 172 (1975).
21. M. G. Payne and M. H. Nayfeh, Phys. Rev. A 13, 595 (1976).
22. S. Geltman, J. Phys. B 9, L1569 (1976).
23. P. L. Knight, J. Phys. B 10, L195 (1976).
24. V. S. Smirnov and A. V. Chaplik, Sov. Phys.-JETP 44, 913 (1976).
25. S. E. Harris and J. C. White, IEEE J. Quant. Elec. QE-13, 972 (1977).
26. P. W. Milonni, J. Chem. Phys. 66, 3715 (1977).
27. G. Nienhuis and F. Schuller, Physica 92C, 397 (1977).
28. K. Lam, I. Zimmerman, J. Yuan, J. R. Laing, and T. F. George, Chem. Phys. 25, 455 (1977).
29. A. M. Lau, Phys. Rev. A. 16, 1535 (1977).
30. T. F. George, J. M. Yuan, I. H. Zimmerman, and J. R. Laing, Disc. Faraday Soc. 62, 246 (1977).
31. I. I. Ostroukhova, B. M. Smirnov, and G. V. Shlyapnikov, Sov. Phys.-JETP 46, 86 (1977).
32. S. P. Andreev and V. S. Lisitsa, Sov. Phys.-JETP 45, 38 (1977).
33. S. I. Yakovlenko, Sov. J. Quant. Elec. 8, 151 (1978), and references therein.
34. M. E. Nayfeh, G. S. Hurst, M. G. Payne, and J. P. Young, Phys. Rev. Lett. 41, 302 (1978).
35. J. C. Light and A. Szöke, Phys. Rev. A 18, 1363 (1978).
36. M. G. Payne, V. E. Anderson, and J. E. Turner, Phys. Rev. A 20, 1032 (1979), and references therein.
37. S. Yeh and P. R. Berman, Phys. Rev. A 19, 1106 (1979), and references therein.
38. E. J. Robinson, J. Phys. B 12, 1451 (1979).
39. Y. Rabin and A. Ben-Reuven, J. Phys. B 13, 2011 (1980).
40. E. J. Robinson, J. Phys. B 13, 2359 (1980).
41. K. Burnett, J. Cooper, R. J. Ballagh, and E. W. Smith, Phys. Rev. A 22, 2005 (1980).

COMBINED RADIATION FIELD — COLLISIONAL EXCITATION

42. K. Burnett and J. Cooper, Phys. Rev. A 22, 2027, 2044 (1980).

43. P. R. Berman, Phys. Rev. A 22, 1838, 1848 (1980).

44. G. Nienhuis, J. Phys. B 14, 3117 (1981).

45. S. Reynaud and C. Cohen-Tannoudji, in Laser Spectroscopy V, edited by A. R. W. McKellar, T. Oka, and B. P. Stoichoff (Springer-Verlag, Berlin, 1981) pp. 166-173.

46. R. E. Walkup and D. E. Pritchard (private communication).

47. For transitions within the same electronic manifold, one might find $V_1(t) \simeq V_2(t)$. In that case, $\omega(t) \simeq \omega$ and CARE is not an efficient process.

48. The range of Δ for which instantaneous resonances occur depends on the specific nature of $V_{LS}(t)$. In stating that such resonances always exist for $\Delta < 0$, we implicitly assume that $V_{LS}(b,t) \rightarrow -\infty$ as $b \rightarrow 0$.

49. S. D. Tvorogov and V. V. Fomin, Opt. Spectroscopy 30, 228 (1971).

50. J. Szudy and W. E. Baylis, J. Quant. Spectrosc. Radiat. Trans. 15, 641 (1975), and references therein.

51. B. Cheron, R. Scheps, and A. Gallagher, Phys. Rev. A 15, 651 (1977).

52. A. Gallagher and T. Holstein, Phys. Rev. A 16, 2413 (1977).

53. Although the CARE and RAIC cross sections have the same qualitative features, the specific dependence on Δ is determined by $V_{LS}(t)$ and $V_c(t)$ {e.g. for $V_{LS}(t) \propto [R(t)]^{-6}$ and $V_c(t) \propto [R(t)]^{-3}$, the CARE and RAIC cross sections vary as $\Delta^{-3/2}$ and $\Delta^{-1/2}$, respectively, for $\Delta\tau_c \ll -1$}.

COMMENTS

Comment on "Observation of Subnatural Linewidth in Na D_2 Lines"

In a recent article,[1] Shimizu, Umezu, and Takuma proposed and demonstrated a novel new method for obtaining subnatural linewidths. Their approach can be summarized as follows: (1) A laser field is perpendicularly incident on an atomic beam; the atoms are in their ground state and the laser frequency is nearly resonant with a ground-state–excited-state transition. (2) The phase of the field is suddenly switched (at $t = 0$, for example). (3) The excitation probability is monitored as a function of atom-field detuning Δ for various delay times T following the phase switch. For fixed T, the resulting excitation probability *amplitude* contains contributions from atoms excited before and after the phase switch; the corresponding excitation *probability* contains interference fringes as a function of Δ having a width of order $1/T$. If $1/T$ is less than the natural linewidth associated with the transition, this method enables one to achieve subnatural spectroscopic linewidths. Experimental verification of this phenomenon was reported.[1]

In deriving an expression for the excitation probability, it appears that Shimizu, Umezu, and Takuma[1] did not properly account for the spontaneous decay in the problem. Consequently, as a function of T, their maximum excitation probability decays at *twice* the rate one should expect. In this Comment, a derivation of the excitation probability is given.

The problem is effectively solved by using a density matrix approach. The atoms are approximated by two-level systems which enter the interaction volume in state 1. Using a field interaction representation and neglecting the "antirotating" components of the field, one obtains equations of motion

$$\dot{\rho}_{11} = \Lambda - \gamma_1\rho_{11} + i[\chi(t)\rho_{21} - \chi^*(t)\rho_{12}],$$

$$\dot{\rho}_{22} = -\gamma_2\rho_{22} - i[\chi(t)\rho_{21} - \chi^*(t)\rho_{12}],$$

$$\dot{\rho}_{12} = \dot{\rho}_{21}^* = -(\gamma_{12} + i\Delta)\rho_{12} + i\chi(t)(\rho_{22} - \rho_{11}),$$

where $\chi(t) = \chi e^{i\varphi(t)}$, $\varphi(t) = 0$ for $t < 0$ and $\varphi(t) = \varphi$ for $t > 0$, χ is an atom-field coupling parameter, Λ is an incoherent pump rate, γ_i is the decay rate for state i, and $\gamma_{12} = (\gamma_1 + \gamma_2)/2$. Using perturbation theory, one can easily obtain the upper-state amplitude at time T following the phase switch to be

$$\rho_{22}(T, \Delta) = 2\Lambda\chi^2\gamma_{12}/[\gamma_1\gamma_2(\gamma_{12}^2 + \Delta^2)] - 2\,\mathrm{Re}\,\frac{\Lambda\chi^2(1 - e^{-i\varphi})\{\exp[-(\gamma_{12} + i\Delta)T] - \exp(-\gamma_2 T)\}}{\gamma_1(\gamma_{12} + i\Delta)[\frac{1}{2}(\gamma_2 - \gamma_1) - i\Delta]}. \tag{1}$$

To compare this result with that of Shimizu, Umezu, and Takuma,[1] one evaluates $\rho_{22}(\infty, \Delta) - \rho_{22}(T, \Delta)$, sets $\varphi = \pi$, and takes $\gamma_2 \gg \gamma_1$ since state 1 is the ground state. The signal $I(T, \Delta)$ is

$$I(T, \Delta) = \frac{4\Lambda\chi^2 \exp(-\gamma_2 T/2)[\cos(\Delta T) - \exp(-\gamma_2 T/2)]}{\gamma_1[(\frac{1}{2}\gamma_2)^2 + \Delta^2]} \tag{2}$$

which is to be compared with the line-shape formula

$$I_s(T, \Delta) = \frac{\gamma_2^2 \exp(-\gamma_2 T)}{\gamma_2^2 + \Delta^2}\left(\frac{\gamma_2}{\Delta}\sin(\Delta T) + \cos(\Delta T) - 1\right) \tag{3}$$

given in Ref. 1. Equations (2) and (3) qualitatively predict the same type of subnatural linewidth phenomenon. However, there are important differences between the two results. First, Eq. (2) leads to a central fringe that is narrower and deeper than that of Eq. (3). Second, Eq. (3) predicts a peak intensity (at $\Delta = 0$) which varies as $\exp(-\gamma_2 T)$ while Eq. (2) predicts one which varies as $\exp(-\gamma_2 T/2)$. For $2/\gamma_2 \simeq 32$ ns appropriate to the Na $3P$ levels, the observed peak intensity decay time of 40 ns (Ref. 1) is in reasonable agreement with Eq. (2). Since the line shape represents an interference effect, one expects the decay rate to be that associated with the coherence ρ_{12} (i.e., γ_{12}) rather than that associated with the population ρ_{22} (i.e., γ_2).

Paul R. Berman
Physics Department, New York University
New York, New York 10003

[1] F. Shimizu, K. Umezu, and H. Takuma, Phys. Rev. Lett. **47**, 825 (1981).

Two-level transition probabilities for asymmetric coupling pulses

E. J. Robinson

Physics Department, New York University, 4 Washington Place, New York, New York 10003
(Received 2 March 1981)

In a recent paper, Bambini and Berman [A. Bambini and P. R. Berman, Phys. Rev. A
23, 2496 (1981)] presented analytic solutions to a certain family of coherent-coupling
pulses for a two-level system. They show, for nonresonant temporally asymmetric
members of the class, that there are no solutions corresponding to vanishing transition
probabilities. In this Comment, we examine the problem in greater generality and demon-
strate that this property is the norm for asymmetric pulses, and that a vanishing transi-
tion probability is possible only if severely overdetermined conditions are satisfied.

The problem of a two-level system coupled by an
external field has a long history in physics, dating
back to the 1930's.[1,2] Originally motivated by in-
vestigations on atoms in magnetic fields, theories of
such systems have more recently been applied to
laser-related problems.[3]

Let a_1, a_2 be the amplitudes of the two states.
We assume that the coupling potential connecting
the two states is of variable amplitude and central
frequency Ω, so that, in the rotating wave approxi-
mation, the time-dependent Schrödinger equation
becomes a pair of coupled equations for a_1, a_2:

$$i\dot{a}_1 = V(t)e^{i\Delta t}a_2 , \tag{1a}$$

$$i\dot{a}_2 = V(t)e^{-i\Delta t}a_1 . \tag{1b}$$

Here Δ is the detuning of Ω from the atomic fre-
quency. We work in a system of units where $\hbar = 1$.

For the case where V is a constant in time, the
solution for initial conditions $a_1 = 0$, $a_2 = 1$ at $t = 0$
is

$$a_1 = \frac{-iV}{(\Delta^2/4 + V^2)^{1/2}}e^{i\Delta t/2}\sin[(\Delta^2/4 + V^2)^{1/2}t] .$$

This is the Rabi problem. For this to be
relevant, the approximation that the rise time of
the field is much shorter than other characteristic
times should be a good one. In their paper, Rosen
and Zener[2] considered a case where this sudden ap-
proximation was not valid. They were motivated
by a serious discrepancy between results of the

sudden-approximation theory and experiment.
They analyzed the effect of a smoothly varying
pulse, choosing a hyperbolic secant because of the
exactly solvable nature of the equations that result
from such a time dependence. For the hyperbolic
secant pulse, one may make a change of variable
that transforms the equation of motion into the hy-
pergeometric equation. Robiscoe[4] has shown how
to generalize this to the case of decaying states.

Recently, Bambini and Berman[5] have gone
beyond the Rosen-Zener problem. They show that
there is an entire class of envelope functions that
may be mapped into the hypergeometric equation,
of which the hyperbolic secant pulse is merely one
member. All $V(t)$ in the family, other than the
hyperbolic secant, are asymmetric in time, i.e.,
$V(t) \neq V(-t)$. Bambini and Berman show that for
these asymmetric pulses, there is no case, apart
from exact resonance, where there is a nonvanish-
ing transition probability, a striking and surprising
result.

In the case of the Rabi problem, on the other
hand, for any given detuning, there are always
values of the pulse area for which the amplitude a_1
returns to zero. In the Rosen-Zener case, the am-
plitude $a_1(+\infty)$ goes like $(\sin A)/A$, where A is the
pulse area, so that here too, once the hyperbolic
secant envelope function is specified, one can find
values of the area of the pulse for which $a_1(+\infty)$
vanishes. Similar remarks hold for other sym-
metric potentials, where solutions have been ob-

tained with computers.[6,7] It is a most remarkable feature of the Bambini-Berman problem that it admits no asymmetric envelopes for $\Delta \neq 0$ with a nonvanishing transition probability. That is, it asserts that for asymmetric pulses of the form studied, if the amplitudes $a_2 = 1$ and $a_1 = 0$ at $t = -\infty$, then at time $t = +\infty$, the probability for finding the system in state 1 is nonvanishing, i.e., there will always be some population in state 1 for this class of off-resonant asymmetric pulse. No previous prediction of this kind of behavior seems extant in the literature. It should be understood that only envelopes of a single algebraic sign are being considered, so that, for example, pulses that are completely antisymmetric in time are excluded from this discussion.

Bambini and Berman[5] reach their conclusion by obtaining a complete analytic solution to their problem. Since most pulse shapes do not admit of closed form solutions, it is of interest to inquire whether the nonvanishing of transition probabilities holds for other smooth, asymmetric pulses and whether this property can be demonstrated in a general way, i.e., through the structure of the equations of motion. It is to this question that we address the present work.

Equations (1) may be put in the form of uncoupled second-order equations

$$\ddot{a}_1 - (\dot{V}/V + i\Delta)\dot{a}_1 + V^2 a_1 = 0 , \tag{2a}$$

$$\ddot{a}_2 - (\dot{V}/V - i\Delta)\dot{a}_2 + V^2 a_2 = 0 . \tag{2b}$$

Defining $z = \int_{-\infty}^{t} f(t')dt' - \frac{1}{2}$, with $A = \int_{-\infty}^{\infty} V\,dt$ and $f = V/A$, Eqs. (2) become, in the z plane,

$$a_1'' - i\frac{\Delta}{f}a_1' + A^2 a_1 = 0 , \tag{3a}$$

$$a_2'' + i\frac{\Delta}{f}a_2' + A^2 a_2 = 0 . \tag{3b}$$

We assume, with Bambini and Berman,[5] that $f(t)$ does not change sign, so that the transformation, which differs from theirs, is single valued. If one transforms Eq. (3a) via the substitution

$$b = a_1 \exp\left[(-i\Delta/2)\int_0^z dz'/f(z')\right] = a_1 e^{-i\Delta t/2} ,$$

into an equation with the first derivative missing, we have

$$b'' + \left[\frac{\Delta^2}{4f^2} + \frac{i\Delta f'}{2f^2} + A^2\right]b = 0 , \tag{3a'}$$

or

$$-b'' + \left[\frac{-\Delta^2}{4f^2} - \frac{i\Delta f'}{2f^2}\right]b = A^2 b . \tag{3b'}$$

Equation (3b') resembles a one-dimensional, time-independent Schrödinger equation for a particle of mass $\frac{1}{2}$ moving in the complex "potential"

$$V = -\left[\frac{\Delta^2}{4} + \frac{i\Delta f'}{2}\right]\frac{1}{f^2} ,$$

where $\hbar$ has been set $= 1$.

This equation is to be solved subject to the initial conditions that $b = 0$ at $z = -\frac{1}{2}$. If the dynamics of the problem permit a transition probability of zero for certain pulse areas, this means $b(z = +\frac{1}{2})$ also vanishes for those values of A. In short, we must solve an eigenvalue problem and find those values of A^2 for which the solutions of Eq. (3b') vanish at $z = \pm\frac{1}{2}$. Now, for physical pulses, only real envelopes exist. For these, A^2 is real and positive. If none of the eigenvalues A^2 meet this criterion, A will have an imaginary part for all the eigenfunctions of Eq. (3b'), and none will correspond to a system driven by an actual pulse, i.e., there will be no physically meaningful pulse areas for which the system undergoes a transition probability of zero. In the following, we shall assume a nonvanishing detuning. Note that the case of exact resonance is entirely equivalent to the elementary quantum mechanical problem of a particle in a box, whose eigenvalues A^2 are $n^2\pi^2$. In this way, we confirm the simple result that the transition probability vanishes for pulse areas that are integral multiples of π, if $\Delta = 0$.

We should comment that if one constructs an asymmetric potential from two temporally distinct symmetric pulses, one can, by making each of the component pulses produce a net transition amplitude of zero, cause the overall probability to vanish. To force the components to be exactly nonoverlapping in time requires that they be sharply cut off. Thus, these pulses do not conform to the smoothness criterion of Bambini and Berman.[5]

We consider now pulses where the imaginary term is present. We examine first the case of symmetric pulses. Let A^2 be a typical eigenvalue. If we replace the imaginary term by its negative, then the resulting equation will have A^{2*} for its eigenvalue. Now, since $f(z)$ is symmetric in z, $f'(z)$ will be antisymmetric. Therefore, the transformation $z \rightarrow -z$ reverses the sign of the imaginary term on the left-hand side of Eq. (3b'), but leaves the eigenvalue unchanged. Immediately, $A^2 = A^{2*}$, i.e., all the eigenvalues are real, although not necessarily larger than zero. For asymmetric pulses, the transformation $z \rightarrow -z$ does not reproduce the complex-conjugate equation, and A^2 will not, in

general, be the same as A^{2a}. This does not absolutely rule out the possibility that for particular $f(t)$ and detuning, one might have one or more real and positive eigenvalues, but demonstrates that it could occur only by accident. We shall show in the following that the conditions that must necessarily be fulfilled for A^2 to be real for asymmetric pulses are severely overdetermined.

To proceed, we will analyze the problem from a perturbative viewpoint, and assume that the entire perturbation expansion can be summed. We do not restrict ourselves to the first few terms, but study the parity-related properties of the full series. We take the zero-order problem to be

$$-b_0^{''} - \left[\frac{\Delta^2}{4f^2} \right] b_0 = A_0^2 b_0 . \tag{4}$$

This is Hermitian and identical to a time-independent Schrödinger equation, which has only real eigenvalues. The imaginary term $-i\Delta f'/2f^2$ is to be considered as a perturbation.

We wish to contrast the case of symmetric and asymmetric pulse envelopes. Assume $f(t)$ to be symmetric—$f(z)$ is also symmetric. [If $f(t)$ were not symmetric about $t=0$, $f(z)$ would lack symmetry about its origin.] For this case, the unperturbed eigenfunction b_0 has definite parity, and the perturbation $-i\Delta f'/f^2$ is odd under reflection. It follows directly that if one writes a perturbation series for A^2 as an expansion in the usual way, contributions from odd powers of the "strength" of the "interaction" will be absent. Since only the even orders survive, and the strength parameter is purely imaginary, the resulting eigenvalues will be real.

If the potential $V(t)$ is not symmetric neither $1/f^2$ nor f'/f^2 will be operators of definite parity, nor will unperturbed solutions b_0 possess well-defined inversion properties. Hence, both even and odd terms in the perturbation expansion will be present, and the eigenvalues A^2 will all be complex, unless there is a case where, for a specific detuning, the odd powers of the expansion sum to zero.

The latter is an extremely unlikely circumstance. Equation (3b') is of the form

$$-b'' - \left[\frac{\mu}{f^2} + i\frac{\lambda f'}{f^2} \right] b = A^2 b . \tag{5}$$

We require not only that the odd powers sum to zero, but that they do so for a value of λ that is exactly the square root of μ. We cannot quite exclude this possibility, but it is evidently highly overdetermined.

To summarize, we have shown that the result obtained for particular asymmetric pulses by Bambini and Berman,[5] namely that there are no nonresonant cases for which the transition probability vanishes, is the normal consequence of the general structure of the equations of motion, and applies, apart from some remotely possible accidental cases, to all smoothly varying, asymmetric pulses which possess envelopes of a single algebraic sign.

[1]I. I. Rabi, Phys. Rev. 51, 652 (1937).
[2]N. Rosen and C. Zener, Phys. Rev. 40, 502 (1932).
[3]An extensive compilation of references is given by L. Allen and J. H. Eberly, *Optical Resonance and Two-Level Atoms* (Wiley, New York, 1975).
[4]R. T. Robiscoe, Phys. Rev. A 17, 247 (1978).
[5]A. Bambini and P. R. Berman, Phys. Rev. A 23, 2496 (1981).
[6]S. Yeh and P. R. Berman (private communication).
[7]E. J. Robinson (unpublished).

Comparison between dressed-atom and bare-atom pictures in laser spectroscopy

P. R. Berman and Rainer Salomaa*

Physics Department, New York University, 4 Washington Place, New York, New York 10003

(Received 26 August 1981)

The theory of the interaction between radiation fields and atoms as applied to laser spectroscopy can be approached using either a bare-atom picture (BAP) or dressed-atom picture (DAP). In the BAP, the basis states are those of the free atoms and free field while, in the DAP, the basis states encompass some part of the atom-field interaction. The theory of saturation spectroscopy in three-level systems is discussed using both approaches. Whereas calculations are usually more easily done using the BAP, one can gain useful insight into the underlying physical processes from the DAP. Moreover, when the radiation field strengths (in frequency units) are larger than the relaxation rates in the problem, the DAP equations simplify considerably and lead to line-shape expressions which may be given a simple interpretation. The DAP is used to obtain resonance conditions for traveling-wave fields interacting with three- and four-level atoms and for a standing-wave saturator and traveling-wave probe interacting with a three-level atom. In addition, the DAP is applied to several problems involving optical coherent transients. A comparison is made between the various advantages of the BAP and DAP and an interesting duality between the two approaches is noted.

I. INTRODUCTION

There exists today a wide variety of "Doppler-free" methods for obtaining absorption spectra associated with atomic or molecular transitions.[1-6] The methods are "Doppler free" in that the width normally occurring in linear spectroscopy can be substantially reduced or totally eliminated using nonlinear techniques. This suppression of the Doppler width is generally achieved in one of two ways. First, one can limit those atoms participating in the absorption process to a narrow velocity range (either by use of an atomic beam or by selective excitation with a laser field) leading to a corresponding reduction of the Doppler width. Alternatively, one can arrange for the atoms to interact with two fields such that the resultant frequency seen in the atomic frame is not strongly dependent on velocity (cancellation of Doppler phases). Coherent transient spectroscopy provides another method for obtaining spectral information that is essentially free of the Doppler width. It is also possible to combine the various methods.

There exists a rich literature devoted to the theory of nonlinear saturation spectroscopy.[1-25] The approaches can be divided into roughly three groups. First, there is the so-called bare-atom picture (BAP) in which the atom-field interactions are represented in terms of a basis using the (bare) atomic eigenstates.[7-18] Second, there is the dressed-atom picture (DAP) in which all or part of the atom-field interaction is solved exactly and the resultant atom-field eigenstates are used as the basis for further calculations.[12,19-24] Finally there are resolvent methods which will not be discussed here.[25]

Most calculations were originally performed using the BAP. For two- or three-level atomic systems interacting with two or more radiation fields, the "Doppler-free" absorption spectra were calculated using a density-matrix approach. It soon became appreciated, however, that the DAP approach, previously used to describe optical pumping experiments,[26] could be advantageously applied to laser spectroscopy experiments when one or more of the fields is intense. The dressed-atom approach has proven to be extremely useful in obtaining theoretical expressions for resonance fluorescence spectra when the exciting field is intense.[19,27]

It is the purpose of this paper to provide a comparison of the DAP and BAP, to indicate the relative advantages of each approach, and to apply the

DAP to some cases not previously considered. It is shown that the BAP equations are invariably easier to solve than the corresponding DAP ones as long as one is dealing with single-mode fields interacting with two- or three-level atomic systems. For multilevel atoms or multimode fields, both methods lead to equations that present considerable analytical difficulties.

Although the DAP equations may not provide any analytical simplifications, they do enable one to obtain an interpretation of the ongoing physical processes that may be helpful in understanding the atom-field interactions. When the frequency separation of the dressed-energy states is much greater than the relaxation rates in the problem, an important simplification occurs in the DAP. One can interpret multiphoton interactions of the BAP in terms of noninterfering single-photon transitions in the DAP. The positions (but not necessarily the strengths and widths) of the various atom-field resonances are then easily and naturally predicted using the DAP.

A comparison of the BAP and the DAP also offers an interesting duality between the two approaches. It is shown that the roles played by the atom-field coupling constants and the relaxation rates are interchanged in the BAP and DAP approaches. In coherent transient spectroscopy, what appears as an optical nutation signal in the BAP now appears as a free-induction decay in the DAP. Other features of the two approaches are discussed as applied to three-level spectroscopy, four-level spectroscopy, saturation spectroscopy involving multimode fields, and coherent transient spectroscopy.

It should be stressed that the DAP discussed in this work differs in spirit from that of conventional theories.[19-22,26] In the conventional DAP, the electromagnetic field is quantized and the dressed states are eigenstates of the atom plus field; consequently, these dressed states represent linear combinations of products of atomic and quantized-field eigenstates. In our case, the field is taken to be classical. However, by using a field-interaction representation for the various state amplitudes and forming appropriate linear combinations of the atomic-state eigenstates, one arrives at equations that are mathematically equivalent to the conventional dressed-atom ones, provided the field strengths are large enough to be treated classically. Thus, even though the DAP eigenstates using classical and quantized fields differ in a fundamental way, the conclusions and interpretations using both

approaches may be similar. It is in this sense that we refer to a "dressed-atom" picture, although our dressed states are not the conventional ones appearing in quantized-field treatments.[19-22,26]

In Sec. II the basic formalism is described and a comparison between the BAP and DAP is given in Sec. III. The DAP is applied to the saturation spectroscopy of homogeneously and inhomogeneously broadened three-level atoms in Secs. IV and V, respectively. In Sec. VI, we discuss the manner in which the DAP can be applied to multilevel atoms or multimode fields and in Sec. VII, coherent transient effects are discussed using the DAP. Some conclusions concerning the relative merits of the two approaches are given in Sec. VIII.

Much of the material presented in Secs. II–V is not new, but is reassembled there to provide the basis for a comparison between the BAP and DAP and to lay the foundation for the material that follows.

II. GENERAL FORMALISM

We consider an idealized three-level moving atom which interacts with a linearly polarized electromagnetic field of the form

$$\vec{E}(z,t) = \hat{e}_x [E_1 \cos(\Omega_1 t - K_1 z + \varphi_1)$$
$$+ E_2 \cos(\Omega_2 t - K_2 z + \varphi_2)] . \qquad (2.1)$$

The atom-field interaction is of the form $\mu_x E(z,t)$ where $-\mu_x$ is the x component of the atomic dipole operator. It is assumed that the wave (E_1, Ω_1) couples the atomic states $|1\rangle$ and $|2\rangle$ only and (E_2, Ω_2) the states $|2\rangle$ and $|3\rangle$ only. Within the rotating-wave approximation,[28] the reduced density matrix of the atom in the field-interaction representation[29] obeys the master equation[12,19]

$$\dot{\tilde{\rho}} = (i\hbar)^{-1} [\tilde{H}, \tilde{\rho}] + \dot{\tilde{\rho}}_{rel} + \Lambda . \qquad (2.2)$$

Equation (2.2) contains three contributions. The first of these involves an effective Hamiltonian $\tilde{H}$ and represents the atom-field interaction. The matrix $\tilde{H}$ is given by

$$\tilde{H} = \hbar \begin{bmatrix} -\tilde{\Delta}_{21} & \alpha_1 & 0 \\ \alpha_1 & 0 & \alpha_2 \\ 0 & \alpha_2 & \tilde{\Delta}_{32} \end{bmatrix} , \qquad (2.3)$$

where we have denoted the Doppler-shifted detun-

ings by

$$\tilde{\Delta}_{21} = \Delta_{21} + k_1 v , \tag{2.4a}$$

$$\tilde{\Delta}_{32} = \Delta_{32} + k_2 v , \tag{2.4b}$$

where

$$\Delta_{21} = \omega_{21} - \text{sgn}(\omega_{21})\Omega_1 ,$$

$$\Delta_{32} = \omega_{32} - \text{sgn}(\omega_{32})\Omega_2 , \tag{2.4c}$$

$$k_1 = \text{sgn}(\omega_{21})K_1 ,$$

$$k_2 = \text{sgn}(\omega_{32})K_2 , \tag{2.4d}$$

and the Rabi frequencies by

$$\alpha_1 = \mu_{21}E_1/2\hbar , \tag{2.5a}$$

$$\alpha_2 = \mu_{32}E_2/2\hbar , \tag{2.5b}$$

in which ω_{ij} is the energy spacing (in units $\hbar$) between levels i and j, $\mu_{ij} = \mu_{ji}$ is the x component of the ij dipole matrix element (notice $\mu_{31} = 0$), and v is the z component of the atomic velocity. The second term in Eq. (2.2) describes relaxation processes and is of the form[30]

$$(\dot{\tilde{\rho}}_{\text{rel}})_{ij} = \sum_{k,l} R_{ij;kl}\tilde{\rho}_{kl} , \tag{2.6}$$

where the elements $R_{ij;kl}$ represent the effects of spontaneous emission or collisional relaxation. The spontaneous emission can lead either to decay *outside* of the three-level system or to a transfer of population between some of the levels. The final term in Eq. (2.2) is an incoherent pumping matrix whose elements are of the form

$$\Lambda_{ij} = \Lambda_i \delta_{i,j} . \tag{2.7}$$

The states $|1\rangle$ and $|2\rangle$ are assumed to be strongly coupled by α_1, whereas α_2 provides a

weak coupling between $|2\rangle$ and $|3\rangle$. Many effects of the strong field are conveniently incorporated by transforming to a "dressed" basis defined by

$$|A\rangle = \cos\theta|1\rangle - \sin\theta|2\rangle , \tag{2.8a}$$

$$|B\rangle = \sin\theta|1\rangle + \cos\theta|2\rangle , \tag{2.8b}$$

$$|C\rangle = |3\rangle , \tag{2.8c}$$

with

$$\sin\theta = \{\tfrac{1}{2}[1 - \tilde{\Delta}_{21}(\tilde{\Delta}_{21}^2 + 4\alpha_1^2)^{-1/2}]\}^{1/2} , \tag{2.9a}$$

$$\cos\theta = \{\tfrac{1}{2}[1 + \tilde{\Delta}_{21}(\tilde{\Delta}_{21}^2 + 4\alpha_1^2)^{-1/2}]\}^{1/2} . \tag{2.9b}$$

In the discussion that follows, the states $|i\rangle$ $(i = 1,2,3)$, will be referred to as states in a bare-atom picture (BAP) and the states $|\alpha\rangle$ $(\alpha = A,B,C)$, will be referred to as states in a dressed-atom picture (DAP).

The transformation (2.8) may be written

$$|\alpha\rangle = T_{\alpha i}|i\rangle , \tag{2.10}$$

where the summation convention is adopted and elements $T_{\alpha i}$ are given by

$$T_{\alpha i} = (T^{-1})_{i\alpha} = \langle i|\alpha\rangle . \tag{2.11}$$

In terms of the T matrix the transformation between the dressed and bare density matrices is

$$\tilde{\rho}_B = T^{-1}\tilde{\rho}_D T , \tag{2.12}$$

which is used to transform Eq. (2.2) into

$$\dot{\tilde{\rho}}_D = (i\hbar)^{-1}[\tilde{H}_D, \tilde{\rho}_D] + \dot{\tilde{\rho}}_{D,\text{rel}} + \Lambda_D , \tag{2.13}$$

where

$$\tilde{H}_D = T\tilde{H}_B T^{-1} = \hbar \begin{bmatrix} -\tfrac{1}{2}\tilde{\Delta}_{21} - \tfrac{1}{2}\omega_{BA} & 0 & -\alpha_2\sin\theta \\ 0 & -\tfrac{1}{2}\tilde{\Delta}_{21} + \tfrac{1}{2}\omega_{BA} & \alpha_2\cos\theta \\ -\alpha_2\sin\theta & \alpha_2\cos\theta & \tilde{\Delta}_{32} \end{bmatrix} , \tag{2.14}$$

$$\omega_{BA} = (\tilde{\Delta}_{21}^2 + 4\alpha_1^2)^{1/2} , \tag{2.15}$$

$$(\dot{\tilde{\rho}}_{D,\text{rel}})_{\alpha\beta} = (R_D)_{\alpha\beta;\gamma\delta}(\tilde{\rho}_D)_{\gamma\delta} , \tag{2.16}$$

$$(R_D)_{\alpha\beta;\gamma\delta} = T_{\alpha i}T_{\beta j}T_{\gamma k}T_{\delta l}R_{ij;kl} , \tag{2.17}$$

$$(\Lambda_D)_{\alpha\beta} = T_{\alpha i}T_{\beta i}\Lambda_i . \tag{2.18}$$

[The angle θ in Eq. (2.9) is taken to lie in the range $0 < \theta < \pi/2$ such that $\cos\theta$ and $\sin\theta$ are positive. With this choice, dressed state B always has a greater energy than dressed state A. In the limit

that $\alpha_1 \to 0$, states $|A\rangle, |B\rangle \to |1\rangle, |2\rangle$ if $\tilde{\Delta}_{21} > 0$ and $|A\rangle, |B\rangle \to |2\rangle, |1\rangle$ if $\tilde{\Delta}_{21} < 0$.]

The transformation T has been chosen to diagonalize the $A - B$ submatrix of $\tilde{H}_D$. In the limit that $\alpha_2 \to 0$, $\tilde{H}_D$ is diagonal and one has a complete solution to the problem. The DAP will be particularly useful when α_2 is small, enabling one to carry out a perturbation expansion in this parameter. Although the matrix $\tilde{H}_D$ has a simple structure, the relaxation and pumping terms are now more complicated. The pumping matrix, which is diagonal in the BAP, has *both* diagonal and off-diagonal elements in the DAP as given in Eq. (2.18). Moreover, the relaxation terms are most naturally expressed in the BAP, where one can typically take (no sum)

$$R_{ij;kl} = -\gamma_{ij}\delta_{i,k}\delta_{j,l}(1 - \delta_{i,j})$$
$$-\Gamma_i\delta_{i,j}\delta_{i,k}\delta_{i,l} + \Gamma_{kl}\delta_{i,j}\delta_{k,l}(1 - \delta_{i,k})$$

(2.19)

leading to a relaxational time rate of change of $\tilde{\rho}$ of the form

$$(\dot{\tilde{\rho}}_{rel})_{ij} = -\gamma_{ij}\tilde{\rho}_{ij} \quad (i \neq j) , \qquad (2.20)$$

$$(\dot{\tilde{\rho}}_{rel})_{ii} = -\Gamma_i\tilde{\rho}_{ii} + \sum_{j(\neq i)} \Gamma_{ji}\tilde{\rho}_{jj} , \qquad (2.21)$$

where Γ_i is the total decay rate of state i and Γ_{ji} describes population transfer from j to i due to spontaneous emission or collisions. While the relaxational decay and coupling in the BAP given by Eqs. (2.20) and (2.21) is fairly simple, the corresponding coupling in the DAP given by Eqs. (2.16)–(2.17) involves many more terms. Explicit expressions for the relaxation rates are given in Appendix A.

To compare the BAP and DAP we write down the equations of the components of the density-matrix elements in both representations. For simplicity, we adopt a relaxation scheme in which $\Gamma_{ij} = 0$ and $\gamma_{ij} = \frac{1}{2}(\Gamma_i + \Gamma_j)$, corresponding to the case in which each level decays to some states *other* than states 1, 2, or 3. In the BAP, one has

$$\dot{\tilde{\rho}}_{11} = \Lambda_1 - \Gamma_1\tilde{\rho}_{11} + 2\alpha_1 \operatorname{Im}(\tilde{\rho}_{21}) , \qquad (2.22a)$$

$$\dot{\tilde{\rho}}_{22} = \Lambda_2 - \Gamma_2\tilde{\rho}_{22} - 2\alpha_1 \operatorname{Im}(\tilde{\rho}_{21}) + 2\alpha_2 \operatorname{Im}(\tilde{\rho}_{32}) , \qquad (2.22b)$$

$$\dot{\tilde{\rho}}_{33} = \Lambda_3 - \Gamma_3\tilde{\rho}_{33} - 2\alpha_2 \operatorname{Im}(\tilde{\rho}_{32}) , \qquad (2.22c)$$

$$\dot{\tilde{\rho}}_{21} = -(\gamma_{21} + i\tilde{\Delta}_{21})\tilde{\rho}_{21} + i\alpha_1(\tilde{\rho}_{22} - \tilde{\rho}_{11}) - i\alpha_2\tilde{\rho}_{31} , \qquad (2.22d)$$

$$\dot{\tilde{\rho}}_{32} = -(\gamma_{32} + i\tilde{\Delta}_{32})\tilde{\rho}_{32} + i\alpha_2(\tilde{\rho}_{33} - \tilde{\rho}_{22}) + i\alpha_1\tilde{\rho}_{31} , \qquad (2.22e)$$

$$\dot{\tilde{\rho}}_{31} = -(\gamma_{31} + i\tilde{\Delta}_{21} + i\tilde{\Delta}_{32})\tilde{\rho}_{31} + i\alpha_1\tilde{\rho}_{32} - i\alpha_2\tilde{\rho}_{21} , \qquad (2.22f)$$

$$\tilde{\rho}_{ij} = \tilde{\rho}_{ji}^* , \qquad (2.22g)$$

while in the DAP, the corresponding equations read:

$$\dot{\tilde{\rho}}_{AA} = \Lambda_A - \Gamma_A\tilde{\rho}_{AA} + 2\beta \operatorname{Re}(\tilde{\rho}_{BA}) + 2\alpha_A \operatorname{Im}(\tilde{\rho}_{CA}) , \qquad (2.23a)$$

$$\dot{\tilde{\rho}}_{BB} = \Lambda_B - \Gamma_B\tilde{\rho}_{BB} + 2\beta \operatorname{Re}(\tilde{\rho}_{BA}) + 2\alpha_B \operatorname{Im}(\tilde{\rho}_{CB}) , \qquad (2.23b)$$

$$\dot{\tilde{\rho}}_{CC} = \Lambda_C - \Gamma_C\tilde{\rho}_{CC} - 2\alpha_A \operatorname{Im}(\tilde{\rho}_{CA}) - 2\alpha_B \operatorname{Im}(\tilde{\rho}_{CB}) , \qquad (2.23c)$$

$$\dot{\tilde{\rho}}_{CA} = -(\gamma_{CA} + i\omega_{CA})\tilde{\rho}_{CA} + i\alpha_A(\tilde{\rho}_{CC} - \tilde{\rho}_{AA})$$
$$- i\alpha_B\tilde{\rho}_{BA} + \beta\tilde{\rho}_{CB} , \qquad (2.23d)$$

$$\dot{\tilde{\rho}}_{CB} = -(\gamma_{CB} + i\omega_{CB})\tilde{\rho}_{CB} + i\alpha_B(\tilde{\rho}_{CC} - \tilde{\rho}_{BB})$$
$$- i\alpha_A\tilde{\rho}_{AB} + \beta\tilde{\rho}_{CA} , \qquad (2.23e)$$

$$\dot{\tilde{\rho}}_{BA} = \Lambda_{BA} - (\gamma_{BA} + i\omega_{BA})\tilde{\rho}_{BA} + \beta(\tilde{\rho}_{AA} + \tilde{\rho}_{BB})$$
$$+ i\alpha_A\tilde{\rho}_{BC} - i\alpha_B\tilde{\rho}_{CA} , \qquad (2.23f)$$

$$\tilde{\rho}_{\alpha\beta} = \tilde{\rho}_{\beta\alpha}^* , \qquad (2.23g)$$

where

$$\Lambda_A = \Lambda_1 \cos^2\theta + \Lambda_2 \sin^2\theta , \qquad (2.24a)$$

$$\Lambda_B = \Lambda_1 \sin^2\theta + \Lambda_2 \cos^2\theta , \qquad (2.24b)$$

$$\Lambda_C = \Lambda_3 , \qquad (2.24c)$$

$$\Lambda_{BA} = \Lambda_{AB} = \frac{1}{2}(\Lambda_1 - \Lambda_2)\sin 2\theta , \qquad (2.24d)$$

$$\Gamma_A = \Gamma_1 \cos^2\theta + \Gamma_2 \sin^2\theta , \qquad (2.25a)$$

$$\Gamma_B = \Gamma_1 \sin^2\theta + \Gamma_2 \cos^2\theta , \qquad (2.25b)$$

$$\Gamma_C = \Gamma_3 , \qquad (2.25c)$$

$$\gamma_{\alpha\beta} = \frac{1}{2}(\Gamma_\alpha + \Gamma_\beta) , \qquad (2.25d)$$

$$\alpha_A = -\alpha_2 \sin\theta , \qquad (2.26a)$$

$$\alpha_B = \alpha_2 \cos\theta , \qquad (2.26b)$$

$$\beta = \frac{1}{4}(\Gamma_2 - \Gamma_1)\sin 2\theta , \qquad (2.27)$$

$$\omega_{CA} = \tilde{\Delta}_{32} + \frac{1}{2}\tilde{\Delta}_{21} + \frac{1}{2}(\tilde{\Delta}_{21}^2 + 4\alpha_1^2)^{1/2} , \qquad (2.28a)$$

$$\omega_{CB} = \tilde{\Delta}_{32} + \frac{1}{2}\tilde{\Delta}_{21} - \frac{1}{2}(\tilde{\Delta}_{21}^2 + 4\alpha_1^2)^{1/2} . \qquad (2.28b)$$

The physical observables are the populations $\tilde{\rho}_{ii}$ and terms proportional to either $\text{Re}(\tilde{\rho}_{ij})$ or $\text{Im}(\tilde{\rho}_{ij})$ giving the dispersion or absorption, respectively, for the saturator $(i,j=2,1)$ or probe $(i,j=3,2)$. Using Eqs. (2.8)–(2.12), one can express these BAP elements in terms of the DAP elements $\tilde{\rho}_{\alpha\beta}$ by

$$\tilde{\rho}_{11}=\cos^2\theta\,\tilde{\rho}_{AA}+\sin^2\theta\,\tilde{\rho}_{BB}+\sin2\theta\,\text{Re}(\tilde{\rho}_{BA})\,,$$

$$(2.29a)$$

$$\tilde{\rho}_{22}=\sin^2\theta\,\tilde{\rho}_{AA}+\cos^2\theta\,\tilde{\rho}_{BB}-\sin2\theta\,\text{Re}(\tilde{\rho}_{BA})\,,$$

$$(2.29b)$$

$$\tilde{\rho}_{33}=\tilde{\rho}_{CC}\,,\qquad(2.29c)$$

$$\tilde{\rho}_{21}=\tfrac{1}{2}\sin2\theta(\tilde{\rho}_{BB}-\tilde{\rho}_{AA})+\cos^2\theta\,\tilde{\rho}_{BA}-\sin^2\theta\,\tilde{\rho}_{AB}\,,$$

$$(2.29d)$$

$$\tilde{\rho}_{32}=\cos\theta\,\tilde{\rho}_{CB}-\sin\theta\,\tilde{\rho}_{CA}\,.\qquad(2.29e)$$

It might be noted that the above equations, together with the quantum regression theorem, could also be used to calculate the spectrum of resonance fluorescence from these levels.[12,19,31]

III. COMPARISON BETWEEN BAP AND DAP: APPROXIMATE SOLUTIONS

The DAP equations are more complicated than the corresponding BAP equations, even for the simplified relaxation scheme adopted in Sec. II. One may, in particular, note the following features:

(i) In the DAP, in contrast to the BAP, the off-diagonal element $\tilde{\rho}_{BA}$ has a source term Λ_{BA}. This disappears only when $\Lambda_1=\Lambda_2$ or $\alpha_1\rightarrow0$.

(ii) All direct coupling between $\tilde{\rho}_{AA},\tilde{\rho}_{AB},\tilde{\rho}_{BA},$ $\tilde{\rho}_{BB}$ is proportional to the difference between the relaxation rates Γ_1 and Γ_2. The coupling parameter is of order β given in Eq. (2.27).

(iii) If we neglect Λ_{AB} and β, the DAP and BAP equations are equivalent with the replacements $\alpha_A\leftrightarrow\alpha_1$, $\alpha_B\leftrightarrow\alpha_2$, and $A,B,C\leftrightarrow1,3,2$. The prominent difference between the two representations is that, in the DAP, all couplings are of order α_2 (weak), whereas in the BAP, states 1 and 2 are strongly coupled by α_1. These features are illustrated in Fig. 1.

Clearly the BAP equations are easier to solve than those of the DAP. However, for a strong saturator, there are definite advantages in using the DAP. Moreover, the simple model configuration

considered here partly hides the power of DAP. A better comparison could, perhaps, be obtained by studying a case where both pictures must be solved approximately. Some applications along these lines are presented in Secs. VI and VII. For the present, we consider the three-level scheme of Fig. 1 since it allows for comparison with well-known results.[1–25]

Regardless of the level structure, the DAP simplifies the interpretation of the probe-absorption spectrum when the saturating field is intense. As an example, consider a three-level system for which two peaks appear in the probe-absorption spectrum at $\tilde{\Delta}_{32}\simeq0$ and $\tilde{\Delta}_{32}\simeq-\tilde{\Delta}_{21}$. If α_1 is weak these resonances can be labeled as stepwise and two photon in the BAP, but this interpretation breaks down if α_1 cannot be treated in lowest-order perturbation theory. In the limit of large α_1, however, the DAP allows one to interpret the two peaks as single-photon transitions between the dressed states A-C and B-C.

One way to solve the density-matrix equations approximately is based on the assumption that the off-diagonal components are small. In the BAP this leads to ordinary perturbation solutions in powers of α_1. The expansion converges rapidly provided that $|\tilde{\Delta}_{21}|$ or the relaxation constants are much larger than α_1. In the DAP, the role of the γ's and α_1 is interchanged; therefore, the corresponding approximate solution holds in the limit that $|\tilde{\Delta}_{21}|$ or α_1 is much larger than the relaxation rates. Thus, for strong fields α_1, a perturbative approach works well in the DAP but not at all in the BAP.
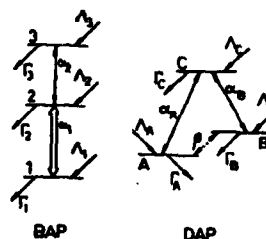

BAP   DAP

FIG. 1. A three-level system in both the BAP and DAP. In the BAP, there is incoherent pumping to and decay from each of the states. Levels 1 and 2 are coupled by a strong field α_1 and levels 2 and 3 by a weak probe field α_2. In the DAP, both couplings α_A and α_B between the dressed states are weak. However, there is now a collisional coupling β of states A and B as well as a "coherent pumping" Λ_{AB} which is not present in the BAP.

For the present, we assume (validity conditions to be stated below) that $\widetilde{\rho}_{BA}$ is negligible. Then, to zeroth order in α_2 it follows immediately that the steady-state solutions to Eq. (2.23) are

$$\widetilde{\rho}_{\alpha\beta}^{0}=(\Lambda_{\alpha}/\Gamma_{\alpha})\delta_{\alpha,\beta}=n_{\alpha}^{0}\delta_{\alpha,\beta} . \tag{3.1}$$

Using Eqs. (2.23) and (2.29) one obtains

$$\widetilde{\rho}_{32}=\frac{i\alpha_2\cos^2\theta(n_C^0-n_B^0)}{\gamma_{CB}+i\omega_{CB}}$$
$$+\frac{i\alpha_2\sin^2\theta(n_C^0-n_A^0)}{\gamma_{CA}+i\omega_{CA}} . \tag{3.2}$$

The steady-state value of $\widetilde{\rho}_{32}$, is related to the probe-induced polarization. It can be seen in Eq. (3.2) that the probe-field polarization may be viewed as originating from two noninteracting single-photon transitions between the dressed states C-B (corresponding strength $\alpha_2\cos^2\theta$) and C-A (strength $\alpha_2\sin^2\theta$).

An exact solution for $\widetilde{\rho}_{32}$ (to first order in α_2) is given in Appendix B where it is shown that Eq. (3.2) is valid provided that both

$$(\widetilde{\Delta}_{21}^2+4\alpha_1^2)^{1/2}>>\tfrac{1}{2}\,|\,\Gamma_2-\Gamma_1\,| \tag{3.3a}$$

and

$$|\,n_C^0-n_B^0\,|\cos^2\theta ,$$

$$|\,n_C^0-n_A^0\,|\sin^2\theta>>\tfrac{1}{4}\frac{|\,\Lambda_1-\Lambda_2\,|}{\omega_{BA}}\sin^22\theta . \tag{3.3b}$$

Roughly speaking, Eqs. (3.3) are satisfied if the decay rates are much less than the frequency separation ω_{BA} between states A and B.

The widths γ_{CA}, γ_{CB} and the positions $\omega_{CB}=0$, $\omega_{CA}=0$ of the resonances given in Eq. (3.2) are accurate if (3.3a) is satisfied. Equation (3.3a) enables one to ignore any interference effects between the two single-photon transitions of the DAP. Mathematically, this assumption involves the neglect of the $\beta\widetilde{\rho}_{CB}$ and $\beta\widetilde{\rho}_{CA}$ terms in Eqs. (2.23d) and (2.23e), respectively, which, in turn, implies that $\widetilde{\rho}_{CA}$ and $\widetilde{\rho}_{CB}$ are decoupled. Equation (3.3b), on the other hand, is the requirement that terms involving $\widetilde{\rho}_{BA}$ in Eqs. (2.23d)−(2.23e) are small enough to be neglected. Roughly speaking Eq. (3.3b) is valid when $(\Gamma_1+\Gamma_2)/\omega_{BA}<<1$. This condition is not sufficient if two of the dressed-state populations are equal. In this case one of the resonances in Eq. (3.2) disappears, whereas in the exact solution, the resonance does not totally vanish but is down in magnitude by a factor of order Γ/ω_{BA}.

IV. HOMOGENEOUSLY BROADENED SYSTEMS

We consider first a homogeneously broadened system in which all the detunings $\widetilde{\Delta}_{ij}$ are independent of v as may be the case when laser beams interact with an atomic beam such that $\vec{k}\cdot\vec{v}=0$. Once Eq. (3.2) is valid the interpretation of the probe-absorption spectrum is extremely simple. We define the probe-absorption spectrum $I(\Delta_{32})$ as[32]

$$I(\Delta_{32})=\frac{1}{\alpha_2}\,\mathrm{Im}\{\widetilde{\rho}_{32}\} , \tag{4.1}$$

which is obtained by combining Eqs. (4.1) and (3.2) to give

$$I(\Delta_{32})=\frac{\gamma_{CB}\cos^2\theta(n_C^0-n_B^0)}{\gamma_{CB}^2+\omega_{CB}^2}$$
$$+\frac{\gamma_{CA}\sin^2\theta(n_C^0-n_A^0)}{\gamma_{CA}^2+\omega_{CA}^2} . \tag{4.2}$$

The two resonances are Lorentzians (which may overlap) having the following properties:
C-B transition

$$\Delta_{32}=-\tfrac{1}{2}\Delta_{21}+\tfrac{1}{2}(\Delta_{21}^2+4\alpha_1^2)^{1/2} \text{ (position) },$$

$$\gamma_{CB}=\gamma_{31}\sin^2\theta+\gamma_{32}\cos^2\theta \text{ (width) },$$

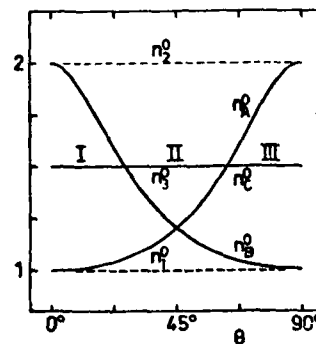$$\cos^2\theta(n_C^0-n_B^0)/\gamma_{CB} \text{ (height) }, \tag{4.3}$$

FIG. 2. Dressed-state populations n_A^0, n_B^0, n_C^0 as a function of the BAP→DAP transformation angle θ. The BAP populations n_1^0, n_2^0, and $n_3^0=n_C^0$ are determined by the incoherent pumping and relaxation rates. The gain factors for the CA and CB transitions can be read directly from this graph. For the case shown ($\Gamma_1=4\Gamma_2$; $n_1^0:n_2^0:n_3^0=1:2:1.5$), region I corresponds to absorption for the CB transition and gain for CA, region II to gain for both the CA and CB transitions, and region III to gain for the CB transition and absorption for CA.

C-A transition

$$\Delta_{32}=-\tfrac{1}{2}\Delta_{21}-\tfrac{1}{2}(\Delta_{21}^2+4\alpha_1^2)^{1/2}\quad\text{(position)},$$

$$\gamma_{CA}=\gamma_{31}\cos^2\theta+\gamma_{32}\sin^2\theta\quad\text{(width)},$$

$$\sin^2\theta(n_C^0-n_A^0)/\gamma_{CA}\quad\text{(height)}.\qquad(4.4)$$

The dependence of the heights and the nature (i.e., absorption or stimulated emission) of the reso-

nances on n_A^0, n_B^0, and n_C^0 is easily carried out with graphs like that shown in Fig. 2 which is constructed using Eqs. (2.24), (2.25), and (3.1). The linewidths always remain below $\max\{\gamma_{32},\gamma_{31}\}$ which implies that there is no "power broadening" in these spectra.

One can note some interesting limiting forms of Eq. (4.2). If field α_1 is very strong ($\alpha_1>>|\Delta_{21}|$) such that $\theta\simeq\pi/4$, then Eq. (4.2) becomes

$$I(\Delta_{32})\simeq\frac{1}{4}\left[\frac{\Lambda_3}{\Gamma_3}-\frac{\Lambda_2+\Lambda_1}{\Gamma_2+\Gamma_1}\right]\left\{\frac{\Gamma_3+\gamma_{21}}{\tfrac{1}{4}(\Gamma_3+\gamma_{21})^2+(\Delta_{32}+\tfrac{1}{2}\Delta_{21}-\alpha_1)^2}+\frac{\Gamma_3+\gamma_{21}}{\tfrac{1}{4}(\Gamma_3+\gamma_{21})^2+(\Delta_{32}+\tfrac{1}{2}\Delta_{21}+\alpha_1)^2}\right\},$$

$$(4.5)$$

which reveals two resonances of the *same* amplitude and *same* width, centered at $\Delta_{32}=\pm\alpha_1-\tfrac{1}{2}\Delta_{21}$.

On the other hand, if $\Gamma_i<<\alpha_1<<|\Delta_{21}|$, then $\theta<<1$ and the $C-B$ resonance takes the form

$$I(\Delta_{32})_{CB}\simeq\gamma_{32}(n_3^0-n_2^0)\left[\gamma_{32}^2+\left(\Delta_{32}-\frac{\alpha_1^2}{\Delta_{21}}\right)^2\right]^{-1}$$

$$\simeq\frac{\gamma_{32}(n_3^0-n_2^0)}{\gamma_{32}^2+\Delta_{32}^2}\left[1+\frac{2\alpha_1^2\Delta_{32}}{\Delta_{21}(\gamma_{32}^2+\Delta_{32}^2)}\right],$$

$$(4.6)$$

which is a Lorentzian with a small AC Stark shift. If only the nonlinear part proportinal to α_1^2 is monitored, the C-B resonance has a dispersionlike shape.[33]

plotted as a function of $\tilde{\Delta}_{21}$. A distribution of $\tilde{\Delta}_{21}$ is indicated schematically by the vertical-hatched column; the intersection of this hatched column with the ω_A and ω_B curves indicates the range of allowed values for ω_A and ω_B for this specific dis-

V. INHOMOGENEOUS BROADENING

According to (3.2) the probe response is negligible except near the resonances $\omega_{CB}=0$ and $\omega_{CA}=0$. The frequencies ω_{CB} and ω_{CA} are functions of $\tilde{\Delta}_{21}$, $\tilde{\Delta}_{32}$, and α_1. Since $\tilde{\Delta}_{21}$ and $\tilde{\Delta}_{32}$ depend on the atomic velocity which is determined by a distribution function and since, in principle, the value of α_1 might also be determined by a distribution function, the general resonance conditions can be satisfied by one or several atomic subgroups in the system. In this inhomogeneous broadening case, the atoms able to satisfy the resonance condition are those responsible for the probe response.

Many features of the probe spectra can be predicted with the aid of the simple graphical analysis given in Fig. 3. To use Fig. 3, it is useful to recall that $\omega_{CB}=\omega_C-\omega_B$ and $\omega_{CA}=\omega_C-\omega_A$, where ω_α is the energy of dressed state $|\alpha\rangle$ in units of $\hbar$ given by the diagonal elements of the Hamiltonian (2.14). In Fig. 3, ω_B and ω_A are

FIG. 3. Dressed-state frequencies ω_A, ω_B, and ω_C as a function of detuning $\tilde{\Delta}_{21}$. (The scales are in arbitrary frequency units.) The vertical strip gives the allowed values of $\tilde{\Delta}_{21}$ for some inhomogeneous distribution. As the probe is tuned, the ω_C line moves vertically and its intersection with the ω_A and ω_B curves gives the regions of probe absorption. These regions are indicated by the horizontal strips in the figure.

tribution of $\tilde{\Delta}_{21}$. The probe frequency (assumed to be independent of $\tilde{\Delta}_{21}$) appears as a horizontal line on this graph which moves vertically as the probe frequency is varied. The intersection of $\omega_C = \tilde{\Delta}_{32}$ with the allowed values of ω_A (or ω_B) gives the range over which the resonance conditions may be satisfied. These regions are indicated by the cross-hatched zones of Fig. 3.

The above analysis is modified somewhat if the variation in $\tilde{\Delta}_{21}$ is due to the Doppler effect.[34] In this case, a distribution of (axial) velocities

$$W(v) = \exp(-v^2/u^2)/\pi^{1/2} u , \qquad (5.1)$$

where u is the most probable speed, leads to frequencies

$$\omega_A = -\tfrac{1}{2}(\Delta_{21} + k_1 v)$$
$$\quad -\tfrac{1}{2}[(\Delta_{21} + k_1 v)^2 + 4\alpha_1^2]^{1/2} , \qquad (5.2a)$$

$$\omega_B = -\tfrac{1}{2}(\Delta_{21} + k_1 v)$$
$$\quad +\tfrac{1}{2}[(\Delta_{21} + k_1 v)^2 + 4\alpha_1^2]^{1/2} , \qquad (5.2b)$$

$$\omega_C = \Delta_{32} + k_2 v . \qquad (5.2c)$$

For the sake of definiteness, we take $k_1 > 0$ and k_2 of arbitrary sign [see Eq. (2.4)] which simply corresponds to a choice of the direction of the positive z direction.

Inhomogeneously broadened three-level systems have been previously analyzed using a graphical approach.[15,17,22] We recall some well-known results and then discuss features not emphasized in earlier works.

To construct a graph similar to that in Fig. 3, we first define the dimensionless parameters

$$x = (\Delta_{21} + k_1 v)/\alpha_1 , \qquad (5.3)$$

$$\omega'_\beta = \omega_\beta/\alpha_1 \quad (\beta = A,B,C) . \qquad (5.4)$$

In terms of these parameters the quantity

$$\omega'_C = v + \frac{k_2}{k_1} x , \qquad (5.5)$$

with

$$v = [\Delta_{32} - (k_2/k_1)\Delta_{21}]/\alpha_1 \qquad (5.6)$$

is a linear function of x with slope of k_2/k_1 and y intercept of v. In Fig. 4, the dimensionless frequencies $\omega'_A, \omega'_B, \omega'_C$ are plotted versus x. For a given Δ_{21} there is a range of x centered about $x = \Delta_{21}/\alpha_1$ of width $2k_1 u/\alpha_1$ which determines

the values of ω'_A and ω'_B present in the system. This range, which simply represents the inhomogeneous broadening in the system owing to the Doppler effect, is indicated by the vertical lines in Fig. 4. The intersection of ω'_C with ω'_A and ω'_B in this region determines possible resonances of the system since it corresponds to $\omega_{CB} = 0$ or $\omega_{CA} = 0$. As Δ_{32} is tuned, the ω'_C curve moves vertically and scans all possible resonances. The factors $\cos^2\theta$, $\sin^2\theta$, n_C^0, n_B^0, and n_A^0 which appear as weight factors for the resonances [see Eq. (3.2)] may be obtained from Fig. 5.

The velocity averaging is easily performed by noticing that for $\gamma_{\alpha\beta} << |\omega_{\alpha\beta}|$ one can write

$$\frac{1}{\gamma_{CB} + i\omega_{CB}} \simeq -i\mathscr{P}\left\{\frac{1}{\omega_{CB}}\right\}$$

$$+ \frac{\pi}{|\partial\omega_{CB}/\partial v|_{v=v_{CB}}}\delta(v - v_{CB}) , \qquad (5.7)$$

where $\omega_{CB}(v_{CB}) = 0$ and $|\partial\omega_{CB}/\partial v|_{v=v_{CB}} \neq 0$ (v_{CB} is a simple zero of ω_{CB}). In the case $k_2/k_1 > 0$ (depicted in Fig. 4) the probe absorption is simply
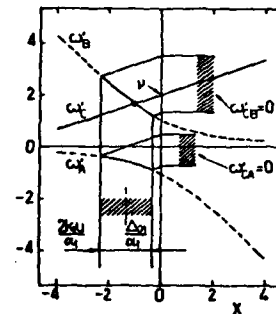

FIG. 4. A curve similar to Fig. 3 in which the dressed-state frequencies $\omega'_A, \omega'_B, \omega'_C$ (in units of α_1) are plotted as a function of velocity through the parameter $x = (\Delta_{21} + k_1 v)/\alpha_1$. Since ω'_C varies linearly with v and, consequently, also linearly with x; the curve $\omega'_C(x)$ is a straight line of slope k_2/k_1 and ω' intercept $v = [\Delta_{32} - (k_2/k)\Delta_{21}]/\alpha_1$. The range of allowed x, indicated by the heavy portions of the ω'_A and ω'_B curves, is centered at Δ_{21}/α_1 and has a width determined by the Doppler distribution, which, in this case, is the inhomogeneous broadening mechanism. Tuning the probe corresponds to a vertical displacement of the ω'_C curve.

$$I(\Delta_{32})=\frac{\pi}{k_1}\left[W\left[\frac{\alpha_1 x-\Delta_{21}}{k_1}\right]\frac{\cos^2\theta(n_C^0-n_B^0)}{|\partial\omega_{CB}'/\partial x|}\bigg|_{x=x_{CB}}+W\left[\frac{\alpha_1 x-\Delta_{21}}{k_1}\right]\frac{\sin^2\theta(n_C^0-n_A^0)}{|\partial\omega_{CA}'/\partial x|}\bigg|_{x=x_{CA}}\right];$$

$$(5.8)$$

where the dimensionless velocity parameter x, Eq. (5.3), has been introduced.

Equation (5.8) together with Figs. 4 and 5 can be used to obtain some qualitative features of the probe spectrum. One first determines the allowed range of x contributing to the spectrum. Using Eq. (5.3) and the fact that $|v|\lesssim u$ it is seen that x must fall within the range defined by

$$\left|x-\frac{\Delta_{21}}{\alpha_1}\right|\lesssim\frac{k_1 u}{\alpha_1}.\qquad(5.9)$$

This range of x, centered at Δ_{21}/α_1 with width of order $2k_1 u/\alpha_1$, is indicated schematically by the heavy portions of ω_A' and ω_B' curves in Fig. 4. Having found the allowed range of x, one then proceeds as follows:

(1) The line $\omega_C'(x)$ [Eq. (5.5)] is drawn for each value of Δ_{32} (or, equivalently v) to determine the position, if any, of resonances $x=x_{CA}(v)$ or $x=x_{CB}(v)$ for which $\omega_C'=\omega_A'$ or $\omega_C'=\omega_B'$, respectively. Notice that a variation of v, which corresponds to varying the probe frequency, is represented in Fig. 4 by a vertical translation of the ω_C' line.

(2) At any resonance positions $x_{CA}(v)$, $x_{CB}(v)$, the corresponding weight functions $\cos^2\theta$, $\sin^2\theta$, $n_C^0-n_B^0$ and $n_C^0-n_A^0$ are read off of Fig. 5, and the velocity distribution $W[(\alpha_1 x-\Delta_{21})/k_1]$ is evaluated at $x=x_{CA}$ or $x=x_{CB}$.

(3) The final factor contributing in Eq. (5.8),

$$\frac{\partial\omega_{C\alpha}'}{\partial x}\bigg|_{x=x_{C\alpha}(v)}=\frac{\partial(\omega_C'-\omega_\alpha')}{\partial x}\bigg|_{x=x_{C\alpha}(v)}\quad(\alpha=A,B),$$

is the *difference in slopes* between the ω_C' and ω_α' curves at the resonance positions. Using the above steps, one can construct the probe spectrum for various values of the parameters α_1, k_2/k_1 and Δ_{21}.

For positive slope $[k_2/k_1>0]$ of $\omega_C'(x)$, it is obvious from Fig. 4 that there always exists some values of v (i.e., probe detunings Δ_{32}) leading to CA and CB resonances. For k_2 negative (recall that we have arbitrarily taken $k_1>0$), both resonances still occur if $k_2(k_1+k_2)>0$ (magnitude of the slope of ω_C' greater than the magnitude of the slopes of the

asymptotes of the ω_B' and ω_A' curves). On the other hand, if $k_2(k_1+k_2)<0$, ω_{CB} resonances are possible only if $v>0$ and ω_{CA} resonances only if $v<0$. There is a range of v

$$v^2\leq v_{cr}^2=4|k_2(k_1+k_2)|/k_1^2\qquad(5.10)$$

for which no resonances are possible and no probe absorption occurs.

Figures 6—9 illustrate the various cases. In Fig. 6 we have graphed $\omega_{CA}'(x,v)=0$ and $\omega_{CB}'(x,v)=0$ for the case $k_2>0$. As discussed above, for each value of x, there is one value of v for which $\omega_{CA}=0$ and one for which $\omega_{CB}=0$. By mapping out a horizontal strip giving the range of allowed x and projecting the intersection of this strip with the $\omega_{CA}'=0$ and $\omega_{CB}'=0$ curves onto the v axis, one obtains the range of $v=[\Delta_{32}-(k_2/k_1)\Delta_{21}]/\alpha_1$ for which significant probe absorption occurs.

If $k_1 u>>\alpha_1$ and $|\Delta_{21}|\lesssim k_1 u$, then x is centered at Δ_{21}/α_1 and the strip of allowed x has a large width $2k_1 u/\alpha_1>>1$ which always includes $x=0$. In this case there is a wide range of v for which resonances occur as shown in Fig. 7(a). The CA and CB resonances overlap, leading to the typical probe spectrum shown in Fig. 7(a). For this case, the probe spectrum is given by (see Appendix C)
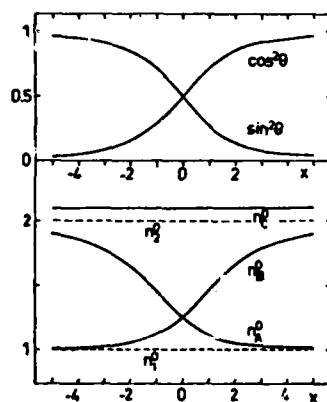

FIG. 5. Curves which give the weight factors $\sin^2\theta$, $\cos^2\theta$, n_α^0 $(\alpha=A,B,C)$ as a function of x. In the example shown, we have taken $n_1^0:n_2^0:n_3^0=1:2:2.1$ and $\Gamma_1:\Gamma_2=3:1$.

$$I(\Delta_{32}) \simeq \frac{\pi^{1/2}}{|k_2|u} \exp\left[-\left[\frac{\Delta_{32}}{k_2} + \frac{\Delta_{32}+\Delta_{21}}{k_1+k_2}\right]^2 \Big/ 4u^2\right]$$

$$\times \left[(n_3^0 - n_2^0) + \frac{|k_2|}{\Gamma_2 k_1}(n_2^0 - n_1^0)\frac{\alpha_1^2 \gamma_{\text{eff}}}{[\Delta_{32}-(k_2/k_1)\Delta_{21}]^2 + \gamma_{\text{eff}}^2 \alpha_1^2/\Gamma_1\Gamma_2}\right],$$

$$(5.11)$$

where

$$\gamma_{\text{eff}} = \Gamma_1 \frac{|k_2|}{k_1} + \Gamma_2 \frac{|k_1+k_2|}{k_1} .$$

$$(5.12)$$

It consists of a broad background term representing linear absorption plus a strongly power-broadened Lorentzian of width $\alpha_1(\gamma_{\text{eff}}^2/\Gamma_1\Gamma_2)^{1/2}$. Although the ω_{CB} and ω_{CA} terms are not themselves Lorentzian, their sum is. Equation (5.11) may be obtained from Eq. (24) of Ref. 13 in the limit of large α_1^2.

For large detunings, $|\Delta_{21}| >> \alpha_1, k_1 u$, the situation is depicted in Fig. 7b. The ω_{CB} and ω_{CA} resonances are now nonoverlapping, leading to the spectrum shown. In this limit

$$\omega_{CB} \simeq \Delta_{32} - \frac{\alpha_1^2}{\Delta_{21}} + k_2 v ,$$

$$(5.13a)$$

$$\omega_{CA} \simeq \Delta_{32} + \Delta_{21} + \frac{\alpha_1^2}{\Delta_{21}} + (k_1+k_2)v ,$$

$$(5.13b)$$

and $\cos^2\theta \approx 1$, $\gamma_{CB} \approx \gamma_{32}$, $\gamma_{CA} \approx \gamma_{31}$. The resulting spectrum is the sum of two Voigt profiles

$$I(\Delta_{32}) \simeq \frac{n_3^0 - n_2^0}{|k_2|u} Z_I\left[\frac{\Delta_{32}-\alpha_1^2/\Delta_{21}+i\gamma_{32}}{|k_2|u}\right] + \frac{\alpha_1^2}{\Delta_{21}^2}\frac{n_3^0-n_1^0}{|k_1+k_2|u}Z_I\left[\frac{\Delta_{32}+\Delta_{21}+\alpha_1^2/\Delta_{21}+i\gamma_{31}}{|k_1+k_2|u}\right],$$

$$(5.14)$$

where Z_I is the imaginary part of the plasma-dispersion function.[35] The spectral components are Gaussians if the arguments of Z_I have magnitude much less than unity and Lorentzians in the opposite limit.

For large intensities, $|\alpha_1| >> |\Delta_{21}|, k_1 u$, the situation is depicted in Fig. 7c. In this limit both the central value and the range of x is much less than unity; the resulting spectrum arises from nonoverlapping CA and CB resonances. For this case we have

$$\omega_{CB} \simeq \Delta_{32} + \tfrac{1}{2}\Delta_{21} - \alpha_1 + \left[k_2 + \tfrac{1}{2}k_1 - \frac{\Delta_{21}}{4\alpha_1}k_1\right]v - \frac{\Delta_{21}^2 + k_1^2 v^2}{8\alpha_1} ,$$

$$(5.15a)$$

$$\omega_{CA} \simeq \Delta_{32} + \tfrac{1}{2}\Delta_{21} + \alpha_1 + \left[k_2 + \tfrac{1}{2}k_1 + \frac{\Delta_{21}}{4\alpha_1}k_1\right]v + \frac{\Delta_{21}^2 + k_1^2 v^2}{8\alpha_1} ,$$

$$(5.15b)$$

$\sin^2\theta \approx \cos^2\theta \approx \tfrac{1}{2}$, and $\gamma_{CB} \approx \gamma_{CA} \approx \tfrac{1}{2}(\gamma_{31}+\gamma_{32})$. Two (nearly) symmetric resonances appear at $\Delta_{32} = -\tfrac{1}{2}\Delta_{21} \pm \alpha_1$ and the spectrum is the sum of two Voigt profiles

$$I(\Delta_{32}) \simeq \frac{1}{2}\left[\frac{\Lambda_3}{\Gamma_3} - \frac{\Lambda_2+\Lambda_1}{\Gamma_2+\Gamma_1}\right]\frac{1}{|k_2+\tfrac{1}{2}k_1|u}\left[Z_I\left[\frac{\Delta_{32}+\tfrac{1}{2}\Delta_{21}-\alpha_1+i\gamma_{CB}}{|k_2+\tfrac{1}{2}k_1|u}\right] + Z_I\left[\frac{\Delta_{32}+\tfrac{1}{2}\Delta_{21}+\alpha_1+i\gamma_{CA}}{|k_2+\tfrac{1}{2}k_1|u}\right]\right],$$
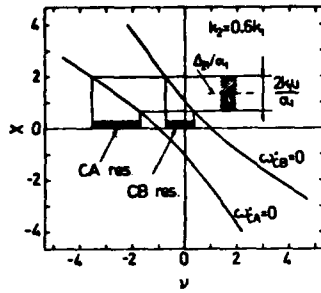
$$(5.16)$$

FIG. 6. Curves representing the resonance conditions $\omega'_{CA}(x,v)=0$ and $\omega'_{CB}(x,v)=0$ for the case $k_2>0$. For a range of allowed x determined by the detuning (Δ_{21}/α_1) and Doppler width (k_1u/α_1), one can find the regions of probe detuning (v) for which absorption can occur. Conversely, for any value of probe detuning v, one can determine whether or not any resonant velocity subset (x) can contribute to the signal. When $k_2>0$, there exists, for each value of v, values of x for which both $\omega'_{CA}=0$ and $\omega'_{CB}=0$.

which are approximately Gaussians if the magnitude of the arguments of the Z_i functions are much less than unity. [In arriving at Eq. (5.16), we neglected the small $(\Delta_{21}^2+k_1^2v^2)/8\alpha_1$ terms in Eq. (5.15).]

The analysis is virtually unchanged if $k_2<0$ and $k_2(k_1+k_2)>0$. The ω'_A, ω'_B curves of Fig. 6 are rotated by 90° about the origin, but the same type of resonance conditions occur. If $k_1u>>\alpha_1$ and $|\Delta_{21}|\lesssim k_1u$, Eqs. (5.11) and (5.12) are still valid; γ_{eff} is now smaller than in the copropagating case owing to some Doppler-phase cancellation. Equations (5.14) and (5.16) remain valid for the large detuning and intense field limits. It is now possible, however, to have a narrow resonance in the large detuning case, provided that $k_2\simeq -k_1$.[36]

The remaining case $k_2(k_1+k_2)<0$ is represented in Fig. 8. As discussed above, there is a range of detunings v $(v^2<v_{\text{cr}}^2)$ for which no resonance values of x may be found. For $v>v_{\text{cr}}$ two values of x correspond to the ω_{CB} resonance and, for $v<-v_{\text{cr}}$, two values of x correspond to the ω_{CA} resonance. The spectrum for the case $k_1u>>\alpha_1$, $|\Delta_{21}|\lesssim k_1u$ is shown in Fig. 9(a). For any $|v|>v_{\text{cr}}$, there are two velocity subgroups of atoms which contribute independently to the probe spectrum except in a region of width $\approx\Gamma$ near $|v|=v_{\text{cr}}$ where both contributions overlap. It is just this overlap region which gives rise to the non-power broadened resonances shown in Fig. 9(a). As derived in Appendix C, the spectrum for this case $(|v|\gtrsim v_{\text{cr}})$ is
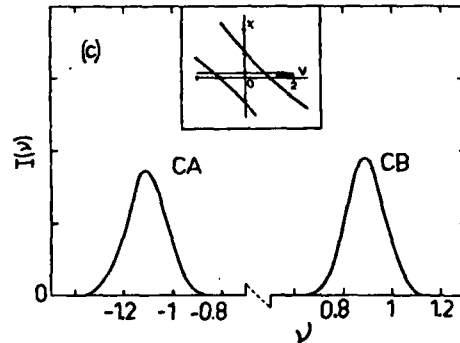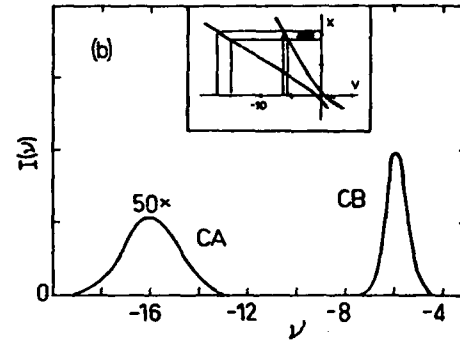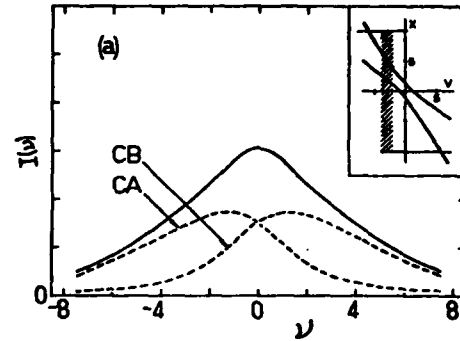

FIG. 7. Typical probe-absorption spectra (in arbitrary units) for the case $k_2=0.6k_1>0$ in the three limits (a) $k_1u>>\alpha_1$, $k_1u>|\Delta_{21}|$, (b) $|\Delta_{21}|>>\alpha_1$, k_1u, and (c) $\alpha_1>>k_1u$, $|\Delta_{21}|$. In drawing these curves, we have taken $n_1^0:n_2^0:n_3^0=1:3:4$ and $\Gamma_1=\Gamma_2<<\alpha_1$. In (a), $\Delta_{21}=0$ and $k_1u=10\alpha_1$; in (b), $\Delta_{21}=10\alpha_1$ and $k_1u\approx\alpha_1$; in (c), $\Delta_{21}=k_1u=0.1\alpha_1$. The inserts are curves analogous to Fig. 6 and indicate the resonant-velocity subgroups which contribute to the probe absorption at a given value of v.

$$I(\nu) = \frac{1}{k_1 u} \left[\frac{2\pi(k_1 + k_2)}{|k_2|} \right]^{1/2} \exp\left[- \left[\Delta_{21} - \alpha_1 \frac{(k_1 + 2k_2)}{[|k_2|(k_1 + k_2)]^{1/2}} \right]^2 \Big/ k_1^2 u^2 \right]$$

$$\times \left[(n_3^0 - n_2^0) + \frac{\Gamma_1 |k_2|(n_2^0 - n_1^0)}{\Gamma_1 |k_2| + \Gamma_2 |k_1 + k_2|} \right] \mathrm{Re} \left\{ \left[|\nu| - \nu_{cr} - \frac{i}{\alpha_1} \left[\frac{|k_2|}{k_1} \gamma_{31} + \frac{k_1 + k_2}{k_1} \gamma_{32} \right] \right]^{-1/2} \right\}.$$

$$(5.17)$$

The large detuning and large field intensity limits are depicted in Figs. 9(b) and 9(c), respectively. Equations (5.14) and (5.16) may still be used to describe these profiles. For the intense field case, a narrow resonance occurs if $k_2 \simeq -k_1/2$.

The Doppler-free nature of the narrow resonances which may occur when $\alpha_1 >> k_1 u$ or $|\Delta_{21}| >> k_1 u$, α_1 arises from a cancellation of Doppler phases. All atoms contribute equally to these resonances; this feature is easily seen in Fig. 4. If $\alpha_1 >> k_1 u$, the range of allowed values of x narrows considerably and the heavy portions of the ω_A' and ω_B' curves reduce to points. If the ω_C' curve is tangent to the ω_A' or ω_B' curves at these points, then all atoms contribute to the resonance. This condition is

$$\frac{k_2}{k_1} = -\frac{1}{2} \pm \frac{1}{2} \frac{\Delta_{21}}{(\Delta_{21}^2 + 4\alpha_1^2)^{1/2}} \qquad (5.18)$$

leading to narrow resonances centered at

$$\Delta_{32} = -\tfrac{1}{2}\Delta_{21} \pm \tfrac{1}{2}(\Delta_{21}^2 + 4\alpha_1^2)^{1/2}, \qquad (5.19)$$

where the upper (lower) signs refer to the $\omega_C' = \omega_B'$ ($\omega_C' = \omega_A'$) resonance. If $|\Delta_{21}| >> k_1 u, \alpha_1$, the allowed x values are located on the asymptotes of
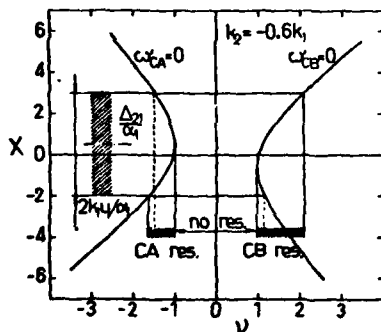
FIG. 8. Resonance conditions $\omega_{CA}'(x,\nu) = 0$ and $\omega_{CB}'(x,\nu) = 0$ for the case $-k_1 < k_2 < 0$. There is now a range of $|\nu| < \nu_{cr}$ for which there are no resonant-velocity groups of atoms.
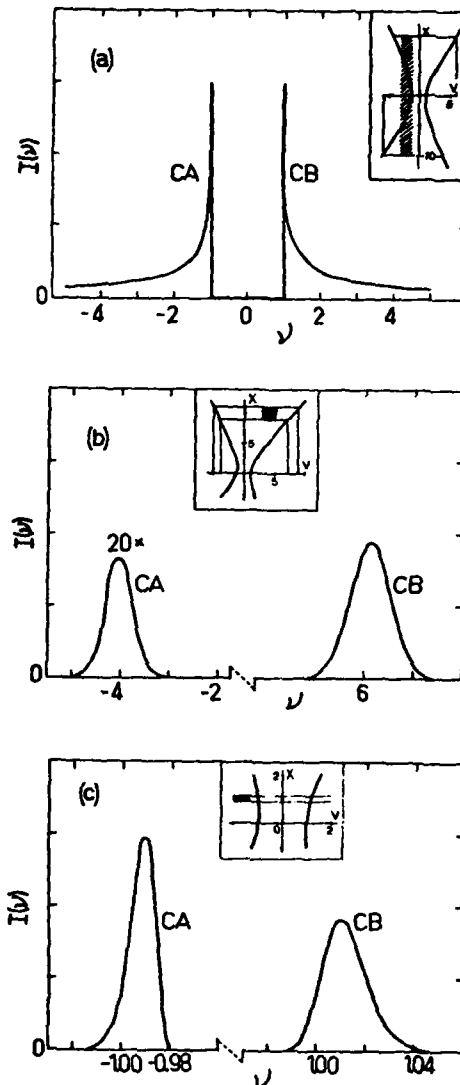

FIG. 9. Probe-absorption spectra for the case $k_2/k_1 = -0.6$, but otherwise the same conditions as in Fig. 7. Note that, owing to Doppler-phase cancellation, the resonances are narrower than those in the corresponding spectra of Fig. 7.

the ω'_A and ω'_B curves. By having $k_2 = -k_1$, the ω'_C curve coincides with these asymptotes so that all atoms once again contribute. Since the resonance condition is the same for all the atoms, the resulting resonance is narrow.

On the other hand, when $\alpha_1 << k_1 u, |\Delta_{21}| \lesssim k_1 u$ only a limited velocity subset of atoms, determined by the pump intensity and detuning (i.e., $|k_1 v + \Delta_{21}| \lesssim \alpha_1$), contribute to the probe absorption. The resulting linewidths are smaller than the Doppler width, reflecting the narrower range of contributing velocity groups.

VI. EXTENSIONS OF THE DAP APPROACH

The DAP allows one to gain physical insight into problems involving more complicated atom-field interactions. The dressed-energy levels of a multilevel atom can be solved exactly or approximately. The weight factors of the spectra which involve elements of the transformation matrix from the bare to dressed picture are generally more difficult to obtain. For dressed-energy-level separations much greater than the natural widths of the levels, a rate-type solution to the DAP equations may be used. In this section, some features of a four-level problem and a three-level problem involving a standing-wave pump field are discussed. In Sec. VII some aspects of coherent transients are examined using the DAP formalism.

A. Strongly coupled three-level system[12,15,19,37-41]

We first consider a three-level system in which one must now diagonalize the complete Hamiltonian. The eigenvalue equation

$$\omega(\omega + \tilde{\Delta}_{21})(\omega - \tilde{\Delta}_{32}) - \alpha_2^2(\omega + \tilde{\Delta}_{21})$$
$$- \alpha_1^2(\omega - \tilde{\Delta}_{32}) = 0 \qquad (6.1)$$

always has three real roots ω_α $(\alpha = A, B, C)$. Equations (2.23) now take the form

$$\dot{\tilde{\rho}}_{\alpha\alpha} = \Lambda_\alpha - \Gamma_\alpha \tilde{\rho}_{\alpha\alpha} + \sum_{\sigma,\delta} R_{\alpha\alpha;\sigma\delta} \tilde{\rho}_{\sigma\delta} , \qquad (6.2a)$$

$$\dot{\tilde{\rho}}_{\alpha\beta} = \Lambda_{\alpha\beta} - (\gamma_{\alpha\beta} + i\omega_{\alpha\beta})\tilde{\rho}_{\alpha\beta} + \sum_{\sigma,\delta} R_{\alpha\beta;\sigma\delta}\tilde{\rho}_{\sigma\delta} ,$$
$$(6.2b)$$

where the coefficients are functions of the transformation matrix elements $\langle i | \alpha \rangle$. The coupling

coefficients $R_{\alpha\beta,\sigma\delta}$ are all proportional to differences between decay rates Γ_l. The $\omega_{\alpha\beta} = \omega_\alpha - \omega_\beta$ are the frequency separations between the dressed states. If $|\omega_{\alpha\beta}| >> \Gamma_l$, the off-diagonal density-matrix elements are small and an approximate solution to Eqs. (6.2) is

$$\tilde{\rho}_{\alpha\alpha}^0 = \Lambda_\alpha / \Gamma_\alpha = n_\alpha^0 , \qquad (6.3a)$$

$$\tilde{\rho}_{\alpha\beta}^0 = -i \left[\Lambda_{\alpha\beta} + \sum_\sigma R_{\alpha\beta;\sigma\sigma} n_\sigma^0 \right] \omega_{\alpha\beta}^{-1} . \qquad (6.3b)$$

Transforming back to the coordinate system $|i\rangle$ we obtain the observables $\tilde{\rho}_{ll}$, $\tilde{\rho}_{21}$, or $\tilde{\rho}_{32}$. In the special case when all Γ's are equal $(\Gamma_l = \gamma)$, the coupling coefficients $R_{\alpha\beta,\sigma\delta}$ vanish, and the exact solution is simply

$$\tilde{\rho}_{\alpha\alpha}^0 = \Lambda_\alpha / \gamma , \qquad (6.4a)$$

$$\tilde{\rho}_{\alpha\beta}^0 = \Lambda_{\alpha\beta} / (\gamma + i\omega_{\alpha\beta}) . \qquad (6.4b)$$

In this limit, the absorption spectrum for field α_2 is

$$I(\Delta_{32}) = -\frac{1}{\alpha_2} \sum_{\alpha,\beta} \frac{\omega_{\alpha\beta} \langle 3 | \alpha \rangle \langle \beta | 2 \rangle \Lambda_{\alpha\beta}}{\gamma^2 + \omega_{\alpha\beta}^2} ,$$
$$(6.5)$$

where $\Lambda_{\alpha\alpha} \equiv \Lambda_\alpha$ and $\omega_{\alpha\alpha} = 0$. Once the transformation matrix elements are known this formula is useful for analyzing the strong-field absorption (cf. the corresponding rather lengthy expression of the BAP). The solution is more complicated when interlevel relaxation is allowed or the decay rates differ greatly. Then the spectrum must be obtained using Eq. (6.2) or (6.3) together with the transformation back to the BAP.

B. Four-level systems[42-44]

As shown previously, the DAP is especially transparent when one of the fields is weak and the strongly coupled part satisfies the rate-type solution. This result can be applied to a four-level system in which levels 1,2,3 are strongly coupled by fields α_1 and α_2 and one of these levels is weakly coupled by a probe field to level 4. The corresponding dressed states are labeled A, B, C, D where D is the weakly coupled state. To obtain the resonance positions we have to solve Eq. (6.1). A graphical solution is shown in Fig. 10 for fixed α_2 as a function of α_1. Whenever $\omega_D = \omega_\alpha$ $(\alpha = A, B, C)$ a probe resonance results. A rate-type solution obviously requires that the anticrossing in Fig. 10 is
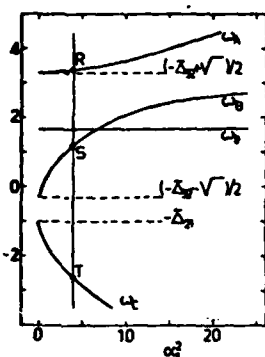
FIG. 10. Dressed-atom frequencies as a function of α_1^2 for $\alpha_2=1$, $\tilde{\Delta}_{21}=1$, and $\tilde{\Delta}_{32}=3$ (all frequencies are in arbitrary units and it is assumed that all relaxation parameters have values much less than one in these units). The horizontal broken lines give the dressed-atom frequencies when $\alpha_1=0$. For a fixed α_1, there are generally three possible probe resonances as the probe frequency $\omega_D=\tilde{\Delta}_D$ is varied. For $\alpha_1^2=4$, these positions are indicated by the points R, S, and T.
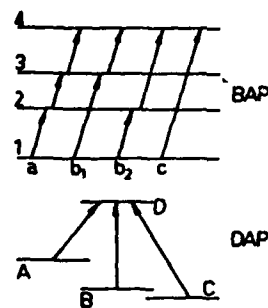

FIG. 11. A classification of the atom-field interactions for four-level systems in both the BAP and DAP. The BAP interpretation, valid only to lowest orders in the fields, is (a) stepwise absorption of α_1, α_2, α_3, (b_1) two-photon absorption of α_1 and α_2 followed by absorption of α_3, (b_2) absorption of α_1 followed by two-photon absorption of α_2 and α_3, and (c) three-photon absorption of α_1, α_2, and α_3. In the DAP, valid at any field intensities, there are three, single-photon processes which contribute to the absorption. For intense fields α_1 and α_2 the single-photon processes do not interfere.

large compared to relaxation rates.

If Doppler broadening is present one may ask whether a splitting similar to the one appearing in three-level systems with $k_2(k_1+k_2)<0$ also occurs in four-level systems. In three-level systems, the splitting shown in Fig. 9 is caused by the absence of resonant-velocity subgroups of atoms over a range of probe detunings. In a four-level system, a resonance occurs when $\omega_D \equiv \Delta_D+k_D v$ is equal to any of the solutions $\omega_a(v)$ of Eq. (6.1). Using the Doppler-shifted values of all the detunings $\tilde{\Delta}_{ij}$ and substituting ω_D for ω in Eq. (6.1), one obtains a cubic equation for v which always has at least one real root.[45] This result implies that there is always at least one resonant-velocity subgroup for all probe detunings of the four-level system. Thus, the mechanism operative in three-level systems leading to the split spectrum of Fig. 9 cannot occur here. The details of the probe spectrum may

depend on the number of resonant velocity subgroups contributing (i.e., one or three), but this feature has yet to be investigated. (Notice that in a five-level system, the quartic eigenvalue equation can have 0, 2, or 4 real roots. The absence of real roots signals a splitting effect similar to that shown in Fig. 9.)

A comparison between the BAP and DAP pictures for a four-level system is shown in Fig. 11 in which the probe acts between levels 3 and 4. The BAP nomenclature is valid in the small-intensity limit only. Note that the processes a and b_1 have the same resonance condition $(\tilde{\Delta}_{43}=0)$ and provide two interfering channels for this resonance. The DAP consists of three noninterfering single-photon transitions allowing for a very simple physical interpretation.

In some special cases, Eq. (6.1) is easily solved, e.g.,

(i) $\tilde{\Delta}_{21}=\tilde{\Delta}_{32}=0$; $\omega_{A,C}=\pm(\alpha_1^2+\alpha_2^2)^{1/2}$, $\omega_B=0$;

(ii) $\tilde{\Delta}_{21}=\tilde{\Delta}_{32}, \alpha_1^2=\alpha_2^2$; $\omega_{A,C}=\pm(\tilde{\Delta}_{21}^2+2\alpha_1^2)^{1/2}$, $\omega_B=0$;

(iii) $\tilde{\Delta}_{21}=-\tilde{\Delta}_{32}, \alpha_1^2=\alpha_2^2$; $\omega_{A,C}=-\frac{1}{2}\tilde{\Delta}_{21}\pm\frac{1}{2}(\tilde{\Delta}_{21}^2+8\alpha_1^2)^{1/2}$, $\omega_B=-\tilde{\Delta}_{21}$.

As an example let us consider the case (ii) in which $\alpha_1=\alpha_2=\alpha$. The transformation is now

$$|A\rangle=\frac{1}{2}\left[1-\frac{\tilde{\Delta}_{21}}{\Omega_R}\right]|1\rangle+\frac{\alpha}{\Omega_R}|2\rangle+\frac{1}{2}\left[1+\frac{\tilde{\Delta}_{21}}{\Omega_R}\right]|3\rangle ,$$ (6.6a)

$$|B\rangle = (\alpha|1\rangle + \tilde{\Delta}_{21}|2\rangle - \alpha|3\rangle)/\Omega_R , \tag{6.6b}$$

$$|C\rangle = \frac{1}{2}\left[1 + \frac{\tilde{\Delta}_{21}}{\Omega_R}\right]|1\rangle - \frac{\alpha}{\Omega_R}|2\rangle + \frac{1}{2}\left[1 - \frac{\tilde{\Delta}_{21}}{\Omega_R}\right]|3\rangle , \tag{6.6c}$$

where $\Omega_R = (\Delta_{21}^2 + 2\alpha^2)^{1/2}$, $\omega_A = \Omega_R$, $\omega_B = 0$, and $\omega_C = -\Omega_R$. If the probe couples levels 4 and 2 $(\omega_D = \tilde{\Delta}_{42})$, if all the γ's are equal and if only level 4 is initially populated the response is simply

$$I(\tilde{\Delta}_{42}) = \frac{\gamma n_4^0}{\Omega_R^2}\left[\frac{\alpha^2}{\gamma^2 + (\tilde{\Delta}_{42} - \Omega_R)^2} + \frac{\tilde{\Delta}_{21}^2}{\gamma^2 + \tilde{\Delta}_{42}^2} + \frac{\alpha^2}{\gamma^2 + (\tilde{\Delta}_{42} + \Omega_R)^2}\right]. \tag{6.7}$$

The absorption spectrum consists of three Lorentzians.[19]
  Equation (6.7) is applicable to the level scheme in Fig. 12 $(k_1 = -k_2 = k_D = k)$ for which

$$\tilde{\Delta}_{21} = \Delta_{21} + kv \ (\Delta_{21} = \omega_{21} - \Omega_1) , \quad \tilde{\Delta}_{32} = -\Delta_{21} + kv , \quad \tilde{\Delta}_{42} = -\Delta_{24} - kv \ (\Delta_{24} = \omega_{24} - \Omega_2) .$$

If $\Delta_{21} = 0$, the conditions for (6.7) are satisfied $(\tilde{\Delta}_{32} = \tilde{\Delta}_{21} = kv, \ \alpha_1^2 = \alpha_2^2 = \alpha^2)$ and we get

$$I(\Delta_{24}) = \frac{n_4^0 \gamma}{(k^2 v^2 + 2\alpha^2)}\left[\frac{\alpha^2}{\gamma^2 + [\Delta_{24} + kv + (k^2 v^2 + 2\alpha^2)^{1/2}]^2}\right.$$

$$\left. + \frac{k^2 v^2}{\gamma^2 + (\Delta_{24} + kv)^2} + \frac{\alpha^2}{\gamma^2 + [\Delta_{24} + kv - (k^2 v^2 + 2\alpha^2)^{1/2}]^2}\right]. \tag{6.8}$$

The velocity-averaged probe-absorption spectrum (assuming $ku >> \gamma$) is given by

$$I(\Delta_{24}) \simeq \frac{n_4^0 \pi^{1/2}}{ku}\exp\left[-\frac{\Delta_{24}^2}{k^2 u^2}\right]. \tag{6.9}$$

There is no narrow structure in the spectrum. The result should be contrasted with the structure obtained when a standing-wave saturator is used (see Fig. 12 and the discussion below).
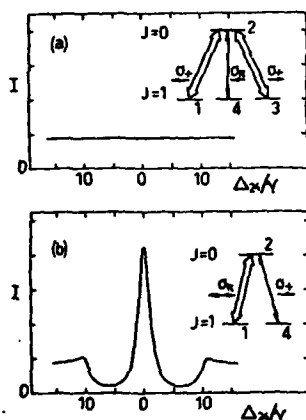

FIG. 12. (a) A four-level scheme in which levels 1,3,4 are degenerate levels of a $J = 1$ state while level 2 is a $J = 0$ state. The strong fields counterpropagate, are circularly polarized, and are resonantly tuned $(\Delta_{21} = 0)$. The probe field is π polarized and acts on the 2-4 transition. The probe absorption spectrum I for this case is flat. (b) For comparison, the probe-absorption spectrum for a three-level system with a standing-wave saturator is shown (see Ref. 53).

C. Standing-wave saturator (two-mode pump)[46-59]

As is well known, the interpretation of the spectra obtained with a standing-wave (SW) saturator is considerably more complicated than the running-wave case.[46-53] Similar difficulties are encountered when the saturator is composed of two running-wave fields having different frequencies.[54-59] The question arises as to whether or not the DAP offers any simplifications.

In the rotating-wave approximation the equation of motion of the density-matrix retains a periodic time dependence owing to the beat frequency $\delta = \Omega_2 - \Omega_1$ between the two saturator modes; in the SW case, this beat frequency is twice the Doppler shift, $\delta = 2k_1 v$. According to the Floquet theorem,[54] the stationary solution to the system contains Fourier components with frequencies $\omega_{A,B}(n) = \omega_{A,B} + n\delta$ $(n = 0, \pm 1, \ldots)$, where ω_A and ω_B are functions of the mode amplitudes and detunings and are chosen such that $|\omega_{AB}| < |\delta|$. These frequencies are related to the eigenfrequen-

cies of the DAP. The states $|1,n_1,n_2\rangle$ and $|2,m_1,m_2\rangle$ are nearly degenerate if

$$n_1+n_2=m_1+m_2+1=N ,$$

where n_i and m_i are the number of photons in mode i and we have assumed $\omega_{21}>0$. For a fixed total number of photons N there is an "infinite" ($\simeq 2\times N$) number of bare-atom states which must be diagonalized. The diagonalization, which can be performed using continued fractions, is not done here. Instead we concentrate on some qualitative aspects of the problem.

If the mode spacing δ is fixed, a rate-type solution in the DAP is valid provided that both $|\delta-\omega_{BA}|>>\gamma$ and $\omega_{AB}>>\gamma$ ($\omega_{BA}=\omega_B-\omega_A>0$). Similarly to the running-wave case, probe resonances are found when $\omega_C=\omega_{A,B}+n\delta$, where $\omega-$ corresponds to the probe detuning (recall that the probe couples to a third, unperturbed level). The heights of the various peaks generally depend in a complicated way on the detunings and amplitudes of the saturator modes.

For a SW saturator the beat frequency $\delta=2k_1v$ is velocity dependent. Difficulties arise since, for slow enough atoms, the energy levels in the DAP form a quasicontinuum. Thus a rate-type solution for the DAP is clearly not applicable for $|2k_1v|\lesssim\gamma$. This region must be described by other approximations. For instance, in the limit $v\rightarrow 0$, the atoms are stationary and the probe response is readily calculated.[52]

Some qualitative understanding of the SW problem is obtained by constructing DAP energy-level diagrams similar to those of the running-wave case (see Fig. 4). Two examples are shown in Figs. 13 and 14.

In Fig. 13, we display the dressed-energy levels as a function of k_1v for a SW saturator with detuning $|\Delta_{21}|>\alpha$. The standing wave consists of two running-wave components labeled by $(\alpha_+, k_+=k_1>0)$ and $(\alpha_-, k_-=-k_1)$. In the region $k_1v<<-\gamma$ (assuming $\Delta_{21}>0$), we can, to a first approximation, use the unperturbed energy levels $\omega_{A,B}$ associated with the running wave α_+ since the wave α_- is strongly detuned and acts only as a perturbation in the region $k_1v<<-\gamma$. The dressed-level frequencies associated with the α_+ wave are given by [see Eq. (5.2)]

$$\omega_{A,B}(n)\approx-\tfrac{1}{2}(\Delta_{21}+k_1v)$$

$$\mp\tfrac{1}{2}[(\Delta_{21}+k_1v)^2+4\alpha_+^2]^{1/2}+2nk_1v .$$

(6.10)

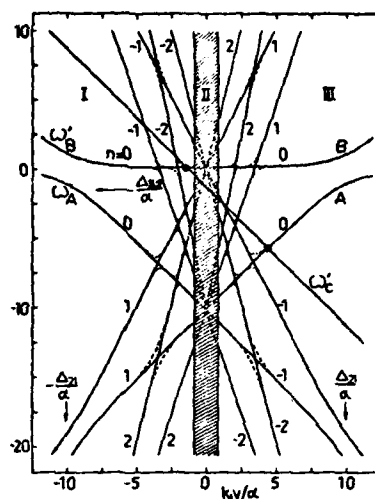
FIG. 13. Dressed-state frequencies $\omega'_A(n)=\omega'_A$ $+2nk_1v/\alpha$, $\omega'_B(n)=\omega'_B+2nk_1v/\alpha$, and $\omega'_C=(\Delta_{32}+k_2v)/\alpha$ ($k_2\simeq-k_1$) as a function of k_1v for a large-field detuning $|\Delta_{21}|>>\gamma$. Values for n are given by the integers labeling each curve. All frequencies are expressed in units of α; the detunings are $\Delta_{21}/\alpha=10$ and $\Delta_{32}/\alpha=-1$. In the range $\gamma<|k_1v|<|\Delta_{21}|$, the frequencies $\omega_A(n)$ and $\omega_B(n)$ are approximately given by $\omega_A(n)=-\Delta_{21}+|k_1v|+2nk_1v$ and $\omega_B(n)=2nk_1v$. The diagram may be used to determine resonance conditions in regions I and III, but not in region II where the rate-type solutions of the DAP break down. Resonant-velocity groups are determined by the intercept of the ω'_C curve with the curves $\omega'_{A,B}(n)$. In the example shown, the major contributions to the probe response arise from the crossings denoted by the large dots (see Fig. 4 of Ref. 53).

Equation (6.10) is not strictly applicable at any value of k_1v where two of the eigenfrequencies are degenerate. At such points, we must use degenerate perturbation theory: the net result is that the crossings are transformed into anticrossings owing to the action of the saturator mode α_-. The energy levels are sketched in Fig. 13.

In the region $k_1v>>\gamma$, the roles of α_+ and α_- are interchanged; the corresponding dressed-level frequencies are given by Eq. (6.10) with the replacement of k_1 by $-k_1$ and α_+ by α_-.

In the intermediate region $-\gamma<k_1v<\gamma$, the rate-type solution of DAP fails. There one may, as a first approximation, use the results valid for $v=0$ discussed in Sec. IV modified to incorporate the standing-wave nature of the saturator. In this region Eq. (6.10) is replaced by

$$\omega_{A,B}\simeq-\tfrac{1}{2}\Delta_{21}\mp\tfrac{1}{2}[\Delta_{21}^2+4\alpha(z)^2]^{1/2} ,$$

(6.11)

where

$$\alpha(z) = |\alpha_+ e^{-ik_1 z} + \alpha_- e^{ik_1 z}| . \qquad (6.12)$$

The inhomogeneity in $\omega_{A,B}$, owing to the z dependence of $\alpha(z)$, can be treated by the methods outlined at the beginning of Sec. V.

Tuning the probe corresponds to moving the line $\omega_C = \Delta_{32} + k_2 v$ vertically. For each value of Δ_{32} there exists an infinite number of resonant subgroups v satisfying the condition $\omega_C(v) = \omega_{A,B}(v, n)$. Whether these resonance subgroups really manifest themselves in the probe absorption depends on the magnitude of the various weight factors derived from the BAP→DAP transformation. For example, in the case shown in Fig. 13, the two major resonant-velocity subgroups are determined at the intersection parts of the ω_C' and dressed states shown in the figure. For other detunings, one can map out the contributing resonant-velocity subgroups and obtain qualitative agreement with the numerically calculated curves of Fig. 4 of Ref. 53.

Figure 14 represents the case of a resonantly tuned SW saturator ($\alpha_+ = \alpha_- = \alpha$) for which the exact DAP energy levels are given by[46-59]

$$\omega_{A,B}(n) = nk_1 v$$

$$\omega_A(n) = -|k_1 v| + 2nk_1 v , \quad \omega_B(n) = 2nk_1 v .$$

The method for determining possible resonant-velocity subgroups remains the same. It should be stressed that this method indicates the positions of possible resonant structure. The determination of
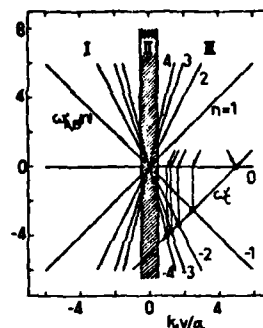

FIG. 14. A diagram corresponding to Fig. 13 for a resonantly tuned ($\Delta_{21} = 0$), standing-wave saturator. In this case, the exact dressed-level frequencies are given by $\omega_{A,B}'(n) = nk_1 v/\alpha$ [$\omega_A(n) = -|k_1 v| + 2nk_1 v$; $\omega_B(n) = 2nk_1 v$]. We have chosen a probe with detuning $\Delta_{32}/\alpha = -5$ and propagation vector $\vec{k}_2 \simeq \vec{k}_1$ such that $\omega_C' \simeq -5 + k_1 v/\alpha$. Some of the resonant-velocity groups indicated by the arrows manifest themselves as distinct peaks in the velocity-dependent probe response (see Fig. 2 of Ref. 53).

the weights associated with these resonances represents a much more complicated problem.[46-59] The striking difference in probe response for running- and standing-wave saturators is illustrated in Fig. 12. The structure observed in Fig. 12(b) has its origin in the various harmonics which enter when a standing-wave saturator is used (but are absent for traveling-wave saturators).

VII. DAP TRANSIENTS

A. Two-level system

The steady-state spectra have been given a simple physical interpretation using the DAP. It is interesting to study also transient behavior using the DAP.[60] For simplicity we assume that $\Gamma_2 = \Gamma_1 = \gamma$ in which case the DAP equation of motion for the AB system is simply

$$\dot{\tilde{\rho}}_{AA} = \Lambda_A - \gamma\tilde{\rho}_{AA} , \qquad (7.1a)$$

$$\dot{\tilde{\rho}}_{BB} = \Lambda_B - \gamma\tilde{\rho}_{BB} , \qquad (7.1b)$$

$$\dot{\tilde{\rho}}_{BA} = \Lambda_{BA} - (\gamma + i\omega_{BA})\tilde{\rho}_{BA} . \qquad (7.1c)$$

[Notice that we have assumed $\alpha_1 = $ constant; therefore, Eq. (7.1) can be applied only for stepwise changes of α_1.]

Assume that field α_1 is switched on at time $t = 0$ leading to an optical nutation signal in the BAP. The solution of the DAP equations (7.1) is

$$\tilde{\rho}_{aa}(t) = (\Lambda_a/\gamma)(1 - e^{-\gamma t}) + \tilde{\rho}_{aa}(0)e^{-\gamma t} , \qquad (7.2a)$$

$$\widetilde{\rho}_{BA}(t)=\left[\frac{\Lambda_{BA}}{\gamma+i\omega_{BA}}\right](1-e^{-(\gamma+i\omega_{BA})t})+\widetilde{\rho}_{BA}(0)e^{-(\gamma+i\omega_{BA})t}. \tag{7.2b}$$

The populations show a simple exponential decay towards their new equilibrium. The oscillatory nutation-type behavior is contained in $\widetilde{\rho}_{BA}$. The initial conditions, obtained from (2.29) for an incoherent initial state, are given by

$$\widetilde{\rho}_{AA}(0)=n_1^0\cos^2\theta+n_2^0\sin^2\theta, \tag{7.3a}$$

$$\widetilde{\rho}_{BB}(0)=n_1^0\sin^2\theta+n_2^0\cos^2\theta, \tag{7.3b}$$

$$\widetilde{\rho}_{BA}(0)=\tfrac{1}{2}(n_1^0-n_2^0)\sin2\theta. \tag{7.3c}$$

Using Eqs. (2.24) and (7.3) in Eqs. (7.2), we find

$$\widetilde{\rho}_{\alpha\alpha}(t)=\widetilde{\rho}_{\alpha\alpha}(0), \tag{7.4a}$$

$$\widetilde{\rho}_{BA}(t)=\tfrac{1}{2}(n_1^0-n_2^0)\sin2\theta\left[\frac{\gamma}{\gamma+i\omega_{BA}}(1-e^{-(\gamma+i\omega_{BA})t})+e^{-(\gamma+i\omega_{BA})t}\right]. \tag{7.4b}$$

The dressed-atom populations remain constant during the transient. If $\omega_{BA}\gg\gamma$ we can write

$$\widetilde{\rho}_{BA}(t)=\widetilde{\rho}_{BA}(0)e^{-(\gamma+i\omega_{BA})t}. \tag{7.5}$$

Nutation in the BAP corresponds to free-induction decay in the DAP. In the BAP the switching on of α_1 creates the coherence $\widetilde{\rho}_{21}$, while, in the DAP, the same change destroys the initial coherence $\widetilde{\rho}_{BA}(0)$. According to (2.29) all the observables $\widetilde{\rho}_{11}$, $\widetilde{\rho}_{22}$, and $\widetilde{\rho}_{21}$ depend on $\widetilde{\rho}_{BA}$ and, therefore, reflect the decay of $\widetilde{\rho}_{BA}$.

The DAP does not offer any substantial advantages over the BAP in calculating the free-induction decay or photon echo of a two-level system (although it may be useful for nutation echoes).[61] In both cases, the field is off for a long time period between the pulses when the BAP and DAP coincide. The DAP is a more natural approach when a strong-field—atomic-interaction occurs.

B. Three-level transients[62-72]

The DAP can provide a useful description of three-level transients. For a strong pump field α_1 and a weak probe α_2, Eqs. (2.23) give the time evolution of the system in the dressed basis. The DAP is most useful if either (1) field α_1 is constant and field $\alpha_2(t)$ undergoes some transient behavior leading to optical nutation, free-induction decay, photon echo, etc. on the BC and AC transitions (see Fig. 1) or (2) the field α_1 is switched on at some time and α_2 may have an arbitrary time dependence.

We consider first the case when α_1 is constant and α_2 is switched on at $t=0$. Equations (2.23) and (2.29) describing the probe response are (assuming $\Gamma_1=\Gamma_2=\gamma$)

$$\dot{\widetilde{\rho}}_{CA}=-(\gamma_{CA}+i\omega_{CA})\widetilde{\rho}_{CA}-i\alpha_2\sin\theta(\widetilde{\rho}_{CC}^0-\widetilde{\rho}_{AA}^0)-i\alpha_2\cos\theta\widetilde{\rho}_{BA}^0, \tag{7.6a}$$

$$\dot{\widetilde{\rho}}_{CB}=-(\gamma_{CB}+i\omega_{CB})\widetilde{\rho}_{CB}+i\alpha_2\cos\theta(\widetilde{\rho}_{CC}^0-\widetilde{\rho}_{BB}^0)+i\alpha_2\sin\theta\widetilde{\rho}_{AB}^0, \tag{7.6b}$$

$$\dot{\widetilde{\rho}}_{32}=\cos\theta\widetilde{\rho}_{CB}-\sin\theta\widetilde{\rho}_{CA}, \tag{7.7}$$

subject to the initial conditions $\widetilde{\rho}_{CA}(0)=\widetilde{\rho}_{CB}(0)=0$.

The $\widetilde{\rho}_{\alpha\beta}^0$ are the steady-state dressed-atom density-matrix elements. Solving Eqs. (7.6) using the steady-state values $\widetilde{\rho}_{\alpha\alpha}^0=\Lambda_\alpha/\gamma=n_\alpha^0$, $\widetilde{\rho}_{AB}^0\simeq0$, and $\widetilde{\rho}_{BA}^0\simeq0$, we obtain

$$\widetilde{\rho}_{32}(t)=\frac{i\alpha_2\sin^2\theta(n_C^0-n_A^0)}{\gamma_{CA}+i\omega_{CA}}(1-e^{-(\gamma_{CA}+i\omega_{CA})t})+\frac{i\alpha_2\cos^2\theta(n_C^0-n_B^0)}{\gamma_{CB}+i\omega_{CB}}(1-e^{-(\gamma_{CB}+i\omega_{CB})t}). \tag{7.8}$$

The oscillatory behavior which appears in homogeneously broadened systems may disappear if inhomogeneous broadening is present. The oscillations may, however, remain observable if ω_{CA} or ω_{CB} depend only

weakly on the atomic velocity. As an example let us consider the case when (5.15) is valid. The velocity-averaged CA contribution is (taking $n_1^0 = n_2^0 = 0$)

$$\langle \widetilde{\rho}_{32}(t) \rangle_{CA} = -\frac{\alpha_2 n_C^0}{2k'u} \left[Z\left(\frac{a+i\gamma}{k'u} \right) - \exp[-(\gamma - ia)t - \tfrac{1}{4}k'^2 u^2 t^2] Z\left(\frac{a+i\gamma}{k'u} + \tfrac{1}{2}ik'ut \right) \right]^* , \qquad (7.9)$$

where $Z(\xi)$ is the plasma-dispersion function,

$$k' = |k_2 + \tfrac{1}{2}k_1| , \quad \gamma = \tfrac{1}{2}(\Gamma_3 + \Gamma_1)$$

(recall $\Gamma_1 = \Gamma_2$), and $a = \Delta_{32} + \alpha_1 + \tfrac{1}{2}\Delta_{21}$. The time-dependent part in (7.9) disappears in a characteristic time $min[(k'u)^{-1}, \gamma^{-1}]$. If $k'u >> \gamma$, velocity dephasing is the dominant decay mechanism; in the case $k'u << \gamma$, the system behaves as a homogeneous one decaying at a rate γ and oscillating with a frequency $(\Delta_{32} + \alpha_1 + \tfrac{1}{2}\Delta_{21})$.

In a second example, field α_2 is kept constant and α_1 is switched on at $t = 0$. The probe response reflects the decay of the initial $\widetilde{\rho}_{BA}$ coherence (recall that $\widetilde{\rho}_{AA}^0$ and $\widetilde{\rho}_{BB}^0$ remain unchanged). Assuming that (7.5) is valid, we obtain from (7.6)

$$\widetilde{\rho}_{CA}(t) = \widetilde{\rho}_{CA}(0)e^{-(\gamma_{CA} + i\omega_{CA})t} - \frac{i\alpha_2 \sin\theta (n_C^0 - n_A^0)}{\gamma_{CA} + i\omega_{CA}}(1 - e^{-(\gamma_{CA} + i\omega_{CA})t})$$

$$-\frac{i\alpha_2(n_1^0 - n_2^0)\sin 2\theta \cos\theta}{2(\gamma_{CA} - \gamma + i\omega_{CB})}(e^{-(\gamma + i\omega_{BA})t} - e^{-(\gamma_{CA} + i\omega_{CA})t}) , \qquad (7.10a)$$

$$\widetilde{\rho}_{CB}(t) = \widetilde{\rho}_{CB}(0)e^{-(\gamma_{CB} + i\omega_{CB})t} + \frac{i\alpha_2 \cos\theta (n_C^0 - n_B^0)}{\gamma_{CB} + i\omega_{CB}}(1 - e^{-(\gamma_{CB} + i\omega_{CB})t})$$

$$+\frac{i\alpha_2(n_1^0 - n_2^0)\sin 2\theta \sin\theta}{2(\gamma_{CB} - \gamma + i\omega_{CA})}(e^{-(\gamma - i\omega_{BA})t} - e^{-(\gamma_{CB} + i\omega_{CB})t}) , \qquad (7.10b)$$

with initial conditions

$$\widetilde{\rho}_{CA}(0) = -i\alpha_2 \sin\theta (n_3^0 - n_2^0)(\gamma_{32} + i\widetilde{\Delta}_{32})^{-1} , \qquad (7.11a)$$

$$\widetilde{\rho}_{CB}(0) = i\alpha_2 \cos\theta (n_3^0 - n_2^0)(\gamma_{32} + i\widetilde{\Delta}_{32})^{-1} . \qquad (7.11b)$$

The assumption $\Gamma_1 = \Gamma_2 = \gamma$ implies that $\gamma_{CB} = \gamma_{CA} = \tfrac{1}{2}\Gamma_3 + \tfrac{1}{2}\gamma$.

The velocity averaging of (7.10) is by no means easy except in the special cases when ω_{CA} or ω_{CB} is nearly independent of v (Doppler-free cases). The labeling of the various terms in (7.10) is obvious: The first term gives the decay of the initial coherence, the second one describes the transient to the new steady state, and the third one is due to the decay of the initial $\widetilde{\rho}_{BA}$ coherence (nutation in the $1 \leftrightarrow 2$ system). The various terms in Eqs. (7.10) can be isolated by a proper choice of experimental parameters [e.g., by choosing α_1 such that $n_C^0 = n_A^0$ the second term in Eq. (7.10a) can be eliminated].

The advantage of the DAP over the BAP is that the DAP gives directly the correct eigenfrequencies ω_{CB} and ω_{CA} (in the BAP one is required to fully solve the problem using Laplace-transform techniques[71] to obtain these values).

VIII. CONCLUSION

The DAP offers little computational advantage over the BAP for most calculations. However, when the frequency separations of the dressed states are much greater than the relaxation rates of these states, the equations of the DAP simplify considerably. In this case, it appears that the dressed basis is the natural one in which to do calculations. Interpretations of the results in both the stationary and transient regime are straightforward in this representation. The positions of the resonances in saturation spectroscopy as well as the oscillation frequencies observable in coherent transient experiments appear as fundamental parameters in the DAP.

When the relaxation rates are comparable with the field strengths, the BAP is generally an easier representation to use than the DAP. In some cases

it may be difficult to interpret the results obtained using the BAP in terms of fundamental physical processes, but the calculations needed to arrive at these results are much more readily done in the BAP. Moreover, the BAP has the advantage of directly supplying the physical observables.

The DAP may be useful when applied to the analysis of atom-field interactions involving multilevel atoms or multimode fields. It also seems to be a convenient basis to use in solving coherent transient problems of the type discussed in Sec. VII.

APPENDIX A: RELAXATION SCHEME IN THE DAP

The relaxational coupling and decay in the DAP is obtained by transforming the relaxation terms of the BAP, Eq. (2.19), with the aid of (2.8), (2.11), and (2.17). To slightly simplify the equations we assume $\Gamma_{13}=\Gamma_{31}=0$ (no collisional mixing of states 1 and 3), and find for the nonvanishing diagonal elements

$$R_{AA,AA} = -\Gamma_1\cos^2\theta - \Gamma_2\sin^2\theta - \tfrac{1}{4}(\varphi - \Gamma_{12} - \Gamma_{21})\sin^2 2\theta , \tag{A1a}$$

$$R_{AA,BB} = \tfrac{1}{4}\varphi\sin^2 2\theta + \Gamma_{12}\sin^4\theta + \Gamma_{21}\cos^4\theta , \tag{A1b}$$

$$R_{AA,CC} = \Gamma_{32}\sin^2\theta , \tag{A1c}$$

$$R_{AA,AB} = R_{AA,BA} = \tfrac{1}{4}\sin 2\theta(\Gamma_2 - \Gamma_1 + \varphi\cos 2\theta - 2\Gamma_{21}\cos^2\theta + 2\Gamma_{12}\sin^2\theta) , \tag{A1d}$$

$$R_{BB,AA} = \tfrac{1}{4}\varphi\sin^2 2\theta + \Gamma_{12}\cos^4\theta + \Gamma_{21}\sin^4\theta , \tag{A2a}$$

$$R_{BB,BB} = -\Gamma_1\sin^2\theta - \Gamma_2\cos^2\theta - \tfrac{1}{4}(\varphi - \Gamma_{12} - \Gamma_{21})\sin^2 2\theta , \tag{A2b}$$

$$R_{BB,CC} = \Gamma_{32}\cos^2\theta , \tag{A2c}$$

$$R_{BB,AB} = R_{BB,BA} = \tfrac{1}{4}\sin 2\theta(\Gamma_2 - \Gamma_1 - \varphi\cos 2\theta + 2\Gamma_{12}\cos^2\theta - 2\Gamma_{21}\sin^2\theta) , \tag{A2d}$$

$$R_{CC,CC} = -\Gamma_3 , \tag{A3a}$$

$$R_{CC,AA} = \Gamma_{23}\sin^2\theta , \tag{A3b}$$

$$R_{CC,BB} = \Gamma_{23}\cos^2\theta , \tag{A3c}$$

$$R_{CC,AB} = R_{CC,BA} = -\tfrac{1}{2}\Gamma_{23}\sin 2\theta , \tag{A3d}$$

where

$$\varphi = 2\gamma_{21} - \Gamma_1 - \Gamma_2 \tag{A4}$$

gives a measure of the effect of phase-changing collisions. The nonvanishing terms involved in the off-diagonal elements are given by

$$R_{BA,BA} = -\gamma_{21} + \tfrac{1}{4}(\varphi - \Gamma_{12} - \Gamma_{21})\sin^2 2\theta , \tag{A5a}$$

$$R_{BA,AB} = \tfrac{1}{4}(\varphi - \Gamma_{12} - \Gamma_{21})\sin^2 2\theta , \tag{A5b}$$

$$R_{BA,AA} = \tfrac{1}{4}\sin 2\theta(\Gamma_2 - \Gamma_1 + \varphi\cos 2\theta + 2\Gamma_{21}\sin^2\theta - 2\Gamma_{12}\cos^2\theta) , \tag{A5c}$$

$$R_{BA,BB} = \tfrac{1}{4}\sin 2\theta(\Gamma_2 - \Gamma_1 - \varphi\cos 2\theta + 2\Gamma_{21}\cos^2\theta - 2\Gamma_{12}\sin^2\theta) , \tag{A5d}$$

$$R_{BA,CC} = -\tfrac{1}{2}\Gamma_{32}\sin 2\theta , \tag{A5e}$$

$$R_{CA,CA} = -\gamma_{31}\cos^2\theta - \gamma_{32}\sin^2\theta \; , \tag{A6}$$

$$R_{CB,CB} = -\gamma_{31}\sin^2\theta - \gamma_{32}\cos^2\theta \; , \tag{A7}$$

$$R_{CA,CB} = R_{CB,CA} = \tfrac{1}{2}(\gamma_{32} - \gamma_{31})\sin 2\theta \; , \tag{A8}$$

with the remaining elements given by the symmetry property $R_{\alpha\beta,\sigma\delta} = R_{\beta\alpha,\delta\sigma}$. Note that either Γ_{ij} or Γ_{ji}, depending on the configuration, vanishes if states i and j are not mixed by collisions. When phase-changing collisions are absent, i.e., $\gamma_{ij} = \tfrac{1}{2}(\Gamma_i + \Gamma_j)$, and all $\Gamma_{ij} = 0$, the relaxation terms are those given in (2.23). In a general case all the terms (A1)−(A8) differ from zero, leading to a complicated relaxation scheme in the DAP.

APPENDIX B: PROBE AND SATURATOR RESPONSES

The solution of Eqs. (2.22) to zeroth order in α_2 is given by

$$\tilde{\rho}_{11}^0 = n_1^0 + \frac{2\alpha_1^2}{\Gamma_1}\gamma_{21}n_{21}^0(\tilde{\Delta}_{21}^2 + \Gamma^2)^{-1} \; , \tag{B1a}$$

$$\tilde{\rho}_{22}^0 = n_2^0 - \frac{2\alpha_1^2}{\Gamma_2}\gamma_{21}n_{21}^0(\tilde{\Delta}_{21}^2 + \Gamma^2)^{-1} \; , \tag{B1b}$$

$$\tilde{\rho}_{33}^0 = n_3^0 \; , \tag{B1c}$$

$$\tilde{\rho}_{21}^0 = i\alpha_1 n_{21}^0(\gamma_{21} - i\tilde{\Delta}_{21})(\tilde{\Delta}_{21}^2 + \Gamma^2)^{-1} \; , \tag{B1d}$$

where $n_i^0 = \Lambda_i/\Gamma_i$, $n_{21}^0 = n_2^0 - n_1^0$, and

$$\Gamma^2 = \gamma_{21}^2 + 2\alpha_1^2\gamma_{21}(\Gamma_1^{-1} + \Gamma_2^{-1})$$
$$= \tfrac{1}{4}(\Gamma_1 + \Gamma_2)^2(1 + 4\alpha_1^2/\Gamma_1\Gamma_2) \tag{B2}$$

[the last step follows from the assumption $\gamma_{21} = \tfrac{1}{2}(\Gamma_1 + \Gamma_2)$]. The components $\tilde{\rho}_{32}^0$ and $\tilde{\rho}_{31}^0$ vanish. The corresponding DAP equations read

$$\tilde{\rho}_{AA}^0 = n_A^0 + \frac{2\beta^2}{\Gamma_A}\gamma_{BA}n_{BA}^0(\omega_{BA}^2 + \Gamma_{BA}^2)^{-1} \; , \tag{B3a}$$

$$\tilde{\rho}_{BB}^0 = n_B^0 + \frac{2\beta^2}{\Gamma_B}\gamma_{BA}n_{BA}^0(\omega_{BA}^2 + \Gamma_{BA}^2)^{-1} \; , \tag{B3b}$$

$$\tilde{\rho}_{CC}^0 = n_C^0 \; , \tag{B3c}$$

$$\tilde{\rho}_{BA}^0 = \beta n_{BA}^0(\gamma_{BA} - i\omega_{BA})(\omega_{BA}^2 + \Gamma_{BA}^2)^{-1} \; , \tag{B3d}$$

where $n_\alpha^0 = \Lambda_\alpha/\Gamma_\alpha$,

$$n_{BA}^0 = n_B^0 + n_A^0 + \Lambda_B \tag{B4a}$$

$$\Gamma_{BA}^2 = \gamma_{BA}^2 - 2\beta^2\gamma_{BA}(\Gamma_A^{-1} + \Gamma_B^{-1}) = \tfrac{1}{4}(\Gamma_B + \Gamma_A)^2(1 - 4\beta^2/\Gamma_A\Gamma_B) \; , \tag{B4b}$$

and β is defined by Eq. (2.27). In terms of the BAP variables, the "population inversion" n_{BA}^0 and the effective width Γ_{BA} can be written as

$$n_{BA}^0 = -\frac{\Gamma_2 + \Gamma_1}{\Gamma_2 - \Gamma_1}n_{21}^0\left[1 + \frac{(\Gamma_2 - \Gamma_1)^2}{4\Gamma_1\Gamma_2}\sin^2 2\theta\right]^{-1} \; , \tag{B5a}$$

$$\Gamma_{BA}^2 = \tfrac{1}{4}(\Gamma_1 + \Gamma_2)^2\left[1 + \frac{(\Gamma_2 - \Gamma_1)^2}{4\Gamma_1\Gamma_2}\sin^2 2\theta\right]^{-1} \; . \tag{B5b}$$

[Notice that n_{BA}^0 enters only in the product βn_{BA}^0 which is nonsingular for $(\Gamma_1 - \Gamma_2) = 0$.]
To first order in α_2 we find from (2.22e) and (2.22f)

$$\tilde{\rho}_{32} = i\alpha_2\frac{[\gamma_{31} + i(\tilde{\Delta}_{32} + \tilde{\Delta}_{21})](\tilde{\rho}_{33}^0 - \tilde{\rho}_{22}^0) - i\alpha_1\tilde{\rho}_{21}^0}{[\gamma_{31} + i(\tilde{\Delta}_{32} + \tilde{\Delta}_{21})](\gamma_{32} + i\tilde{\Delta}_{32}) + \alpha_1^2} \; . \tag{B6}$$

In the DAP we obtain from (2.23d), and (2.23e)

$$\tilde{\rho}_{CA} = -i\alpha_2\{(\gamma_{CB} + i\omega_{CB})[\sin\theta(\tilde{\rho}_{CC}^0 - \tilde{\rho}_{AA}^0) + \cos\theta\tilde{\rho}_{BA}^0]$$
$$- \beta[\cos\theta(\tilde{\rho}_{CC}^0 - \tilde{\rho}_{BB}^0) + s\,n\theta\tilde{\rho}_{AB}^0]\}[(\gamma_{CA} + i\omega_{CA})(\gamma_{CB} + i\omega_{CB}) - \beta^2]^{-1} \; , \tag{B7a}$$

$$\tilde{\rho}_{CB} = i\alpha_2\{(\gamma_{CA}+i\omega_{CA})[\cos\theta(\tilde{\rho}_{CC}^0-\tilde{\rho}_{BB}^0)+\sin\theta\tilde{\rho}_{AB}^0]$$
$$-\beta[\sin\theta(\tilde{\rho}_{CC}^0-\tilde{\rho}_{AA}^0)+\cos\theta\tilde{\rho}_{BA}^0]\}[(\gamma_{CA}+i\omega_{CA})(\gamma_{CB}+i\omega_{CB})-\beta^2]^{-1}, \qquad \text{(B7b)}$$

which after insertion into (2.29e) yield the observable $\tilde{\rho}_{32}$. The DAP solution Eq. (B7) is clearly much more complicated than the BAP expression (B6).

The DAP solution simplifies considerably in the limit $\omega_{BA} \gg \gamma_{BA}, \Gamma_{BA}$. The lowest-order terms are given by

$$\tilde{\rho}_{\alpha\alpha}^0 = n_\alpha^0 + O(\gamma^2/\omega_{BA}^2), \qquad \text{(B8a)}$$

$$\tilde{\rho}_{BA}^0 = -i\beta n_{BA}^0/\omega_{BA} + O(\gamma^2/\omega_{BA}^2). \qquad \text{(B8b)}$$

[The corresponding solutions in the BAP would be

$$\tilde{\rho}_{ii}^0 = n_i^0, \quad \tilde{\rho}_{21}^0 = i\alpha_1 n_{21}^0/(\gamma_{21}+i\Delta_{21}),$$

according to (B1).] As $\beta \simeq \gamma$ we see that $\tilde{\rho}_{BA}^0$ is roughly a factor γ/ω_{BA} smaller than the diagonal elements $\tilde{\rho}_{\alpha\alpha}^0$. The rate-type solution (3.2) is obtained by neglecting $\tilde{\rho}_{BA}^0$ and terms proportional to β in (B7). This approximation is equivalent to keeping only the lowest-order terms in a power expansion in terms of γ/ω_{BA}. In the following, we study in some detail the accuracy of (3.2).

Strongly coupled transition 1↔2

If we insert (B8) into (2.29), we obtain, after going back to the BAP variables,

$$\tilde{\rho}_{11}^0 \simeq n_1^0 + \frac{2\alpha_1^2}{\Gamma_1}\gamma_{21}n_{21}^0(\tilde{\Delta}_{21}^2+4\gamma_{21}^2\alpha_1^2/\Gamma_1\Gamma_2)^{-1}, \qquad \text{(B9a)}$$

$$\tilde{\rho}_{22}^0 \simeq n_2^0 - \frac{2\alpha_1^2}{\Gamma_2}\gamma_{21}n_{21}^0(\tilde{\Delta}_{21}^2+4\gamma_{21}^2\alpha_1^2/\Gamma_1\Gamma_2)^{-1}, \qquad \text{(B9b)}$$

$$\tilde{\rho}_{21}^0 \simeq i\alpha_1 n_{21}^0(\gamma_{21}-i\tilde{\Delta}_{21})(\tilde{\Delta}_{21}^2+4\gamma_{21}^2\alpha_1^2/\Gamma_1\Gamma_2)^{-1}. \qquad \text{(B9c)}$$

A comparison between (B1) and (B9) reveals that the approximation is good provided that

$$\tilde{\Delta}_{21}^2+4\alpha_1^2\gamma_{21}^2/\Gamma_1\Gamma_2 \gg \gamma_{21}^2. \qquad \text{(B10)}$$

This condition is satisfied when either $|\tilde{\Delta}_{21}| \gg \gamma_{21}$ or $\alpha_1^2 \gg \frac{1}{4}\Gamma_1\Gamma_2$. Note that if we neglect (B8b) there is no absorption of the strong field α_1 [the first term in (2.29d) is real and describes dispersion only].

Probe response

We can express the exact result (B6) in a form[13]

$$\tilde{\rho}_{32} = i\alpha_2[W_+(Z_++i\tilde{\Delta}_{32})^{-1}+W_-(Z_-+i\tilde{\Delta}_{32})^{-1}], \qquad \text{(B11)}$$

where

$$Z_\pm = \frac{1}{2}(\gamma_{32}+\gamma_{31}+i\tilde{\Delta}_{21})\mp\frac{1}{2}i[(\tilde{\Delta}_{21}+i\gamma_{32}-i\gamma_{31})^2+4\alpha_1^2]^{1/2}, \qquad \text{(B12)}$$

$$W_\pm = \frac{1}{2}(\tilde{\rho}_{33}^0-\tilde{\rho}_{22}^0)\pm[\frac{1}{2}(\tilde{\rho}_{33}^0-\tilde{\rho}_{22}^0)(\tilde{\Delta}_{21}+i\gamma_{32}-i\gamma_{31})-\alpha_1\tilde{\rho}_{21}^0][(\tilde{\Delta}_{21}+i\gamma_{32}-i\gamma_{31})^2+4\alpha_1^2]^{-1/2}. \qquad \text{(B13)}$$

An expansion of (B12) and (B13) in terms of the assumedly small parameter

$$\epsilon = (\gamma_{32}-\gamma_{31})/(\tilde{\Delta}_{21}^2+4\alpha_1^2)^{1/2} \qquad \text{(B14)}$$

yields

$$Z_++i\tilde{\Delta}_{32} \simeq \gamma_{CB}+\frac{1}{4}\alpha_1\sin4\theta\epsilon^3+i\omega_{CB}+\frac{1}{2}i\alpha_1\sin2\theta\epsilon^2, \qquad \text{(B15a)}$$

$$Z_-+i\tilde{\Delta}_{32} \simeq \gamma_{CA}-\frac{1}{4}\alpha_1\sin4\theta\epsilon^3+i\omega_{CA}-\frac{1}{2}i\alpha_1\sin2\theta\epsilon^2, \qquad \text{(B15b)}$$

$$W_+ \simeq (n_C^0 - n_B^0)\cos^2\theta + \tfrac{1}{2} i\epsilon \sin^2 2\theta n_C^0 + \tfrac{1}{4} i \sin^2 2\theta (\Lambda_1 - \Lambda_2)/\omega_{BA} \ , \tag{B16a}$$

$$W_- \simeq (n_C^0 - n_A^0)\sin^2\theta - \tfrac{1}{2} i\epsilon \sin^2 2\theta n_C^0 - \tfrac{1}{4} i \sin^2 2\theta (\Lambda_1 - \Lambda_2)/\omega_{BA} \ . \tag{B16b}$$

A finite value of ϵ slightly changes the widths and positions of the resonances. The corrections are negligible when $(\tilde{\Delta}_{21}^2 + 4\alpha_1^2)^{1/2} \gg \tfrac{1}{2}|\Gamma_1 - \Gamma_2|$ which is a relatively mild condition. The expressions (B16) for the weight factors $W_\pm$ are accurate to order $O(\epsilon^2; \epsilon\gamma/\omega_{BA}; \gamma^2/\omega_{BA}^2)$ and coincide with those given in (3.2) provided that $|\epsilon| \ll 1$ and

$$|n_C^0 - n_B^0| \gg |\Lambda_1 - \Lambda_2| \sin^2\theta/\omega_{BA} \ , \tag{B17a}$$

$$|n_C^0 - n_A^0| \gg |\Lambda_1 - \Lambda_2| \cos^2\theta/\omega_{BA} \ . \tag{B17b}$$

The correction terms given in (B16) are purely imaginary and, therefore, introduce a *dispersive-type change* in the absorption spectrum ($\sim \mathrm{Im}\,\tilde{\rho}_{32}$). This change causes a small shift in the position of the resonances, but does not appreciably affect their height.

APPENDIX C: DOPPLER-BROADENED PROBE SPECTRA

Introducing the dimensionless parameters (5.3)—(5.6) into (5.2) and solving the equations $\omega_C = \omega_{A,B}$ for x, we obtain

$$x_{1,2} = -\frac{k_1(2k_2 + k_1)}{2k_2(k_1 + k_2)} v \pm \frac{k_1^2}{2k_2(k_1 + k_2)} \left[v^2 + \frac{4k_2(k_1 + k_2)}{k_1^2} \right]^{1/2} \ . \tag{C1}$$

If $k_2(k_1 + k_2) > 0$, both the roots in (C1) are real. The root with the plus (minus) sign satisfies the CB (CA) resonance condition when $k_2 > 0$ ($k_2 < 0$). If $k_2(k_1 + k_2) < 0$, $x_{1,2}$ are complex in the region (5.10); otherwise both roots belong to the branch $\omega_{CB} = 0$ for $v > v_{cr} > 0$ and to the branch $\omega_{CA} = 0$ when $v < -v_{cr}$. In all cases the solutions (C1) must fall within the Doppler profile [see Eq. (5.9)] so that the Doppler-distribution function is not negligibly small.

Case $k_2(k_1 + k_2) > 0$

Inserting (C1) into (5.8), we obtain after lengthy algebraic manipulations

$$I(v) = \frac{\pi}{2|k_2|} W(v_{CB}) \left[(n_3^0 - n_2^0) \left[1 - \frac{v\,\mathrm{sgn}(k_2)}{[v^2 + 4k_2(k_1 + k_2)/k_1^2]^{1/2}} \right] + (n_2^0 - n_1^0) \frac{|k_2|}{k_1 \Gamma_2} \frac{\gamma_{\text{eff}}}{v^2 + \gamma_{\text{eff}}^2/\Gamma_1 \Gamma_2} \right.$$

$$\left. \times \left[1 - \frac{v[k_2\Gamma_1 - (k_1 + k_2)\Gamma_2]/k_1 \gamma_{\text{eff}}}{[v^2 + 4k_2(k_1 + k_2)/k_1^2]^{1/2}} \right] \right] + \frac{\pi}{2|k_2|} W(v_{CA})[v \rightarrow -v] \ , \tag{C2}$$

where $\omega_{CB}(v_{CB}) = 0$, $\omega_{CA}(v_{CA}) = 0$, and where γ_{eff} is defined by (5.12). Provided that

$$\left[v^2 + \frac{4k_2(k_1 + k_2)}{k_1^2} \right] \left| v + \frac{2k_2(k_1 + k_2)\Delta_{21}}{k_1(2k_2 + k_1)\alpha_1} \right| \ll \frac{k_2^2(k_1 + k_2)^2 u^2}{k_1 |2k_2 + k_1| \alpha_1^2} \tag{C3}$$

the Gaussians in (C2) are approximately equal,

$$W(v_{CA}) \simeq W(v_{CB}) \simeq \exp\left[-\left[\frac{\Delta_{32}}{k_2} + \frac{\Delta_{32} + \Delta_{21}}{k_1 + k_2} \right]^2 \bigg/ 4u^2 \right] \bigg/ \pi^{1/2} u \tag{C4}$$

and the simple result given in the text, Eq. (5.11), is valid. When (C3) is violated the dominant structure in the absorption spectrum arises from the Gaussians, and Eqs. (5.14) and (5.16) become applicable.

Case $k_2(k_1 + k_2) < 0$

If $v > v_{cr} > 0$, both of the roots (C1) satisfy the equation $\omega_{CB} = 0$ (if $v < -v_{cr}$ the equation $\omega_{CA} = 0$). Thus

only the CB transition contributes, and we can approximate

$$\tilde{\rho}_{32} \simeq i\alpha_2 \cos^2\theta (n_C^0 - n_B^0)(\gamma_{CB} + i\omega_{CB})^{-1} . \tag{C5}$$

This can be written as

$$\tilde{\rho}_{32} \simeq -\frac{\alpha_2}{\gamma_{CB}} g(x) \cos^2\theta (n_C^0 - n_B^0)[(x - x_1)(x - x_2) + ig(x)]^{-1} , \tag{C6}$$

where

$$g(x) = -\frac{\gamma_{CB} k_1^2}{\alpha_1 k_2 (k_1 + k_2)} \left[v + \left[\frac{k_2}{k_1} + \frac{1}{2} \right] x + \frac{1}{2}(x^2 + 4)^{1/2} \right] . \tag{C7}$$

The last factor can be expanded as

$$\text{Im}\{[(x - x_1)(x - x_2) + ig]^{-1}\} \simeq \text{Im} \left[[(x_2 - x_1)^2 + 4ig]^{-1/2} \right.$$
$$\left. \times \left[\mathscr{P}\frac{1}{x - x_1} - i\pi\delta(x - x_1) - \mathscr{P}\frac{1}{x - x_2} - i\pi\delta(x - x_2) \right] \right] , \tag{C8}$$

where the complex square root has to be evaluated so that its imaginary part is positive (assume $x_2 > x_1$). The principal values in (C8) are negligible, because for $(x_2 - x_1) \gg \gamma/\alpha_1$ the complex square root is real and for $x_2 \simeq x_1$ they cancel. Inserting (C8) into (C6), we obtain

$$I_{CB}(v) \simeq \frac{k_1 \pi^{1/2}}{|k_2| |k_1 + k_2| u} \sum_{i=1}^{2} \exp\left[- \left[\frac{\alpha_1 x_i - \Delta_{21}}{k_1 u} \right]^2 \right]$$
$$\times [n_C^0 - n_B^0(x_i)] \left[v + \frac{k_1 + k_2}{k_1} x_i \right] \text{Re}\{[(x_2 - x_1)^2 + 4ig(x_i)]^{-1/2}\} . \tag{C9}$$

In the limit $x_2 \to x_1$, this gives, after insertion of the explicit expressions (C1) for x_1 and x_2

$$I_{CB}(v) \simeq \frac{1}{k_1 u} \left[\frac{2\pi(k_1 + k_2)}{|k_2|} \right]^{1/2} \left[(n_3^0 - n_2^0) + \frac{\Gamma_1 |k_2|}{\Gamma_1 |k_2| + \Gamma_2 |k_1 + k_2|}(n_2^0 - n_1^0) \right]$$
$$\times \exp\left[- \left[\Delta_{21} - \alpha_1 \frac{k_1 + 2k_2}{(|k_2(k_1 + k_2)|)^{1/2}} \right]^2 / k_1^2 u^2 \right]$$
$$\times \text{Re}\left\{ \left[v - v_{cr} - \frac{i}{\alpha_1} \left[\frac{|k_2|}{k_1} \gamma_{31} + \frac{k_1 + k_2}{k_1} \gamma_{32} \right] \right]^{-1/2} \right\} , \tag{C10}$$

when $x_2 - x_1 \gg \gamma/\alpha_1$, Eq. (C9) reduces to

$$I(\Delta_{32}) \simeq \frac{\pi^{1/2}}{2|k_2|u} \exp\left[- \left[\frac{\alpha_1 x_2 - \Delta_{21}}{k_1 u} \right]^2 \right]$$
$$\times \left\{ (n_3^0 - n_2^0) \left[1 + \frac{v}{(v^2 - v_{cr}^2)^{1/2}} \right] \right.$$
$$\left. + (n_2^0 - n_1^0) \frac{k_2}{k_1^2 \Gamma_2} \left[\Gamma_1 k_2 \left[1 + \frac{v}{(v^2 - v_{cr}^2)^{1/2}} \right] + \Gamma_2(k_1 + k_2) \left[1 - \frac{v}{(v^2 - v_{cr}^2)^{1/2}} \right] \right] \right\}$$
$$\times \left[v^2 + \left[\Gamma_1 \frac{k_2}{k_1} + \Gamma_2 \frac{k_1 + k_2}{k_1} \right]^2 \frac{1}{\Gamma_1 \Gamma_2} \right]^{-1} \right\} + \text{term}[(v^2 - v_{cr}^2)^{1/2} \to -(v^2 - v_{cr}^2)^{1/2}] . \tag{C11}$$

In the limit $v \to \infty$, (C11) gives just the flat background absorption. Both (C10) and (C11) agree with the limiting intense-field results given in Ref. 13.

*Permanent address: Technical Research Centre of Finland, SF 02150 Espoo 15, Finland.

[1]*Laser Spectroscopy III*, edited by J. L. Hall and J. L. Carlsten (Springer, New York, 1977). This reference, as well as Refs. 2−6 below, contain many review articles in the general area of laser spectroscopy.

[2]*Laser Spectroscopy IV*, edited by H. Walther and K. W. Rothe (Springer, Berlin, 1979).

[3]*High Resolution Laser Spectroscopy*, edited by K. Shimoda (Springer, New York, 1976).

[4]*Laser Spectroscopy of Atoms and Molecules*, edited by H. Walther (Springer, New York, 1976).

[5]V. S. Letokhov and V. P. Chebotaev, *Non-Linear Laser Spectroscopy* (Springer, New York, 1977).

[6]*Frontiers in Laser Spectroscopy*, edited by R. Balian, S. Haroche, and S. Liberman (North-Holland, Amsterdam, 1977).

[7]G. E. Notkin, S. G. Rautian, and A. A. Feoktistov, Zh. Eksp. Teor. Fiz. **52**, 1673 (1967) [Sov. Phys.—JETP **25**, 1112 (1967)].

[8]M. S. Feld and A. Javan, Phys. Rev. **177**, 540 (1969).

[9]T. W. Hänsch and P. E. Toschek, Z. Phys. **236**, 213 (1970).

[10]S. Haroche and F. Hartmann, Phys. Rev. A **6**, 1280 (1972).

[11]I. M. Beterov and V. P. Chebotaev, Prog. Quantum Electron. **3**, 1 (1974), and references therein.

[12]R. M. Whitley and C. R. Stroud, Phys. Rev. A **14**, 1498 (1976).

[13]R. Salomaa and S. Stenholm, J. Phys. B **8**, 1795 (1975); **9**, 1221 (1976).

[14]R. Salomaa, J. Phys. B **10**, 3005 (1977).

[15]R. Salomaa, Physica Ser. **15**, 251 (1977).

[16]C. J. Borde in Ref. 1, p. 121.

[17]C. Delsart and J. C. Keller, J. Phys. (Paris) **39**, 350 (1978).

[18]P. R. Berman, P. F. Liao, and J. E. Bjorkholm, Phys. Rev. A **20**, 2389 (1979).

[19]C. Cohen-Tannoudji and S. Reynaud, J. Phys. B **10**, 345 (1977); **10**, 365 (1977).

[20]C. Cohen-Tannoudji and S. Reynaud, J. Phys. B **10**, 2311 (1977).

[21]S. Reynaud, thesis, University of Paris, 1977 (unpublished).

[22]F. Hoffbeck, thesis, University of Paris, 1978 (unpublished).

[23]E. Arimondo and P. Glorieux, Phys. Rev. A **19**, 1067 (1979).

[24]M. Himbert, thesis, University of Paris, 1980 (unpublished).

[25]See, for example, A. Ben Reuven and L. Klein, Phys. Rev. A **4**, 753 (1971); L. Klein, M. Giraud and A. Ben Reuven, *ibid.* **10**, 682 (1974); Y. Rabin and A. Ben Reuven, J. Phys. B **13**, 2011 (1980).

[26]C. Cohen-Tannoudji, in *Cargese Lectures in Physics* (Gordon and Breach, New York, 1968), Vol. 2, p. 347.

[27]G. Nienhuis and F. Schuller, J. Phys. B **12**, 3473 (1979).

[28]Neglect terms of order $|\Omega_2-|\omega_{32}||/(\Omega_2+|\omega_{32}|)$ and $|\Omega_1-|\omega_{21}||/|\Omega_1+|\omega_{21}||$.

[29]Our field interaction representation is defined by

$$\tilde{\rho}_{21}=\rho_{21}\exp[i\,\mathrm{sgn}(\omega_{21})(\Omega_1 t-K_1 z+\varphi_1)]\,,$$

$$\tilde{\rho}_{32}=\rho_{32}\exp[i\,\mathrm{sgn}(\omega_{32})(\Omega_2 t-K_2 z+\varphi_2)]\,,$$

$$\tilde{\rho}_{31}=\rho_{31}\exp[\,i\,\mathrm{sgn}(\omega_{21})(\Omega_1 t-K_1 z+\varphi_1)$$
$$+i\,\mathrm{sgn}(\omega_{32})(\Omega_2 t-K_2 z+\varphi_2)]\,,$$

$$\tilde{\rho}_{ii}=\rho_{ii}\,.$$

[30]In a more general case, the relaxation is described by an integral equation to account for velocity-changing collisions. See, for example, P. R. Berman, Phys. Rep. **43**, 101 (1978).

[31]M. Lax, Phys. Rev. **172**, 350 (1968). B. R. Mollow, Phys. Rev. A **12**, 1919 (1975), and references therein; A. V. Kruglikov, Opt. Spektrosk. **47**, 1033 (1979) [Opt. Spectrosc. (USSR) **47**, 573 (1979)]; G. Nienhuis and F. Schuller, J. Phys. B **13**, 2205 (1980).

[32]The power absorption coefficient of the probe wave (in units of m^{-1}) is obtained by multiplying $I(\Delta_{32})$ by a factor $(\Omega_2\mu_{32}^2/\hbar c\epsilon_0)$. A positive value of $I(\Delta_{32})$ indicates that there is probe gain in the V and cascade configurations and probe absorption in the Λ configuration.

[33]See Fig. 5 of Ref. 18.

[34]Recall that our rate-type approximation is valid provided

$$\omega_{R4}=[(\Delta_{21}+k_1 v)^2+4\alpha_1^2]^{1/2}>2\alpha_1\gg\Gamma\,.$$

[35]The plasma-dispersion function is defined by

$$Z(\psi)=\pi^{-1/2}\int_{-\infty}^{\infty}dt\,\exp(-t^2)(t-\psi)^{-1}$$

with $\mathrm{Im}\psi>0$; it may be related to the complex error function.

[36]For reviews of this subject, see, G. Grynberg and B. Cagnac, Rep. Prog. Phys. **40**, 791 (1977); and M. Salour, Rev. Mod. Phys. **50**, 667 (1978).

[37]K. Shimoda, Appl. Phys. (Germany) **9**, 239 (1976).

[38]M. F. H. Schuurmans, Phys. Lett. **A63**, 25 (1977).

[39]R. L. Panock and R. J. Temkin, IEEE J. Quantum Electron. QE **13**, 425 (1977).

[40]B. Sobolewska, Opt. Commun. **20**, 378 (1977).

[41]C. Mavroyannis, Opt. Commun. **29**, 80 (1979).

[42]Z. Bialynicka-Birula and I. Bialynicki-Birula, Phys. Rev. A **16**, 1318 (1977).

[43]S. J. Petuchowski, J. D. Oberstar, and T. A. DeTemple, Phys. Rev. A **20**, 529 (1979).

[44]D. J. Kim and P. D. Coleman, IEEE J. Quantum Electron. QE **16**, 300 (1980).

[45]If $k_D(k_D+k_1)(k_D-k_2)=0$ (or if either $\alpha_1^2=0$ or $\alpha_2^2=0$), Eq. (6.1) with $\omega=\Delta_D+k_D v$ reduces to a second-order equation in v, and the analysis is as in Sec. V.

[46]S. G. Rautian and I. I. Sobelman, Zh. Eksp. Teor. Fiz. **44**, 934 (1963) [Sov. Phys.—JETP **17**, 635 (1963)].

(1963)].

[47]B. J. Feldman and M. S. Feld, Phys. Rev. A $\underline{5}$, 899 (1972).

[48]N. Skribanowitz, M. J. Kelly, and M. S. Feld, Phys. Rev. A $\underline{6}$, 2302 (1972).

[49]E. V. Baklanov, I. M. Beterov, B. Ya. Dubetskii, and V. P. Chebotaev, Pis'ma Zh. Eksp. Teor. Fiz. $\underline{22}$, 289 (1975) [Sov. Phys.—JETP Lett. $\underline{22}$, 134 (1975)].

[50]P. R. Berman and J. Ziegler, Phys. Rev. A $\underline{15}$, 2042 (1977).

[51]E. Kyrölä and S. Stenholm, Opt. Commun. $\underline{30}$, 37 (1979).

[52]E. Kyrölä and R. Salomaa, Appl. Phys. (Germany) $\underline{20}$, 339 (1979).

[53]E. Kyrölä and R. Salomaa, Phys. Rev. A $\underline{23}$, 1874 (1981).

[54]J. H. Shirley, Phys. Rev. $\underline{138}$, B979 (1965).

[55]S. Feneuille, J. Phys. B $\underline{7}$, 1981 (1974).

[56]S. Feneuille, M.-G. Schweighofer, and G. Oliver, J. Phys. B $\underline{9}$, 2003 (1976).

[57]A. M. Bonch-Bruevich, T. A. Vartanyan, and N. A. Chigir, Zh. Eksp. Teor. Fiz. $\underline{77}$, 1899 (1974) [Sov. Phys.—JETP $\underline{50}$, 901 (1979)].

[58]S. P. Goreslavskii and V. P. Krainov, Opt. Spektrosk. $\underline{47}$, 825 (1979) [Opt. Spectrosc. (USSR) $\underline{47}$, 457 (1979)]; S. P. Goreslavskii, N. B. Delone and V. P. Krainov, J. Phys. B $\underline{13}$, 2659 (1980).

[59]S. Geltman, Phys. Lett. $\underline{A81}$, 27 (1981).

[60]For a general survey of coherent transient effects see Refs. 1—6; R. Shoemaker, in *Laser and Coherence Spectroscopy*, edited by J. I. Steinfeld (Plenum, New York, 1978), p. 197; and R. G. Brewer, Physics Today $\underline{30}$, 50 (1977).

[61]F. Rohart, P. Glorieux, and B. Macke, J. Phys. B $\underline{10}$, 3835 (1977); N. C. Wong, S. S. Kano, and R. G. Brewer, Phys. Rev. A $\underline{21}$, 260 (1980).

[62]D. Grischkowsky, Phys. Rev. A $\underline{7}$, 2096 (1973).

[63]D. Grischkowsky, M. M. T. Loy, and P. F. Liao, Phys. Rev. A $\underline{12}$, 2514 (1975).

[64]R. G. Brewer and E. L. Hahn, Phys. Rev. A $\underline{11}$, 1641 (1975).

[65]M. Sargent III and P. Horwitz, Phys. Rev. A $\underline{13}$, 1962 (1976).

[66]D. P. Hodginson and J. S. Briggs, Opt. Commun. $\underline{22}$, 45 (1977).

[67]J. R. Ackerhalt and B. W. Shore, Phys. Rev. A $\underline{16}$, 277 (1977); B. W. Shore and J. R. Ackerhalt, Phys. Rev. A $\underline{15}$, 1640 (1977).

[68]M. Ducloy, J. R. R. Leite, and M. S. Feld, Phys. Rev. A $\underline{17}$, 623 (1978); M. Ducloy and M. S. Feld, in Ref. 1, p. 243; J. R. R. Leite, R. L. Sheffield, M. Ducloy, R. D. Sharma, and M. S. Feld, Phys. Rev. A $\underline{14}$, 1151 (1976); M. S. Feld in Ref. 6, p. 203.

[69]M. P. Silverman, S. Haroche, and M. Gross, Phys. Rev. A $\underline{18}$, 1507 (1978).

[70]T. W. Mossberg, R. Kachru, S. R. Hartmann, and A. M. Flusberg, Phys. Rev. A $\underline{20}$, 1976 (1979), and references therein.

[71]A. Schenzle and R. G. Brewer, Phys. Rev. A $\underline{14}$, 1756 (1976); Phys. Rep. $\underline{43}$, 455 (1978).

[72]L. Kancheva, D. Pushkarov, and S. Rashev, J. Phys. B $\underline{14}$, 573 (1981).

Semiclassical picture of depolarizing collisions: Application to collisional studies using laser spectroscopy

J.-L. Le Gouët

*Laboratoire Aumé Cotton, * Centre National de la Recherche Scientifique, Bâtiment 505, 91405 Orsay-Cedex, France*

P. R. Berman

Physics Department, New York University, 4 Washington Place, New York, New York 10003

(Received 2 April 1981)

An extension of the Jeffreys-Wentzel-Kramers-Brillouin approximation to inelastic processes is used to obtain the scattering amplitude which describes the collisionally induced depolarization of magnetic substate coherences. It is found that the scattering amplitudes contain contributions from two overlapping regions. For large interatomic separations, the different Zeeman sublevels are shifted and mixed by collisions, but follow a common collision trajectory. For small interatomic separations, it is possible to find adiabatic eigenstates which follow distinct collision trajectories. The theory is used to investigate the nature of the depolarizing collision kernels and rates which enter into the analysis of laser spectroscopy experiments.

I. INTRODUCTION

Laser saturation spectroscopy experiments are beginning to provide an important probe of collisional processes occurring in low pressure gases.[1] The elimination of the broad Doppler background encountered in standard spectroscopy permits a more sensitive measure of the manner in which collisions perturb the energy levels and alter the velocity of atoms.

A particularly interesting process that may be studied in such experiments is the way in which collisions perturb *superposition* states in atoms that have been created by an atom-field interaction. Since the various internal states comprising the superposition state are generally shifted and scattered *differently* in a collision, one is led to a somewhat complicated description of the entire scattering process for the superposition state, especially if collisions can also couple the superposition levels. Formal theories[2,3] have been developed to describe the scattering and time evolution of atomic superposition states via a quantum-mechanical transport equation, but little progress has been made in obtaining solutions or physical interpretations of the results. It is the purpose of this paper to provide a simplification of the transport equation and some additional physical insight into the scattering process. Methods of semiclassical scattering theory are used to achieve these goals.

The specific problem we choose to study involves the scattering of atoms prepared in a linear superposition of magnetic substates of a level characterized by internal-angular-momentum quantum number j. The way in which collisions couple, shift, and scatter the various magnetic substates is investigated. Coherent superpositions of magnetic substates (magnetic moments, Zeeman coherences) are conveniently created and probed using the "three-level" system of Fig. 1. The 1-2 transition is excited with a nearly monochromatic laser beam and the 2-3 transition is probed with another colinear laser beam. Level 2 (shown for $j = 1$) is $(2j + 1)$ fold degenerate; Zeeman coherences within level 2 may be produced and detected using a proper choice of the laser beam polarizations. Owing to the Doppler effect, the excitation-detection scheme excites or probes only those atoms having a specific velocity component along the laser beam direction. Thus, any collision-induced modification of the Zeeman coherences for atoms having a specific longitudinal velocity can be monitored in such a system. The Zeeman coherences tend to be destroyed by inseparable contributions from collisional effects on the internal (shifting and mixing of magnetic sublevels) and external (state-dependent scattering for the different magnetic sublevels) atomic degrees of freedom. In such experiments, the collisional relaxation is determined by the number of collisions per lifetime of the level under con-
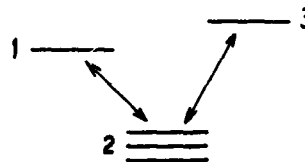

FIG. 1. "Three-level" scheme for depolarizing collision studies. Levels 1 and 3 are nondegenerate. Level 2 has three substates which, though separately indicated in the figure, are assumed to be energy degenerate.

sideration and the specific interatomic potential.

It should be noted that collisional depolarization studies are not new. Optical pumping techniques have been used to investigate depolarizing collisions between optically oriented excited state atoms and ground-state perturbers.[4] However the general nature of such optical pumping work (broadband sources, total cross-section measurements) does not lead to results that are overly sensitive to velocity-changing effects. Recent laser saturation experiments[5] based on schemes similar to that shown in Fig. 1 provide a more sensitive measure of such effects.

In attempting to analyze the scattering process for an atom in a linear superposition of magnetic substates one is naturally led to examine the applicability of the classical pictures shown in Fig. 2. The first drawing represents the single-trajectory limit. The dependence of the deflection on internal state is negligible so that the internal and the translational motions are decoupled. The second scheme depicts the situation where a diagonal representation has been found. Then each sublevel obeys the rules of elastic scattering along a substate-labeled trajectory. When none of these extreme situations holds, is a classical picture still possible? Answering this question would help to complete the blanks in the third drawing of Fig. 2. It should be noticed that the existence of a classical picture is questionable since depolarizing collisions imply a coupling between the internal motion, which is highly quantumlike due to the smallness of the electronic angular momentum, and the translational motion which can be quasiclassical.[6] We shall discuss applicability of the various limits and approximations in terms of standard treatments of collision problems.

In Sec. II various methods available for treating inelastic scattering, when the de Broglie wavelength of the colliding particle is much smaller than the characteristic dimension of the interaction region, are reviewed. In Sec. III exact equations for the scattering amplitudes are obtained

and those expressions are evaluated in the various semiclassical limits discussed in Sec. II. In Sec. IV we return to the problem encountered in laser spectroscopy and examine the semiclassical limit of the transport equation for atomic multipoles of a degenerate level. A summary is given in Sec. V.

II. APPROXIMATIONS IN INELASTIC SCATTERING THEORY

A few years ago, the development of research in the fields of collisional rotational and vibrational excitation of molecules,[7,8] and of electronic excitation and charge transfer in atoms[9] stimulated efforts for obtaining a semiclassical description of inelastic collisions,[10-16] which should be, by far, more tractable than a purely quantum approach. Since certain procedures in these theories are similar to those encountered in obtaining semiclassical limits of elastic scattering, it is useful to recall that two semiclassical approximation schemes[17] may be used to calculate the elastic scattering amplitude,

$$ f(\theta) = \frac{1}{2iK} \sum_l (2l+1)(e^{2i\eta_l} - 1) P_l(\cos\theta) \qquad (1) $$

(where K is the magnitude of the atomic wave vector and η_l is the phase shift of the l-labeled partial wave).

(i) The first method is the semiclassical phase shift approximation, which is valid when the de Broglie wavelength $\lambdabar$ is much smaller than the distance of closest approach r_c. In this form of the JWKB approximation, each η_l is calculated along a classical path which is characterized by the initial velocity and the impact parameter $(l+\frac{1}{2})/K$. Although the η_l are calculated along classical trajectories, the classical correspondence between scattering angle θ and impact parameter is lost in Eq. (1) since a large range of l values contribute to scattering at angle θ.

(ii) The second method, valid under the more stringent condition $\sqrt{\lambdabar} \ll \sqrt{r_c}$, is the classical trajectory limit. The condition $\sqrt{\lambdabar} \ll \sqrt{r_c}$ permits one to retain in Eq. (1) only those l values such that the impact parameter $(l+\frac{1}{2})/K$ corresponds to classical scattering at angle θ.

A number of papers have explored the conditions for generalizing the JWKB approximation to inelastic processes[10-15] using an approach which was initiated by Kemble.[16] They have concluded that such an extension is possible only when the atomic translational motion is nearly independent of the internal states. In the case when the additional condition $\sqrt{\lambdabar} \ll \sqrt{r_c}$ is fulfilled, the JWKB
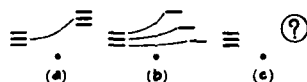
FIG. 2. Schematic representation of atomic trajectories during a depolarizing collision. In (a) an atom in a superposition state is scattered along a trajectory common to the three substates which are mixed by the collision. In (b) a distinct trajectory is associated with each substate and no transition between substates is induced by the collision. In (c) the single-trajectory approximation is not valid and transitions are induced between substates: What trajectory does the atom follow?

Errata

Erratum: Semiclassical picture of depolarizing collisions: Application to collisional studies using laser spectroscopy
[Phys. Rev. A **24**, 1831 (1981)].

J.-L. Le Gouët and P. R. Berman

Equation (2) should read

$$f_{MM'}^{hel}(\psi,\theta,\varphi) = \frac{(-1)^{M-M'}}{2iK}\sum_J (2J+1)(S_{MM'}^J - \delta_{MM'})\mathscr{D}_{MM'}^{J*}(\varphi,\theta,\psi),$$

where (φ,θ,ψ) are the Euler angles of a reference frame constructed on the final velocity. In the text, $f_{MM'}^{hel}(\theta,\varphi)$ stands for $f_{MM'}^{hel}(0,\theta,\psi)$.

In the next to the last line, p. 1838, the relation should read $\mathscr{D}_{MM'}^J(\varphi,\theta,\psi) = \sum_{M''}\mathscr{D}_{M''M}^{J*}(\mathscr{R}')\mathscr{D}_{M''M'}^J(\mathscr{R})$, where $(\varphi,\theta,\psi) = \mathscr{R}'^{-1}\mathscr{R}$....

Equation (36) reads

$$\gamma_{mm'}^{m''m'''} = \frac{4\pi^2 N}{K^2}\sum (-1)^{m''-m+Q+Q'}(2J+1)(2J'+1)(2f+1)\begin{bmatrix} j & j & f \\ m & -m' & q \end{bmatrix}\begin{bmatrix} j & j & f \\ m'' & -m''' & q \end{bmatrix}$$

$$\times \begin{bmatrix} J & J' & f \\ M & -M' & Q \end{bmatrix}\begin{bmatrix} j & j & f \\ M & -M' & Q \end{bmatrix}\begin{bmatrix} j & j & f \\ M'' & -M''' & Q' \end{bmatrix}\begin{bmatrix} J & J' & f \\ M'' & -M''' & Q' \end{bmatrix}$$

$$\times \int dv_r W_r(v_r)v_r^3(\delta_{MM''}\delta_{M'M'''} - S_{M''M}^J S_{M'''M'}^{J'*}).$$

Erratum: Theory of electron—hydrogen-atom collisions in the presence of a laser field
[Phys. Rev. A **17**, 1900 (1978)]

H. S. Brandi, Belita Koiller, L. C. M. Miranda, and J. J. Castro

The STA1 is unsuitable to treat bound states in the presence of electromagnetic fields. All matrix elements are of the form

$$V_{\alpha\beta} \propto \begin{cases} \langle \alpha | \vec{F} | \vec{\beta} \rangle \simeq \langle \alpha || H_0, \vec{p} || \beta \rangle, \\ (E_\alpha - E_\beta)\langle \alpha | \vec{p} | \vec{\beta} \rangle = 0. \end{cases}$$

The numerical results of the Refs. 1−3 as listed below are wrong.

[1]H. S. Brandi, B. Koiller, and H. G. P. Lins de Barros, Phys. Rev. A **19**, 1058 (1979).
[2]H. G. P. Lins de Barros and H. S. Brandi, Can. J. Phys. **57**, 1886 (1979).
[3]H. G. P. Lins de Barros and H. S. Brandi, *Proceedings of the Eleventh ICPEAC, Kyoto, 1979*, edited by K. Takayanagi and N. Oda (The Society for Atomic Collision Research, Kyoto, 1979), p. 916.

extension is thus possible only when atoms follow the same common spatial trajectory in any of the coupled internal states as in Fig. 1(a). A completely different approach has been developed under the name of classical S-matrix theory by Miller and Marcus.[10,11] They treat the internal degrees of freedom quasiclassically, retaining only the interference properties of quantum mechanics, since they calculate scattering amplitudes. In these papers there is no apparent condition of common trajectory. A special mention must be made to the work of Pechukas[16] which bypasses the common trajectory condition at the expense of complications with a noncausal interaction.

In light of these general methods let us examine the depolarizing collision problem. A ground-state spinless particle, the perturber, collides with an atom having internal angular momentum $\vec{j}$. The magnitude of $\vec{j}$ is on the order of a few $\hbar$ and is supposed to be much smaller than that of the translational angular momentum. Since the collision is assumed to result only in a change of direction of $\vec{j}$, the other numbers which characterize the internal state of the active atom are implicit. The effective interatomic potential is a function of the internuclear distance $\vec{r}$ and of the angle $(\vec{r},\vec{j})$.

A classical S-matrix method[10,11] seems very tempting for solving the problem formulated in this manner. With this approach, for given initial and final values for the variables describing the system (internal and interparticle angular momenta, energy), one calculates S-matrix elements classically along the trajectory connecting these initial- and final-state values. A phase $\varphi_c = \int \vec{p} \cdot d\vec{r}/\hbar$ evaluated along each trajectory enables one to account for any quantum interference effect arising from contribution of several trajectories to a given S-matrix element. The classical S matrix has the advantage of eliminating the discussion about common trajectory for the various magnetic substates since it is only the initial- and final-state variables that determine the scattering process. However, the solution of the problem in the frame of classical mechanics is rather difficult: the couple of colliding particles in the center-of-mass system has 8 degrees of freedom and after taking account of the conservation of $|\vec{j}|$, of the total angular momentum J, of total energy E, one is left with three differential equations, two of which are coupled. In general these equations must be solved numerically.

If instead, we adopt a quantum-mechanical formulation of the problem, certain simplifications are possible. Since the interatomic potential depends only on the quantum variable $\vec{r}$ and on the operator $\hat{\vec{j}} \cdot \hat{\vec{r}}$, one immediately notes that, if the "instantaneous" axis of quantization is taken along $\vec{r}$, then the Hamiltonian is a function of $\vec{r}$ and $\hat{j}_z$ and commutes with $\hat{j}_z$ (recall that $[\vec{r}, \hat{\vec{j}}] = 0$ since $\vec{r}$ is the interatomic separation and $\vec{j}$ acts in the active-atom subspace). Thus using this basis, known as the helicity representation after Jacob and Wick,[19] one concludes that the various magnetic sublevels in this representation are coupled only by the rotation of the internuclear axis during a collision. Two limiting cases may be envisioned:

(i) If the various instantaneous magnetic substates experience approximatively the same collisional interaction (the explicit condition is prescribed in the next section), then the notion of a common classical trajectory may be valid. The coupling between magnetic substates induced by the rotation of the internuclear axis can be significant in this case since the "instantaneous" eigenfrequencies differ by less than the inverse duration of a collision (i.e.. the helicity representation is *not* an adiabatic one in this limit). The coupling and scattering of the levels can be calculated using a semiclassical phase-shift approach. One expects that the limit of nearly equal collisional interaction for the different substates is achieved for collisions with large impact parameters.

(ii) In the other extreme, one can imagine that the helicity representation is an adiabatic one. The various magnetic sublevels experience significantly different collisional interactions and are scattered independently according to the equations of classical scattering theory. Normally, one requires small internuclear separations to achieve this adiabatic limit.[20]

It is the classical trajectory limit of these two extreme situations which is illustrated in Figs. 2(a) and 2(b). One might expect that the range of validity of the semiclassical picture could be extended by combining these two approximations. For example, in a given collision, limits (i) and (ii) could be used for large and small internuclear separations, respectively. The precise conditions of validity of these different situations are examined in the next section.

III. CALCULATION OF THE SCATTERING AMPLITUDE

The calculation is performed using the helicity representation which has been defined in the preceding section. During a collision, the z component of the internal angular momentum changes from an initial value $\hbar M$ relative to a quantization axis directed *opposite* to the initial velocity (i.e., in the direction of the interparticle separation

$\vec{r}$) to a final value $\hbar M'$ relative to a quantization axis which is taken along the final direction $\theta\varphi$. The scattering amplitude takes the closed form[17]

$$f^{hel}_{MM'}(\theta, \varphi) = \frac{(-1)^{M-M'}}{2iK} \sum_{J} (2J+1)(S^J_{MM'} - \delta_{MM'})$$
$$\times \mathfrak{D}^{J*}_{MM'}(\varphi, \theta, 0), \qquad (2)$$

where $S^J_{MM'}$ is an S-matrix element and $\mathfrak{D}^J_{MM'}(\varphi, \theta, 0)$ is the rotation matrix of rank J. The internal angular momentum $\vec{j}$ and the relative orbital angular momentum $\vec{l}$ have been coupled into the total angular momentum $\vec{J}$ and the summation is over all allowed values of $\vec{J} = \vec{l} + \vec{j}$. The S-matrix elements can be obtained in terms of the asymptotic form of the radial wave functions $\psi^{lJ}_M(r)$ as (see Appendix A)[21]

$$\lim_{r\to\infty} \psi^{lJ}_M(r) = -\frac{2J+1}{2iK}(-1)^{M'-M+l+J}$$
$$\times [\delta_{-M'M} e^{-iKr} - (-1)^{l+J} S^J_{M'M} e^{iKr}]. \qquad (3)$$

This boundary condition selects appropriate solutions of the radial equation

$$\left(-\frac{\hbar^2}{2\mu}\frac{d^2}{dr^2} - \frac{\hbar^2 K^2}{2\mu} + \langle M|V|M\rangle\right)\psi^{lJ}_M(r)$$
$$= -\sum_{M'\neq M} \langle M|V|M'\rangle \psi^{lJ}_{M'}(r), \qquad (4)$$

which is derived from the Schrödinger equation (see Appendix A). In this equation, μ is the reduced mass, and

$$\langle M|V|M'\rangle = \left(V_M(r) + \frac{J(J+1)}{2\mu r^2}\hbar^2\right)\delta_{MM'}$$
$$- \frac{\hbar^2}{2\mu r^2}[\lambda_+(J,M)\lambda_+(j,M)\delta_{MM'-1}$$
$$- \lambda_-(j,M)\lambda_-(J,M)\delta_{MM'+1}],$$

where $V_M(r)$ is the interatomic potential in substate M and

$$\lambda_\pm(J,M') = [J(J+1) - M'(M'\pm 1)]^{1/2}.$$

In the absence of coupling between the channels, Eq. (4) reduces to

$$\left(-\frac{\hbar^2}{2\mu}\frac{d^2}{dr^2} - \frac{\hbar^2 K^2}{2\mu} + V_M(r) + \frac{J(J+1)}{2\mu r^2}\hbar^2\right)\psi^{lJ}_M(r) = 0. \qquad (5)$$

The general solution of this equation in the JWKB approximation is a linear combination of functions $e^{\pm iQ_{JM}}/\mathcal{P}^{1/2}_{JM}$ where

$$\mathcal{P}_{JM} = \left(\hbar^2 K^2 - \frac{J(J+1)}{r^2}\hbar^2 - 2\mu V_M(r)\right)^{1/2},$$
$$\qquad (6)$$
$$Q_{JM} = \int_{r_1}^{r} \frac{\mathcal{P}_{JM}(r')}{\hbar} dr'.$$

This suggests that one tries solutions to Eq. (4) of the form

$$\psi^{lJ}_M(r) = b^+_{JM}(r)\frac{e^{iQ_{JM}}}{\mathcal{P}^{1/2}_{JM}} + b^-_{JM}(r)\frac{e^{-iQ_{JM}}}{\mathcal{P}^{1/2}_{JM}}. \qquad (7)$$

The standard theory of second-order differential equations states that, in addition to the boundary conditions, a supplementary condition is needed to determine $b^\pm_{JM}(r)$.[14] We have chosen the following condition:

$$b^{+\prime}_{JM}e^{iQ_{JM}} + b^{-\prime}_{JM}e^{-iQ_{JM}} - \frac{1}{2}\frac{\mathcal{P}'_{JM}}{\mathcal{P}_{JM}}(b^+_{JM}e^{iQ_{JM}} + b^-_{JM}e^{-iQ_{JM}}) = 0,$$
$$\qquad (8)$$

which transforms Eq. (4) into the set of first-order differential equations

$$b^{+\prime}_{JM}(r) = \frac{\mathcal{P}'_{JM}}{2\mathcal{P}_{JM}}b^+_{JM}e^{\mp 2iQ_{JM}} \pm \frac{\hbar X^+_{JM}}{2i(\mathcal{P}_{JM}\mathcal{P}_{JM+1})^{1/2}}(b^+_{JM+1}e^{i(Q_{JM+1}\pm Q_{JM})} + b^-_{JM+1}e^{-i(Q_{JM+1}\pm Q_{JM})})$$
$$\pm \frac{\hbar X^-_{JM}}{2i(\mathcal{P}_{JM}\mathcal{P}_{JM-1})^{1/2}}(b^+_{JM-1}e^{i(Q_{JM-1}\pm Q_{JM})} + b^-_{JM-1}e^{-i(Q_{JM-1}\pm Q_{JM})}), \qquad (9)$$

where

$$X^\pm_{JM} = \lambda_\pm(J,M)\lambda_\pm(j,M)/r^2 \qquad (10)$$

and a prime indicates d/dr. Except within a distance of a few $\bar{\lambda}$ from the turning points where $\mathcal{P}_{JM}$ is close to zero, these "exact" equations may be simplified by using the conditions that we have imposed at the beginning. From $\bar{\lambda} \ll r_c$, it follows that $\mathcal{P}'_{JM} \ll \mathcal{P}^2_{JM}/\hbar$ and since $j \ll J$, it follows that $\hbar X_{JM}/2(\mathcal{P}_{JM}\mathcal{P}_{JM+1})^{1/2} \ll \mathcal{P}_{JM}/\hbar$. Using these two inequalities one may neglect the terms having rapidly varying phase factors in Eq. (9)

and obtain

$$b^{+\prime}_{JM} = \sum_{M'} A^+_{MM'}b^+_{JM'}, \qquad (11)$$

where

$$A^+_{MM'} = \pm\frac{\hbar}{2i(\mathcal{P}_{JM}\mathcal{P}_{JM'})^{1/2}}(X^+_{JM}\delta_{M'M+1}$$
$$+ X^-_{JM}\delta_{M'M-1})e^{\pm i(Q_{JM'}-Q_{JM})}.$$

Thus, the inward wave (represented by b^-_{JM}) is decoupled from the outward wave (represented by b^+_{JM}). This is the essence of the semiclassical ap-

proximation and can be considered as an expression of microscopic causality. However, the semiclassical approximation requires, in addition, that a connection can be made between inward and outward waves at the classical turning point. This is accomplished provided one of the two following conditions is fulfilled[14]:

(i) $|\mathcal{P}_{JM} - \mathcal{P}_{JM\pm1}| \ll \mathcal{P}_{JM} + \mathcal{P}_{JM\pm1}$. This condition permits one to define a turning point, which is common to all the channels. When in addition $\sqrt{K} \ll \sqrt{r_c}$, a common trajectory is available.

(ii) $|\mathcal{P}_{JM} - \mathcal{P}_{JM\pm1}| \gg X_{JM}^{\pm} \hbar^2/2(\mathcal{P}_{JM}\mathcal{P}_{JM\pm1})^{1/2}$. In this case the $A_{MM'}$ in Eq. (11) are very rapidly varying functions of r. Thus the substates are not significantly mixed by collisions and the $b_{JM}^{\pm}$ are approximately constant. This decoupling corresponds to the adiabatic approximation.

These explicit requirements for a semiclassical description, correspond, as expected, to the limiting situations that we have evoked in the previous section. In terms of the potential difference between the internal states, the above conditions are, respectively, transformed into

$$|V_M(r) - V_{M\pm1}(r)| \ll (\mathcal{P}_{JM} + \mathcal{P}_{JM\pm1})^2/2\mu = E_1, \qquad (12a)$$

$$|V_M(r) - V_{M\pm1}(r)| \gg X_{JM}^{\pm} \frac{\hbar^2}{4\mu} \frac{\mathcal{P}_{JM} + \mathcal{P}_{JM\pm1}}{(\mathcal{P}_{JM}\mathcal{P}_{JM\pm1})^{1/2}} = E_2. \qquad (12b)$$

Condition (12a) requires that the difference between the scattering potentials for different magnetic substates be small enough to allow for a "single-trajectory" approach to the problem while condition (12b) requires that the potentials *differ* enough so that the collision is adiabatic with regard to the helicity eigenstates. Except in the vicinity of a classical turning point, E_1 is of the order of thermal energy and is much larger than E_2 which is of the order of $\hbar^2 K/\mu r$. Therefore, throughout the classically accessible region, at least one of the inequalities (12) is satisfied by any potential difference. This guarantees the general validity of a semiclassical description of depolarizing collisions.

As an illustration, we consider a simple potential such that $|V_M(r) - V_{M\pm1}(r)|$ is a monotonic, decreasing function of r. Thus if r_0 is a distance such that $E_2 \ll |V_M(r_0) - V_{M\pm1}(r_0)| \ll E_1$, the conditions (12a) and (12b) are fulfilled, respectively, when $r > r_0$ and $r < r_0$. This situation is represented in Fig. 3 which exhibits the overlap of the adiabatic and single-trajectory regions. In this situation one may transform Eq. (11) in order to examine the classical motion character of the problem. We define a set of classical trajectories using a time parameter t. The radial coordinate $r_{JM}(t)$ satisfies the equations
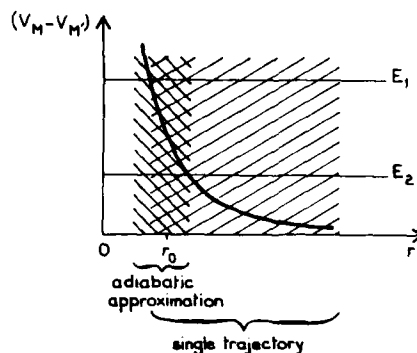

FIG. 3. The spatial domains for adiabatic and single-trajectory approximations are represented in the case of continuously decreasing $|V_M(r) - V_{M'}(r)|$. At r_0 both approximations are valid.

$$\frac{dr_{JM}}{dt} = \begin{cases} -v_{JM}(r_{JM}(t)) & \text{when } t < 0, \\ v_{JM}(r_{JM}(t)) & \text{when } t > 0, \end{cases} \qquad (13)$$

$$r_{JM}(0) = r_{JM}^{(TP)},$$

where the radial speed $v_{JM}(r)$ is

$$v_{JM}(r) = \begin{cases} \mathcal{P}_{JM}(r)/\mu & \text{when } r < r_0, \\ v_J(r) = \langle \mathcal{P}_{JM'}(r) \rangle_M/\mu & \text{when } r > r_0, \end{cases} \qquad (14)$$

and $r_{JM}^{(TP)}$ is the coordinate of the classical turning point in channel M, with angular momentum $\vec{J}$.

Two different situations may be examined in the limits that $r_{JM}^{(TP)}$ is larger or smaller than r_0.

$r_{JM}^{(TP)} < r_0$. The incident particle first reaches the radius r_0 at a time t_J^- which is M independent assuming a common trajectory $r_J(t)$ for $-\infty < t < t_J^-$ (since this interval corresponds to $r > r_0$). In Eq. (11) we replace $b_{JM}^-(r)$ by $c_{JM}(t)$ defined by

$$c_{JM}(t) = b_{JM}^-(r_J(t)), \quad t < t_J^- \qquad (15)$$

and find that $c_{JM}(t)$ obeys the differential equation

$$\frac{d}{dt} c_{JM}(t) = \sum_{M'} B_{MM'}^J(t) c_{JM'}(t), \quad t < t_J^- \qquad (16)$$

where

$$B_{MM'}^J(t) = \frac{\hbar}{2i\mu}[X_{JM}^+(r_J(t))\delta_{M',M+1} + X_{JM}^-(r_J(t))\delta_{M',M-1}]$$

$$\times \exp\frac{i}{\hbar}\int_{t_J^-}^t [V_M(r_J(t')) - V_{M'}(r_J(t'))]dt', \quad t < t_J^-. \qquad (17)$$

In arriving at Eqs. (16) and (17), we set $(\mathcal{P}_{JM}\mathcal{P}_{JM'})^{1/2} \simeq (\mathcal{P}_{JM} + \mathcal{P}_{JM'})/2 \simeq \mu v_J(r)$ and evaluate the phase difference $(i/\hbar)\int_{r_0}^r (\mathcal{P}_{JM} - \mathcal{P}_{JM'})dr'$ to first order in $V_M - V_{M'}$.

In the region $r < r_0$, the $b_{JM}^{\pm}(r)$ are constant owing

to the adiabatic nature of the collision for $r < r_0$. There is a classical trajectory r_{JM} which may be associated with each helicity state and a corresponding classical turning point $r_{JM}^{(TP)}$. The JWKB connection formulas are used at the turning point to relate $b_{JM}^{\pm}(r)$ and one finds

$$ib_{JM}^{+}(r_{JM}^{(TP)})e^{iQ_{JM}(r_{JM}^{(TP)})} = b_{JM}^{-}(r_{JM}^{(TP)})e^{-iQ_{JM}(r_{JM}^{(TP)})} . \quad (18a)$$

Since the $b_{JM}^{\pm}(r)$ are constant for $r < r_0$, Eq. (18a) may be written

$$ib_{JM}^{+}(r_0) = b_{JM}^{-}(r_0)e^{-2iQ_{JM}(r_{JM}^{(TP)})} . \quad (18b)$$

Connection with the time-dependent $c_{JM}(t)$ amplitudes is achieved by associating

$$c_{JM}(t) = \begin{cases} b_{JM}^{-}(r_{JM}(t)), & t < \dfrac{t_J^{-} + t_{JM}^{+}}{2} & (19a) \\[2ex] ib_{JM}^{+}(r_{JM}(t)), & t > \dfrac{t_J^{-} + t_{JM}^{+}}{2} & (19b) \end{cases}$$

where t_{JM}^{+} is the M-dependent time at which a classical particle moving along the r_{JM} trajectory would exit the $r < r_0$ region. Using Eqs. (19), (18), and (6) we find

$$c_{JM}(t_{JM}^{+}) = c_{JM}(t_J^{-})\exp\left(-\frac{i}{\hbar}\int_{t_J^{-}}^{t_{JM}^{+}} \frac{\mathcal{P}_{JM}^2(r_{JM}(\tau))d\tau}{\mu}\right). \quad (20)$$

Finally, for times $t > t_{JM}^{+}$, we are again in the $r > r_0$ zone. Each r_{JM} trajectory created for $r < r_0$ now continues into the $r > r_0$ region without further splitting. *Thus, each trajectory can be labeled by its M value in the $r < r_0$ region.* For $t > t_{JM}^{+}$ (i.e., $r > r_0$) there is again coupling of the $b_{JM}^{\pm}(r)$ along each trajectory. Defining

$$c_{JM}^{M'}(t) = ib_{JM}^{+}(r_{JM'}(t)), \quad t > t_{JM}^{+} \quad (21)$$

where $r_{JM'}(t)$ is the extension of the trajectory associated with $M = M'$ in the $r < r_0$ region, one finds that $c_{JM}^{M'}$ obeys equations analogous to (16) and (17). The final value for $b_{JM}^{+}(\infty)$ is given by a sum over all trajectories, i.e.,
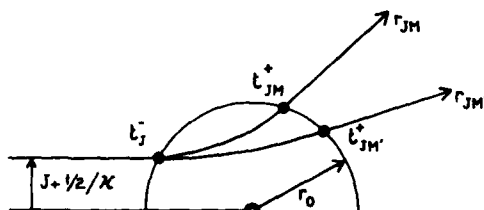

FIG. 4. An atom in a superposition state enters the interaction region with an impact parameter $(J + \frac{1}{2})/K$. From time t_J^{-} to t_{JM}^{+} or $t_{JM'}^{+}$ no transition occurs between substates and their respective trajectories may part from each other. After t_{JM}^{+} or $t_{JM'}^{+}$ a single trajectory starts from the point reached at t_{JM}^{+} or $t_{JM'}^{+}$.

$$ib_{JM}^{+}(\infty) = i\sum_{M'} b_{JM'}^{+}(r_{JM'}(\infty)) = \sum_{M'} c_{JM}^{M'}(\infty) . \quad (22)$$

This equation can be put into a more transparent form if time evolution operators are introduced such that

$$c_{JM}(t) = \sum_{M''} U_{M''M}^{J}(t', t)c_{JM''}(t'), \quad t < t_J^{-} \quad (23a)$$

$$c_{JM}^{M'}(t) = \sum_{M''} U_{M''M}^{JM'}(t', t)c_{JM''}(t'), \quad t > t_{JM'}^{+} . \quad (23b)$$

One can combine Eqs. (22), (23), and (20) to obtain

$$ib_{JM}^{+}(\infty) = \sum_{M''M'} U_{M'M}^{JM'}(t_{JM'}^{+}, \infty)$$

$$\times \exp\left(\frac{i}{\hbar\mu}\int_{t_J^{-}}^{t_{JM'}^{+}} \mathcal{P}_{rJ}^2(r_{JM'}(\tau))d\tau\right)$$

$$\times U_{M''M'}^{J}(-\infty, t_J^{-})b_{JM''}^{-}(-\infty) . \quad (24)$$

Equation (24) may be given a simple physical interpretation (see Fig. 4). In order to calculate the contribution of the Jth partial wave to the scattering amplitude, one starts a collision at $t = -\infty$ with $b_{JM''}^{-}(-\infty)$. For $-\infty < t < t_J^{-}$, collisions mix all states along an average common trajectory and this mixing is represented by $U_{M''M'}^{J}(-\infty, t_J^{-})$. For $t_J^{-} < t < t_{JM}^{+}$, the adiabatic states are not mixed by the collisions and one evaluates elastic scattering phase shifts along each trajectory. Finally, the states are again mixed along each of the final trajectories as represented by $U_{M'M}^{JM'}(t_{JM'}^{+}, \infty)$ (recall that the superscript M' labels the trajectory in the *adiabatic* region). The time-evolution operators describe the mixing and shifting of atomic substates as the atoms move along classical trajectories. The spatial coordinates have been changed from quantum-mechanical variables into time-dependent parameters. However, there subsists in Eq. (24) an exponential phase factor which attests to the quantum-mechanical character of the translational motion in the region where $r < r_0$.

To get expressions for the time-evolution operators, one may use Eqs. (23), (16), and (17) to obtain

$$\frac{d}{dt}U_{M'M}^{J}(t', t) = \sum_{M''} B_{MM''}^{J}(t)U_{M'M''}^{J}(t', t), \quad t < t_J^{-} \quad (25a)$$

$$\frac{d}{dt}U_{M'M}^{JM'}(t_{JM'}^{+}, t) = \sum_{M''} B_{MM''}^{JM'}(t)U_{M'M''}^{JM'}(t_{JM'}^{+}, t), \quad t > t_{JM'}^{+} \quad (25b)$$

subject to

$$U_{M'M}^{J}(t, t) = \delta_{MM'}, \quad U_{M'M''}^{JM'}(t_{JM'}^{+}, t_{JM'}^{+}) = \delta_{M'M''} , \quad (25c)$$

where $B^J_{MM'}$ is given by Eq. (17) and $B^{JM'}_{MM''}(t)$ is also given by Eq. (17) with $r_J(t)$ replaced by $r_{JM'}(t)$ (recall that $r_{JM''}$ indicates the trajectory associated with the M'' helicity state in the *adiabatic* region).

An expression for S-matrix elements is obtained by substituting Eq. (24) into Eq. (7) and making a comparison with Eq. (3). One finds[21]

$$S^J_{-M'M} = (-1)^J \sum_{M''} U^J_{M'M''}(-\infty, t_J^-) U^{JM''}_{M''M}(t_{JM''}^+, \infty)$$
$$\times \exp(i\Delta^{JM''}_{M'M} + 2i\eta_{JM''}), \qquad (26)$$

where

$$\eta_{JM''} = \lim_{r \to \infty} \int_{r^{(TP)}_{JM''}}^r \frac{\mathcal{P}_{JM''}(r')}{\hbar} dr' - Kr + (J + \tfrac{1}{2})\frac{\pi}{2} \qquad (27a)$$

and

$$\Delta^{JM''}_{M'M} = \frac{1}{\hbar} \int_{-\infty}^{t_J^-} [V_{M'}(r_J(\tau)) - V_M(r_J(\tau))] d\tau$$
$$+ \frac{1}{\hbar} \int_{t_{JM''}^+}^{\infty} [V_{M''}(r_{JM''}(\tau)) - V_M(r_{JM''}(\tau))] d\tau, \qquad (27b)$$

$r^{(TP)}_{JM''} > r_0$. In this case the time interval $[t_J^-, t_{JM}^+]$, during which the trajectories part from one another,

er, collapses, so that t_J^- and t_{JM}^+ may be set to 0 in Eq. (22) which reduces to

$$S^J_{-M'M} = (-1)^J U^J_{M'M}(-\infty, \infty) \exp(i\eta_{JM'} + i\eta_{JM}). \qquad (28)$$

where

$$U^J_{M'M}(-\infty, \infty) = \sum_{M''} U^J_{M'M''}(-\infty, 0) U^J_{M''M}(0, \infty).$$

This region corresponds to weak (large impact parameter) collisions.

This is the farthest point which can be reached in the direction of a semiclassical picture under the approximation $\lambda \ll r_c$. As has already been noted in Sec. II, the classical trajectories which have been hitherto considered may not be regarded as actual paths since deflection in direction $\theta\varphi$, which is described by the scattering amplitude [Eq. (2)] involves contribution from all the impact parameters $(J + \tfrac{1}{2})/K$.

The final step of the semiclassical approximation is possible provided $\sqrt{\lambda} \ll \sqrt{r_c}$. It consists in using the stationary-phase method to calculate the scattering amplitude [Eq. (2)]. This calculation is performed in Appendix B. In the simplest case, that of a purely repulsive interaction, one obtains

$$f^{hel}_{-M'M}(\theta, \varphi) = \frac{(-1)^J}{K(\sin\theta)^{1/2}} \sum_{M''} (J_{\theta M''})^{1/2} U^{J_{\theta M''}}_{M'M''}(-\infty, t_J^-) U^{J_{\theta M''}M''}_{M''M}(t_{JM''}^+, \infty) \exp(i\Delta^{J_{\theta M''}M''}_{M'M} + 2i\eta_{J_{\theta M''}M''})$$

$$\times \left(\frac{\partial\theta}{\partial J_{\theta M''}}\right)^{1/2} \exp\left(-\frac{i\pi}{2} - i(M'+M)\frac{\pi}{2} - iJ_{\theta M''}\theta\right) \exp(-iM\varphi), \qquad (29)$$

where $J_{\theta M''}$ is the angular momentum giving rise to scattering at $\theta\varphi$ for an atom following trajectory M'' in the adiabatic region. This result is valid provided that $\sqrt{\lambda} \ll \sqrt{r_0}$ and $J_{\theta M}\theta \gg 1$. The former condition allows one to use a stationary-phase method, and the latter condition implies that validity of Eq. (29) breaks down in the small-angle diffractive region.

As in elastic scattering, the major contribution in the sum over J comes from specific values of J, linking these values and the scattering direction $(\theta\varphi)$. However, Eq. (24) differs from the usual elastic scattering amplitude in the fact that for a given deflection direction $\theta\varphi$, a distinct impact parameter $(J_{\theta M''} + \tfrac{1}{2})/K$ is associated with each intermediate internal substate M''. For more general forms of the interaction potential, a rainbow angle may be defined and when θ is smaller than it, several values of J are generally involved in the scattering amplitude for given θ and M''.

Throughout this section mention has been made of classical trajectories. However, this notion

is actually meaningful, only when collisional effects on observables are considered. Then scattering cross sections instead of scattering amplitudes are involved. The aim of the next section is to discuss the classical trajectory picture of depolarizing collisions on the observables which are accessible in laser spectroscopy.

IV. DEPOLARIZING COLLISIONS IN LASER SPECTROSCOPY

In a gas cell, the quantum-mechanical state of atoms within a small domain of position-velocity space around $(\vec{r}, \vec{v})$ is most conveniently described by the density-matrix elements $\rho_{\alpha\alpha'}(\vec{r}, \vec{v})$ where α and α' label internal states. We shall limit the discussion to the case where α and α' belong to the same j level since we are interested in studying the effect of depolarizing collisions. The general transport equation which determines the collisional evolution of density-matrix elements of "active atoms" immersed in a perturber bath is given by[2]

$$\frac{d}{dt}\rho'_{\alpha\beta}\bigg|_{\text{coll}} = -\sum_{\alpha'\beta'}\Gamma^{\alpha'\beta'}_{\alpha\beta}(\vec{v})\rho'_{\alpha'\beta'}(\vec{r},\vec{v},t) + \sum_{\alpha'\beta'}\int d^3v\, W^{\alpha'\beta'}_{\alpha\beta}(\vec{v}',\vec{v})\rho'_{\alpha'\beta'}(\vec{r},\vec{v}',t),\tag{30a}$$

where

$$\Gamma^{\alpha'\beta'}_{\alpha\beta}(\vec{v}) = N\int d^3v_b\, W_b(\vec{v}_b)\left(\frac{2\pi\hbar}{i\mu}[f_{\alpha\alpha'}(\vec{v}_r,\vec{v}_r)\delta_{\beta\beta'} - f_{\beta\beta'}(\vec{v}_r,\vec{v}_r)\delta_{\alpha\alpha'}]\right)\tag{30b}$$

and

$$W^{\alpha'\beta'}_{\alpha\beta}(\vec{v}',\vec{v}) = N\int d^3v_r\int d^3v_{r'}\,\delta(\vec{v}'-\vec{v}-\vec{Y})W_b(\vec{v}-\vec{v}'_r+\vec{Y})\delta(v_r-v'_r)v_r^{-1}f_{\alpha'\alpha}(\vec{v}'_r,\vec{v}_r)f^*_{\beta'\beta}(\vec{v}'_r,\vec{v}_r),\tag{30c}$$

where $\vec{v}_r$ is the relative velocity between active atom and perturber, $W_b(\vec{v}_b)$ is the perturber equilibrium velocity distribution, $\vec{Y} = (\mu/m)(\vec{v}'_r-\vec{v}_r)$, N is the perturber density, and $f_{\alpha'\alpha}(\vec{v}'_r,\vec{v}_r)$ is the $\alpha',\vec{v}'_r - \alpha,\vec{v}_r$ inelastic scattering amplitude. In our case the internal state is labeled by the magnetic number m and the relevant scattering amplitudes are $f_{mm'}(\vec{v}'_r,\vec{v}_r,\hat{A})$ where m and m' are taken along a fixed quantization axis $\hat{A}$. This scattering amplitude may be expressed as a function of the scattering amplitude in the helicity representation by

$$f_{mm'}(\vec{v}'_r,\vec{v}_r,\hat{A}) = \sum_{MM'}\mathfrak{D}^{j*}_{mM}(\mathfrak{R}')\mathfrak{D}^{j}_{m'M'}(\mathfrak{R})f^{\text{hel}}_{MM'}(\vec{v}'_r,\vec{v}_r),\tag{31}$$

where $\mathfrak{R} = (\varphi_{v_r},\theta_{v_r},0)$ and $\mathfrak{R}' = (\varphi_{v'_r},\theta_{r'_r},0)$ and φ and θ are polar angles with respect to $\hat{A}$.

In traditional optical pumping experiments in which depolarizing collisions are studied,[4] neither the vapor excitation nor the signal detection is velocity selective. In these experiments, the broadband excitation creates density-matrix elements $\rho^j_{mm'}(\vec{r},\vec{v},t)$ in a state of given j and the intensity of radiation emitted (or absorbed) from these mm' substates in a given direction and with a specific polarization is monitored. With broadband excitation and detection, the signal is a function of velocity-averaged density-matrix elements

$$\rho^j_{mm'}(\vec{r},t) = \int d^3v\,\rho^j_{mm'}(\vec{r},\vec{v},t)$$

and provides some measure of the effects of depolarizing collisions in level j. Integrating Eq. (30a) over velocity we find

$$\frac{d}{dt}\rho^j_{mm'}(\vec{r},t)\bigg|_{\text{coll}} = -\sum_{m''m'''}\int d\vec{v}\,\gamma^{m''m'''}_{mm'}(\vec{v})\rho^j_{m''m'''}(\vec{r},\vec{v},t),\tag{32a}$$

where

$$\gamma^{m''m'''}_{mm'} = \Gamma^{m''m'''}_{mm'}(\vec{v}) - \int d^3v\, W^{m''m'''}_{mm'}(\vec{v},\vec{v}').\tag{32b}$$

Equation (32a) does not decouple γ and ρ; however, an approximation that is often made[22] is to neglect the $\vec{v}$ dependence of the γ's. In effect, one replaces $\gamma^{m''m'''}_{mm'}(\vec{v})$ by

$$\gamma^{m''m'''}_{mm'} = \int d^3v\, W(\vec{v})\gamma^{m''m'''}_{mm'}(\vec{v}),\tag{33}$$

where $W(\vec{v})$ is the active atom velocity distribution. A good approximation to Eq. (32a) is then

$$\frac{d}{dt}\rho^j_{mm'}(\vec{r},t)\bigg|_{\text{coll}} = -\sum_{m''m'''}\gamma^{m''m'''}_{mm'}\rho^j_{m''m'''}(\vec{r},t).\tag{34}$$

The $\gamma^{m''m'''}_{mm'}$ describe the (velocity-averaged) coupling between magnetic sublevels and, as such, reflect the nature of the collisional interaction. Thus the structure of the $\gamma^{m''m'''}_{mm'}$ can provide some insight into the collisional process. By combining Eqs. (33), (32b), (30b), and (30c) and performing some of the integrations, one may obtain[2]

$$\gamma^{m''m'''}_{mm'} = N\int d^3v_r W_r(\vec{v}_r)v_r\left(\frac{2\pi}{iK}[f_{m''m}(\vec{v}_r,\vec{v}_r)\delta_{m'm''} - f^*_{m'''m'}(\vec{v}_r,\vec{v}_r)\delta_{mm''}] - \int d\Omega_{v_r}f_{m''m}(\vec{v}'_r,\vec{v}_r)f^*_{m'''m'}(\vec{v}'_r,\vec{v}_r)\right).\tag{35}$$

This expression can be written in terms of S-matrix elements if Eqs. (31) and (2) are used for the scattering amplitudes. The resulting equation can be simplified by using the relation $\mathfrak{D}^j_{MM'}(\theta,\varphi,0)$ $= \sum_{M''}\mathfrak{D}^j_{MM''}(\mathfrak{R})\mathfrak{D}^j_{M''M'}(\mathfrak{R}')$ and other elementary properties of the $\mathfrak{D}$ matrices. The integrals over $d\Omega_{v_r}$ and $d\Omega_{v'_r}$ can be carried out and, after some cancellation of terms, one is left with

$$\gamma_{mm}^{m''n'} = \frac{4\pi^2 N}{K^2} \sum (-1)^q (2J+1)(2J'+1)(2f+1) \begin{pmatrix} j & j & f \\ m & -m' & q \end{pmatrix} \begin{pmatrix} j & j & f \\ m'' & -m''' & q \end{pmatrix} \begin{pmatrix} j & j & f \\ M & -M' & q \end{pmatrix} \begin{pmatrix} J & J' & f \\ M'' & -M''' & q \end{pmatrix}$$

$$\times \begin{pmatrix} J & J' & f \\ M'' & -M''' & q \end{pmatrix} \int dv_r W_r(v_r) v_r^3 (\delta_{MM'} \delta_{M'M'''} - S^J_{M''M} S^{J'*}_{M'''M'}), \tag{36}$$

where the sum is over all repeated indices (except j). Equation (36) contains the selection rule $m - m'' = m' - m'''$ which may also be obtained from symmetry considerations. One can verify that $\sum_n \gamma_{mm}^{m''n'} = 0$, reflecting the conservation of probability $\sum_m d\rho_{mm}(\vec{r}, t)/dt \big|_{coll} = 0$.

Using Eq. (26), one can write the dynamical factor appearing in Eq. (36) as

$$\delta_{M''M'} \delta_{M''M} - S^{J'*}_{M''M'} S^J_{M''M} = \delta_{M''M'} \delta_{M''M} - \sum_{m'n'} U^{J'*}_{-M''m'n'}(-\infty, t_f^-) U^J_{-M'n}(-\infty, t_f^-) U^{J'n*}_{n'M'}(t^+_{J n'}, +\infty)$$

$$\times U^{Jn}_{nM}(t^+_{Jn'}, +\infty) \exp[-i(\Delta^{Jn'}_{-M''M'} - \Delta^{Jn}_{-M''M})] \exp[-2i(\eta_{J'n'} - \eta_{Jn})]. \tag{37}$$

In writing Eq. (37) we have implicitly used the selection rule $|J - J'| \leq j$ which is imposed by the $3 - j$ symbols appearing in Eq. (36). Since $J \gg j$, differences between J and J' can be neglected in all but phase factors. In the previous section it has been shown that the quantum-mechanical aspect of the translational motion is concentrated in the factors $\exp[-2i(\eta_{J'n'} - \eta_{Jn})]$. The other factors describe the evolution of internal substates along classical paths $r_{Jn}(t)$. Let $\hbar J_0$ be the angular momentum for which $r^{(TP)}_{JM} = r_0$. In Eq. (36), the sum over J may be regarded as a sum over the impact parameter $(J + \frac{1}{2})/K$, in analogy with the classical mechanics calculation. In the region where $J > J_0$ [or $r_0 < r^{(TP)}_{JM}$] a common motion approximation is valid. Since $|J - J'| \ll J$, the phase difference in Eq. (37) can be expanded under the form

$$\eta_{J'n'} - \eta_{Jn} = \eta_{Jn'} - \eta_{Jn} + (J' - J)\frac{\partial \eta_{Jn'}}{\partial J}, \tag{38}$$

where $2\partial \eta_{Jn'}/\partial J$ can be identified as the classical deflection angle θ_J (see Appendix B). Then, following Eq. (28) one reduces Eq. (37) to

$$\delta_{M''M'} \delta_{M''M} - S^{J'*}_{M''M'} S^J_{M''M} = \delta_{M''M'} \delta_{M''M} - U^{J'*}_{-M''M'}(-\infty, +\infty) U^J_{-M''M}(-\infty, +\infty)$$

$$\times \exp\frac{i}{\hbar} \int_0^\infty [V_{-M''}(r_J(t)) + V_M(r_J(t)) - V_{-M'}(r_J(t)) - V_M(r_J(t))] dt \exp[-i(J' - J)\theta_J], \tag{39}$$

where $(\eta_{Jn} - \eta_{Jn'})$ have been expanded to lowest order in the potentials. This expression describes the substate mixing along a single trajectory $r_J(t)$.

When $J < J_0$ [or $r_0 > r^{(TP)}_{JM}$], it may be verified that $|\eta_{Jn} - \eta_{J'n'}| \gg 1$ and that the factor $\exp[-2i(\eta_{J'n'} - \eta_{Jn})]$ averages to zero by summation over J and J' for $|n| \neq |n'|$. A classical trajectory r_{Jn} may still be assigned to elements of the density matrix which are diagonal (in the helicity representation) on entering the region $r < r_0$ but the classical picture fails for nondiagonal elements. In other words at $r = r_0$ the magnetic substate populations ρ_{JnJn} are scattered along separate trajectories r_{Jn} but the coherence between substates is lost owing to trajectory separation. After the departure from the region $r < r_0$, substate mixing starts again along each separate trajectory. In some sense the images given in Figs. 2(a) and 2(b) are valid when the interatomic distance r is, respectively, larger or smaller than r_0. To work out this semiclassical picture, the only needed condition on the de Broglie wavelength has been $\lambda \ll r_c$. This condition is not sufficient to regard the atoms as wave packets of dimension much smaller than the interaction distance. Thus, in analogy with JWKB calculations of scattering amplitudes, the classical trajectories that we have mentioned are not really followed by the atoms. A specific evaluation of $\gamma_{mm}^{m''n'}$ will be given in a future work.

Velocity selective laser spectroscopy

In velocity selective laser spectroscopy, the relevant quantity which describes collisional effects is the collision kernel $W_{mm}^{m''n'}(\vec{v}', \vec{v})$. Calculation of this kernel from Eqs. (30c) and (31) requires the knowledge of products of differential scattering amplitudes of the form

$$f_{M''M'}^{\star hel J}(\vec{v}_r', \vec{v}_r) f_{M''M}^{hel J}(\vec{v}_r', \vec{v}_r).$$

The stringent condition $\sqrt{\lambda} \ll \sqrt{r_c}$ is needed to obtain a semiclassical approximation of this quantity. We consider still the simple case of purely repulsive interaction for which a semiclassical

scattering amplitude has been calculated (Eq. 29). Since Eq. (29) is valid only if $J_{\theta_M}\theta \gg 1$, a supplementary assumption is needed to take into account small-angle scattering. We suppose that the width of $\rho_{mm'}(\vec{r}, \vec{v}, t)$ in velocity space is much larger than the velocity change which corresponds to the deflection angle defined by $J_{\theta_M}\theta = 1$. Thus, the collisional transport equation may be written

$$\frac{d\rho_{mm'}}{dt}\bigg|_{\text{coll}} = \sum_{m''m'''} -\Gamma_{mm'}^{m''n'''}(\vec{v})\rho_{m''m'''}(\vec{r}, \vec{v}, t)$$

$$+ \sum_{m''m'''} \rho_{m''m'''}(\vec{r}, \vec{v}, t) \int d^3v\, W_{mm'<}^{m''n'''}(\vec{v}', \vec{v})$$

$$+ \sum_{m''m'''} \int d^3v'\, W_{mm'>}^{m''n'''}(\vec{v}', \vec{v})\rho_{m''m'''}(\vec{r}, \vec{v}', t),$$

$$(40)$$

where $W_{mm'>}^{m''n'''}(\vec{v}', \vec{v})$ describes collisions which are such that $J_{\theta_M}\theta > 1$ and $W_{mm'<}^{m''n'''}(\vec{v}', \vec{v})$ describes the remaining very small-angle collisions. The first two terms may be calculated in the same way as $\gamma_{mm'}^{m''n'''}$.

The semiclassical approximation of scattering amplitudes is needed to determine $W_{mm'>}^{m''n'''}(\vec{v}', \vec{v})$.
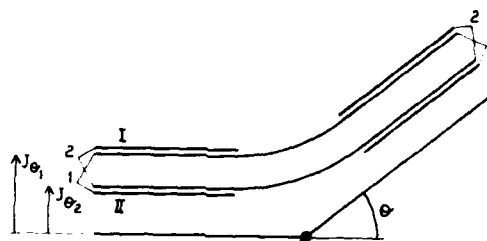

FIG. 5. The scattering of two-substate atoms at angle θ results from the contribution of two trajectories: the one which enters the $r < r_0$ region in substate 1 at impact parameter $(J_{\theta_1} + \frac{1}{2})K$ (I) and the one which enters the $r < r_0$ region in substate 2 at impact parameter $(J_{\theta_2} + \frac{1}{2})/K$ (II). Along each trajectory mixing between substates occurs for $r < r_0$. The trajectories of substate 2 in I and substate 1 in II would lead to scattering at an angle *other than* θ and are, therefore, not continued into the $r < r_0$ region.

As above, two collision regions may be distinguished depending on whether J_{θ_M} is larger or smaller than J_0. When $J_{\theta_M} > J_0$, a single trajectory is available and one obtains

$$f_{M'''M'}^{*\text{hel}}(\theta, \varphi)\, f_{M''M}^{\text{hel}}(\theta, \varphi) = \frac{J_\theta}{K^2 \pi \sin\theta \left|\frac{d\theta}{dJ_\theta}\right|}\, U_{-M'''M'}^{J_\theta}(-\infty, +\infty)^*\, U_{-M''M}^{J_\theta}(-\infty, +\infty)$$

$$\times \exp\frac{i\mu}{\hbar}\int_0^\infty dt[V_{-M'''}(r_{J_\theta}(t)) - V_{-M'}(r_{J_\theta}(t)) + V_M(r_{J_\theta}(t)) - V_{M'}(r_{J_\theta}(t))]$$

$$\times \exp\left(-i(M''' - M'' + M - M')\frac{\pi}{2}\right) \qquad (41)$$

for use in Eqs. (30c) and (31). This result contains the product of a semiclassical elastic differential scattering cross section by a factor which accounts for the MM' transitions along this trajectory.

When $J_{\theta_M} > J_0$, distinct trajectories corresponding to distinct substates may contribute to scattering at $\theta\varphi$ and

$$f_{M'''M'}^{*\text{hel}}(\theta, \varphi)\, f_{M''M}^{\text{hel}}(\theta, \varphi) = \frac{1}{K^2 \pi \sin\theta}\sum_{nn'}(J_{\theta n}J_{\theta n'})^{1/2}U_{-M'''n}^{J_{\theta n}}(-\infty, t_J^-)^*\, U_{-M''n'}^{J_{\theta n'}}(-\infty, t_J^-)U_{nM'}^{J_{\theta n'}n}(t_{Jn}^+, \infty)^*\, U_{n'M}^{J_{\theta n'}n'}(t_{Jn'}^+, \infty)$$

$$\times \exp[-i(\Delta_{-M'''M'}^{J_{\theta n}n} - \Delta_{-M''M}^{J_{\theta n'}n'})]\exp\left(-i(M''' - M' - M'' + M)\frac{\pi}{2} + i(M' - M)\varphi\right)$$

$$\times \left(\frac{\partial\theta}{\partial J_{\theta n}}\frac{\partial\theta}{\partial J_{\theta n'}}\right)^{-1/2}\exp[2i(\eta_{J_{\theta n'}n'} - \eta_{J_{\theta n}n}) + i(J_{\theta n} - J_{\theta n'})\theta]. \qquad (42)$$

The last factor in Eq. (42) represents interference effects between diverging trajectories. Its angular dependence is given by

$$\frac{d}{d\theta}[2(\eta_{J_{\theta n'}n'} - \eta_{J_{\theta n}n}) - (J_{\theta n'} - J_{\theta n})\theta] = J_{\theta n} - J_{\theta n'}. \qquad (43)$$

This angular dependence leads to oscillations of $W_{mm'>}^{m''n'''}(\vec{v}', \vec{v})$ as a function of $\vec{v}$ and $\vec{v}'$. In

$\int W_{mm'>}^{m''n'''}(\vec{v}', \vec{v})\rho_{m''m'''}(\vec{v}')d^3v'$, the integral over v' averages to zero for terms with $|n| \neq |n'|$ *provided* $(\mu/m)_u |J_{\theta n} - J_{\theta n'}|^{-1}$ is much smaller than the width of $\rho_{mm'}(\vec{v})$ in velocity space, where u is the active-atom mean speed.

The net effect of scattering in direction $\theta\varphi$ for a two-level system in this limit is shown in Fig. 5. The angular momenta $J_{\theta_i}(i = 1, 2)$ correspond to scattering of an atom in state i through the

angle $\theta_0\varphi$. For $r > r_0$ the substates are mixed by the collisional interaction along each of the two trajectories I and II. For $r < r_0$ the two states in each of trajectories I and II are split by the collisional interaction, but only *one* trajectory in each leads to scattering at $(\theta\varphi)$. Finally, the states in a given trajectory are again mixed for $r > r_0$. The internal final state is a combination of internal states which have experienced the history shown in Fig. 5. When the above conditions are not fulfilled, no simple picture can be given. It should be noticed that the phase factor in Eq. (42) cannot be clearly separated into a "spatial phase shift" which would represent interference effects between diverging trajectories, and an "internal phase shift" which results from internal substate mixing and which is present along a common classical trajectory.

Thus, the methods used to calculate $\gamma_{mm'}^{m''n'''}$ and $W_{mm'}^{m''n'''}(\vec{v}', \vec{v})$ are perfectly consistent with the JWKB and classical trajectory approximations, respectively, that are used to calculate total and differential scattering cross sections. Assuming $\lambda \ll r_c$, the result for $\gamma_{mm'}^{m''n'''}$ can be interpreted in terms of a large number of partial waves giving rise to scattering at angle $\theta\varphi$ with *no* classical correspondence between impact parameter and scattering angle; however, the relevant *phase shifts and substate coupling are* calculated along classical trajectories (just as the η_l are calculated along classical trajectories in the JWKB evaluation of collision cross sections). Under the more stringent condition $\sqrt{\lambda} \ll \sqrt{r_c}$, the derived expression for the kernel $W_{mm'}^{m''n'''}(\vec{v}', \vec{v})$ can be interpreted as arising from collisions having the appropriate impact parameter to give rise to classical scattering at $\theta\varphi$. There may be a number of such impact parameters reflecting the different interaction potentials for the various magnetic substates.

We have not attempted to give an interpretation to $W_{mm'}^{m''n'''}(\vec{v}', \vec{v})$ under the less restrictive semiclassical condition $\lambda \ll r_c$; in this limit the large number of partial waves contributing to each scattering amplitude leads to a very complicated expression when bilinear products of the scattering amplitudes are taken to form the collision kernel. Only when *total* cross sections, such as those represented by $\gamma_{mm'}^{m''n'''}$, are evaluated does one regain a result with a simple physical interpretation.

V. SUMMARY

In view of understanding the signal formation in laser spectroscopic experiments when depolarizing collisions are present, we have developed a semiclassical theory of these collisions. First

we have shown that single-trajectory approximation and adiabatic approximation can be combined to obtain a generally valid expression for the semiclassical phase shifts (provided $\chi \ll r_c$). An explicit calculation of this phase shift has been outlined in the simple case of a continuously decreasing difference of the substate dependent interatomic potentials. The conditions of validity for using a semiclassical scattering amplitude have been examined and the case of a purely repulsive interaction has been treated in some detail. Using semiclassical approximations to the scattering amplitudes, we investigated the nature of the depolarization collision kernels and rates which enter into laser spectroscopic experiments. For these two quantities a picture of the scattering, in terms of classical trajectories, has been given. In a forthcoming paper, expressions that we have obtained will be used in a numerical calculation of the corresponding signal profiles which could be observed in laser spectroscopic experiments.

APPENDIX A: DERIVATION OF THE RADIAL EQUATION[17]

A convenient set of commuting observables in the center-of-mass frame consists of the Hamiltonian H, j^2, and the total angular-momentum operators J^2, J_z, where J_z is taken along a laboratory fixed axis of quantization Oz. The corresponding eigenfunctions are $\Psi^{JJM_J}(\vec{r}, \vec{\rho})$ where M_J is an eigenvalue of J_z and $\vec{\rho}$ denotes the ensemble of electronic coordinates of the colliding atoms. The total Hamiltonian H is

$$H = H_0(\vec{\rho}) + \frac{P^2}{2\mu} + V(\vec{r}, \vec{\rho}),$$

where $H_0(\vec{\rho})$ is the internal Hamiltonian, $V(\vec{r}, \vec{\rho})$ is the interatomic potential, and

$$P^2 = -\hbar^2 \frac{\partial^2}{\partial r^2} + \frac{(J^2 + j^2 - 2\vec{J}\cdot\vec{j})}{r^2}\hbar^2.$$

The Hamiltonian, without internuclear motion, is

$$H_0 = H_0(\vec{\rho}) + \frac{j^2\hbar^2}{2\mu r^2} + V(\vec{r}, \vec{\rho}).$$

Its eigenfunctions are $\varphi_{M'}^{j}(r, \vec{\rho})$ where M' is the simultaneous eigenvalue of J_z, and j_z, along the

rotating axis of quantization $\hat{r}$. The expansion of $\Psi^{JJM}(\hat{r},\vec{\rho})$ in terms of $\varphi_M^j(r,\vec{\rho})$, and the wave function $\psi_M^{jj}(r)$ describing the scattering is[17]

$$\Psi^{JJM_J}(\hat{r},\vec{\rho}) = \frac{1}{r}\sum_{M'} \mathfrak{D}_{M_J M'}^{J*}(\mathfrak{R})\psi_M^{jj}(r)\varphi_{M'}^j(r,\vec{\rho}),$$

where $\mathfrak{R}$ is the rotation which brings $\hat{r}$ along Oz. We substitute this expression into the Schrödinger equation

$$\frac{\hbar^2 K^2}{2\mu}\Psi^{JJM_J}(\hat{r},\vec{\rho}) = H\Psi^{JJM_J}(\hat{r},\vec{\rho}),$$

where K is the magnitude of the relative motion wave vector. Projection on $\varphi_M^{j*}(r,\vec{\rho})$ leads to the radial equation

$$\left(-\frac{\hbar^2}{2\mu}\frac{d^2}{dr^2} - \frac{\hbar^2}{2\mu}\bar{\pi}\frac{d}{dr} - \frac{\hbar^2 K^2}{2\mu} + \langle M|V|M\rangle\right)\psi_M^{jj}(r)$$

$$= -\sum_{M'=M}\langle M|V|M'\rangle\psi_M^{jj}(r),$$

where

$$\bar{\pi} = \int d\vec{\rho}\,\varphi_M^{j*}(r,\vec{\rho})\frac{\partial}{\partial r}\varphi_M^j(r,\vec{\rho}),$$

$$\langle M|V|M'\rangle = \left(V_M(r) + \frac{J(J+1)-2M^2+j(j+1)}{2\mu r^2}\hbar^2\right)\delta_{MM'}$$

$$-\frac{\hbar^2}{2\mu r^2}[\lambda_+(J,M)\lambda_+(j,M)\delta_{MM'-1}$$

$$+\lambda_-(j,M)\lambda_-(J,M)\delta_{MM'+1}],$$

$\lambda_\pm(J,M') = [J(J+1)-M'(M'\pm1)]^{1/2}$, and $V_M(r)$ is the value of the interatomic potential in substate M. In the diagonal term, the contributions which contain $\bar{\pi}$ and $j(j+1)-2M^2$ may be neglected as they are of the order of λ/r_c.

The boundary-value condition which is necessary to select the appropriate solution of the radial equation is determined by the asymptotic form of a scattered plane wave which is

$$\Psi \to e^{i\vec{K}\cdot\vec{r}}\tilde{\phi}_M^j(\vec{\rho}) + \sum_{M'}\frac{e^{iKr}}{r}f_{MM'}^{\text{hel}}(\theta,\varphi)\varphi_{M'}^j(\infty,\vec{\rho}),$$

where $\tilde{\phi}_M^j(\vec{\rho})$ is the electronic wave function assuming that the quantization axis is along $\vec{K}$, and $f_{MM'}^{\text{hel}}(\theta,\varphi)$ is the scattering amplitude in the helicity representation. The connection between $\tilde{\phi}_M^j(\vec{\rho})$ and $\varphi_{M'}^j(\infty,\vec{\rho})$ is

$$\tilde{\phi}_M^j(\vec{\rho}) = \sum_{M'}\mathfrak{D}_{MM'}^{j*}(\mathfrak{R})\varphi_{M'}^j(\infty,\vec{\rho}).$$

Expansion of the plane-wave function in terms of spherical harmonics leads to

$$e^{i\vec{K}\cdot\vec{r}}\tilde{\phi}_M^j(\vec{\rho}) \to \frac{1}{2iKr}\sum_{lMl'}(2l+1)(2J+1)(e^{iKr}-(-1)^l e^{-iKr})$$

$$\times\begin{pmatrix} l & j & J \\ 0 & M & -M \end{pmatrix}\begin{pmatrix} l & j & J \\ 0 & M' & -M' \end{pmatrix}$$

$$\times\mathfrak{D}_{-M-M'}^J(\mathfrak{R})\varphi_{M'}^j(\infty,\vec{\rho}).$$

Summing over l and using Eq. (2) one finally obtains

$$\Psi \to \frac{1}{2iKr}\sum_{JM'}(2J+1)[-(-1)^{J+j}\delta_{M'-M}e^{-iKr}+S_{MM'}^J e^{iKr}]$$

$$\times(-1)^{M-M'}\mathfrak{D}_{MM'}^{J*}(\mathfrak{R})\varphi_M^j(\infty,\vec{\rho}).$$

Since $\Psi \approx \sum_{JM'}\Psi^{JjM'}(\hat{r},\vec{\rho})$, we see that the asymptotic form of the radial wave function is[21]

$$\lim_{r\to\infty}\psi_M^{jj}(r) = -\frac{2J+1}{2iK}(-1)^{M-M'+j+J}$$

$$\times[\delta_{-MM'}e^{-iKr}-(-1)^{j+J}S_{MM'}^J e^{iKr}].$$

APPENDIX B: STATIONARY-PHASE CALCULATION

The needed approximation for $\mathfrak{D}_{MM'}(\varphi,\theta,0)$ for large J values is given by Brussaard and Tolhoek[23]

$$\mathfrak{D}_{MM'}^J(0,\theta,0) = \left(\frac{\pi}{2}\sin\theta k(\theta)\right)^{-1/2}\sin\left(\frac{\pi}{4}+M\pi+W_{MM'}^J(\theta)\right), \tag{B1}$$

where

$$k(\theta) = [J^2-(M^2+M'^2-2MM'\cos\theta)/\sin^2\theta]^{1/2} \tag{B2}$$

and

$$W_{MM'}^J(\theta) = J\cos^{-1}[(J^2\cos\theta-MM')/(J^2-M^2)^{1/2}(J^2-M'^2)^{1/2}]$$

$$-M\cos^{-1}[(M\cos\theta-M')/\sin\theta(J^2-M^2)^{1/2}] - M'\cos^{-1}[(M'\cos\theta-M)/\sin\theta(J^2-M'^2)^{1/2}]. \tag{B3}$$

This approximation is valid provided $W'_{MM'}(\theta) \gg 1$. This expression is substituted into Eq. (2). The sum of the term involving $\delta_{MM'}$ vanishes[17] and one is left with

$$f^{hel}_{MM'}(\theta,\varphi) = \frac{(-1)^{M-M'}}{2iK} \sum_J (2J+1) S^J_{MM'} \mathfrak{D}^{J\,*}_{MM'}(\varphi,\theta,0),$$
(B4)

where $S^J_{MM'}$ is to be given by Eq. (26). The quantities $U^{JM'}_{MM'}(t,t')$ and $\exp(i\Delta^{JM'}_{M'M})$, appearing in Eq. (26) are slowly varying functions of J with respect to $\exp(2i\eta_{JM'})$. Thus, they can be taken out of the sum over J and evaluated at a point of maximum contribution to the sum. One may use the stationary-phase method to calculate

$$\int dJ \exp[2i\eta_{JM''} \pm iW'_{MM'}(\theta)].$$
(B5)

The stationary-phase condition is $d/dJ\{2\eta_{JM''}$

$\pm W'_{MM'}(\theta)] = 0$ which leads to

$$2\frac{d\eta_{JM''}}{dJ} = \pm \cos^{-1}\left(\frac{J^2\cos\theta - MM'}{(J^2-M^2)^{1/2}(J^2-M'^2)^{1/2}}\right)$$
(B6)

or, when $M \ll J$,

$$2\frac{d\eta_{JM''}}{dJ} = \pm\theta + O\left(\frac{M^2}{J^2}, \frac{MM'}{J^2}, \frac{M'^2}{J^2}\right).$$
(B7)

The classical deflection angle Θ is defined by

$$\Theta = 2\frac{d\eta_{JM''}}{dJ},$$
(B8)

where $d\eta_{JM''}/dJ$ satisfies Eq. (B7) to first order in M'/J. A set of angular momenta $J_{\Theta M''}$ may satisfy Eq. (B8). We restrict now our calculation to the single case of a purely repulsive potential. Then $\theta = \Theta$ and the semiclassical scattering amplitude may be evaluated from Eqs. (B4), (22), and (B1) using the method of stationary phase. One obtains

$$f^{hel}_{-M',M}(\theta,\varphi) = \frac{1}{K(\sin\theta)^{1/2}} \sum_{M''} (J_{\Theta M''})^{1/2} \left(\frac{\partial\theta}{\partial J_{\Theta M''}}\right)^{-1/2} U^{J_{\Theta M''}}_{M'M''}(-\infty,t_J^-) U^{J_{\Theta M''}}_{M''M}(t_{JM''}^+,\infty) \exp(i\Delta^{J_{\Theta M''}M''}_{M'M} + 2i\eta_{J_{\Theta M''}M''})$$

$$\times \exp\left(-i\frac{\pi}{2} - i(M'+M)\frac{\pi}{2} - iJ_{\Theta M'}\theta\right) \exp(-iM\varphi).$$
(B9)

This expression is bound to the validity of the stationary-phase approximation which requires that

$$\left|\frac{\partial^2\theta}{\partial J^2}\left(\frac{\partial\theta}{\partial J}\right)^{-3/2}\right| \ll 1.$$
(B10)

This condition generally reduces to $\sqrt{\lambda} \ll \sqrt{r_c}$. One has to also take account of the condition of validity of the approximation used for $\mathfrak{D}^J_{MM'}(0,\theta,0)$. To first order in M/J the approximation demands that

$$|J_{M''\Theta}\sin\theta| \gg 1.$$
(B11)

The points of stationary phase for channels M and M' are well separated provided that

$$|J_{M\theta} - J_{M'\theta}| \gg (\partial\theta/\partial J)^{-1/2}.$$
(B12)

The fulfillment of this condition implies that the wave packets in channels M and M' do not overlap. When condition (B12) is not fulfilled the distinct wave packets coalesce into a single one, but Eq. (B9) is still valid, since Eq. (B8) still has a single solution for a given value of M''.

*Laboratoire associé à l'Université Paris-Sud.

[1] For a comprehensive bibliography see R. Vetter and P. R. Berman, Comments At. Mol. Phys. 10, 69 (1981).

[2] P. R. Berman, Phys. Rev. A 5, 927; 6, 2157 (1972).

[3] V. A. Alekseev, T. L. Andreeva, and I. I. Sobelman, Zh. Eksp. Teor. Fiz. 62, 614 (1972) [Sov. Phys.— JETP 35, 325 (1972)].

[4] W. Happer, Rev. Mod. Phys. 44, 169 (1972).

[5] M. Gorlicki, A. Peuriot, and M. Dumont, J. Phys. (Paris) Lett. 41, L275 (1980) and private communication; J.-L. Le Gouët and R. Vetter, J. Phys. B 13, L147 (1980).

[6] The scattering can depend strongly on the internal state, although the exchange of angular momentum between internal and external motion is very small with

regard to the translational angular momentum.

[7] W. D. Held, J. Schöttler, and J. P. Toennies, Chem. Phys. Lett. 6, 304 (1970); H. Udseth, C. F. Giese, and W. R. Gentry, J. Chem. Phys. 54, 3643 (1971).

[8] D. Secrest and B. P. Johnson, J. Chem. Phys. 45, 4556 (1966); B. R. Johnson, D. Secrest, W. A. Lester, and R. B. Bernstein, Chem. Phys. Lett. 1, 396 (1967).

[9] H. F. Helbig and E. Everhart, Phys. Rev. 140, 715 (1965); J. C. Houvier, P. Fayeton, and M. Barat, J. Phys. B 7, 1358 (1974).

[10] W. H. Miller, J. Chem. Phys. 53, 1949 (1970); 54, 5386 (1971).

[11] R. A. Marcus, J. Chem. Phys. 54, 3965 (1971); J. N. L. Connor and R. A. Marcus, ibid. 55, 5636 (1971).

[12] M. D. Pattengill, C. F. Curtiss, and R. B. Bernstein,

J. Chem. Phys. **54**, 2197 (1971); C. F. Curtiss, *ibid.* **52**, 4832 (1970).

[13] D. R. Bates and D. S. F. Crothers, Proc. R. Soc. London Ser. A **315**, 465 (1970) and references therein.

[14] J. B. Delos, W. R. Thorson, and S. K. Knudson, Phys. Rev. A **6**, 709 (1972); **6**, 720 (1972).

[15] C. Gaussorgues, C. Le Sech, F. Masnou-Seeuws, and R. MacCaroll, J. Phys. B **8**, 239 (1975); **8**, 253 (1975).

[16] P. Pechukas, Phys. Rev. **181**, 166 (1969); **181**, 174 (1969).

[17] M. S. Child, *Molecular Collision Theory* (Academic, London, 1974). Note we follow the notation of Child when we use $f_{MM'}$ or $S_{MM'}$ to indicate transition from M to M'.

[18] E. C. Kemble, Phys. Rev. **48**, 549 (1935).

[19] M. Jacob and G. C. Wick, Ann. Phys. (N.Y.) **7**, 404 (1959).

[20] In the classical picture of the adiabatic limit, the momentum $\vec{j}$ precesses rapidly around $\vec{r}$ and this motion is much faster than the rotation of the internuclear vector around the center of mass. The classical S-matrix problem is then reduced to the solution of one differential equation for each value of $\vec{j} \cdot \vec{r}/r$.

[21] We insist upon the fact that in $S^{J}_{M'M}$, M' is taken along $\vec{K}$ while M is measured along $\vec{r}$. Thus, in the absence of any collisional interaction, looking in the forward direction one observes a final momentum M along $\vec{r}$, which is equal to the initial momentum M' along direction $\vec{K}$. This implies that $S^{J}_{MM'}$ is diagonal in M. On the other hand, in the adiabatic approximation, as the internal momentum is linked to the internuclear axis, a final momentum M corresponds to the same momentum along the initial internuclear axis, i.e., to the opposite value $-M$ along direction $\vec{K}$. Thus $S^{J}_{MM'}$ is proportional to $\delta_{-MM'}$.

[22] A. Omont, J. Phys. Radium **26**, 26 (1965); P. R. Berman and W. E. Lamb, Phys. Rev. **187**, 221 (1969).

[23] P. J. Brussard and H. A. Tolhoek, Physica (Utrecht) **23**, 955 (1957).

New Results for Transition Probabilities in Two-Level Systems:

The Large Detuning Regime

E. J. Robinson and P.R. Berman
Department of Physics
New York University
4 Washington Place
New York, New York 10003

Abstract

The problem of calculating transition probabilities
in two-level systems is studied in the limit where the
detuning is large compared to the inverse duration of the
interaction. Coupling potentials whose Fourier transforms
$\tilde{V}(\omega)$ are of the form $f(\omega)e^{-(|b\omega|)}$ for large frequencies
give rise to solutions which may be classified into
families according to the form of $f(\omega)$. Within each
family, transition probabilities may be calculated from
formulae that differ only in the numerical value of
a scaling parameter. In cases where the coupling function
has a pole in the complex time plane, the families are
identified with the order of this singularity. In par-
ticular, for poles of first order, a connection with the
Rosen-Zener solution can be made.

The analysis is performed via high-order perturbation
expansions, which are shown to always converge for two-
level systems driven by coupling potentials of finite
pulse area.

I. Introduction

In many areas of physics, one encounters problems involving two states of a quantum-mechanical system coupled by a time-dependent potential.[1-10] In the interaction representation, the equations of motion for a_1 and a_2, the probability amplitudes of levels 1 and 2, are of the form

$$i\dot{a}_1 = V(t) e^{i\omega t} a_2, \tag{1a}$$

$$i\dot{a}_2 = V(t) e^{-i\omega t} a_1, \tag{1b}$$

where ω is the frequency separation of the states and $V(t)$ is the coupling potential. Decay effects are neglected in Eqs. (1) (and throughout this paper) and we work in a system of units in which $\hbar = 1$.

Equations of this type arise in many semiclassical problems. A problem of current interest to which they apply is the coupling of two levels of an atom by a laser pulse that has a temporal width which is small compared to the natural lifetimes of the levels. The pulse, $V(t)$ is of the form

$$V(t) = 2 A(t) \cos \Omega t, \tag{2}$$

where Ω is the central frequency of the pulse, and $2A(t)$ is the envelope function of its amplitude. Assuming that $\frac{|\Omega-\omega|}{\Omega+\omega} \ll 1$, one can recast Eqs. (1) in terms of Δ, the detuning of the pulse from resonance (rotating wave approximation) as

- 2 -

$$i\dot{a}_1 = A(t)\, e^{i\Delta t}\, a_2, \tag{3a}$$

$$i\dot{a}_2 = A(t)\, e^{-i\Delta t}\, a_1. \tag{3b}$$

Eqs. (3) or (1) are deceptively simple in form, and one might, at
first glance, believe that the system must be completely understood, so
that nothing remains to be investigated about the equations or their so-
lution. Actually, there is very little known about the overall qualitative
nature of the solutions to Eqs. (3) for arbitrary $A(t)$. Apart from any in-
trinsic interest one might have in the dynamics of two-level systems, such
information could be useful, for example, in applications where one wished
to choose the pulse shape to maximize the excitation probability for a
given detuning Δ.

To appreciate that our assertion concerning the lack of knowledge
about the behavior of systems described by Eqs. (3) is valid, one need
only recognize that the answer to the following question is not known
in general. "Starting with initial conditions $a_1(-\infty) = 1$, $a_2(-\infty) = 0$, how
does the probability amplitude $a_2(t)$ depend qualitatively on the pulse
area S, defined by

$$S = \int_{-\infty}^{\infty} A(t)\, dt,$$

on the detuning, and on the shape of the envelope function $A(t)$?"

A response to this query can be made for a limited number of cases.
Analytic solutions are available if $A(t)$ belongs to a class of functions[5],
(including the hyperbolic secant of Rosen and Zener[2,3]) mappable into the

- 3 -

hypergeometric equation, or if $A(t) = $ (constant) $\exp(-\alpha|t|)$[9,10] or if $A(t)$ is a step function (Rabi problem), or if the detuning is zero.[*] In addition, there are approximate solutions available in adiabatic[4] or perturbative limits. Yet, there remains a wide range of parameters and pulse shapes for which an answer to the basic question cannot be provided.

In this paper, we shall examine the solutions to Eqs. (3) in the limit where the product of the detuning $|\Delta|$ and the characteristic pulse duration τ has a magnitude greatly in excess of unity. In other words, we are assuming that the pulse does not possess the appropriate Fourier components to significantly compensate for the detuning. In consequence, the transition probability $|a_2(\infty)|^2$ will always be very small (but still great enough to be experimentally measurable in atomic vapors of densities $\sim 10^{12}$ atoms/cm^3). We note that numerical solutions of Eq. (3) in this detuning range may be possible but are very costly in computer time and plagued with technical difficulties.

For the case $|\Delta\tau| \gg 1$, we shall establish the following results: (1) Low-order perturbative approximations for $a_2(\infty)$ are not valid for arbitrary pulse area S, despite the fact that $|a_2(t)|^2 \ll 1$ for all time. (2) An iterative solution to Eqs. (1) always converges for well-behaved envelope functions. (3) Asymptotic solutions for $a_2(t)$, t finite, may be easily found, but expressions for $a_2(\infty)$ are difficult to obtain. (4) Asymptotic solutions for $a_2(\infty)$ can be obtained for a limited class of

[*]Kaplan[7] has also considered cases where the detuning varies as prescribed functions of the amplitude, and obtained closed-form expressions.

- 4 -

pulse envelope functions using contour integration techniques. This is a broader set than that for which exact solutions are known. (5) The asymptotic dependence of $a_2(\infty)$ depends critically on the nature of the singularities of the pulse envelope function $A(t)$, analytically continued into the complex plane. (6) If two pulse functions have the same Fourier transforms in the limit of large frequencies and if the dominant dependence of the transform is an exponential decay in the frequency, then the asymptotic forms of the solutions $a_2(\infty)$ for these functions in the limit of large $|\Delta|$ are simply related. In this paper, we address points (1), (2), (3), and (6); methods for actually obtaining asymptotic solutions (points (4) and (5)) will be discussed in a future article.

II. Asymptotic solutions.

As we have indicated, the Rosen-Zener[2,3] (hyperbolic secant coupling pulse) problem is one of the few for which exact solutions are known. In this case, a simple expression gives the transition amplitude as a function of detuning and area for all values of these parameters. Naturally, since this formula

$$a_2(\infty) = -i\sqrt{2\pi}\ \tilde{V}(\Delta)\ \frac{\sin S}{S},\tag{4}$$

where $\tilde{V}$ is the Fourier transform of $A(t)$, is exact, it is valid in the special case of the asymptotic limit.

We shall show that there is an entire class of pulses for which the asymptotic transition amplitude, as a function of S and Δ, may be written

- 5 -

down by inspection, once the Rosen-Zener problem has been solved. We shall also demonstrate that there are other classes of pulses whose solutions as t $\to \infty$ are unrelated to Rosen-Zener, but are connected to each other in the sense that once one has been solved, the solutions for the entire class may be obtained by inspection.

The existence of these related solutions will be established via term-by-term comparison of nth order perturbation expansions which, under very general conditions, are convergent in two-level problems. (See Appendix). With suitable scaling of the coupling strengths, the series for different members of particular classes will be seen to be identical, in the limit of large detunings.

The particular potentials analyzed in this paper are $A(t)$ whose Fourier transforms for large ω assume the form $p(\omega) \exp(-|b\omega|)$, where p is a slowly varying function of ω, and b a constant. It is convenient to make a variable change, such that $\nu = |b|\omega$ and $x = t/|b|$. Consequently, the exponential decay factor in the Fourier transform becomes $\exp(-|\nu|)$ and the equations of motion transform to

$$i \dot{a}_1 = \beta f(x) e^{i\alpha x} a_2,$$

(3a')

$$i \dot{a}_2 = \beta f(x) e^{-i\alpha x} a_1,$$

(3b')

where $\alpha = |b\Delta|$ and where the dot now signifies differentiation with respect to x. β, previously designated as S, is the pulse area. The reduced potential function $f(x)$ is defined such that $\int_{-\infty}^{\infty} f(x)dx = 1$. The

- 6 -

pulse area is invariant under the indicated change of variable. One may also write Eqs. (3) as a pair uncoupled second-order equations

$$\ddot{a}_1 - \left(\frac{\dot{f}}{f} + i\alpha\right)\dot{a}_1 + \beta^2 f^2 a_1 = 0, \tag{5a}$$

$$\ddot{a}_2 - \left(\frac{\dot{f}}{f} - i\alpha\right)\dot{a}_2 + \beta^2 f^2 a_2 = 0. \tag{5b}$$

There are two aspects to the solutions of Eqs. (3) or (5). These are the calculation of the amplitudes at finite and infinite times, respectively. The former are of interest if the transients are to be used as input to other problems, such as multiphoton ionization[11], while the latter, with which we are mainly concerned here, are the transition amplitudes, $a_2(\infty)$. The two temporal regimes differ greatly in the methods that must be used to perform accurate calculations.

Apart from the Rabi problem, the problem which has attracted the most study is that of Rosen and Zener[2,3], $f(x) = (\operatorname{sech}\pi\, x/2)/2$, for which the solutions are

$$a_1 = {}_2F_1(a, b, c, z), \tag{6a}$$

$$a_2 = -i K z^{1-c^*} {}_2F_1(a - c^* + 1, b - c^* + 1, 2 - c^*, z), \tag{6b}$$

or

$$a_2 = -i K z^{1-c^*}(1-z)^{c^* - a - b} {}_2F_1(1-a, 1-b, 2-c^*, z), \tag{6b'}$$

- 7 -

where $a = -b = \frac{\beta}{\pi}$, $c = \frac{1}{2} - \frac{i\alpha}{4\pi}$,

$$z = \frac{\tanh \frac{\pi x}{3} + 1}{2}, \quad K = \frac{\beta}{4\pi(\frac{1}{2} - \frac{i\alpha}{4\pi})},$$

and $_2F_1$ designates the hypergeometric function. The form of a_2 given by Eq. (6b) is valid for all x, while that given by Eq. (6b') holds only for finite λ, unless β corresponds to an eigenvalue, a pulse area for which $a_2(+\infty)$ vanishes.[6] We recall that $a_2(\infty)$, the transition amplitude for the Rosen-Zener problem is given by Eq. (4).

One may write the solutions to Eqs. (3) as perturbation series in the usual fashion, noting that only even orders enter the expression for a_1, while only odd orders appear in the formula for a_2. The expansion for $a_2(+\infty)$ is

$$a_2 = -i \sum_{k=0}^{\infty} a_2^{(2k+1)} \beta^{2k+1} (-1)^k, \quad \text{where}$$

$$a_2^{(2k+1)} = \int_{-\infty}^{\infty} A(x_1) e^{-i\alpha x_1} dx_1 \prod_{j=2}^{2k+1} \int_{-\infty}^{x_{j-1}} A(x_j) e^{i(-1)^j \alpha x_j} dx_j.$$

In the Appendix, it is shown that this series converges for all finite pulse areas.

For the remainder of the paper we will restrict ourselves to the case of pulses that are symmetric in time and where $|\alpha| \gg 1$ --

- 8 -

the adiabatic or asymptotic limit. The Fourier transform will be
symmetric in ν. We shall begin by comparing the finite and infinite
time solutions of the Rosen-Zener problem, which exemplify relevant
properties of transition amplitudes induced by smooth pulses.

We may obtain the finite time solution by explicitly expanding
the $_2F_1$ function of Eq. (6b')

$$a_2 = - \frac{i\beta}{4\pi(\frac{1}{2} - \frac{i\alpha}{4\pi})} e^{-i\alpha x} \operatorname{sech} \frac{\pi x}{2} \Big[1 +$$

$$\frac{(1 + \frac{\beta}{\pi})(1 - \frac{\beta}{\pi})}{3 - \frac{i\alpha}{2\pi}} (\tanh \frac{\pi x}{2} + 1) + \cdots \Big].$$

For large α, it is sufficient to retain the leading term

$$a_2 \simeq \frac{\beta}{\alpha} e^{-i\alpha x} \operatorname{sech} \frac{\pi x}{2}.$$

This is equivalent to first-order perturbation theory in the adiabatic
limit

$$a_2^{(1)} = -i \int_{-\infty}^{x} V(x') e^{-i\alpha x'} dx' \simeq \frac{V(x)}{\alpha} e^{-i\alpha x},$$

where subsequent parts integrations are neglected, since they are
$O(\frac{1}{\alpha^n})$, $n > 1$. We immediately see that this sequence of parts integrations
is unsuitable for calculation $a_2(\infty)$, since each term separately vanishes
when $x \to \infty$. Even including the third - and higher-order terms in the

- 9 -

perturbation series via analogous sequences of parts integrations does not enable one to obtain a non-zero amplitude as $t \rightarrow \infty$. Consequently, other methods are necessary to calculate for $a_2(\infty)$.

It is clear from the preceding paragraph that for large enough α, first-order perturbation theory is a sufficiently accurate approximation for most purposes, provided x is finite. For infinite times, not only does the adiabatic sequence of parts integrations lead to an incorrect $a_2(\infty)$, but even an exact evaluation of the first order integral may be insufficient. This is typified by the exact Rosen-Zener amplitude, Eq. (4), in which the factor $\sin\beta$ does not reduce to its first order limit of β unless $|\beta|$ is small compared to unity. This failure of the first-order theory occurs no matter how large the detuning becomes. One must retain enough terms in the perturbation expansion to accurately represent the sine function. Thus, for the Rosen-Zener pulse, if the coupling is great enough so that saturation effects would appear at resonance, simple first-order theories can not be used for a nonresonant pulse of the same strength. As we shall see, other smooth pulses also possess this "saturation memory". In fact, in some cases, a higher-order theory is necessary off resonance even for a case where a first-order theory would suffice at resonance. This is exemplified by the formulae of Eqs. (9) below.

Since each coupling function $f(x)$ is different, one might be led to believe that separate calculations must be performed for each individual case. Fortunately, as we have stated earlier, there prove

- 10 -

to be classes of pulses where, if one knows the functional dependence
of the asymptotic transition amplitude on α and β for one member of
the class, one knows it for all members of the class, although the actual
time dependence of the potentials may be drastically different. What is
significant is that their Fourier transforms assume the same form as
$\alpha \to \infty$.

When Rosen and Zener deduced Eq. (4), they suggested that similar
formulae might hold for other smooth pulses.[2] This conjecture proves not
to hold in general. It is manifestly false for asymmetric pulses, nor is
it even valid for all symmetric pulses.[5,6] What we shall show is that a
kind of Rosen-Zener conjecture does apply at large detunings for pulses
in which $f(x)$ has simple poles at $x = i$. This law does not apply to pulses
which have higher order poles at this point, although scaling laws for
these do exist, different for each order.

The following theorem will be established. Let two coupling
pulses $A(x)$ and $A_o(x)$ have Fourier transforms $\tilde{V}(\nu)$ and $\tilde{V}_o(\nu)$. The
Fourier transforms of both approach, for large values of the argument,
the same asymptotic form $\tilde{V}_a(\nu)$. If $\tilde{V}_a$ is of the form, $\phi(\nu)e^{-|\nu|}$ where
$\phi(\nu)$ is a slowly varying function of ν, then the asymptotic transition
amplitudes generated by the two pulses will be the same, provided that
the pulse areas are both finite. A sufficient condition for the indicated
asymptotic behavior of the Fourier transforms is that they be equal, for
large ν, to a contour integration whose value is given by the product of
the residue at $x = i$ and the usual Cauchy factor $2\pi i$. If two such pulses

- 11 -

are to have the same $\phi(\nu)$, they must possess poles of the same order at $x = i$.

The contribution of order $(2k+1)$ to the transition amplitude may be rewritten slightly

$$a_2^{(2k+1)} = \int_{-\infty}^{\infty} A(x_1) e^{-i\alpha x_1} dx_1 \prod_{j=2}^{2k+1} \lim_{\lambda_j \to 0} \int_{-\infty}^{x_{j-1}} A(x_j) e^{\{i(-1)^j \alpha + \lambda_j\} x_j} dx_j .$$

The factors $e^{\lambda_j x_j}$ do not affect the integrals. They are used to remove ambiguities as $x_j \to -\infty$ in the treatment below, where we express the amplitude in terms of integrals in the frequency domain. The limits $\lambda_j \to 0$ are to be taken before the x_1 integration is performed. Expressing each $A(x_j)$, $j \geq 2$, in terms of its Fourier transform, we have

$$a_2^{(2k+1)} = \frac{1}{(2\pi)^{2k}} \int_{-\infty}^{\infty} A(x_1) e^{-i\alpha x_1} dx_1 \prod_{j=2}^{2k+1} \lim_{\lambda_j \to 0}$$
$$\int_{-\infty}^{x_{j-1}} dx_j \int_{-\infty}^{\infty} \tilde{V}(\gamma_j) e^{i(\gamma_j + (-1)^j \alpha - i\lambda_j) x_j} d\gamma_j .$$

By working in the frequency domain, we shall be able to examine the structure of the integrals for $a_2^{(2k+1)}$ and establish that the contribution from regions where the asymptotic form of $\tilde{V}$ is not valid is lower by $O(\frac{1}{\alpha})$ than the contributions from regions where it is valid.

- 12 -

The integrals over the x_i are trivial to perform. We obtain

$$a_2^{(2k+1)} = \lim_{\lambda_\ell \to 0} \frac{1}{(2\pi)^{k-\frac{1}{2}}} \int_{-\infty}^{\infty} d\gamma_2 \cdots d\gamma_{2k+1} \, \tilde{V}\left(\sum_{j=2}^{2k+1} \gamma_j - \alpha\right)$$

$$\prod_{j=2}^{2k+1} \frac{\tilde{V}(\gamma_j)}{\sum_{\ell=2k+3-j}^{2k+1} (\gamma_\ell + (-1)^\ell - i\lambda_\ell)} \; .$$

We now proceed to determine the asymptotic form of these amplitudes.
The analysis is easiest to follow for the third-order contribution $a_2^{(3)}$,
but exactly the same reasoning and conclusions will apply for the higher
order terms. (The theorem is true by inspection in first-order, since
that contribution is, apart from a constant multiplier, just the Fourier
transform itself. Thus, if two coupling functions have Fourier transforms
of the same asymptotic form, their first-order transition amplitudes scale
the same way with β and α. The leading non-trivial term is $a_2^{(3)}$.)

$$a_2^{(3)} = \lim_{\lambda \to 0} \frac{1}{\sqrt{2\pi}} \int_{-\infty}^{\infty}\int_{-\infty}^{\infty} \frac{\tilde{V}(\gamma_1)\,\tilde{V}(\gamma_2)\,\tilde{V}(\gamma_1 + \gamma_2 - \alpha)\, d\gamma_1 \, d\gamma_2}{(\gamma_1 - \alpha - i\lambda)(\gamma_2 + \gamma_1 - i\lambda)} \; .$$

It is convenient to make the change of variable $\nu_i = y_i \, \alpha$.

$$a_2^{(3)} = \lim_{\lambda \to 0} \frac{1}{\sqrt{2\pi}} \int_{-\infty}^{\infty}\int_{-\infty}^{\infty} \frac{\tilde{V}(\alpha y_1)\,\tilde{V}(\alpha y_2)\,\tilde{V}(\alpha[y_1 + y_2 - 1])\, dy_1 \, dy_2}{(y_1 - 1 - i\lambda)(y_1 + y_2 - i\lambda)} \; =$$

- 13 -

$$\frac{1}{\sqrt{2\pi}}\left\{ P\iint_{-\infty}^{\infty}{}_{-\infty}^{\infty} \frac{\tilde{V}(\alpha y_1)\,\tilde{V}(\alpha y_2)\,\tilde{V}(\alpha[y_1+y_2-1])\,dy_1\,dy_2}{(y_1-1)(y_1+y_2)}\right.$$

$$\left. + i\pi \lim_{\lambda\to 0}\int_{-\infty}^{\infty} dy_2 \left[\frac{\tilde{V}(\alpha)(\tilde{V}(\alpha y_2))^2}{1+y_2-i\lambda} + \frac{(\tilde{V}(\alpha y_2))^2\,\tilde{V}(\alpha)}{-y_2-1-i\lambda} \right] \right\},$$

where P indicates that the integrand excludes infinitesimal regions near $y_1 = -y_2$ and $y_1 = 1$. We may formally integrate the last two terms. If, (-1) is factored from the second of the two integrals, they combine to become

$$i\pi \lim_{\lambda\to 0}\int_{-\infty}^{\infty} dy_2\, \tilde{V}(\alpha)(\tilde{V}(\alpha y_2))^2 \left\{ \frac{1}{1+y_2-i\lambda} - \frac{1}{1+y_2+i\lambda} \right\}.$$

It is immediately obvious that if these are partitioned according to the rule

$$\lim_{\varepsilon\to 0}\int \frac{\phi(x)\,dx}{x-x_0-i\varepsilon} = P\int \frac{\phi(x)\,dx}{x-x_0} + i\pi\,\phi(x_0),$$

the principal value contributions exactly cancel, while the $i\pi$ terms are proportional to $e^{-3\alpha}$, and exponentially small compared to $a_2^{(1)}$, which decays only like $e^{-\alpha}$. Terms proportional to exponentials which decay more rapidly than $e^{-\alpha}$ do not contribute to the asymptotic form.

We now proceed to examine the remaining contributions to $a_2^{(3)}$, where it is again understood that the small regions in the neighborhood of $y_2 = -y_1$ and $y_1 = 1$ are excluded from the integrals. For all regions

- 14 -

except where $|y| < |\frac{a}{\alpha}|$, where a is a number of order unity, $\widetilde{V}(\alpha y) \to \widetilde{V}_a(\alpha y)$.

Thus, for the entire y_1-y_2 plane, except where $y_1 \sim 0$, $y_2 \sim 0$ (but not both simultaneously) and $y_1 + y_2 \simeq 1$, the numerator of the integrand is well represented by its asymptotic form. Furthermore, since at most **one** of the three Fourier transform factors departs from its asymptotic form in any given region of space, the area in the $y_1 - y_2$ plane over which one of the $\widetilde{V}$ both departs from its asymptotic form and decays no more rapidly than $e^{-\alpha}$ is $O(1/\alpha)$. It is, of course implicitly assumed that the exact and asymptotic forms of the Fourier transforms remain bounded as their arguments $\to 0$. For the former, this is equivalent to the requirement, which we have already stated, that β be finite.

Now consider that portion of the y_1-y_2 plane where all factors in the numerator are well-approximated by their asymptotic forms. Examine in particular the exponential decay factors

$$e^{-\alpha|y_1|} \quad e^{-\alpha|y_2|} \quad e^{-\alpha|y_1+y_2-1|} .$$

The only portion of the plane where the combined effect of the exponential factors leads to an overall decay that is not faster than $e^{-\alpha}$ is the range $0 < y_1 < 1$, $0 < y_2 < 1-y_1$. The integrand does not change sign in this portion of y_1-y_2 space, which encompasses an area $\sim 1/2$, compared to the area $1/\alpha$, which is the corresponding extent in which the nonasymptotic integrand decays no more rapidly than $e^{-\alpha}$. Note that there is no portion of the plane in which the integrand decays more slowly than $e^{-\alpha}$. Thus the nonasymptotic integrand contribution

is $O(\frac{1}{\alpha})$ compared to that of the asymptotic integrand.

Similar considerations enable one to deduce that one may also replace the Fourier transforms in the higher-order integrals by their asymptotic forms.

We thus conclude that if the time-dependences of two coupling functions are such that the asymptotic forms of their Fourier transforms are identical and of the indicated form, the large detuning transition amplitudes are the same.

As we have indicated, a sufficient condition that two pulses have the same $a_2(\infty)$ for large α is that both asymptotic Fourier transforms be equal to contour integrations given by $(2\pi i)$ $(\text{Res}(x=i))$. We compare the hyperbolic secant of Rosen and Zener, $f = \frac{1}{2}$ sech $\frac{\pi x}{2}$ with the Lorentzian $f = \frac{1}{\pi} (1+x^2)^{-1}$. The corresponding $A(x)$ are

$$A_L(x) = \frac{\beta}{\pi} \left(1+x^2\right)^{-1},$$

$$A_H(x) = \frac{\beta}{2} \, sech \, \frac{\pi x}{2}.$$

The transforms for both may be calculated via contour integrations. The Lorentzian case is trivial and applies to all ν, not just large frequencies. We choose a contour that runs along the real axis from $-R$ to $+R$ and is closed by a semicircle in the upper half plane. The contribution to the contour integral from the arc vanishes as $R \to \infty$, so that the Fourier transform is identical to the contour integral, whose value is determined by the residue at the simple pole at $x = i$.

- 16 -

The result is

$$\tilde{V}_L = \frac{\beta}{\sqrt{2\pi}}\, e^{-|\gamma|} . \tag{7a}$$

For the hyperbolic secant we choose a rectangular contour which runs from $-R$ to $+R$ along the real axis, that is continued by rectangular segments parallel to the imaginary from the points $(\pm R, 0)$ to the points $(\pm R, 2i)$, and is closed by a line parallel to the real axis which runs from $(R, 2i)$ to $(-R, 2i)$. The two vertical segments give vanishing contributions as $R \to \infty$, and the horizontal segment off the real axis goes exponentially to zero compared to the segment along the real axis as $\nu \to \infty$. Thus, for the hyperbolic secant, **the Fourier transform is identical to that of the Lorentzian in the asymptotic region. For large ν it is given by**

$$\tilde{V}_H \simeq \frac{2\beta}{\sqrt{2\pi}}\, e^{-|\gamma|} . \tag{7b}$$

Since the Rosen-Zener solution gives the transition amplitude for all detunings, according to Eq. (4), as $-i\sqrt{2\pi}\, f(\alpha)\sin\beta$, this formula must be valid asymptotically also. As we have shown that the asymptotic Fourier transforms of the Lorentzian and hyperbolic secant are proportional for large detunings, the Lorentzian must induce **a transition amplitude that** obeys a formula similar to Eq. (4). From Eqs. (7), we see that to construct the Lorentzian and hyperbolic secant Fourier transforms so that **they are asymptotically identical, it is necessary to choose the Lorentzian**

pulse area β_L to be twice that of β_h. This immediately gives the large detuning scaling law for the Lorentzian

$$a_{2L} = -i \sqrt{2\pi} \; 2 \, \overset{\sim}{f_L}(\alpha) \sin \frac{\beta}{2} . \qquad (8a)$$

This result has been independently obtained by carrying out an asymptotic solution of Eqs. (3).[12]   One can also show that for the pulse $A_c = \beta_c \, \mathrm{cosech}\,\pi x$, the appropriate scaling law is

$$a_{2c} = -i \frac{\sqrt{2\pi}}{2} \, \overset{\sim}{f_c}(\alpha) \sin 2\beta . \qquad (8b)$$

For the hyperbolic secant pulse, the transition amplitude vanishes for pulse areas $\beta = n\pi$, n integral for all detunings. The Lorentzian, on the other hand, has eigenvalues $\beta = n\pi$ for zero detuning, while those for large detuning are $\beta = 2n\pi$. The eigenvalues of A_c go from $n\pi$ at $\alpha = 0$ to $\frac{n\pi}{2}$ as $\alpha \to \infty$.

The existence of a pole at $x=i$ is a sufficient, but not a necessary condition that the asymptotic Fourier transform of a coupling pulse $\sim p(\omega)e^{-|\omega|}$. For example, the function $(1+x^2)^{-3/2}$ has an asymptotic Fourier transform proportional to $\nu^{1/2} e^{-\nu}$. The factor $\nu^{1/2}$ precludes deducing the asymptotic transition amplitude from the Rosen-Zener formula. Similarly, the squares of the hyperbolic secant and of the Lorentzian each have poles of second order at $x=i$, with the consequence that, for both of these, $\tilde{V}_a \sim \nu^1 e^{-|\nu|}$, so that while these will have asymptotic transition amplitudes that are related to each other, they cannot be obtained by scaling from Eq. (4). In our next paper, we shall show

- 18 -

how to calculate asymptotic transition amplitudes when the coupling

pulse has second- and higher-order poles at x=i. For now, we merely

present the formulae for the transition amplitudes generated by the

squares of the hyperbolic secant and Lorentzian

$$a_2(H2) = -i \frac{2\pi}{C^2} e^{-|\alpha|} \sin\left[C\sqrt{\frac{|\alpha\beta|}{\pi}}\right] \sinh\left[C\sqrt{\frac{|\alpha\beta|}{\pi}}\right] \quad (9a)$$

$$a_2(L2) = -i \frac{2\pi}{C^2} e^{-|\alpha|} \sin\left[C\sqrt{\frac{|\alpha\beta|}{2\pi}}\right] \sinh\left[C\sqrt{\frac{|\alpha\beta|}{2\pi}}\right], \quad (9b)$$

where $C = 1 + \frac{1}{6} + \frac{1}{56} + \frac{1}{182} + \simeq 1.194$. Equation (9a) can be obtained

from Eq. (9b) by scaling techniques derived in this paper.

III. Summary and Conclusion

In this paper, we have demonstrated that pulse shapes $A(t)$

whose Fourier transforms asymptotically approach the form $\phi(\nu)e^{-|\nu|}$,

where ϕ is slowly varying, may be categorized into families which differ

according to the function ϕ. Within each family, the transition ampli-

tudes $a_2(\infty)$ are related by simple scaling laws, so that if one is able

to derive an expression for the transition amplitude generated by one

member of the family, corresponding formulae for all other members of

the family may be written down by inspection.

A sufficient condition that the Fourier transform be of the

required form is that it be obtainable in the asymptotic region as a

contour integral evaluated from the residue at a single pole on the

imaginary time axis. For the case where $A(t)$ has simple poles, $a_2(\infty)$

may be inferred from the solution of the Rosen-Zener problem[2,3], known for fifty years, by a trivial scaling operation.

Our results were obtained by examining the structure of the terms in perturbation expansions for transition amplitudes. (We have demonstrated that these sequences always converge in two-level problems provided that the pulse areas are finite. Low-order approximations, however, are frequently not useful for $t \to \infty$ even when they are valid at finite times.) With suitable choices of ratios of pulse areas, corresponding terms in the series for different members of the same family **will be identical.**

In a future paper[12], we shall present methods for explicitly calculating transition amplitudes that apply to higher-order, as well as simple poles. Thus, we are not restricted in practice to writing scaling laws for pulses which may be compared in the asymptotic region to the hyperbolic secant.

Appendix – Convergence of Perturbation Theory for the Transition

Amplitude

We demonstrate here that the perturbation series for a_2 converges
for all finite pulse areas. The contribution of order $(2k+1)$ is

$$b_1^{(k)} = -i\beta^{2k+1} a_2^{(2k+1)} =$$

$$-i\beta^{2k+1}(-1)^k \int_{-\infty}^{\infty} f(x_1)e^{-i\alpha x_1} dx_1 \prod_{j=2}^{2k+1}\int_{-\infty}^{x_{j-1}} f(x_j)e^{i(-1)^j \alpha x_j} dx_j. \tag{A-1}$$

Now assume that $A(x)$ is of a single algebraic sign. Without loss of
generality we may take this to be positive. We compare the series with
the corresponding expansion for $\alpha = 0$.

$$b_{10}^{(k)} = -i\beta^{2k+1}(-1)^k \int_{-\infty}^{\infty} f(x_1)dx_1 \prod_{j=2}^{2k+1}\int_{-\infty}^{x_{j-1}} f(x_j)dx_j = \tag{A-2}$$

$$-i\beta^{2k+1}(-1)^k \int_{-\infty}^{\infty}|f(x_1)|dx_1 \prod_{j=2}^{2k+1}\int_{-\infty}^{x_{j-1}}|f(x_j)|dx_j. \tag{A-2'}$$

Invoking the theorems on repeated integrals of the same function

$$b_{10}^{(k)} = \frac{-i\beta^{2k+1}}{(2k+1)!}(-1)^k \left(\int_{-\infty}^{\infty} f(x)dx\right)^{2k+1},$$

and the terms are recognized as identical to those for the series $-i\sin\beta$.

Now consider the series

$$F(\beta) = \sum \left| b_{10}^{(k)} \right| = \sum \frac{\left| \beta^{2k+1} \right|}{(2k+1)!} \left(\int_{-\infty}^{\infty} f(x)\,dx \right)^{2k+1}$$

$$= \sum \frac{\left| \beta^{2k+1} \right|}{(2k+1)!} .$$

This is evidently the series for $\sinh\beta$, which converges so long as β is finite. Hence, the series of Eq. (A-2) is absolutely convergent. Now

$$\left| b_1^{(k)} \right| = \frac{\left| \beta^{2k+1} \right|}{} \left| \int_{-\infty}^{\infty} f(x_1) e^{-i\alpha x_1}\,dx_1 \prod_{j=2}^{2k+1} \int_{-\infty}^{x_{j-1}} f(x_j) e^{i(-1)^j \alpha x_j}\,dx_j \right|$$

$$\leq \left| \beta^{2k+1} \right| \int_{-\infty}^{\infty} \left| f(x_1) \right|\,dx_1 \prod_{j=2}^{2k+1} \int_{-\infty}^{x_{j-1}} \left| f(x_j) \right|\,dx_j$$

$$\leq \left| b_{10}^{(k)} \right| ,$$

so that the series, Eq. (A-1) is also absolutely convergent, and our result is established.

We note that the same arguments will apply to perturbation series at finite times, provided merely that $\int_{-\infty}^{x} f(x')\,dx' = \beta(x)$ is of one sign and finite. If $f(x)$ changes sign, the results will still be valid provided the generalized area $\int_{-\infty}^{x} \left| f(x') \right|\,dx'$, is finite.

A simple case where the convergence theorem does not apply is the coupling function $A(x) = (\text{const})\,(\tanh\pi x/2)/x$, since β is logarithmically divergent. In addition, since the pulse area is proportional to the

Fourier transform at zero frequency, the multiple integrals in the

frequency domain for the third- and higher-order contributions to the

perturbation series contain regions where the integrands blow up, so

that the individual terms beyond first order may not even exist. (The

first-order contribution will be finite, since the Fourier transform for

this pulse exists for $\nu \neq 0$. In this case, we note that the infinite

area does not imply a pulse of infinite energy, so that it theoretically

could exist. One evidently cannot use the methods developed here to

describe the dynamics. At the very least, decay would have to be in-

cluded in the analysis, and a completely non-perturbative treatment

utilized.)

References

1. L. Allen and J.H. Eberly, <u>Optical Resonance and Two-Level Atoms</u>, (Wiley, New York, 1975). This work includes an extensive bibliography for the two-level problem.

2. N. Rosen and C. Zener, Phys. Rev. A <u>40</u>, 502 (1932).

3. R.T. Robiscoe, Phys. Rev. A <u>17</u>, 247 (1978).

4. R.T. Robiscoe, Phys. Rev. A <u>25</u>, 1178 (1982).

5. A. Bambini and P.R. Berman, Phys. Rev. A <u>23</u>, 2496 (1981).

6. E.J. Robinson, Phys. Rev. A <u>24</u>, 2239 (1981).

7. A.E. Kaplan, Sov. Phys. - JETP <u>41</u>, 409 (1976).

8. M.G. Payne and M.H. Nayfeh, Phys. Rev. A <u>13</u>, 595 (1976).

9. D.S.F. Crothers and J.G. Hughes, J. Phys. B <u>10</u>, L557 (1977).

10. D.S.F. Crothers, J. Phys. B <u>11</u>, 1025 (1978).

11. E.J. Robinson, J. Phys. B <u>13</u>, 2243 (1980).

12. P.R. Berman and E.J. Robinson, (unpublished).

O'ROURKE*, and S. M. MUDARE, Georgia Institute of Technology.**--The resonance Raman profiles of a number of vibrational lines of copper tetraphenylporphyrin in a nitrogen matrix have been measured throughout the Q(0-0) and Q(0-i) absorption region. Based on absorption spectra analysis, the nitrogen matrix provides an environment approximating the gas phase.[1] The major features in the excitation profiles can be analyzed using a simple adiabatic theory.[2] From spectra taken with excitation near the Soret band, it is possible to explain the strong enhancement of the 392 cm^{-1} profile at frequencies 1200-1600 cm^{-1} removed from the Q(0-0) band as weak Hertzberg-Teller (HT) coupling of the 392 cm^{-1} mode and strong HT coupling of these higher frequencies. The strength of the 392 cm^{-1} Raman intensity is due to a strong Franck-Condon effect for this mode. Additional structure observed in the profiles is attributed to interference between fundamental and combination terms in the scattering intensity equation.
*Current address: E. I. Dupont Savannah River Laboratory.
**Supported by NSF Grant DMR-7907758.
[1]D. C. O'Shea, P. E. O'Rourke and S. M. Mudare, Paper KE2, San Francisco APS Meeting.
[2]P. E. O'Rourke and D. C. O'Shea, this session.

BH 14   Radiative Mean Lifetimes of the Excited States of the Hydrogen-Like Atoms. K. OMIDVAR, NASA/Goddard Space Flight Center--Using Kramers' semi-classical formula for the oscillator strength of the hydrogen-like atoms[1], it is shown that the mean lifetime of an excited state with a principal quantum number n behaves with respect to n as $(\mu Z^*)^{-1}n^3/\ln(n)$, where u is the atomic reduced mass, and Z is the effective charge of the point charge coulomb field acting on the running electron. Using this result, it is shown that the mean lifetime of a state specified by the principal and angular momentum quantum numbers n and ℓ behaves as $(\mu Z^*)^{-1}n^3\ell^2$. Agreement with selected measured mean lifetimes of the excited and rydberg states of He and alkalide atoms will be shown.

[1]H. Supported by the U.S. Office of Naval Research under Contract No. N00014-77-C-0553.

BH 15   Collisionally Aided Radiative Excitation Studies in Sodium*, M. TAWIL, P.R. LERMAN, E. GIACOBINO†, O. REDI, H.H. STROKE, R. VETTER††, NYU - A study is being made of the interaction of light from a ring dye laser with Na undergoing collisions, to understand better the physics of the processes beyond the impact region leading to line asymmetry and possible heating and cooling. In one experiment, the 4D state was excited far off resonance in a two-photon transition (578.7 nm) with Ar at pressures p=0-55 Torr. For p≠0, fluorescence was observable for detuning ≈10 Doppler widths. At ≈20 Torr small (Na₂?) peaks were observed in the wings. They vanished without Ar. In a second experiment, stepwise excitation with 2 photons from a single laser (568.4 nm) is used to populate the 4D level in the presence of Ar or He. The intermediate 3P atoms appear to be heated in the process. The width is studied by the hole made in the 3P-3S fluorescence as the 3P-4D transition is scanned, or by the 4P-3S cascade transition. Results are compared to theoretical predictions by one of us (PPL).
*Supported in part by NSF grants PHY-7909173/02 and INT-7921530, and by the Office of Naval Research.
†Permanent address: Ecole Normale Supérieure, Paris.
††Permanent address: Laboratoire Aimé Cotton, Orsay.

BH 16   Measurement of Static Electric Field Ionization Rate $\Gamma_T(F)$ of Helium 20 ≤ n ≤ 60 Rydberg States Preliminary Results.* D.R. MARIANI, W. VAN de WATER, P.M. KOCH, Yale Univ.--An experiment is in progress to measure precisely the F-dependence of $\Gamma_T(F)$ over the range $10^5 - 10^8$ s^{-1} near the "saddle-point" ionization limit $n^4F = 1/16$ au. The fast-beam, ^{12}C ^{16}O, cw laser spectroscopic method is similar to that used previously[1]

to measure $\Gamma_T(F)$ for individual Stark substates of hydrogen, which ionize at larger values of $n^4F = 0.1-0.3$ au. We have adapted programs kindly furnished by Zimmerman et al.[2] to calculate needed He Stark maps. $\Gamma_T(F)$ is extracted from least-squares computer fits to signal-averaged ionization curves. $^4He(1sns)^3S_1$ $\Gamma_T(F)$-curves on semilog plots rise rapidly between 10^5-10^6 s^{-1}, but bend over between 10^7-10^8 s^{-1} much more than those for H Stark substates. Data for these and other states will be presented and interpreted.
*Supported by NSF Grant PHY80-26548
[1]P.M. Koch and D.R. Mariani, Phys. Rev. Lett. 46, 1275 (1981).
[2]M.L. Zimmerman et al., Phys. Rev. A20, 2251 (1979).

BH 17   Microwave Multiphoton Ionization of Rydberg Atoms: Helium Compared to Hydrogen. P.M. KOCH, W. VAN de WATER, and D.R. MARIANI, Yale U.*--An experiment is in progress to measure with high relative precision the F_0-dependences of the rate W (over the range $10^5-10^6 s^{-1}$) of the microwave ionization of $^{12}C^{16}O_2$ laser-excited helium and hydrogen Rydberg atoms (20 ≤ n < 60) in a fast beam (>6 keV). We use a microwave electric field F(t)= $F_0\cos\omega t$ (linearly polarized parallel to the beam axis) at discrete frequencies $\omega/2\pi$ between 8 and 12 GHz. Slopes k of log-log plots of W vs. F_0^2 can be dramatically different for H and He atoms with nearly the same binding energy; e.g. at $\omega/2\pi = 9.91$ GHz, $k[H(n=42)] \geq 20$ where as $k[He(1s4ls)^3S_1] \leq 2$. Additional data for other H and He states and for other frequencies (especially near observed hydrogen "resonance" frequencies[1]) will be presented and interpreted.
*Supported by NSF Grant PHY80-26548
[1]J.E. Bayfield, L.D. Gardner, and P.M. Koch, Phys. Rev. Lett. 39, 76 (1977).

POSTER SESSIONS

SESSION BXa: HEAVY ION REACTIONS I
Monday afternoon, 26 April 1982
Empire Room at 2:00 P.M.

BXa 1
Velocity Measurements of Evaporation Residues. Y. CHAN, M. MURPHY, R. STOKSTAD, I. TSERRUYA, Lawrence Berkeley Laboratory; A. BUDZANOWSKI, LBL and INP, Cracow, and M. Blann Lawrence Livermore Lab.*--The velocities of the heavy products from the reactions $^{16}O+^{27}Al, ^{40}Ca, ^{58}Ni$ were measured with a TOF spectrometer and beams of ^{16}O at 140, 217 and 313 MeV from the LBL 88-Inch Cyclotron. Evaporation-residue-like products for $^{16}O+^{40}Ca$ at the higher energies show mean velocities less than those expected for complete fusion and equilibrium decay. A similar effect has been reported for $^{20}Ne+Ca$.[1] The energy, mass, and angular dependence of the mean velocities will be discussed.
*This work was supported by the Director, Office of Energy Research, Division of Nuclear Physics of the High Energy and Nuclear Physics and by Nuclear Sciences of the Basic Energy Sciences Program of the U.S. Department of Energy under Contract No.W-7405-ENG-48.
1) D. G. Kovar et al. BAPS 26, 1133 (1981).

BXa 2   Systematics of Light Ion Emission from Heavy Ion Reactions. J.B. BALL, R.L. AUBLE, F.E. BERTRAND, C.B. FULMER, I.Y. LEE, R.L. ROBINSON, P.H. STELSON, Oak Ridge National Laboratory*, D.L. HENDRIE, Lawrence Berkeley Laboratory, H. BREUER, H.D. HOLMGREN, and J.R. SILK, University of Maryland--Energy spectra of Z=1,2 particles from 51, 100, 147 MeV/amu ^{16}O-induced reactions have been measured using beams from the LBL Bevalac. At $E(^{16}O) = 100$ MeV/amu, targets of Al, Ni, Sn, and Au were used to study target mass (A_T) effects. High energy proton yields are found to vary as $A_T^{1/3}$ at

DATE FILMED

8